

# Methodology for the Design of Dynamic Rock Supports in Burst Prone Ground

By

**D Raju Guntumadugu**

A thesis submitted to McGill University in partial fulfillment of the  
requirements for the degree of Doctorate of Philosophy



Department of Mining and Materials Engineering,  
McGill University, Montreal, Canada

August, 2013

© G D Raju, 2013

## Dedication

This work is dedicated to my elder brother and sister-in-law: G.P. Raju and G. Amara, who looked after me as their own son, and without whom I would not have continued my education this long.

## Acknowledgments

I am greatly indebted to Prof. Hani Mitri, my supervisor for his excellent guidance, encouragement, constructive criticism, sustained interest and continuing support throughout this research and preparation of the thesis. While admitting the fact that the tireless efforts, continuous guidance, and friendly behavior provided by you were priceless, I gratefully acknowledge the financial assistance you provided, without which, it was almost impossible for me to get an opportunity to study at McGill. It was a great pleasure to be associated with you.

I would like to also thank Dr. V. Venkateswarlu and Dr. P.C. Nawani – Present and Past Directors of NIRM, Kolar Gold Fields, India – for allowing me to pursue a PhD at McGill by granting me a study leave and for all the encouragement during the study. I am thankful to Dr. G.M.N. Rao, HOD, Rock Fracture Mechanics Division, NIRM, India, who is also my superior at NIRM, for giving me valuable advice throughout this study and sparing me to do my research. I thank also my other colleagues in the department, Mr. Uday Kumar and Ms. Praveena Das Jennifer for sharing the burden and always encouraging me towards my research.

Moreover, I would like to thank Dr. R.V. Rao, President (designs) at K.U. Hydro, New Delhi, Dr. S. Gangadhara, Professor (Civil Engineering), at Bangalore University and Dr. H.S. Venkatesh, HOD, Rock Blasting and Excavation Engineering Division, NIRM, India for their continuous help, guidance, and encouragement before and during this study. It would be almost impossible to complete this task without the contributions from Dr. Denis Thibodeau and Ms. Lindsay Moreau-Verlaan at Garson Mine of Vale Ltd., Sudbury.

I would like to thank my long time associate and undergraduate classmate Mr. D.R. Chinnasane, and my long time college in India Mr.

Narayan Mamidi, both Senior Ground Control Engineers at Vale Ltd., Sudbury for all their help and inspiration they gave me to come to McGill and to make me feel at home whenever I visited Sudbury.

All my colleagues at the Mine Design Lab, McGill, have been very supportive during this stay at McGill, particularly Dr. Shahé Shnorhokian, Dr. Tarek Hamade, Mr. Zaka Emad, Mr. Wael Abdellah, and Mr. Atsushi Sainoki. For all the good discussions, arguments, and cheerful moments we had in Rooms 104 and 102 will be remembered forever.

I had a very good support from the administration of the Department of Mining and Materials Engineering, and to name a few, Barbara, Marina and Ruth.

I also want to thank Mr. Ilaya Raj of Sathyam Computers (working for Bombardier Aerospace, Montreal), who has been my roommate for most of my stay in Montreal, for his help in accommodating me and for cooking the homely food, and I also thank all my childhood friends and colleagues who always encouraged me even from a long distance.

As usual, last but not least, the biggest thank you goes to my family – my wife, Parameswari, and my children, Sahithi and Sudhir, for tolerating all pains due to my absence from their midst. I deeply regret for all the times, which belongs to them, when I could not be with them since this is most important in their lives.

# Table of Contents

Acknowledgments .....	iii
Table of Contents .....	v
List of Tables .....	viii
List of Figures .....	x
Abstract .....	xv
Résumé .....	xvii
1 Introduction .....	1-1
1.1 General.....	1-1
1.2 Rockburst Damage.....	1-3
1.3 Scope and Objectives.....	1-5
1.4 Thesis outline .....	1-6
2 Literature Review on Drift Support.....	2-1
2.1 General.....	2-1
2.2 Classification .....	2-1
2.3 Empirical approach.....	2-3
2.3.1 Brief Review of Empirical Methods .....	2-6
2.3.2 Rule of thumb by Lang, 1961 .....	2-7
2.3.3 Rock Quality Designation (RQD) .....	2-7
2.3.4 Rock Structure Rating (RSR).....	2-10
2.3.5 Rock Mass Rating (RMR) .....	2-11
2.3.6 The Rock Mass Quality (Q)-System.....	2-15
2.3.7 Discussion on empirical approach .....	2-20
2.4 Typical drift support pattern .....	2-25
2.5 Characteristics of drift support system.....	2-29
2.5.1 Support functions .....	2-30
2.5.2 Strength of drift support elements .....	2-32
3 Dynamic Supports for Burst Prone Ground.....	3-1
3.1 General.....	3-1
3.2 Current technologies .....	3-4
3.2.1 Cone bolt .....	3-6

3.2.2	The D-Bolt.....	3-8
3.2.3	The Yield-Lok.....	3-11
3.2.4	Durabar .....	3-14
3.2.5	Garford dynamic bolt.....	3-17
3.2.6	DSI dynamic bolt.....	3-19
3.2.7	Discussion on current technologies .....	3-21
4	Case study .....	4-1
4.1	Introduction.....	4-1
4.2	Geo mining conditions of Garson Mine.....	4-2
4.3	Drift Support practice at Garson mine .....	4-4
4.4	Evaluation of current drift support behavior .....	4-7
4.5.1	Numerical Modeling – Static analysis .....	4-9
4.5.2	Mining sequence simulation.....	4-11
4.5.3	Structural elements in FLAC .....	4-16
4.5.4	Analysis and results .....	4-20
4.5.5	Load distribution along the fully grouted rebar .....	4-29
4.5.6	Parametric study .....	4-31
5	Model Calibration .....	5-1
5.1	Introduction.....	5-1
5.2	U-cell .....	5-3
5.3	Instrumentation program .....	5-6
5.3.1	No 1 Shear east – 4900 level.....	5-6
5.3.1	No 1 Shear east – 5000 level.....	5-9
5.3.2	No 1 Shear east – 5100 level.....	5-12
5.3.3	Summary of instrumentation results.....	5-15
6	Dynamic Modeling of Drift Performance .....	6-1
6.1	Introduction.....	6-1
6.1.1	Dynamic Modeling Setup .....	6-2
6.1.2	Boundary Conditions.....	6-2
6.1.3	Application of Dynamic Input .....	6-4
6.1.4	Mechanical damping .....	6-8

6.2	Dynamic analysis .....	6-9
6.2.1	Dynamic performance of drift without support.....	6-9
6.2.2	Dynamic performance of drift primary support .....	6-12
6.2.3	Dynamic performance of drift secondary support .....	6-15
6.2.4	Summary of yielding and wall damage .....	6-18
6.2.5	Summary of bolt axial loads.....	6-21
6.2.6	Drift wall displacements .....	6-24
7	Dynamic Rock Support Selection/Design Methodology .....	7-1
7.1	General.....	7-1
7.2	Current design methods .....	7-2
7.3	Summary of existing methods .....	7-12
7.4	Proposed methodology for design of dynamic rock supports ..	7-13
7.4.1	General .....	7-13
7.4.2	Proposed methodology .....	7-19
8	Conclusions and Suggestions for Future research .....	8-1
8.1	Case study numerical modeling .....	8-1
8.2	Dynamic modeling.....	8-2
8.3	Suggestions for future research .....	8-4
8.4	Statement of Contribution.....	8-5
9	References.....	9-1
10	Appendix.....	10-1
A-1	FLAC 2D Code for static analysis.....	10-2
A2	- Pictures of field instrumentation and others during this study.	10-21

## List of Tables

Table 2-1: Classification of Existing empirical systems for underground support design (Palmstrom, 1995) .....	2-4
Table 2-2: Correlation between RQD and rock mass quality (Deere, 1968) .....	2-9
Table 2-3 Description of three parameters used in RSR.....	2-10
Table 2-4 Rock Mass Rating and rock class correlation ( Bieniawski, 1989) .....	2-12
Table 2-5 Meaning of rock mass classes and rock mass classes determined from total ratings ( Bieniawski, 1978).....	2-13
Table 2-6 Rock Mass classification based on Q -values (Barton et al., 1974) .....	2-17
Table 2-7 Primary rock support specifications in mine developments (refer to Figure 1) .....	2-27
Table 2-8 Secondary rock support specifications in mine developments (refer to Figure 2) .....	2-28
Table 2-9 Strength properties of popular drift supports( Stillborg, 1994 & Mansour mining inc, 2012) .....	2-34
Table 4-1 Primary rock support specifications in mine developments(refer to Figure 4-4) .....	4-5
Table 4-2 Secondary rock support specifications in mine developments (refer to Figure 4-5).....	4-6
Table 4-3 Rockmass properties (Itasca, 2009) .....	4-15
Table 4-4 Rebar mechanical and grout interface properties .....	4-20
Table 5-1 Details of instruments at 1 Sh East 4900 level.....	5-7
Table 5-2 Details of instruments at 1 Sh East 5000 level.....	5-9
Table 5-3 Details of instruments at 1 SH E – 5100 level .....	5-12
Table 5-4 Initial loads on rockbolts, soon after installation.....	5-16
Table 5-5 Axial loads on rebars by insitu measurements (kN).....	5-17
Table 5-6 Comparison of computed and measured axial loads (kN) .....	5-18
Table 5-7 Summary of deformation in 5100L .....	5-18

Table 7-1 Rockburst damage mechanisms and nature of the anticipated damage (CAMIRO-Mining Division, 1990-95) .....	7-8
Table 7-2 Drift wall damage for various levels of ppv due to dynamic load .....	7-30
Table 7-3 Kinetic Energy w.r.t peak particle velocity and the associated wall damage .....	7-32

## List of Figures

Figure 2-1 Generalised support classification ( Mitri, 2000).....	2-3
Figure 2-2 Estimating RQD from a drill core (Deere, 1968).....	2-8
Figure 2-3 RQD based support guidelines ( Merritt, 1972) .....	2-9
Figure 2-4 RMR based chart for maximum stable unsupported span and stand-up time (Bieniawski, 1989) .....	2-14
Figure 2-5 support pressure, Cablebolt length and density guidelines with respect to span and RMR based on Unal, 1983 ( Hutchinson & Diederichs, 1996) .....	2-15
Figure 2-6 Rock support selection guide lines based on Q-values and excavation support ratio (Grimstad and Barton, 1993) .....	2-18
Figure 2-7 Support selection guidelines with RMR and Q-system correlations.....	2-19
Figure 2-8 Enhanced supports installed in burst prone areas (Yao et al. 2009) .....	2-25
Figure 2-9 Primary support system in ore and rock development.....	2-27
Figure 2-10 Secondary support system during in ore and rock developments.....	2-28
Figure 2-11 Effect of yielding support in a dynamic environment (CANMET, 2008).....	2-30
Figure 2-12 Primary support functions (McCreath and Kaiser, 1992) ....	2-31
Figure 2-13 Load deformation curves for typical drift supports( Hoek, 1995) .....	2-32
Figure 2-14 Load deformation curves for typical drift supports including Cone bolt ( CRRP:1990-95) .....	2-32
Figure 3-1 Main functions of supports (CAMIRO Mining Division, 1990- 1995) .....	3-2
Figure 3-2 Modified cone bolt ( MCB), ( Mansur mining.com) .....	3-6
Figure 3-3 Laboratory static test on Fully deboned MCB33( CANMET- MMSL, 2012) .....	3-7

Figure 3-4 Laboratory dynamic test on fully deboned MCB33 (CANMET-MMSL, 2012).....	3-8
Figure 3-5 The D-Bolt with different types of anchors (www.dynamicrocksupport.com).....	3-10
Figure 3-6 D-Bolt (O-anchor) laboratory static test results (CANMET-MMSL, 2012) .....	3-10
3-7 D- Bolt Laboratory dynamic testing results (CANMET-MMSL, 2012)..	3-11
3-8 Yield-Lok Bolt and the function of polymer coating and upset head	3-12
Figure 3-9 Static test results of Yield-Lok Dynamic and static bolts (CANMET- MMSL, 2012).....	3-13
3-10 Dynamic test results of Yield-Lok dynamic bolt( CANMET-MMSL, 2012) .....	3-14
Figure 3-11 The Durabar Yielding bolt (Duraset, www.avengman.com)	3-15
Figure 3-12 Static test results of DURABAR and regular rebar(CANMET-MMSL, 2012) .....	3-16
Figure 3-13 Dynamic test results of DURABAR yieldable bolt(CANMET-MMSL, 2012) .....	3-16
Figure 3-14 The Garford dynamic bolt.....	3-17
3-15 Dynamic test results of Garford dynamic bolt (Varden et al, 2008)	3-18
Figure 3-16 DSI dynatork- dynamic bolt (dsiunderground.com).....	3-19
Figure 3-17 Static and dynamic laboratory test results of DSI-Dynatork bolt, conducted at CANMET facility (dsiunderground.com) .....	3-20
Figure 3-18 Summary of yielding supports tested (CANMET-MMSL, 2012) .....	3-22
Figure 3-19 Comparison between the measured and simulated responses conebolt under dynamic conditions.....	3-24
Figure 4-1 Garson Mine location map .....	4-3
Figure 4-2 Geological units of Garson Mine (Shnorhokian et al, 2013) ...	4-3
Figure 4-3 Typical level plan of 1 shear east zone of the study area .....	4-4
Figure 4-4 Primary support system .....	4-5

Figure 4-5 Secondary or enhanced support system .....	4-6
4-6 Axial load distribution along rock bolt.....	4-7
Figure 4-7 Axial load distribution along fully grouted rockbolt .....	4-9
Figure 4-8 Basic explicit calculation process in FLAC (Itasca, 2011).....	4-11
Figure 4-9 Model geometry with drift .....	4-12
Figure 4-10 Primary support system of fully grouted rebars: Model 1....	4-13
Figure 4-11 Primary and secondary support system: Model 2 .....	4-14
Figure 4-12 Basic model of rockbolt element (Tang et al. 2000).....	4-15
Figure 4-13 Maximum axial loads on primary supports during different mining stages – Model 1 .....	4-22
4-14 Maximum axial loads on primary supports during different mining stages – Model 2 .....	4-23
Figure 4-15 Extent of rock mass yielding around the drift .....	4-29
Figure 4-16 Axial load distribution along fully grouted rebar .....	4-30
Figure 4-17 Axial load distribution along fully grouted MCB .....	4-31
Figure 4-18 Axial loads with various rockmass modulus in primary supports .....	4-32
Figure 5-1 Conventional hollow load cell.....	5-2
Figure 5-2 The U-cell, typical dia 31mm for 16mm or 19mm rockbolts, and 35mm dia for 22mm rockbolts.....	5-3
Figure 5-3 The U-cell portable readout unit and the new generation U-cells .....	5-5
Figure 5-4 Typical calibration of U-cell in the lab .....	5-5
Figure 5-5 Typical field installation of U-cell in a fully grouted rebar .....	5-6
Figure 5-6 Plan showing the location of instruments, 4900 level-1 SHE ..	5-8
Figure 5-7 Plan showing the location of instruments, 5000 level-1 SHE	5-11
Figure 5-8 Plan showing the location of instruments, 5100 level-1 SHE	5-14
Figure 5-9 deformations at 5100L-SW-Pillar nose bet 3181 sill and 3221 sill(MPBX - ID-4-South Wall) .....	5-19
Figure 5-10 Deformations at 5100L-NW- opposite to SW pillar nose bet 3181 sill and 3221 sill(MPBX-ID-6-NW) .....	5-20

Figure 5-11 Wall damage that caused high surface deformations at 5100L-SW pillar nose bet 3181 sill and 3221 sill.....	5-22
Figure 6-1 Quiet boundary conditions.....	6-3
Figure 6-2 Model geometry with input loading and boundary conditions for dynamic modeling .....	6-6
Figure 6-3 Two types of waves for dynamic loading (Genis and Gercek, 2003) .....	6-8
Figure 6-4 Drift behaviour under dynamic loading without supports and no mining.....	6-11
Figure 6-5 Drift behavior under dynamic loading with primary supports	6-15
Figure 6-6 Drift behavior with primary and secondary support without mining sequence under dynamic condition.....	6-18
Figure 6-7 Wall damage around the drift faces – without mining .....	6-20
Figure 6-8 Rock mass yielding around the drift – without mining.....	6-21
Figure 6-9 Axial loads on primary supports under dynamic condition....	6-22
Figure 6-10 Axial loads on primary and secondary supports under dynamic condition – No mining sequence.....	6-23
Figure 6-11 Displacements around drift opening due to dynamic load ..	6-26
Figure 6-12 Displacements around drift opening plotted against ppv ....	6-27
Figure 7-1 Example of various charts provided for aiding the design process in CRRP, 1990-1995(CAMIRO-Mining Division (1990-95)).....	7-7
Figure 7-2 Enhanced supports installed in burst prone area (Yao et al, 2009) .....	7-12
Figure 7-3 Configuration of slab thickness and dimension loaded by stress ( McGarr, 1997) .....	7-16
Figure 7-4 Slab formation around underground excavation, after MUHLHAUS, 1993(McGarr, 1997).....	7-18
Figure 7-5 Wall damage around the drift with primary and secondary support for various levels of PPV due to seismic event.....	7-24
Figure 7-6 Flow chart of proposed design methodology for dynamic rock support design .....	7-25

Figure 7-7 Wall damage around drift due to 1.5m/s ppv at the surface of the wall .....	7-26
Figure 7-8 Reported damage threshold w.r.t peak particle velocity by Brinkmann et al.1987 (Saharan et al. 2006) .....	7-29
Figure 7-9 Wall damage due to various peak particle velocity .....	7-31
7-10 Kinetic energy, PPV and corresponding bolt density(based on bolt energy capacity of 16kJ) .....	7-33
7-11 Shear failure at higher levels of peak particle velocities .....	7-33
Figure 7-12 Effect of dynamic rock supports, cone bolts in this case ( Simser et al. 2007) .....	7-35
Figure 7-13 Field observation of rockbolt failure ( C.C.Li, 2010) .....	7-36
Figure 7-14 Field observation of conebolt failure in shear from the case study mine .....	7-38

## **Abstract**

The depth at which underground mines operate has been increasing continuously which is particularly true in the case of hard rock mining. The stability issues associated with mining at great depth pose tough challenges to engineers and researchers alike. Long-term mine developments in deep hard rock mines such as haulage drifts need to be functional during the entire life of the mine plan without posing any major stability concerns, which will otherwise hamper the production and other logistics associated with mining operations. High convergence and rockburst hazards are the main problems due to high stress and mining-induced seismicity in deep hard rock mining. In such circumstances, the understanding of drift support behavior under static and dynamic conditions is crucial for mining engineers when dealing with drift stability in deep, hard rock mines. In this thesis, current design methods for selecting drift support systems are reviewed, which are mostly dependent on empirical approaches and are geared towards static support design. Based on this, the current research focuses on ground support analysis under both static and dynamic conditions to understand drift support behavior with respect to nearby mining. Numerical modeling of drift primary and secondary supports is performed by developing two models using the 2-dimensional FLAC code. Axial loads induced in the drift support system under static and dynamic conditions are estimated for the case study hard rock mine in Canada at a depth of 1500 m. The results of numerical modeling are obtained in terms of axial loads in the drift support system, wall damage due to tension under dynamic conditions, and the extent of rock mass yielding around the drift. It is found that mining on the same level is critical to drift stability under static conditions, and rock mass yielding in the south wall of the drift (towards the ore body) extends beyond the bolting horizon once this stage begins. The results also show that by providing secondary support before same level mining commences, drift stability is greatly enhanced. The static model is

calibrated through the implementation of an in-situ monitoring program of axial loads induced at the head of the rockbolt. A new load monitoring device called U-cell is successfully used for this purpose. Measured and estimated axial loads are then compared and found to be in good agreement. The preliminary dynamic analysis shows that a peak particle velocity of 2.0 m/s at the periphery of the drift will cause wall damage more than 1.0 m when only primary supports are provided, and around 0.5 m when secondary supports are installed along with the primary ones, and when there is no nearby mining taking place. The effects of lower level and same level mining under dynamic conditions are also examined, and wall damage and rock mass yielding are estimated. The estimation of wall damage depth is crucial in designing dynamic rock supports. It is demonstrated that wall damage due to various levels of ground motion can be estimated by dynamic numerical modeling. Finally, a methodology for the design of dynamic rock supports is presented, which is based on the selection of yielding support type and pattern, the estimation of the ejection velocity, and the volume of wall damage as obtained from dynamic modeling.

## Résumé

La profondeur des mines souterraines a augmenté de manière continue, particulièrement en ce qui concerne les mines en roches dures. Les problèmes de stabilité associés aux mines profondes représentent comme des défis pour les exploitants, comme pour les chercheurs. Les développements miniers à longue durée de vie dans les mines profondes, tels que les galeries de roulage, doivent rester fonctionnels pour toute la durée de l'exploitation, sans poser de soucis majeurs, qui, sinon, nuiraient à la productivité et à l'organisation des opérations minières. Les fortes convergences et le risque de coup de terrain constituent les principaux problèmes dus aux fortes concentrations de contraintes et à la sismicité minière induite dans les mines profondes en roches dures. Dans de telles circonstances, la compréhension du comportement du soutènement des galeries sous l'effet de chargements statiques et dynamiques est essentielle pour les ingénieurs miniers confrontés aux questions de stabilité dans les mines profondes en roches dures.

Dans cette thèse, nous exposons les méthodes courantes de dimensionnement du soutènement des galeries, qui reposent principalement sur des approches empiriques et ont pour objectif d'assurer la stabilité sous chargement statique. Sur cette base, la recherche se concentre sur des méthodes de dimensionnement du soutènement sous des charges statiques et dynamiques, dans le but de comprendre le comportement du soutènement des galeries adjacentes aux zones en cours d'exploitation. La modélisation numérique du soutènement primaire et secondaire des galeries est réalisée en développant deux méthodes recourant au code bidimensionnel FLAC.

Les charges axiales dans le soutènement des galeries sont estimées sous des sollicitations statiques et dynamiques, dans le cas d'une mine canadienne en roche dure, à 1500 m de profondeur. Les résultats de la modélisation numérique sont présentés en termes de charge axiale dans

le soutènement, d'endommagement des parois sous l'effet des tractions induites par les sollicitations dynamiques et de l'extension de la zone rompue autour des galeries. Nous montrons ainsi que l'exploitation sur le même niveau a des conséquences importantes sur la stabilité des galeries en chargement statique, et qu'au niveau du parement sud (i.e. du côté du gisement), la zone rompue s'étend au-delà de la longueur des boulons au début de cette étape.

Les résultats montrent aussi que la stabilité de la galerie de roulage est très nettement améliorée si un soutènement secondaire est mis en œuvre lorsque commence l'exploitation sur le même niveau. Le modèle statique est calibré en utilisant des mesures in situ de la charge axiale sur les têtes de boulons. Pour ce faire, un nouveau dispositif de mesure de la charge, appelé « U-cell » a été utilisé avec succès. Les mesures de charge et les résultats de la modélisation sont comparés et sont en bon accord. L'étude dynamique préliminaire montre que des vitesses de points matériels de l'ordre de 2.0 m/s à la périphérie de la galerie de roulage induisent un endommagement au delà de 1.0 m de profondeur lorsque seul le soutènement primaire est mis en œuvre, et au delà de 0.5 m lorsqu'un soutènement secondaire est installé, pour peu qu'il n'y ait pas de zone en exploitation à proximité.

Les effets de l'exploitation sur le même niveau et sur un niveau inférieur sont également comparés; l'endommagement des parois et la rupture de massifs rocheux sont estimés. L'estimation de l'endommagement de la paroi est essentielle afin de dimensionner le soutènement dynamique. On montre que l'endommagement de la paroi peut être estimé par modélisation numérique, pour différents niveaux de vitesses du terrain. Pour finir, une méthodologie pour le dimensionnement du soutènement dynamique est présentée; elle est basée sur la sélection du type et de la géométrie du soutènement. La vitesse d'éjection et l'endommagement de la paroi sont estimés par modélisation numérique.

# 1 Introduction

## 1.1 General

Mining depth is increasing day by day, particularly in the case of hard rock mining. The stability issues associated with mining at great depth are posing tough challenges to both engineers and researchers alike. Permanent mine openings in deep hard rock mines such as haulage drifts need to be functional during the entire life of the mine without posing any major stability concerns, which would hamper the production and other logistics in running the mining operations. Keeping in mind the service life of the haulage drifts in hard rock mining and the purpose they serve, the stability and safety of these drifts becomes of utmost importance. Design of underground structures is generally based on empirical approaches. However, the empirical design methods are based on ratings assigned to underground structures. These ratings are based on estimates of rock strength, characteristics of discontinuities, seepage conditions, etc. Some of them can only be determined after opening an excavation. These empirical methods do not account for the in-situ stresses, direction of discontinuities, interaction of multiple openings, etc. The efficiency of the support system cannot be evaluated based on performance data in the empirical design methods. Application of principles of rock mechanics, and numerical modeling would lead to the development of qualitative and quantitative approaches for the effective design of underground openings. Mine openings are constructed in rock mass environment that usually exhibit heterogeneous, anisotropic and discontinuous behavior. The long term stability of the excavation is of primary concern, particularly in the case of haulage drifts in deep hard rock mines. Haulage drifts are used for the transportation of blasted ore

from the draw point to nearby ore pass or dumping point in sublevel mining systems. During production, haulage drifts are occupied by mine operators and haulage equipment, and thus must remain functional and safe during their service life.

In deep hard rock mines, the rock mass is highly stressed and excavations will often become unstable. Appropriate support measures to control these instabilities must then be adopted to contain the falling rock mass in a safe manner. In such conditions managing the damage due to mining induced seismicity by appropriate support measures forms a key factor. Kaiser et al. (1997) make it clear that the design of such support requires consideration of the nature of seismic hazard (e.g. rockburst), the additional demand placed on the support by dynamic-forces and the capacity of the support system to meet that demand.

Rockburst is a dynamic form of rock failure, and is one of the most serious calamities in deep mining. Rockburst phenomena in deep underground hard rock mines are generally classified into two main categories: fault slip and strainburst. Strainbursts are characterized by a sudden release of energy in a highly stressed rock mass, more often, causes a local violent failure of the rock mass around the openings. Although strainbursts generally involve small amounts of rock, and relatively small size seismic events, they account for the great majority of rockburst accidents in underground mines. Examples of such phenomena are sill and crown pillar bursts associated with cut-fill mining, abutment pillar failure in a block-caving production level (Mitri et al. 1999). Strainbursts have also been experienced in coal mines, where it is called coal bump. On the other hand fault-slip bursts occur when the shear stress along a geological structure exceeds the normal stress or clamping force acting on the structure, generally due to nearby stope excavation ( Blake and Hedley, 2003). Rockbursts are experienced in underground

mining at various localities in the world, causing fatalities and injuries to mine operators and damage to mine workings.

## **1.2 Rockburst Damage**

Rockbursts can cause excavation and support damage apart from being an impending danger to the life of men and the safety of mining equipment. The damage mechanisms generally include volume expansion (bulking) of the rock due to fracturing, violent ejection of blocks due to seismic energy transfer and seismically-induced rock falls. Damage due to such mechanisms may vary according to the severity of each event.

The specific damage mechanism involved, and the severity of the damage caused will vary depending upon a number of parameters such as the preexisting stress levels in the rock, the quality of the rock mass around the excavation, the excavation shape, and the seismic source characteristics.

Each of the rockburst damage mechanisms may result in different levels of damage to an excavation and its support system. On the basis of field studies of rock damage and support damage levels, Kaiser et al. (1993) define various damage levels that were observed to occur in association with rockburst phenomena. The damage severity depends on many factors including;

- Failure potential near the opening
- Support effectiveness
- Local mine stiffness
- Magnitude of seismically induced stresses, rock accelerations or velocities
- Opening geometry, size and orientation
- Geological structure

Also haulage drifts have to undergo the effect of nearby mining activity such as stoping and other excavations. Blasting employed in creating excavations also induces stresses temporarily in the rock mass around. Sometimes, irreversible deformations along the discontinuities may occur. Therefore, the underground openings often need internal support to improve their stability and safety. The support system could be passive or active. The choice of the support system will invariably depend on the geological conditions, equipment intended for drift development, cost of support systems, and available expertise.

Numerical modeling is increasingly being used to study rock mechanics problems associated with the multiple underground openings in complex geological formations. Mine openings that are driven in rock medium usually exhibit heterogeneous, anisotropic and discontinuous behavior. The analysis of underground excavations involve the evaluation of displacements, extent of yielding zones in static conditions, and the extent of yielding around the excavation and the energy associated with ejection of rock due to a seismic event to assess the stability and to perform an effective design of the same.

Monitoring the behavior of underground rock openings may be recognized today as an important and essential tool for the design and construction of mine openings. Systematic in situ monitoring of the performance of both the rock mass and the support systems through instrumentation has been found to be one of the crucial issues in underground mining. As the mining depth is increasing all over the world, stability issues with mining at great depths are inevitable. Monitoring the in situ performance of the support system and the surrounding rock mass forms a key objective of the ground control programs which aim to

- provide basis for design modifications during development of openings i.e. adaptation of the design to the geological conditions actually encountered;
- monitor the performance of the support system; and
- confirm when the mining induced movements have been controlled.

Furthermore the results of numerical modeling can be compared with those from the instrumentation program. The comparison gives confidence in the methodology adopted for the design of appropriate support system to effectively control the ground under dynamic conditions as well as the effect of the nearby mining.

### **1.3 Scope and Objectives**

It is evident from the depths at which the hard rock mines are being operated today that the mine workings at great depths have to deal with high stress and seismicity. The supports thus selected/designed should sustain high stress and dynamic forces. The long term stability of the service openings is of primary concern, particularly in case of haulage drifts in deep hard rock mines. The haulage drifts are the most occupied openings in the mine, and are occupied by men and equipment.

The scope of this research is focused on deep hard rock mining of steeply dipping, tabular ore bodies. The haulage drift is subjected to

- a) The effect of nearby stope sequencing
- b) The effect of dynamic event on drift support

The above-mentioned factors will be examined with reference to a case study from the Garson Mine of Vale Ltd in Sudbury, Canada. The scope of the study is the #1 Shear East ore body located between levels 4900 and 5100.

The main objectives of this study include

- Numerical modeling of the haulage drift of the case study mine to estimate the response of the walls with respect to the nearby stoping activities
- Numerical modeling of the haulage drift opening to study the performance of the support system under static and dynamic conditions
- Monitoring of in situ load on supports and displacements around the opening with appropriate instrumentation system
- Validation of the numerical models with field measurements namely rock support loads
- To propose a methodology for dynamic rock support selection and design

#### **1.4 Thesis outline**

Including this chapter which presents the general overview of the scope and objective of this thesis has the following chapters.

Chapter 2 presents a review of literature on current support selection/design methods and the typical drift support pattern in deep hard rock mines. The existing empirical method for drift support design is discussed.

Chapter 3 presents a detailed review on the current support technologies available for burst prone ground support. The various types of supports their principle of working and the specifications are presented in this chapter to understand the current technologies.

Chapter 4 presents the case study that includes the static analysis of drift support system with respect to nearby mining. FLAC 2D of Itasca is used to conduct the numerical modeling and the effect of the mining sequence on the drift support performance is examined.

Chapter 5 presents the Instrumentation program in the case study area. The results of the in situ loads measured on rockbolts are used to compare with the numerical modeling results to calibrate the model.

Chapter 6 presents the dynamic modeling of the case study, with a view to examine the response of the drift performance due to the dynamic event. Wall damage and extent of yielding for various levels of ground motion is obtained and also the bolt axial load under the dynamic event is obtained.

Chapter 7 presents the importance of the wall damage for designing the dynamic rock supports in a burst prone area. The result obtained in Chapter 6 is used to estimate the kinetic energy of the rock block that is ejected to estimate the kinetic energy. After successfully performing the dynamic modeling and the results such as, location and extent of wall damage, displacements, a methodology for designing/selecting dynamic rock supports is proposed.

Chapter 8 presents the research conclusions and recommendations for further research.

## **2 Literature Review on Drift Support**

### **2.1 General**

Design of underground structures is generally based on empirical and intuitive approaches. However, the empirical design methods are based on ratings assigned to underground structures. These ratings are based on estimates of rock strength, characteristics of discontinuities, seepage etc. Some of them can only be determined after opening an excavation. These empirical methods do not account for the in-situ stresses, direction of discontinuities, etc. The efficiency of the support system cannot be evaluated based on performance data in the empirical design methods

### **2.2 Classification**

One of the main reasons for using supports in underground mining is to maintain the inherent strength of the rock mass to support itself after it has been disturbed by an excavation. Supports act as reinforcing elements, i.e., they help transfer the weight of loose rocks to intact and solid rocks. In civil engineering projects, it is the custom to describe support as being temporary or permanent. Temporary support is installed to ensure safe working conditions during the construction period, and, permanent support is installed for the long term stability of the excavation.

Support systems may be classified into two broad categories: internal and external, which can be either active or passive. A support becomes active when stresses are induced in it at the time of installation. Therefore, such supports reinforce the rock mass structure by exerting an "induced" stress on the ground immediately after its installation (Brady & Brown, 1993). The common examples are pretensioned rock bolts or cables, hydraulic props, expandable segmented concrete linings and powered supports for long wall faces. Active supports are applied in situations where an excavation is believed to cause excessive deformation

in the ground (Stillborg, 1994). An example of this situation is separation of rock wedges from the rock mass. Passive supports do not reinforce the rock mass immediately after installation, but their effect is seen as subsequent mining activities take place. Examples of passive supports are steel arches, timber sets, composite packs and un-tensioned bolts (e.g. rockbolts, cable bolts, reinforcing bars, etc.).

External supports are generally of the passive type. They are placed around the boundary of the excavation to help restrain the movement of the rock walls and avoid the failure of rock mass. Steel arches, wooden cribs and fiber reinforced shotcrete are some types of external supports. Backfill is another common type of external, passive support used in hard rock mining. Internal supports continue to see technological developments in the mining industry. The basic mechanism of internal support is to bound rocks together to maintain the overall stability of the rock mass around an excavation. Internal supports which are pretensioned at the time of installation are considered to be of the active type. Swellex, Split Sets, grouted bars and mechanical anchors are some of the common examples of internal supports. A general classification of support systems is given in Figure 2.1 (Mitri, 2000).

Support design of underground permanent openings is generally based on empirical and intuitive approaches. However, the empirical design methods are based on ratings assigned to underground structures. These ratings are based on estimates of rock strength, characteristics of discontinuities, seepage etc. Some of them can only be determined after opening an excavation and there are many such approaches exist. This chapter deals with the review of such methods available globally

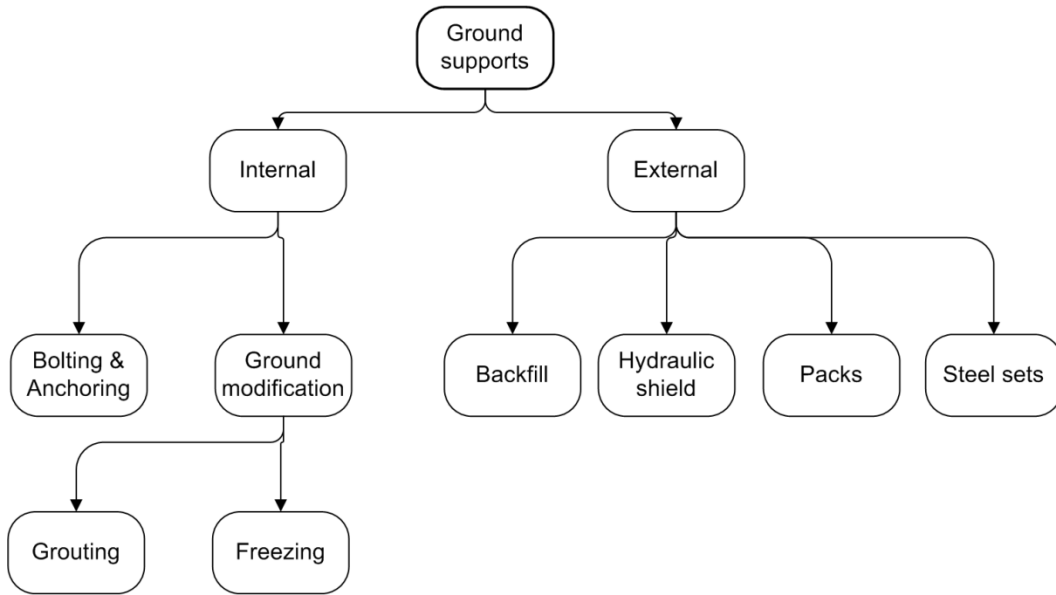


Figure 2-1 Generalised support classification ( Mitri, 2000)

### 2.3 Empirical approach

Empirical methods assess the stability of the underground excavations by the use of statistical analysis of the underground observations. The engineering rock mass classifications are the best-known empirical approach for assessing the stability of the underground openings. Classification systems in use for underground support design are given in Table 2-1(Palmstrom, 1995). Some of the empirical approaches consider the design of support systems on the basis of empirical formulae based on rules of thumb combined with the past and similar experiences. These approaches presented a number of charts and tables for the convenient use. Syed(2004), after investigating a few case studies, where empirical methods of support design was adopted, opines that the two main empirical approaches namely RMR and Q systems of rock mass classification though include main governing parameters, their use provides some overall guidance for the selection of support system, and however, they are not stand alone.

Table 2-1: Classification of Existing empirical systems for underground support design (Palmstrom, 1995)

<b>Name of the Classification</b>	<b>Form And Type</b>	<b>Main Applications</b>	<b>Reference</b>
The terzaghi rock load classification System	Descriptive and behaviouristic form functional type	For design of steel support in tunnels	Terzaghi, 1946
Lauffer's stand-up time classification	Descriptive form General Type	For input in tunneling design	Lauffer, 1958
The new Austrian tunneling method ( NATM)	Descriptive and behavioristic form tunneling concept	For excavation and design in incompetent ( overstressed ) ground	Rabcewicz, Miller and Pacher, 1958 - 64
Rock classification for rock mechanical purposes	Descriptive form General type	For input in Rock mechanics	Patching and Coats, 1968
The unified classification of soils and rocks	Descriptive form General type	Based on particles and blocks for communication	Deere et al., 1969

The rock quality designation ( RQD)	Numerical Form General type	Based on Core Logging: used in other classification systems	Deere et al. 1967
The Size-strength Classification	Numerical Form Functional type	Based on rock strength and block diameter; used mainly in mining	Franklin, 1975
The rock structure rating (RSR) classification	Numerical form Functional type	For design of (steel) supports in tunnels	Wickham et al. 1972
The rock mass rating (RMR) classification	Numerical form Functional type	For use in tunnel, mine and foundation design	Bieniawski., 1973
The 'Q' classification system	Numerical form Functional type	For design of support in underground excavations	Barton et al. 1974
The typological classification	Descriptive form General type	For use in communication	Matula and Holzer, 1978
The unified rock classification system	Descriptive form general type	For use in communication	Williamson, 1980

Basic Geotechnical Classification ( BGD)	Descriptive form General type	For general use	ISRM, 1981
The Geological Strength Index ( GSI )	Numerical form Functional type	For design of supports in underground excavations and use in Numerical modeling as input	Hoek, 1994
The Rock Mass index ( Rmi ) system	Numerical form Functional type	For general Characterisation, design of support, TBM progress	Palmstrom, 1995

### 2.3.1 Brief Review of Empirical Methods

There are many number of classification systems available and are well documented by many authors (Palmstrom, 1995; Singh and Goel, 1999; Edelbro, 2003). Rock mass classification systems can be of considerable use when there is not enough geotechnical data of the project is available, particularly during the initial stages of project. All the classification systems are not meant for support selection/design, only some of them are used for the support design purposes where as the other classification systems are used for the rock characterization purposes. In the present review only those empirical systems that are used for designing/selecting supports for underground openings are briefly described. The classification system takes in to consideration the factors which are believed to affect the stability of the opening. The parameters are therefore often related to the discontinuities such as the number of joint sets, joint distance, roughness, alteration and filling of joints.

### 2.3.2 Rule of thumb by Lang, 1961

In 1961, Lang proposed the rule of thumb for estimating the support requirements as below:

Minimum bolt length, L=

- Twice the bolt spacing, S; (L=2S)
- Three times the width of critical and potentially unstable rock blocks defined by the average discontinuity spacing, b;
- 0.5B for spans of B < 6m, 0.25B for spans of B = 18-30 m.

Farmer and Shelton(1980), also proposed another rule of thumb for selecting the supports based on the rock mass discontinuity sets and the span from the case histories collected from numerous authors.

### 2.3.3 Rock Quality Designation (RQD)

In 1964, Deere introduced an index to assess rock quality quantitatively, called rock quality designation (RQD). The RQD is a core recovery percentage that is indirectly based on the number of fractures and the amount of softening in the rock mass that is observed from the drill cores. Only the intact pieces with length longer than 100mm are summed and divided by the total length of the core run (Deere, 1968)

$$RQD = \frac{\sum \text{Length of core pieces} > 10cm}{\text{Total Core length}} \times 100\%$$

This means that the RQD is simply a measurement of the percentage of “good” rock recovered from borehole cores. An example of estimating the

length of core pieces more than 10cm from a drill core is shown in Figure 2-2.

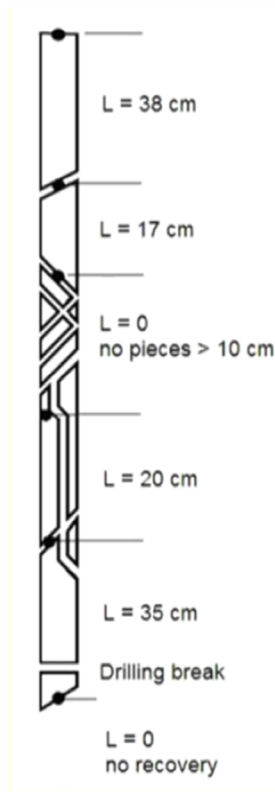


Figure 2-2 Estimating RQD from a drill core (Deere, 1968)

According to Deere (1968), all the artificial fractures should be ignored while counting the core length for RQD and also all pieces that are not hard and sound even if they pass the requisite 100mm length. Rock support selection chart based on RQD and the span of the opening as presented by Merritt, (1972) is shown in Figure 2-3.

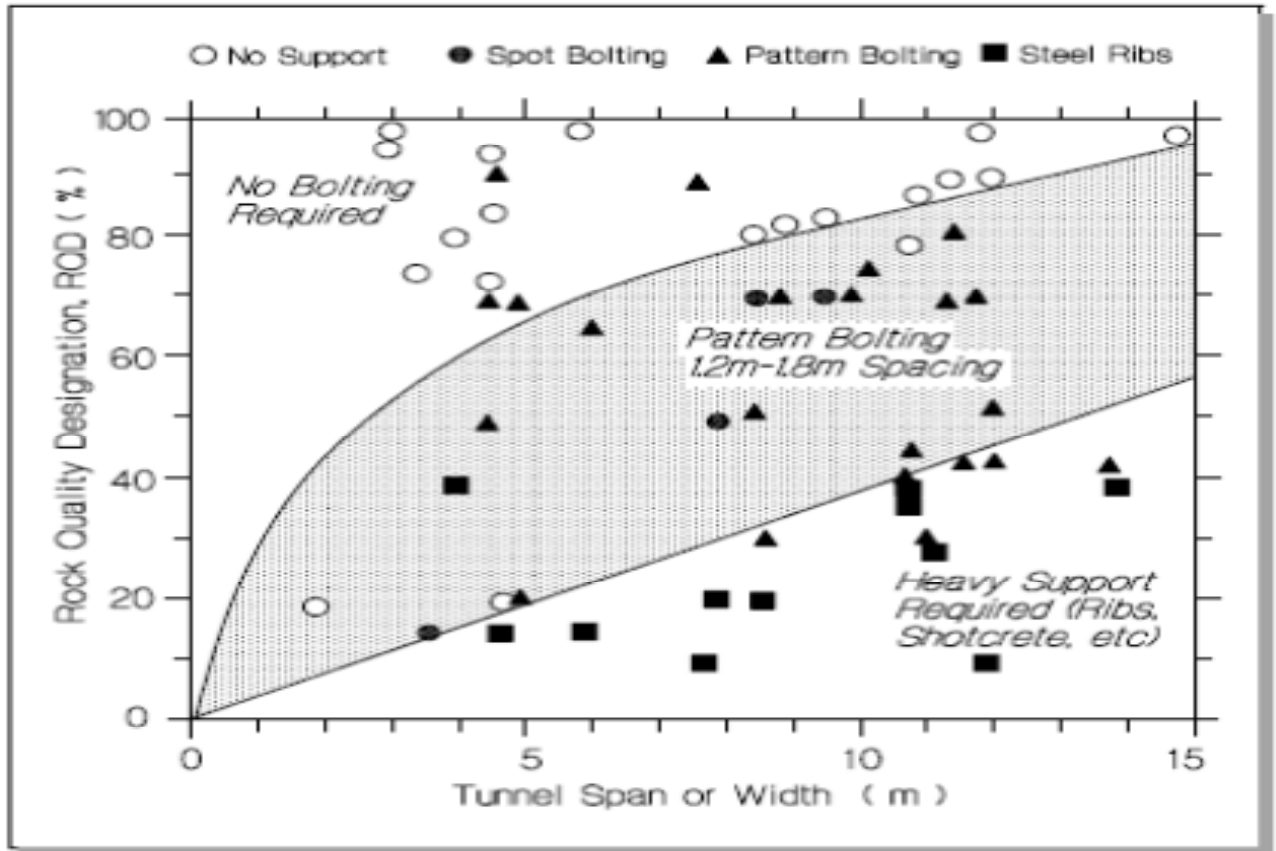


Figure 2-3 RQD based support guidelines ( Merritt, 1972)

The International society for Rock Mechanics ( ISRM) recommends at least NX( size 54.7 mm) core size. However from the experience of the Deere, the other core sizes and drilling techniques are applicable for recording RQD measurements (Deere and Deere., 1988). Correlation between RQD and rock mass quality is presented in Table 2-2

Table 2-2: Correlation between RQD and rock mass quality (Deere, 1968)

RQD (%)	<25	25-50	50-75	75-90	90-100
Rock Quality	Very Poor	Poor	Fair	Good	Excellent

### 2.3.4 Rock Structure Rating (RSR)

Wickham et al., (1972) introduced a quantitative method for describing the quality of rock mass and the required support system. The Rock Structure Rating (RSR) is the first to introduce numerical ratings of the rock mass properties and said to be the precursor to the two most used classification systems today i.e. the RMR and the Q-System (Palmstrom, 2003). The numerical value of RSR ranges from 0 to 100 and is the sum of weighted numerical values determined by three parameters called A, B and C. The description of each of the parameter is given Table 2-3

Table 2-3 Description of three parameters used in RSR

Parameter	Description
A	Combine the generic rock type with an index value for rock strength along with the general type of structure in the rock mass studied
B	Relates the joint pattern with respect to the direction of the drive
C	The degree of joint weathering, alteration and the amount of water inflow and Considers the overall rock quality with respect to parameters A and B

Further developments with RSR to make this method simple and easy to use for prediction of the support requirements are reported by (Skinner, 1988). A detailed description of assigning ratings to various parameters and classifying the rock mass using RSR is given by Hoek, (2000).

### 2.3.5 Rock Mass Rating (RMR)

In 1973 Bieniawski introduced the Geomechanics Classification also named the Rock Mass Rating ( RMR), at the South African Council of Scientific and Industrial Research (CSIR). The rating system was based on his experiences in shallow tunnels in sedimentary rocks. Originally, the RMR system involved 49 unpublished case histories. According to Bieniawski (1989) the RMR has been applied in more than 268 case histories such as in tunnels, underground chambers, mines, slopes and rock caverns. The reasons for using RMR according to him, the ease of use and the versatility in engineering practice. When applying this classification system, one divides the rock mass into a number of structural regions and classifies each region separately. The RMR system uses the following six parameters, whose ratings are added to obtain a total RMR-value

- i. UCS of intact rock material
- ii. RQD
- iii. Joint spacing
- iv. Joint condition
- v. Ground water condition
- vi. Joint orientation

The first five parameters represent the basic parameters ( $RMR_{basic}$ ) in the classification system. The sixth parameter is treated separately because the influence of discontinuity orientations depends up on engineering applications. Each of these parameters is given a rating that symbolizes the rock quality description. All the ratings are algebraically summarized

for the first five given parameters and can be adjusted depending on the joint and tunnel orientation by the sixth parameter as shown in the following equation

$$RMR = RMR_{basic} + \text{adjustment for joint orientation}$$

The Final RMR values are grouped in to five rock mass classes as shown in Table 2-4, where the rock mass classes are in groups of twenty ratings each. The various parameters are not equally important for the overall classification of the rock mass, since they are given different ratings. Higher rock mass rating indicates better rock mass condition.

Table 2-4 Rock Mass Rating and rock class correlation ( Bieniawski, 1989)

RMR	< 20	21-40	41-60	61-80	>80
Rock Class	Very Poor	Poor	Fair	Good	Very Good

Rock reinforcement selection guidelines based on the RMR value was published by Bieniawski (1989). The guidelines presented in Table 2-5 are based on a 10m span horseshoe-shaped tunnel, constructed using drill and blast methods (Palmstrom, 2003). Since the shape, size, and depth are different in a mine, care must be taken when using it in mines. According to Palmstrom (2003), factors such as in situ stress, tunnel size and shape and the method of excavation affect the guidelines. Also the recommended support is the permanent support and not the primary support.

Table 2-5 Meaning of rock mass classes and rock mass classes determined from total ratings (Bieniawski, 1978)

Parameter/properties of rock mass	Rock Mass Rating ( Rock class)				
	100-81	80-61	60-41	40-21	<20
Ratings	100-81	80-61	60-41	40-21	<20
Classification of rock mass	Very Good	Good	Fair	Poor	Very Poor
Average stand - up time	10 years for 15 m span	6 months for 8 m span	1 week for 5 m span	10 hours for 2.5m span	30 minutes for 1 m span
Cohesion of the rock mass	>400kPa	300-400kPa	200-300 kPa	100-200 kPa	<100 kPa
Friction angle of the rock mass	>45°	35°-45°	25°-35°	15°-25°	<15°

The classification parameters are obtained from bore hole data or underground mapping and can be used for selecting the permanent support system. Most of the applications of RMR system have been in the field of tunneling but also in various types of slopes for slope stability, foundation stability, caverns and different mining applications. Figure 2-4 shows the chart giving the guidelines on maximum stable unsupported span and unsupported stand up time based on RMR.

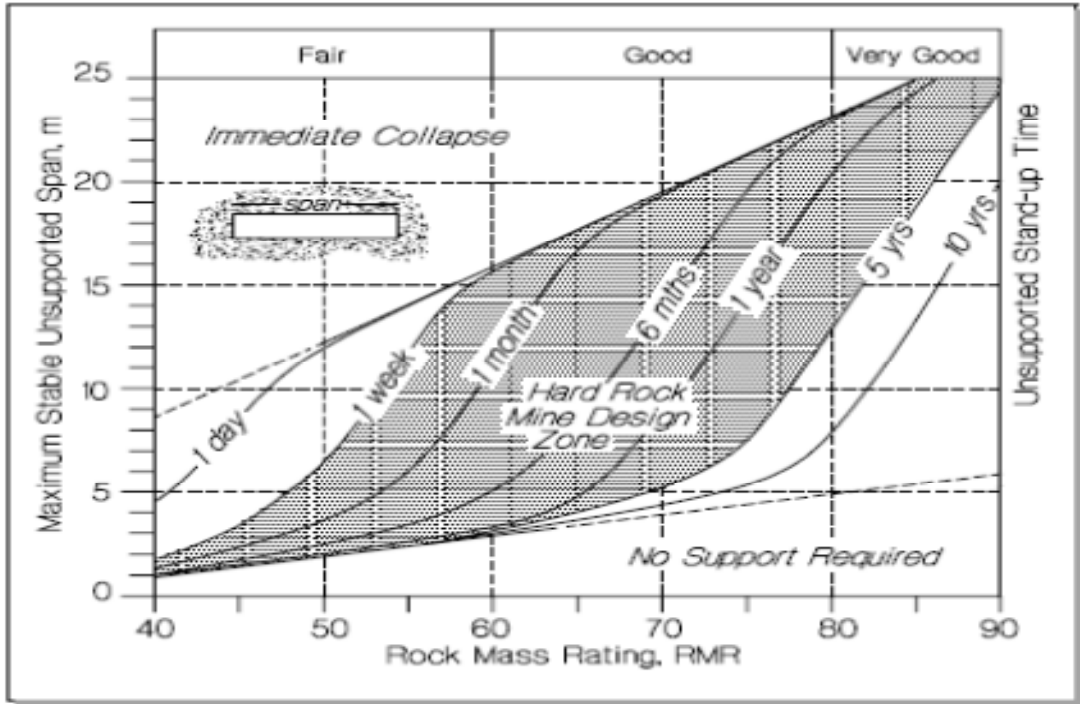


Figure 2-4 RMR based chart for maximum stable unsupported span and stand-up time (Bieniawski, 1989)

Another chart, which provides cable bolt support guidelines based on RMR developed by Unal (1983) is shown in Figure 2-5. According to Diedrichs and Hutchinson, the concept of this is simple and yet it produces reasonable results for cable bolt length and moderately conservative recommendations for cable bolt density for mining applications. The cablebolt densities as shown in Figure 2-5 are calculated for a rock specific weight of  $26\text{kN/m}^3$  and for steel capacities of 20 tonnes (200kN) for single strand and 40 tonnes for double strand cablebolts for permanent installations. For temporary and non-critical openings, 25 and 50 tonnes can be used respectively. This results in a 20% decrease in cablebolt density as also pointed in Figure 2-5.

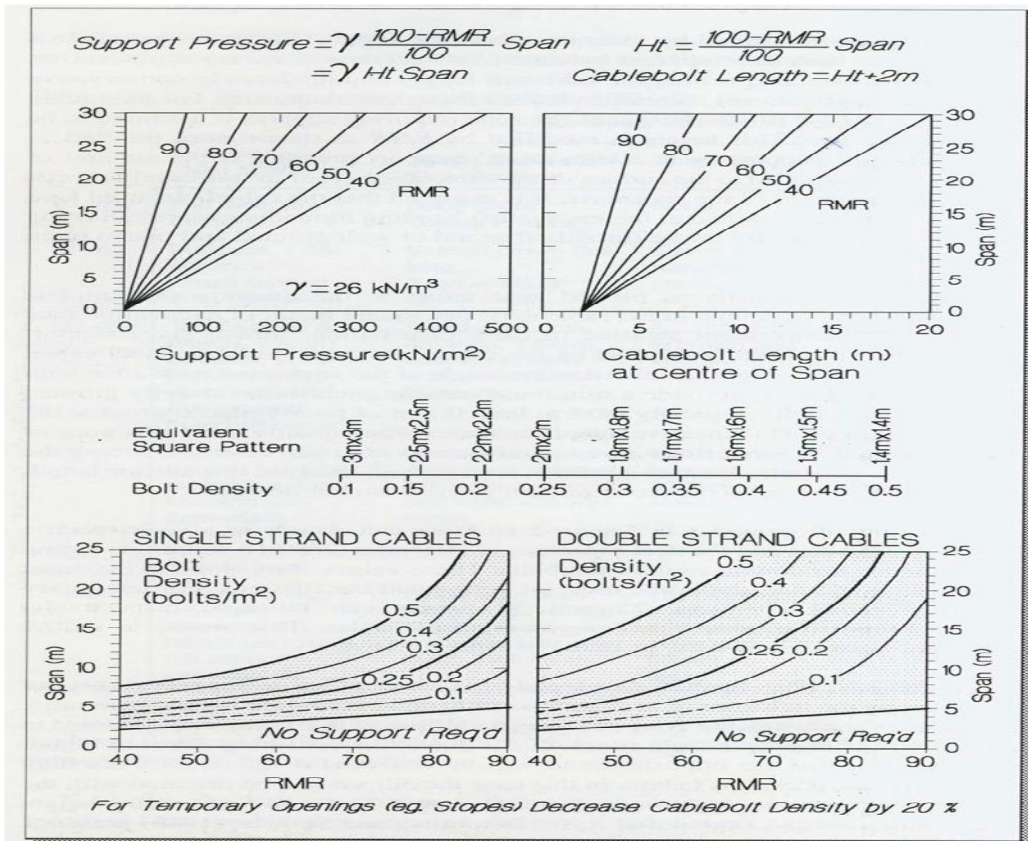


Figure 2-5 support pressure, Cablebolt length and density guidelines with respect to span and RMR based on Unal, 1983 (Hutchinson & Diederichs, 1996)

### 2.3.6 The Rock Mass Quality (Q)-System

Barton et al. first introduced the rock tunneling Quality index, the Q-system in 1974. This is based on 212 case records. The studied cases ranged from unsupported 1.2m wide pilot tunnels to unsupported 100m wide mine caverns. The excavation depth ranged from 5 to 2500m where the most common depths were between 50 and 250m. Updating of the Q-system has taken place on several occasions. The original parameters of the Q-system have not been changed, but the rating for the stress reduction factor (SRF) has been altered by Grimstad and Barton (1993), when 1050 new case records were included. In 2002, some new Q-value correlations were presented by Barton, which also included new footnotes

for  $J_w$ ,  $J_a$  and SRF. According to Barton (1988) the fundamental geotechnical parameters are,

- Block size
- Minimum inter-block shear strength, and
- Active stress

These fundamental geotechnical parameters are represented by the following ratios (Barton, 2002):

Relative block size =  $RQD / J_n$

Relative frictional strength (of the least favourable joint set or filled discontinuity) =  $J_r / J_a$

Active stress =  $J_w / SRF$

The rock mass quality is defined as (Barton et al., 1974):

$$Q = \frac{RQD}{J_n} \times \frac{J_r}{J_a} \times \frac{J_w}{SRF}$$

Where

RQD = Deere's Rock Quality Designation (Deere et al., 1968),

$J_n$  = joint set number,

$J_r$  = joint roughness number (of least favorable discontinuity or joint set),

$J_a$  = joint alteration number (of least favorable discontinuity or joint set),

$J_w$  = joint water and pressure reduction factor, and

SRF = stress reduction factor-rating for faulting, strength/stress ratios in hard massive rocks, and squeezing and swelling rock.

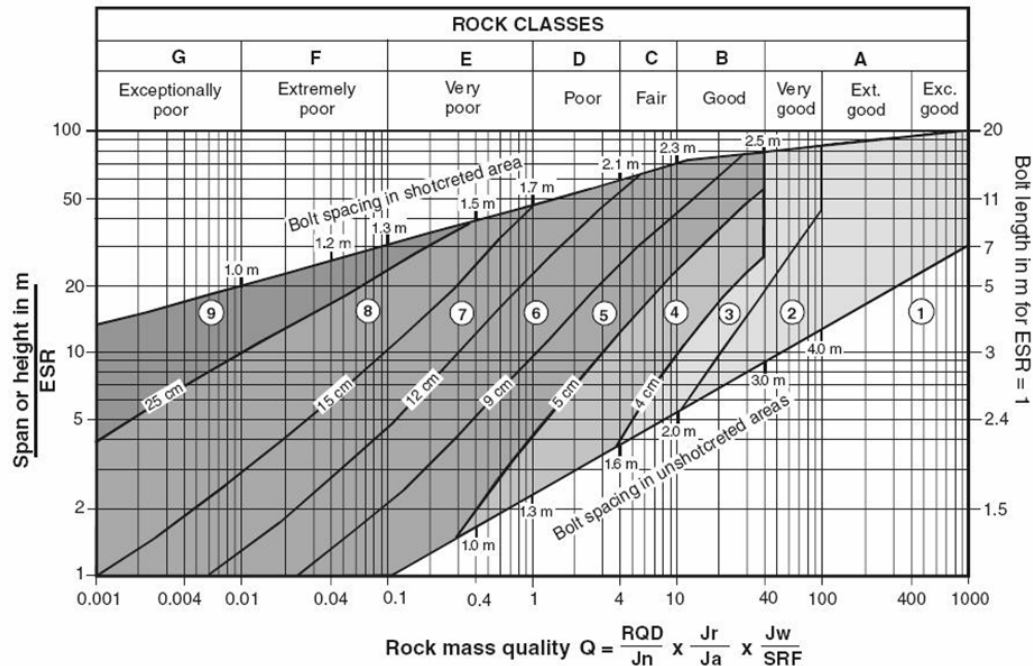
The use of the Q-system is specifically recommended for tunnels and caverns with an arched roof. The rock mass has been classified into

nine categories based on the Q- value and accordingly the supports can be selected by using the charts provided. Classification of rock mass according to the Q value is presented in Table 2-6

Table 2-6 Rock Mass classification based on Q -values  
(Barton et al. 1974)

Q	Group	Classification
10-40 40-100 100-400 400-1000	1	Good Very Good Extremely Good Exceptionally Good
0.10-1.0 1.0-4.0 4.0-10.0	2	Very Poor Poor Fair
0.001-0.01 0.01-0.1	3	Exceptionally Poor Extremely Poor

Barton (2002), presented the new Q-value correlations and are mainly focused on the applicability of the Q – system in site characterization and tunnel design. The chart detailing the support selection guidelines based on Q-system is shown in Figure 2-6.



**REINFORCEMENT CATEGORIES:**

- |   |   |
|---|---|
| <ul style="list-style-type: none"> <li>1) Unsupported</li> <li>2) Spot bolting</li> <li>3) Systematic bolting</li> <li>4) Systematic bolting, (and unreinforced shotcrete, 4 - 10 cm)</li> <li>5) Fibre reinforced shotcrete and bolting, 5 - 9 cm</li> </ul> | <ul style="list-style-type: none"> <li>6) Fibre reinforced shotcrete and bolting, 9 - 12 cm</li> <li>7) Fibre reinforced shotcrete and bolting, 12 - 15 cm</li> <li>8) Fibre reinforced shotcrete, &gt; 15 cm, reinforced ribs of shotcrete and bolting</li> <li>9) Cast concrete lining</li> </ul> |
|---|---|

Figure 2-6 Rock support selection guide lines based on Q-values and excavation support ratio (Grimstad and Barton, 1993)

Based on case studies, Bieniawski (1976) was the first author to suggest a correlation between the RMR-system and the Q-system (Edelbro, 2003):

- $RMR = 9.0 \ln Q + 43.$
- $RMR = 5.9 \ln Q + 43.$  (Rutledge and Preston (1978))
- Other correlations are:
  - $RMR = 5.4 \ln Q + 55.2,$  Moreno(1980)
  - $RMR = 5 \ln Q + 60.8,$  Cameron et al. (1981)
  - $RMR = 10.5 \ln Q + 41.8,$  Abad et al. (1984)

According to Goel et al., (1995), these correlations are not reliable, as they do not take in to account the same parameters. He evaluated these correlations on the basis of 115 case histories. Figure 2-7 shows the support selection guidelines with RMR and Q-system correlations.

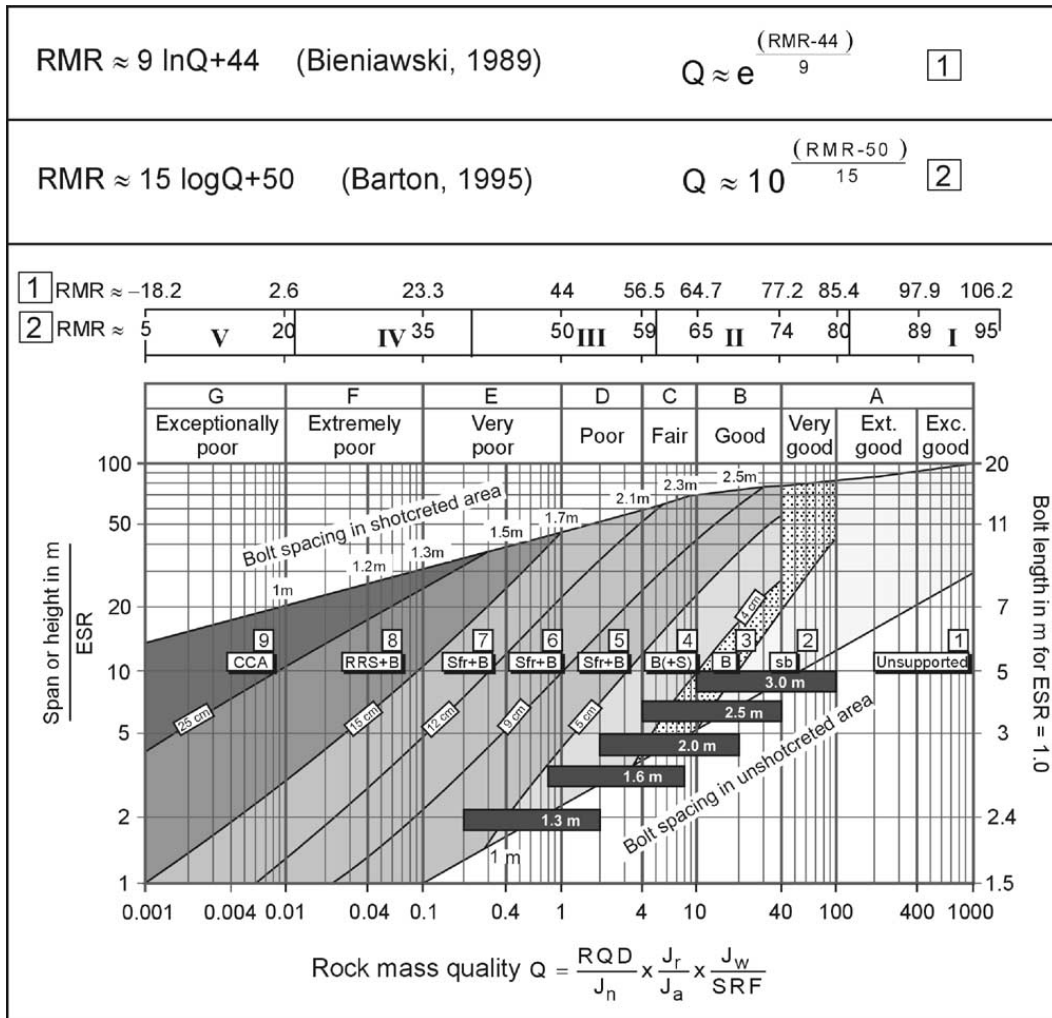


Figure 2-7 Support selection guidelines with RMR and Q-system correlations

### **2.3.7 Discussion on empirical approach**

A major contribution of the classification systems for use in underground openings is that, they provide a way of quantifying the quality and capability of the rock mass, which can be understood in a global context. Their exactness is not of interest in decimals. With careful and respectful application, in Norway and in other parts of the world, those systems serve as useful tools both in design and construction. Being used in combination with other classification systems and together with; engineering judgment; analytical and numerical analysis, monitoring and observation of the tunnel behavior, the tunneling engineer has a powerful toolbox in hand. It is important to keep in mind that the appropriate application of these systems, both during the design and construction phases. Site specific considerations and modifications are needed to enable the most appropriate application of any of these classification systems.

Singh and Goel(1999) put it that in all of the classification system poorest rock mass is assigned a minimum rating and the maximum rating is assigned to the excellent rock mass. Thus, every parameter of a classification plays a more dominant role as overall rating decreases. Obviously, many classifications are accurate in both excellent and poor rock conditions. Reliability may decrease for medium rock conditions (Singh and Goel, 1999). Hoek and Brown (1997) have realized that a classification system must be non-linear to classify poor rock masses realistically. In other words, the reduction in strength parameters with classification should be non-linear unlike RMR in which strength parameters decrease linearly with decreasing RMR. However Mehrotra (1992) has found that strength parameters decrease non-linearly with RMR for dry rock masses. empirical approaches as mentioned above have limitations for their use in detailed design, as they cannot provide

effective solution whenever the excavation come across with the following features:-

- Joint orientation, intersection of joints resulting in kinematically unstable mechanisms.
- Interaction of multiple excavations.
- Sequence of excavation and time lag in installation of supports.
- Rock cover.
- Failure mechanisms.
- Time dependent material property

'Q' and RMR system are most widely used for the design. However in many of the field situation, these system leads to under or over estimation of the support system. Sayed, (2004) mentions some field situations where this system could not take in to account the actual conditions of the excavations include

- In case of Bhatan Twin Tunnel, the interaction between the two tunnels cannot be taken up by these two systems. It is also observed that the failure is mainly due to slip and separation of the joints rather than the stress-based failure, which these two systems could not be able to identify
- In case of Ghatghar Hydro Electric Project, the interaction of the powerhouse cavern, the transformer cavern and the connecting tunnels could not be taken up by these two systems. The presence of different types of basaltic rock

with different values of RQD varying across the depth could not be accounted. The rock bolts generally will not be effective if the joints run perpendicular to the longitudinal direction of the cavern, which these two systems could not be able to identify

- In case of Sardar Sarovar Project, the interaction of the powerhouse cavern and connecting tunnels could not be taken up at a time. Thereby restricting the utility of the systems. The higher in situ stresses perpendicular to the longitudinal direction of the cavern coupled with many shear zones, which are causing the distress along the walls could not be identified. The failures (cracks and distress) observed in the walls than the roof could be attributed to the factors mentioned above
- In case of Tala Hydro Electric Project, the interaction of the powerhouse, transformer cavern and connecting tunnels could not be taken up thereby restricting the utility of the systems. The collapse of the roof occurred could not be predicted which may be attributed to high rock cover, delay in implementation of support system for stage excavations and inadequate support system

The classification systems are often used for other applications than rock mass stability, such as calculation of different rock mechanical parameters. The results from such calculations should only be considered as rough estimates. However, since it is often difficult to carry out exact field measurements of such parameters. Stability analysis of underground

engineering works has been a challenging and difficult subject in geomechanics, from the early rock load theories to the three dimensional numerical analysis methods available today (Sotirios vardakos, 2003).

The two most commonly used rock mass classification systems today is the RMR and the 'Q' system. These classification systems include the rock quality designation (RQD), which was introduced by Deere in 1964 as an index of assessing rock quality quantitatively. Since different classification systems pay attention to different parameters, it is often recommended that at least two methods should be used when classifying a rock mass (Hoek, 2000). The most commonly used parameters are intact rock strength, joint strength, joint spacing and ground water condition.

When using rock mass classification systems, it has often been suggested (RQD, RMR, Q-system) that only the natural discontinuities, which are of geological or geomorphologic origin, should be taken into account. However, it is often difficult, if not impossible, to judge whether a discontinuity is natural or artificial, after activities such as drilling blasting and other excavation activities.

From the above, it is also clear that most of the methods available to design an underground cavern / opening are based mostly on empirical approaches which have the inputs from RMR / Q-system; hence, there is a need for scientific and rational design of support system for the stability of the underground excavation using numerical modeling and field instrumentation. More over all these empirical approaches are confined to static support design/selection and none of them considers the dynamic conditions, which most of the deep hard rock mines and the deep tunnels are sure to experience. The only exception is that the one proposed by the CAMIRO mining division (1990-1995) as part of the Canadian Rockburst Research Program (CRRP), which discuss about the support

requirements under dynamic conditions based on some case studies and proposes number of charts for selecting the dynamic supports for burst prone ground. However these charts need to be validated through the field measurements particularly under the dynamic condition. Some deep hard rock mines facing the burst problems have designed their own support system for the burst prone ground based on their own experiences in their own or group of mines. One such method is proposed by Yao et al(2009).The approach adopted here was risk based approach to design highly yielding support to sustain future seismic impact after gaining experience from the major rockburst. A risk rating system to determine where enhanced support system is required was evolved by taking the following six parameters in to consideration and then assigning numerical rating to the parameters.

- Historic Seismic data of the area
- Ground condition
- Efficacy of the existing ground support
- Deteriorated infrastructures in the proximity
- Anticipated mining induced stress
- Other geological structures in the proximity

The total risk rating is found after summing up the individual ratings. The threshold rating of the risk is established by back analysis of a number of areas within the mine. If the total risk rating crosses this threshold rating, then enhanced support is required in the form of yielding supports in that area. Also the type of enhanced support is determined using the five-step methodology (Yao et al, 2009). Typical burst prone area supported using this methodology is shown in Figure 2-8



Figure 2-8 Enhanced supports installed in burst prone areas (Yao et al. 2009)

## 2.4 Typical drift support pattern

Primary support systems in Canadian mines typically employ 3/4 inch resin grouted rebar in the back and shoulder. In low stress environment, jointed/fractured rock mass for short term openings (2 year life or less), the efficiency of resin grout is not warranted, hence the use of 5/8 inch and 3/4 inch mechanical rockbolts with expansion shell. Typical support length is 6 to 7 feet (1.8 to 2.1 m) for drifts of spans in the range of 4 to 5 m and for the drift spans of more than 5m, support lengths of 8 ft(2.4m) in the back and 6 ft(1.8m) in the wall is employed. On the other hand, sidewall support systems employ more ductile support such as Swellex and Split-Sets. These supports offer greater ability to accommodate sidewall deformations due to mining-induced convergence. A typical primary and secondary support systems practiced at some of the mines in Canada, where a high horizontal stress causes the instability are shown in Figure 2-9 and Figure 2-10. The specifications of the support

system are presented in Table 2-7 and Table 2-8.

As can be seen from figure 2-9, it is evident that the rebar of 6 or 8 ft is the primary support system during the regular rock development. In the ore development the primary support in the sidewall consists of split sets. The secondary or enhanced support system consists of 8ft(2.4m) long Modified cone bolt(MCB) or MN12 Swellex bolt along with '0'gage mine mesh as shown in figure 2-10. It is understood that the secondary or enhanced support system has the yielding capacity to resist the dynamic loading. This sort of support system will enhance the haulage drift stability against seismic loads. Apart from this reinforced shotcrete with "0" gage mesh or with steel fibres is also employed to have a stable back and walls in burst prone ground.

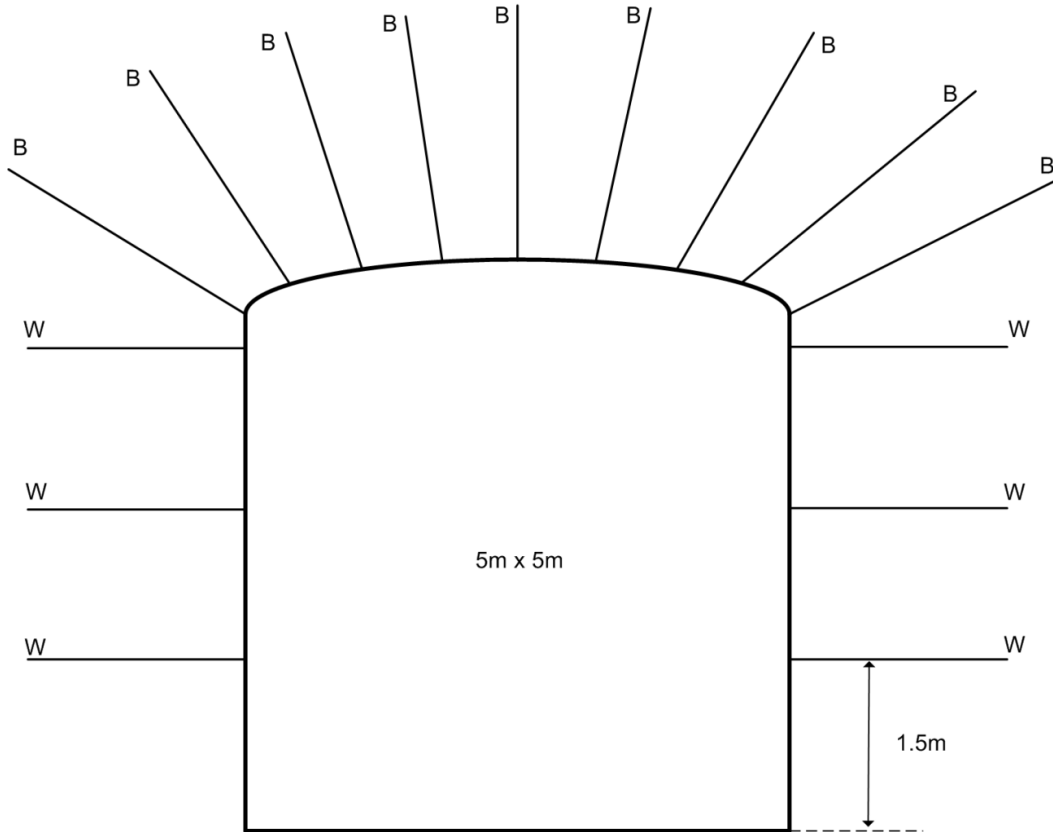


Figure 2-9 Primary support system in ore and rock development

Table 2-7 Primary rock support specifications in mine developments (refer to Figure 2-9)

Regular Rock Development	Excavation width < 6m		Excavation width > 6m
	B	6ft-Rebar	8ft-Rebar
W	6ft-Rrebar	6ft-Rebar	
Development in Ore	B	6ft-Rrebar	8ft-Rebar
	W	6-ft 6-inch FS46 Split-Set	6-ft 6-inch FS46 Split-Set

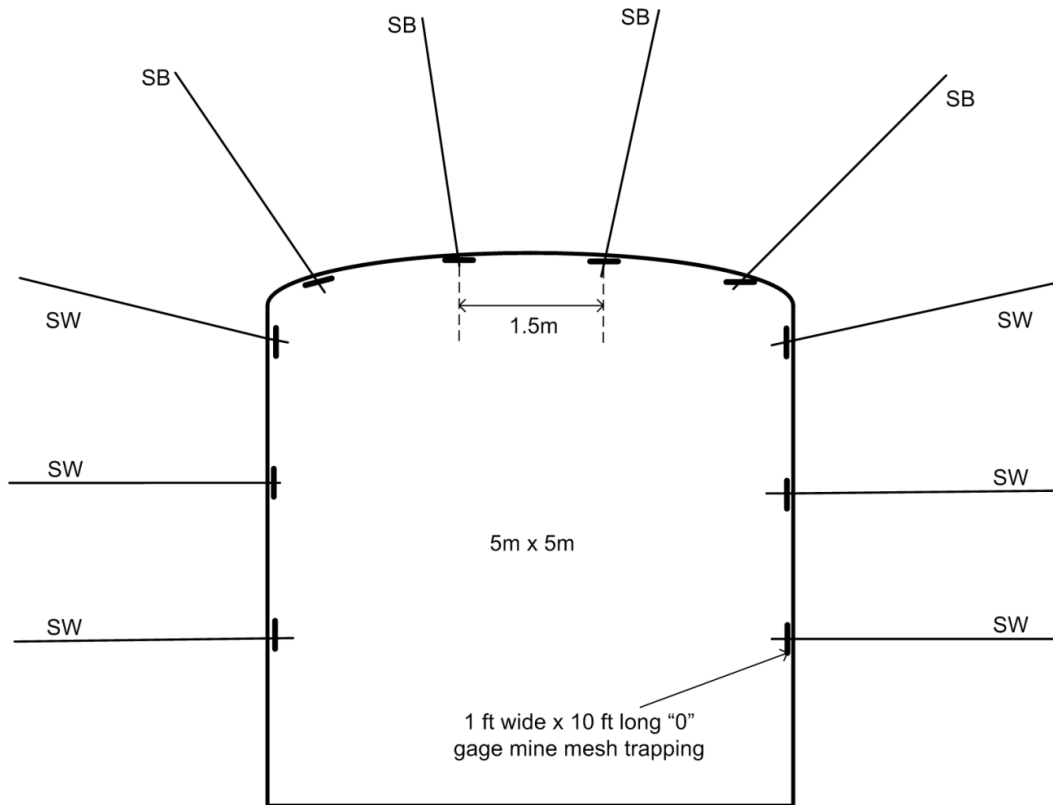


Figure 2-10 Secondary support system during in ore and rock developments

Table 2-8 Secondary rock support specifications in mine developments (refer to Figure 2-10)

Secondary support	Type of secondary support	
	SB	8 ft long Modified Cone Bolts ( MCB) Or MN12 Swellex bolts
SW		

## **2.5 Characteristics of drift support system**

Most of the underground openings particularly the deep ones require ground support to improve the stability of the openings and there by ensure a safe working conditions for the personnel and operating machinery. The adequate and appropriate ground support design matches the characteristics of support elements such as steel tendon, screen, straps, plates, shotcrete. etc ( CANMET, 2008). One has to consider both static (supporting the weight of the surrounding rock with rigid ground support elements) and dynamic conditions (surviving additional forces, energy absorption), which may be imposed suddenly and without warning through using yielding ground support systems. Wagner (1984), Hedley (1992), Ortlepp (1992), Kaiser (1993), Daehnke et al. (2001), Hoek (2007a) mentioned that, dynamic conditions are very difficult to predict and design for in practice.

The static behavior of most commonly used support systems has been widely investigated and documented over the years ( Schach et al. (1979), Stillborg (1994), Hoek et al. (1995), Hutchinson and Diedrichs (1995), Hadjigeorgiou and Charette (2001), Stille (2001), Windsor (2001), Beauchamp (2006)).

Mining depths are increasing and the mine openings are being made under the highly stressed rock conditions, which are prone to rock bursts. Due to this fact the dynamic characteristics of the ground support are becoming important parameters for the selection of the same and the design of support systems in over stressed rock and highly dynamic environment.

The importance of the design of supports for burst prone ground conditions is highly evident, that the MSHA Ground Control committee has made tendon support design under such conditions a key research priority

and a research project was launched in February 2007 to investigate the subject (CANMET 2008).

The effect of dynamic support, when properly designed is evident from Figure 2-11. It shows the two adjacent openings in a same mine, the photo on the left shows the standard ground support, while the photo on the right side shows with the yielding support.

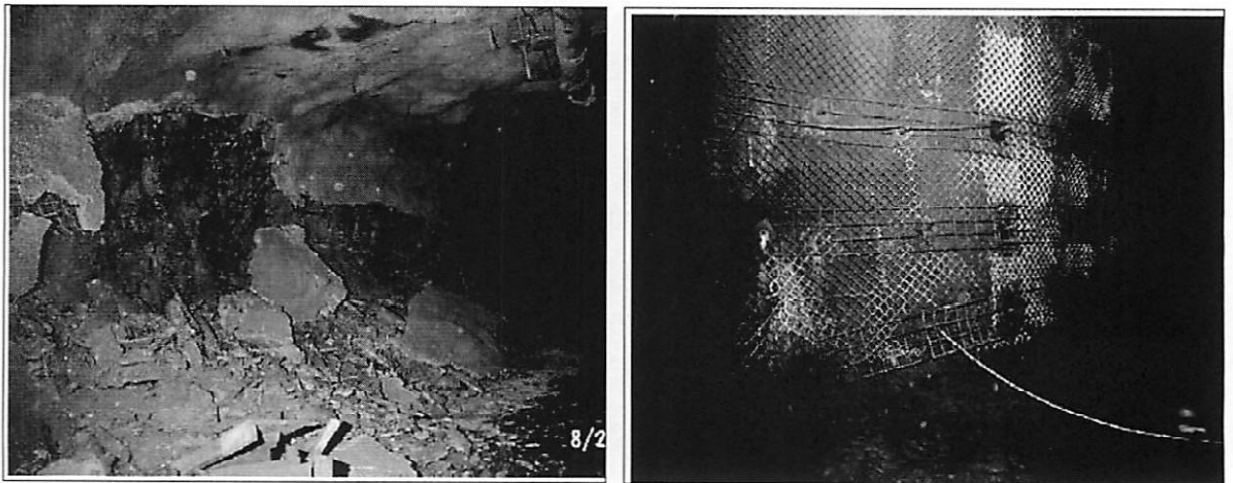


Figure 2-11 Effect of yielding support in a dynamic environment (CANMET, 2008)

### 2.5.1 Support functions

McCreath and Kaiser (1992) explained the function of each element in a support system and noted that it is complex and depends on its interaction with the ground. The functions of the support elements as given by them are shown in Figure 2-12. As can be seen from the Figure, there are three primary support functions, i.e to reinforce the rock mass, to retain broken rock, and to securely hold loose rock or tie back the retaining elements.

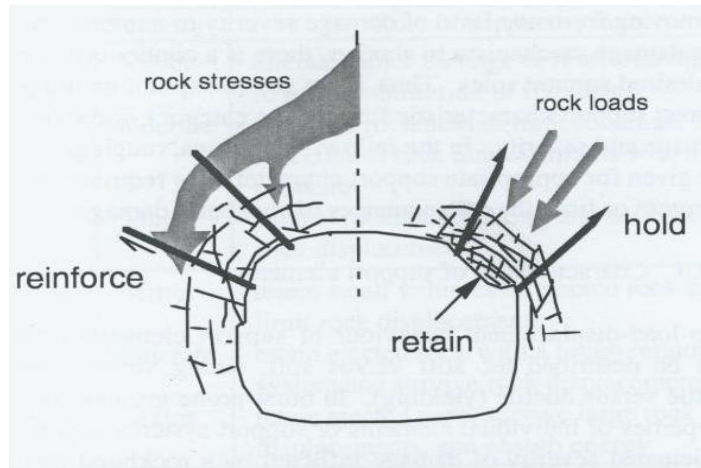


Figure 2-12 Primary support functions (McCreath and Kaiser, 1992)

The goal of reinforcing the rock mass is to strengthen it, thus enabling the rock mass to support itself (Hoek & Brown 1980). The Canadian rockburst research program (1990-95) explains the above three primary functions of the support elements. Reinforcing mechanisms generally restrict and control the bulking of the rock mass. Typically, reinforcing elements such as grouted rebars or dowels behave as stiff support elements, where as split set bolts, yielding swellex or Cone bolts, may behave as ductile or yielding elements under high stress or deformation conditions. The holding function is generally aimed to tie the retaining elements of the support system and loose rock back to stable ground. A mechanical rockbolt performs the holding function. While retaining broken rock at the excavation surface may be required for safety reasons. McCreath and Kaiser (1992) observe that full areal coverage by retaining elements becomes increasingly important as the level of rockburst severity increases. Retaining elements may be either stiff and strong, such as a cast concrete liner or a closed-ring shotcrete membrane, or they may be ductile and able to yield, such as chain-link or welded-wire mesh (CRRP, 1990-95).

## 2.5.2 Strength of drift support elements

The load deformation characteristics of typical support elements are shown in Figure 2-13 and Figure 2-14.

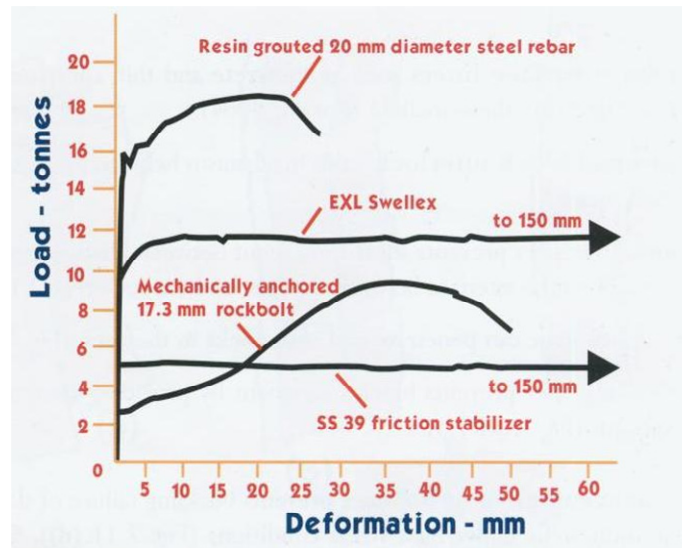


Figure 2-13 Load deformation curves for typical drift supports( Hoek, 1995)

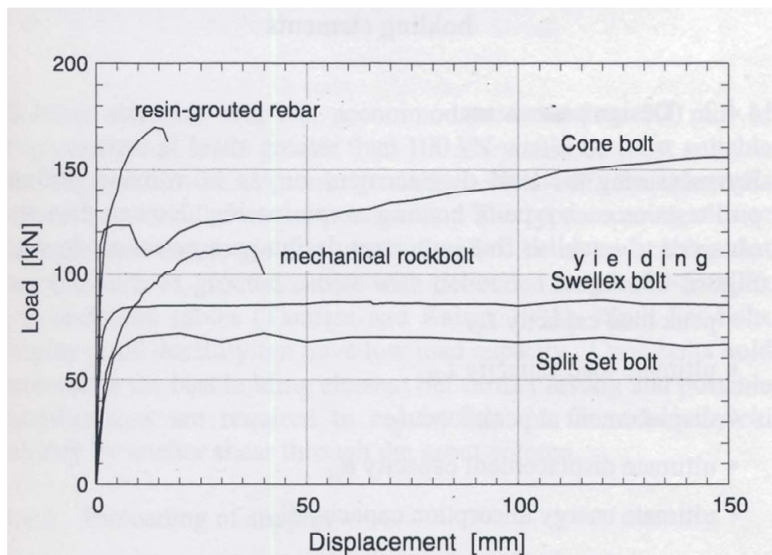


Figure 2-14 Load deformation curves for typical drift supports including Cone bolt ( CRRP:1990-95)

It can be observed from Figure 2-13 that the support elements, such as grouted rebars, absorb little energy. However, grouted rebars resist bulking and hold fractured rock together which can be of great help to the nearby yielding bolts such as cone bolts when installed as part of the support system to dissipate energy, even if the rebars fail locally. The general load displacement curve including Cone bolt is shown in Figure 2-14. As can be seen from the Figure the ductility of the Cone bolt is very high than the regular grouted rebar and mechanical rockbolt. Also, yielding Swellex has considerable displacement capacity with fewer loads compared to Cone bolt. These bolts will have good energy absorption capacity with load capacity of 90-140kN in case of Cone bolt.

The strength parameters of popular drift support elements are presented in Table 2-9. It can be noted from the table that both mechanically anchored and grouted (cement and resin) rockbolt strengths are presented. According to Stillborg(1994), the resin bond is stiffer compared to cement bond as the local fracture as well as bond failure found in and near the joint is limited, which resulted in comparatively smaller total rockbolt deformation. Also on the Shear component he notes that if a rockbolt is subjected to some shear component, the load bearing capacity is reduced compared to a bolt which is loaded in pure tension. The reduction in strength depends up on the bolt type and the angle between the bolt and the joint surface.

Table 2-9 Strength properties of popular drift supports( Stillborg, 1994 & Mansour mining inc, 2012)

Rockbolt type	Diameter, mm	Tensile strength, kN	Function
Rebar ( resin and cement grouted)	16	79	Primary
	20	120	Primary
	22	161	Primary
Mechanical rockbolt	16	100.5	Primary
	19	148.6	Primary
Swellex	26	100	Primary/Secondary
	36	205	
Split set	39	90	Primary/secondary
	46	135	
Cablebolt	15.2	250	Secondary

Potvin et al. (2004) in a book on Surface support in Mining reported the results of research by Stacy and Ortlepp for more than five years on the dynamic behavior of various surface supports. Various types of wire mesh and shotcrete, which have been used for rock support for many years, as well as other containment support system, were tested during their program. The containment support systems tested include

- Welded wire mesh,
- Chain link wire mesh
- Various types of special wire mesh
- Some of the above with wire rope lacing
- Special wire mesh with yielding wire rope lacing
- Shotcrete
- Shotcrete reinforced with welded wire mesh
- Dramix and monofilament polypropylene fiber reinforced shotcrete with wire rope lacing

The standard materials used in the mine support systems were also used in the dynamic test programs. Three categories of support liners are:

Category I: Wire mesh support components on their own

Category II: Wire mesh and wire rope lacing support systems

Category III: Shotcrete based support components and systems

Based on the summarized results of the dynamic testing, after interpretation of those results, they made following conclusions.

- Some wire mesh support systems are capable of absorbing large amounts of energy whilst providing support and containing failed rock

- The energy absorbing capacity of wire mesh and fiber reinforced shotcrete surface support is increased by a factor of between two and seven with the addition of wire rope lacing.
- The use of yielding rock bolts can be expected to add significantly to the energy absorption capacity of the surface support, and
- Failure of one component of the surface support system generally leads to failure of the overall system. It is most important, therefore, that all of the components making up the support system are matched in terms of their capacities.

## **3 Dynamic Supports for Burst Prone Ground**

### **3.1 General**

As the mining depth increases, mine openings at great depths will often become unstable due to the fact that the rock mass is subjected to high stresses. Such instabilities must be controlled by adopting appropriate support measures to control the falling rock mass to maintain safe workings. Managing the damage due to mining induced seismicity, in such conditions by appropriate energy absorbing support systems is a key factor. Design of such support system requires consideration of the nature of seismic hazard, the additional demand placed on the support by dynamic forces, and the capacity of the support system to meet that demand (Kaiser et al, 1997).

The effectiveness of the support system for the particular condition is the deciding factor in achieving the safe mining conditions. Conventional support design methodologies utilize empirical rock mass classification systems to design the supports, mostly for a static condition. However, in burst prone environment, conventional support design methods are not suitable as dynamic conditions or pseudo dynamic conditions (large deformations) prevail. The supports for these conditions require yielding /energy absorption capabilities to have stable and safe working conditions. A design methodology involving a rational approach will be able to serve this purpose. Also it is appropriate to look into the characteristics of the support system, both static and dynamic and match with the all support elements in a support system.

As part of research on Canadian rock burst research program (1990-1995), McCreath & Kaiser(1992) conducted a study to evaluate current support practices in burst prone ground worldwide and found that based on South African experience, mine openings can be designed to

survive fairly large rockburst events, when using cable lacing support systems (McCreath & Kaiser 1992). The support system firstly should reinforce the rock mass in order to control the failure of the rock. When this is not successful, it then has to hold the failed rock and control the amount of the displacement that occurs. Finally, it has to retain the failed rock and absorb the energy with which this material is being forcibly driven. The first two functions, reinforcing and holding, are accomplished within the volume of the rock mass, usually by bolts or rebars or cables, while the third function is accomplished only on the surface of the rock mass, usually by mesh or increasingly by shotcrete (McCreath & Kaiser. 1992) as shown in Figure 3-1.

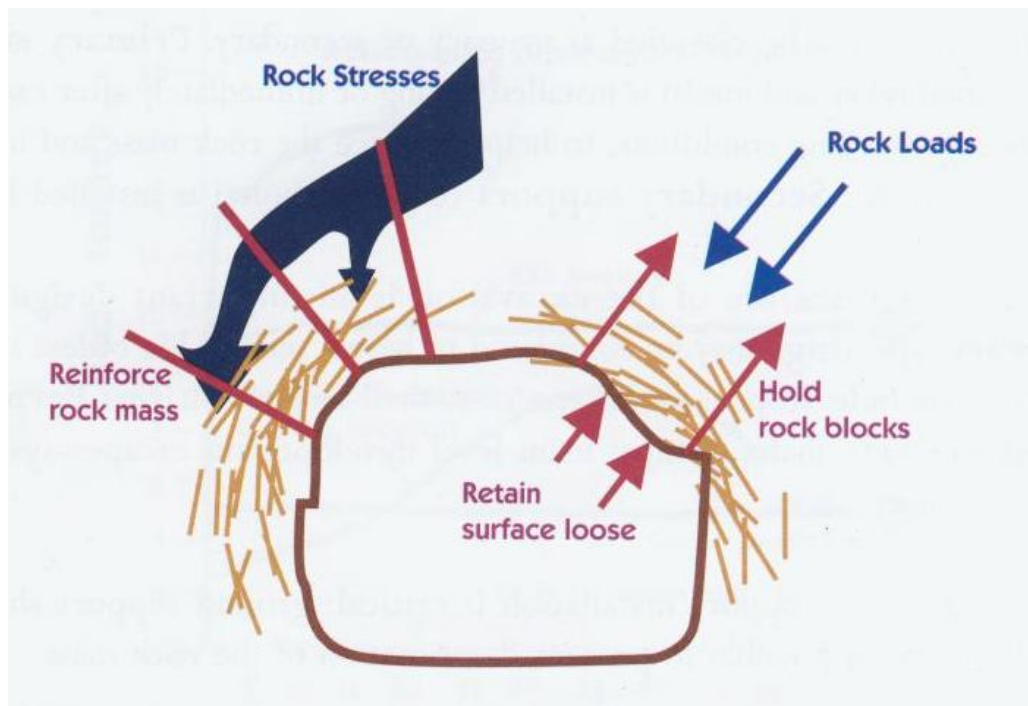


Figure 3-1 Main functions of supports (CAMIRO Mining Division, 1990-1995)

The extensive studies as part of the Canadian rockburst research published by the CAMIRO Mining division (1990-1995), provides the specific damage mechanism involved, and the severity of the damage caused due to dynamic event and vary depending upon a number of

parameters such as the pre existing stress levels in the rock, the quality of the rock mass around the excavation, the excavation shape, and the seismic source characteristics. Also it is obvious that, nature of the damage mechanism and the severity of the resulting damage, when taken together define the demand that will be placed upon any installed support system. Once the nature of this demand is understood, then it becomes possible to select a support system in a rational manner, one that has the capacity to respond effectively to the demands imposed by the above damages. Three distinct mechanisms that are involved in most of the damage caused by rockbursts have also been explained by the above study. In order of priority or frequency of occurrence, these mechanisms are

- Sudden volume expansion or bulking of the rock due to fracturing of the rock mass around an excavation. **It also expresses that Rock mass bulking is a major cause of damage to support in burst-prone ground and its significance of assessing the amount of bulking and controlling the bulking process has not been recognized previously. It is now evident that it accounts for a substantial amount of the damage that is observed in Canadian mines.**
- Rock falls ( or fall of ground), which have been induced by seismic shaking, are the second most common cause of damage in Canadian burst-prone ground
- Ejection of rock due to energy transfer from a remote seismic source may be a major cause of damage in the deep South African mines, but is far less common in rockburst prone Canadian mines.

The above study by CAMIRO(1990-1995) suggest that in dealing with support selection for burst prone conditions, the fore most step is to

estimate the type of damage mechanism involved and the likely severity of the resulting damage. Also it is useful to understand the conditions that lead to or trigger a rockburst. It is worth noting here that for the purpose of support selection, a primary goal is to assess the anticipated thickness of the rock that could be involved in the damage process. Each of the rockburst damage mechanisms may result in different levels of damage to an excavation and its support system. On the basis of field studies of rock damage and support damage levels, Kaiser (1993) defined various damage levels that were observed to occur in association with rockburst phenomena. The damage severity depended on many factors including;

- Failure potential near the opening
- Support effectiveness
- Local mine stiffness
- Magnitude of seismically induced stresses, rock accelerations or velocities
- Opening geometry, size and orientation
- Geological structure

And the damage severity can be estimated by previous rockburst observations, stress –to-strength ratio of the rock mass and peak particle velocity.

### **3.2 Current technologies**

In this section, the current support technologies available for burst prone ground that have energy absorption/yielding capacity are reviewed. Load displacement characteristics of these support systems in comparison with the rigid supports also presented.

As already mentioned, in regard to rock support, a conventional support device performs one or more of the three functions: (1) reinforcement of the rock mass, (2) retaining of broken rock and (3)

holding of the retaining devices (McCreath and Kaiser, 1992). In the case of a rock bolt, its functions involve reinforcement of the rock and holding the retaining. Li and Doucet (2012) explain the instabilities caused in static and dynamic situations. Instabilities are mainly caused by gravitational rock falls in static and low-stress rock conditions, and the theory of rock bolting in this case is that rock bolts must be strong enough to compensate the dead weight of the potentially falling block. Thus, under static condition the strength of the bolt is crucial for static rock support design. However in dynamic loading conditions like rockburst, it is the energy released from the rock rather than simply load or displacement that has to be dealt with. Either strain or fault-slip rockbursts will release a good amount of energy. The released energy of an ejected rock block is expressed as  $1/2 mv^2$ ; where,  $m$  is the mass of the ejected block and  $v$  the ejection velocity. This amount of energy must be absorbed by the support devices in a support system in order to avoid rock ejection. The energy absorption of a support device is expressed as its average load multiplied by the displacement (Li and Doucet, 2012). In addition to the transfer of energy, the interaction between the ejected rock and the support devices also involves a transfer of momentum. The momentum of the ejected rock is expressed as  $mv$ . This amount of momentum must be fully transferred to the support devices involved if the ejection is to be avoided. A yield support system is composed of yield support devices. Yield support devices are needed in burst-prone rock conditions in order to avoid rock ejections. Support devices for dynamic rock support must be not only deformable but also strong, that is, they must have a satisfactory energy-absorbing capacity. Rock bolt is an important type of support device in a support system. Conventional rock bolts such as encapsulated rebar and Split Set absorb little energy because of their small deformation capacity (rebar) or their small load bearing capacity (Split Set) displacement (Li and Doucet, 2012). Recognising this fact the cone bolt was invented in South Africa as early as in the 1990s (Ortlepp 1992, 1994)

probably the first type of energy-absorbing rock bolt used by the mining industry (Jager 1992; Ortlepp and Stacey 1995).

### 3.2.1 Cone bolt

As mentioned in the previous section the cone bolt is first invented in South Africa and it consists of a smooth steel bar with a flattened conical flare forged onto one end. The smooth bar is coated with a thin layer of wax, so that it will be easily de-bonded from the grout under pull loading. The cone bolt was originally designed for use with cement grout, but was later modified for resin grout (Simser 2001). Later this cone bolt was modified by adding a blade at the end of the bolt to facilitate the resin mixing and this is called Modified Cone Bolt (MCB) shown in Figure 3-2



Figure 3-2 Modified cone bolt (MCB), (Mansur mining.com)

The MCB developed by Noranda, Canada is a smooth bar threaded at its outer end, with a forged cone and mixing blade at the other end. The smooth bar has a plastic sleeve debonding agent to reduce the friction and bonding effect of the resin. Under Dynamic loading conditions, the MCB will yield or plough through the resin, thus absorbing the energy through controlled deformation (Mansour mining Inc). In a static loading condition, the cone functions as a wedge-style mechanical anchor similar to standard mechanical rockbolts. The MCB is tensionable, thus capable

of being installed on a single pass and/or used as either a primary or secondary support. The cone bolt can be installed using conventional equipment such as jacklegs, stopers or mechanized bolters. Tests conducted by CANMET-MMSL (2012) on Modified cone bolts under static and dynamic condition are shown in Figure 3-3 and Figure 3-4 respectively. Cone bolts of different types show the energy capacities of 16 to 30 kJ as per the tests conducted at CANMET.

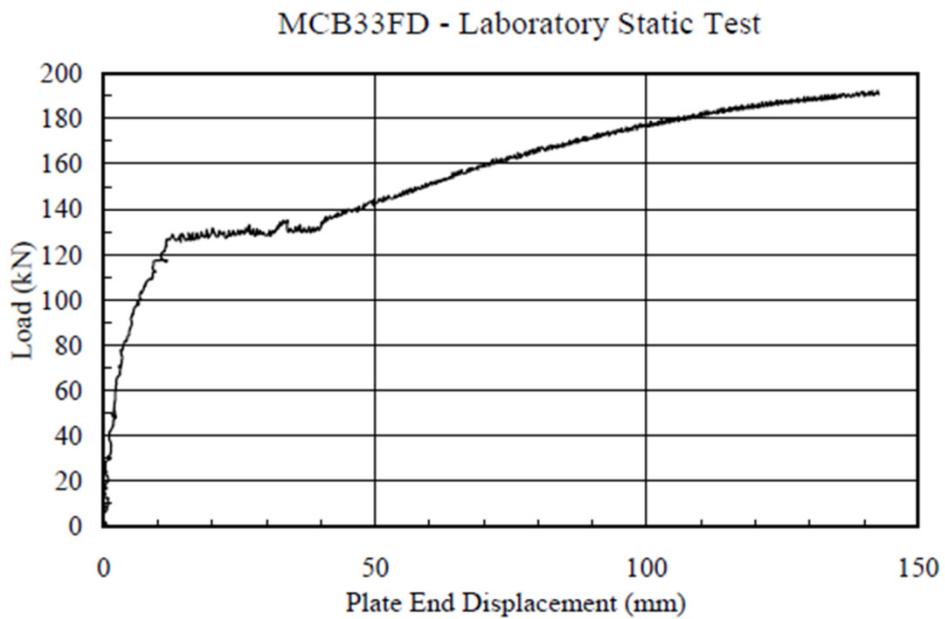
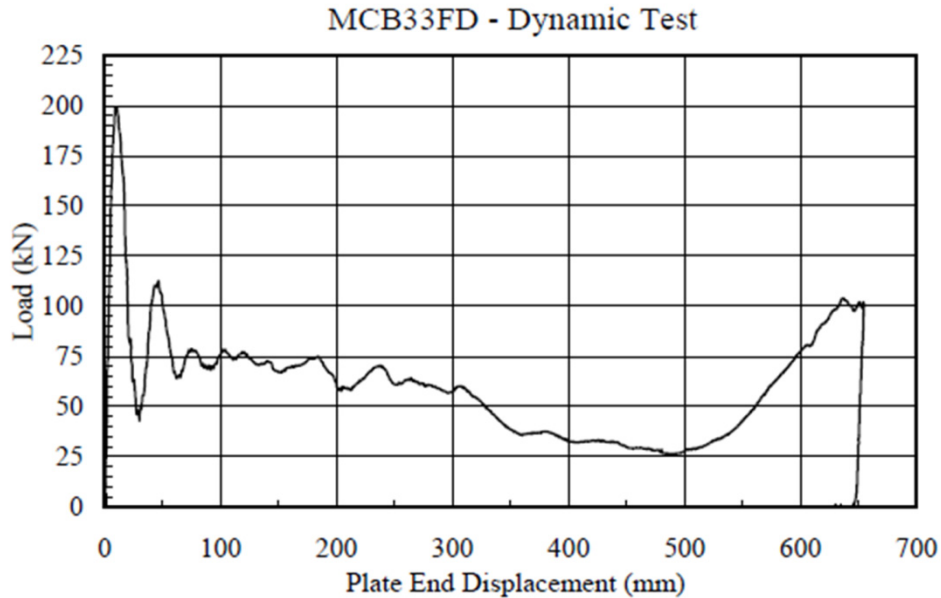


Figure 3-3 Laboratory static test on Fully deboned MCB33( CANMET-MMSL, 2012)



**Figure 3-4** Laboratory dynamic test on fully deboned MCB33 (CANMET-MMSL, 2012)

### 3.2.2 The D-Bolt

The D-bolt is a new type of energy-absorbing rock bolt. It differs from the above-yielding rock bolts in structure. The D-bolt is made of a smooth steel bar with a limited number of anchors spaced along the length of the bar. The sections between anchors are designed to be approximately 1 m long. The bolt is fully encapsulated in a borehole with either cement or resin grout. The anchors are firmly fixed in the grout, while the bar sections have very weak or no bonding to the grout because of the smooth surface. The bar sections elongate plastically to absorb energies when subjected to dynamic shocks. The bolt has a high energy absorption capacity. For instance, 22-mm bolts can absorb 40 kJ of kinetic energy per metre of bolt shank. Because of the layout of the multi-anchors, the bolt has a reliable anchoring mechanism (Li and Doucet, 2012).

A D-Bolt reinforces the rock by constraining rock dilation between anchors. The anchors are loaded when the rock dilates and then the smooth sections between the anchors become stretched. The load in the smooth sections increases quickly with a small increase in the rock dilation until the yield load is reached. After that, the sections elongate plastically until failure. The D-Bolt absorbs the rock dilation energy through fully mobilizing the strength and deformation capacities of the bolt material. The smooth sections of a D-Bolt independently provide reinforcement functions to the rock. Failure of one section would not affect the reinforcement function of other sections of the bolt. Li (2010, 2011b) presents more details of the layout and principle of the D-bolt. An extensive dynamic testing program was undertaken to examine the dynamic performance of the bolt. Li and Doucet (2012) present the major findings of the tests as well as relevant analyses. A D-bolt with different types of anchors is shown in Figure 3-5. Results of laboratory tests conducted on O-anchor D-bolt under static and dynamic conditions are shown in Figure 3-6 and Figure 3-7 respectively.

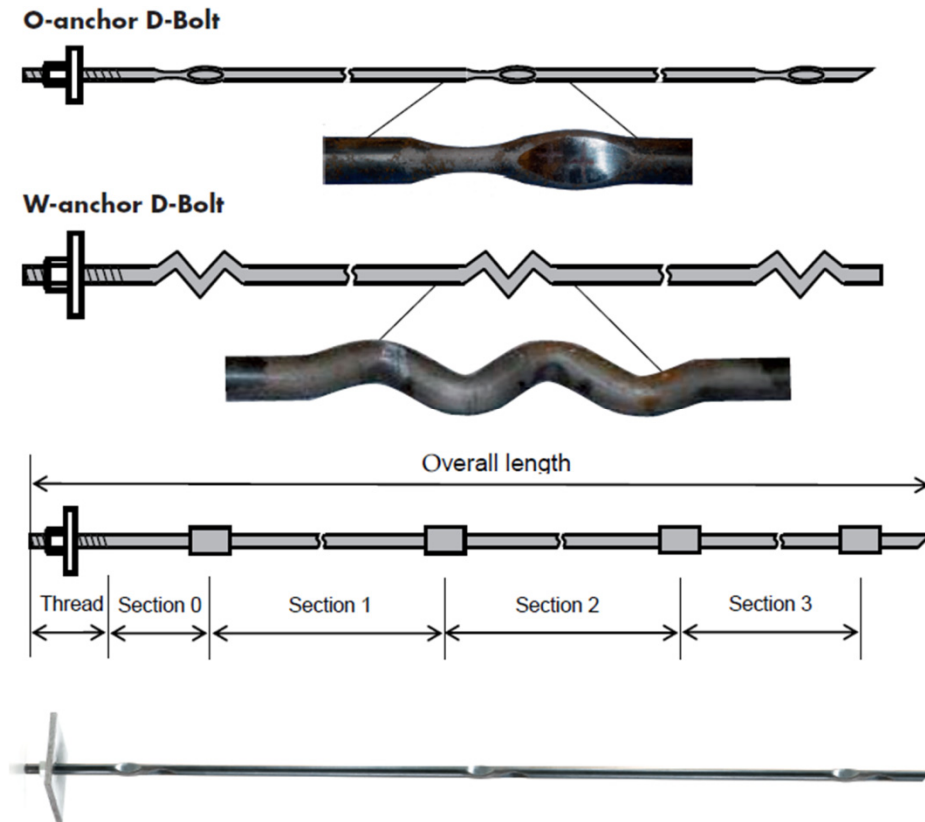


Figure 3-5 The D-Bolt with different types of anchors  
[www.dynamicrocksupport.com](http://www.dynamicrocksupport.com)

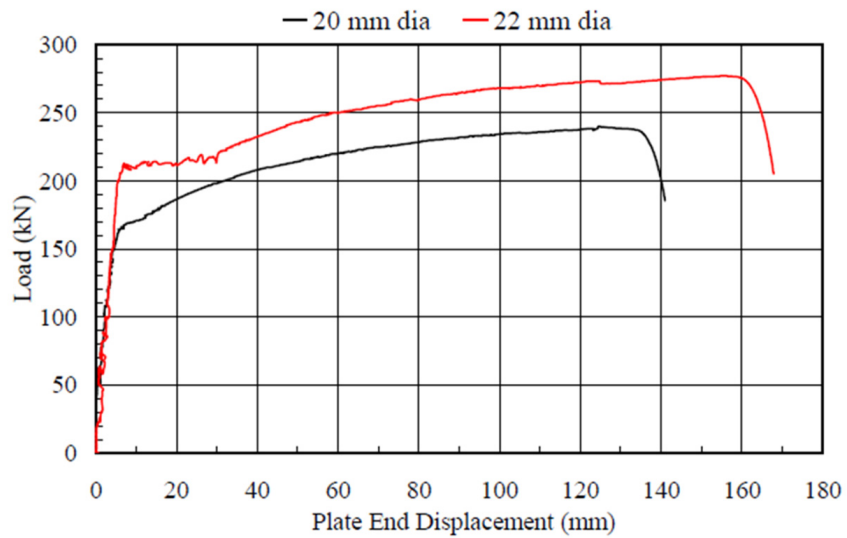
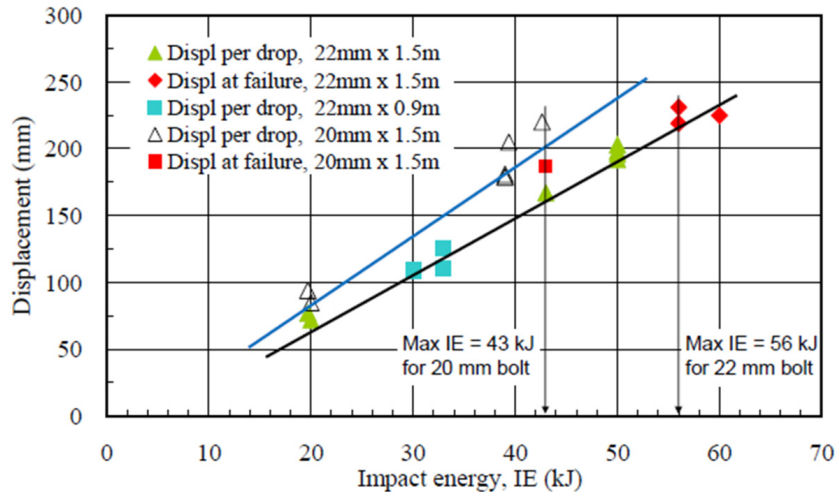


Figure 3-6 D-Bolt (O-anchor) laboratory static test results (CANMET-MMSL, 2012)

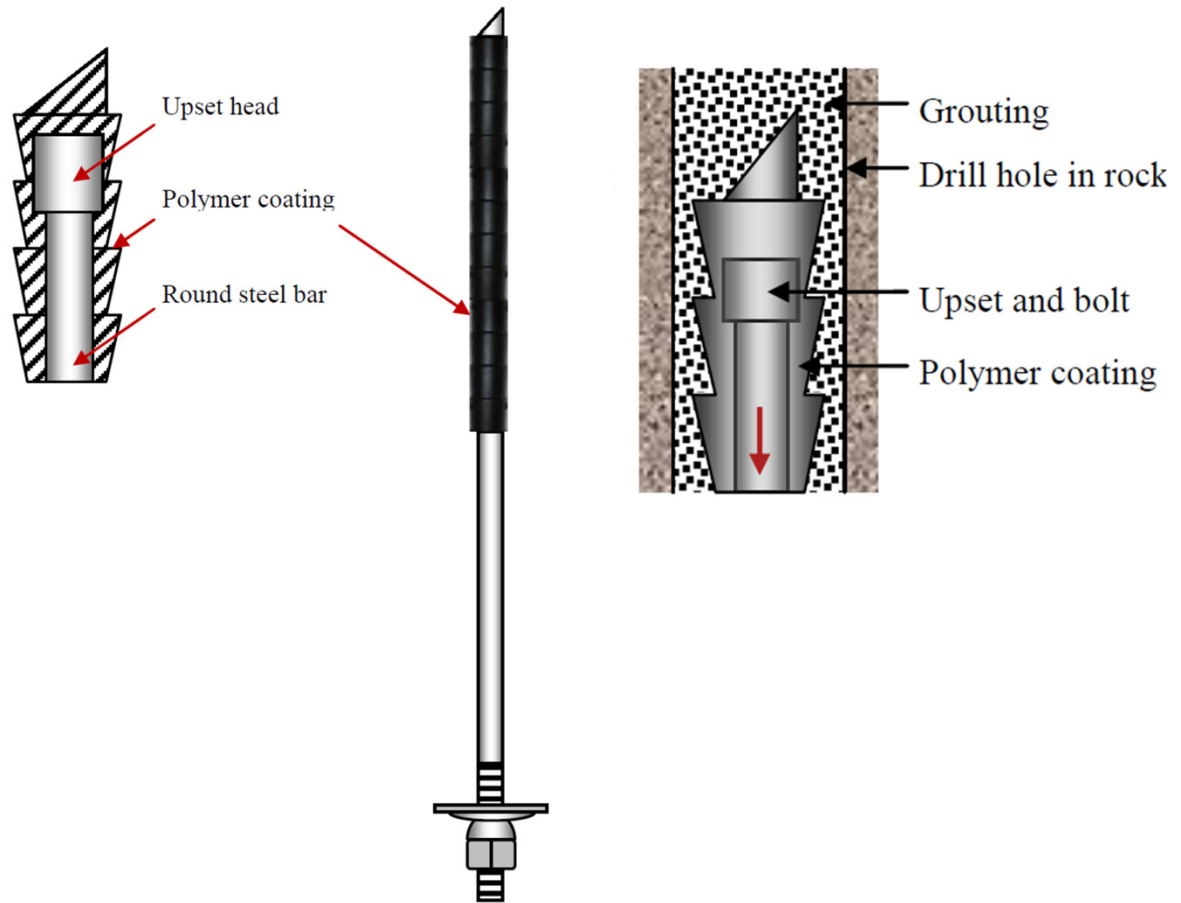


3-7 D- Bolt Laboratory dynamic testing results (CANMET-MMSL, 2012)

### 3.2.3 The Yield-Lok

Yield-Lok (Wu and Oldsen 2010) was recently introduced on the market. The anchor of the bolt is pre encapsulated in engineered polymer to build its yielding device. The Yield-Lok bolt is fully or partially grouted with resin or cement mortar. The principle of yielding performance is based on the interactions between the upset, the polymer coating and the grouting media. The function of each element is shown Figure 3-8. The angled head of the polymer coating aids to shred resin cartridge packing during insertion of the bolt into resin and enhances anchorage. Resin mixing is facilitated by deformations on polymer coating similar to rebar. As such, the Yield-Lok bolt can be fully inserted without rotation, and then spun afterwards to mix the resin. The bolt is tensioned and provides immediate primary support on installation. In static loading conditions, the Yield-Lok bolt performs completely similar to a rebar bolt, providing stiff reinforcement and containment of rock mass. In dynamic loading conditions, the upset transfers the impacts on the surrounding polymer coating, resulting in confined compression, thermal softening and flow of the polymer around the upset, creating the plowing effect. The dynamic energy is therefore absorbed by pulling or plowing the upset through the

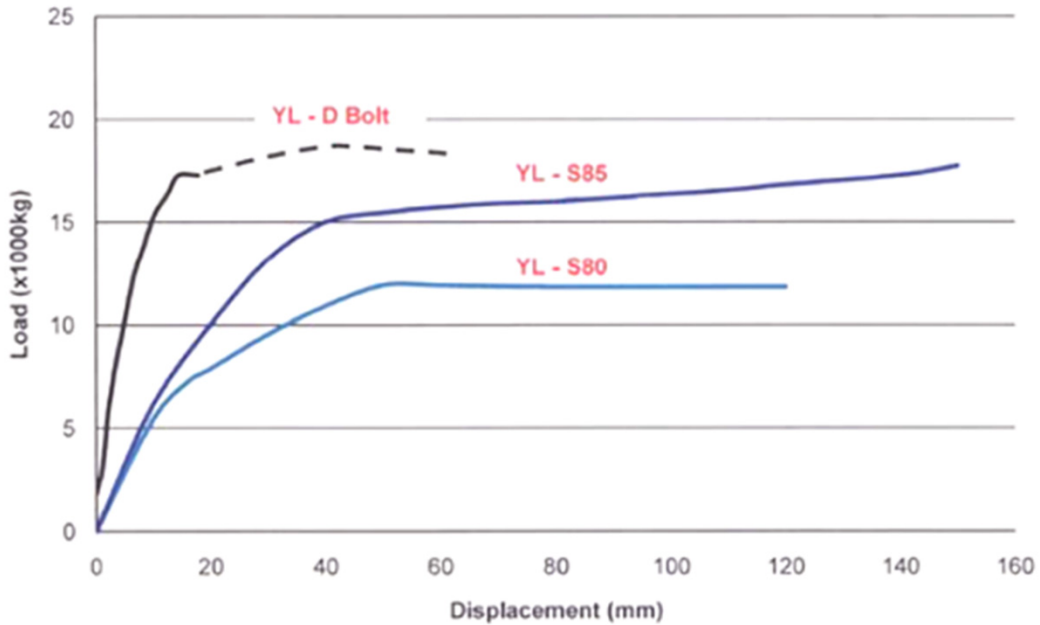
polymer. Part of the dynamic energy is consumed in the friction between the smooth bar and the Polymer coating (Wu and Oldsen 2010).



### 3-8 Yield-Lok Bolt and the function of polymer coating and upset head

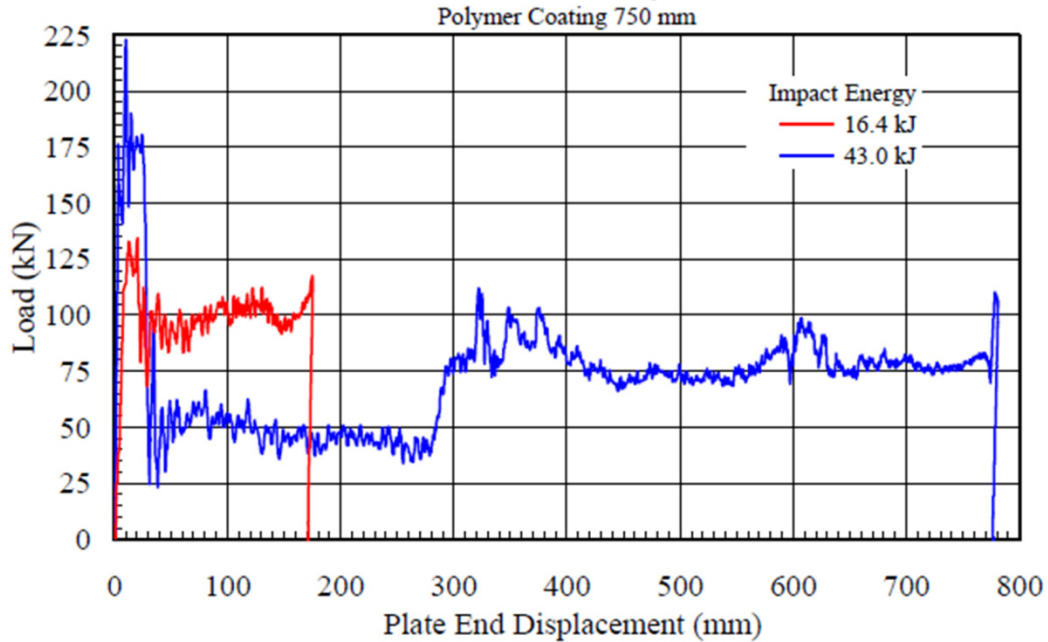
According to Wu and Oldsen (2010), the yielding elements (upset and the polymer coating) are controlled in engineering design and manufacturing, the quality can be well controlled, which can ensure the steady performance of the Yield-Lok bolt throughout the full length of polymer encapsulation. Also the function of grouting media in Yield-Lok bolt is to provide confinement of the polymer, instead of working as a yielding element as in the case of cone bolts. It means that if the bolt is fully grouted and solidly confined, the performance of Yield-Lok bolt is independent of the type of grouting agent, the mixing status and drill hole

diameter. Since the displacement mechanism is contained within the polymer, debonding agents such as grease are not required to achieve the specified plow effect and consistent performance (Wu and Oldsen, 2010). Results of laboratory dynamic tests conducted on Yield-Lok bolt under static and dynamic conditions is shown in Figure 3-9 and Figure 3-10 respectively.



© Jenmar of Canada, 2011. YL-D: Yield-Lok dynamic: YL-S: Yield-Lok static

Figure 3-9 Static test results of Yield-Lok Dynamic and static bolts  
(CANMET- MMSL, 2012)



3-10 Dynamic test results of Yield-Lok dynamic bolt( CANMET-MMSL, 2012)

### 3.2.4 Durabar

Durabar<sup>R</sup> also from South Africa is another type of yielding rock bolt. As shown in Figure 3-11, the rod is bent to form a wave and act as a ductile anchor. The collar end is terminated with either an eye to facilitate cable lacing or with a threaded section for nut and washer. The bar is coated with wax on its entire length except at the collar end to enhance debonding. The hole is injected with cement grout ([www.avengman.com](http://www.avengman.com)).

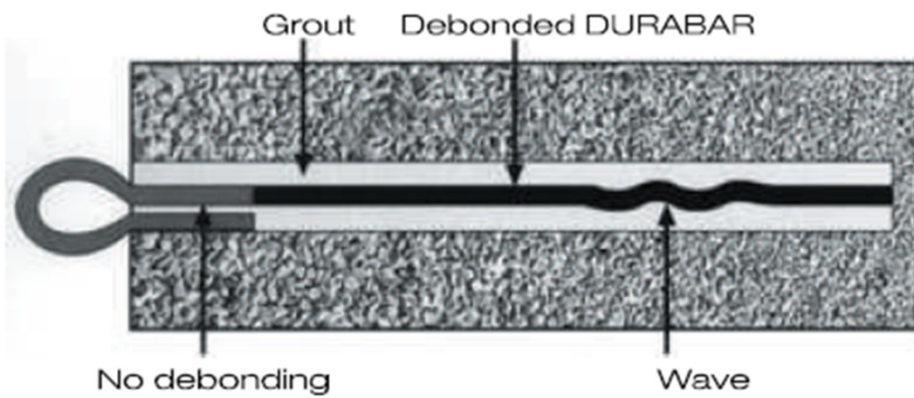
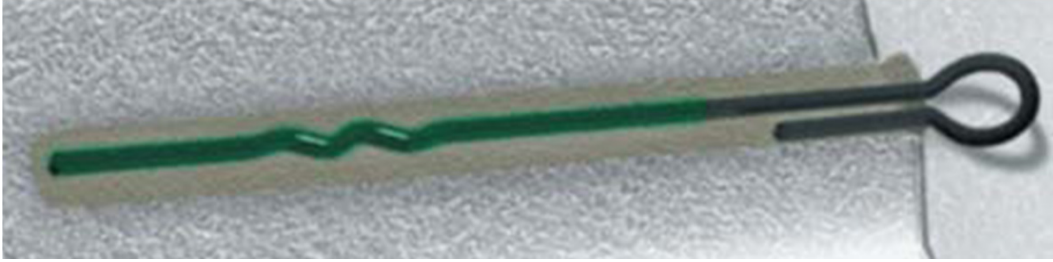


Figure 3-11 The Durabar Yielding bolt (Duraset, [www.avengman.com](http://www.avengman.com))

The anchor of Durabar is a crinkled section of the smooth bar. When the face plate is loaded, the anchor slips along the crinkled profile in the cement grout at a certain pull load (Li and Doucet, 2012). The results of laboratory static and dynamic tests are shown in Figure 3-12 and Figure 3-13.

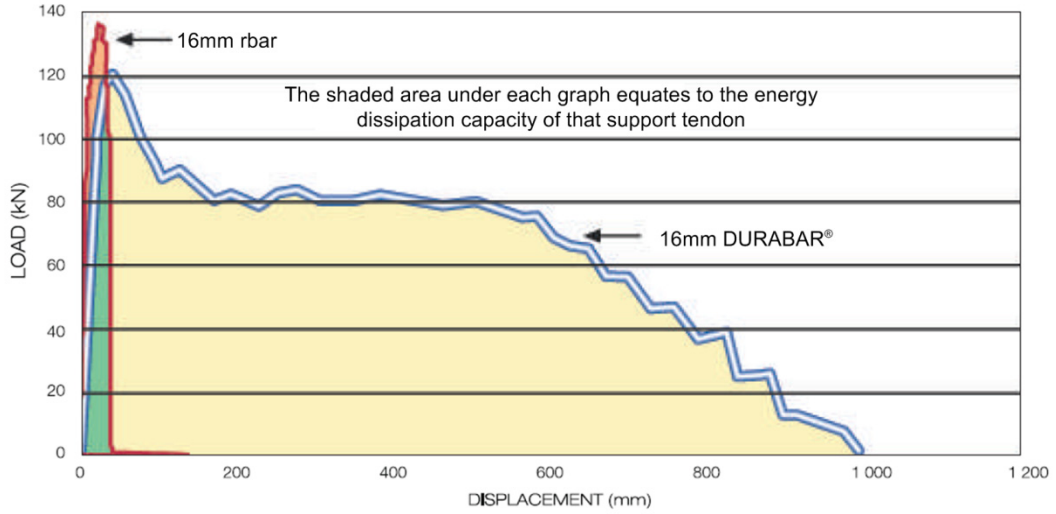


Figure 3-12 Static test results of DURABAR and regular rebar(CANMET-MMSL, 2012)

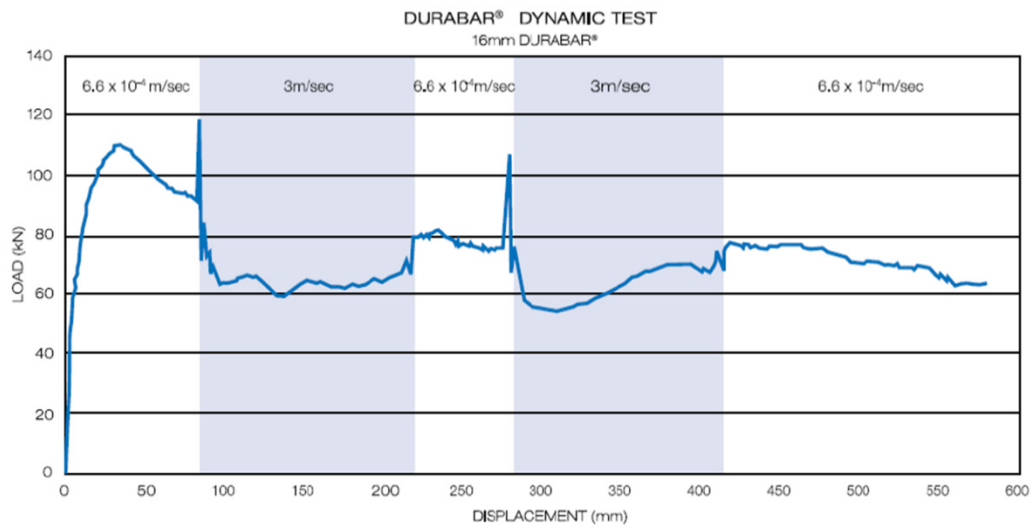


Figure 3-13 Dynamic test results of DURABAR yieldable bolt(CANMET-MMSL, 2012)

### 3.2.5 Garford dynamic bolt

The Garford dynamic bolt is invented in Australia and consists of a solid steel bar, an anchor and a coarse-threaded steel sleeve at the end. This bolt is characterized by its engineered anchor which allows the bolt to stretch by a large amount when the rock dilates (Li and Doucet, 2012). Figure 3-14 shows the Garford dynamic bolt. Varden et al(2008) presented some tests and selection of the garford dynamic bolt for use under dynamic conditions and explains that the bolt consists of a 20 mm mild steel solid bar with resin mixing device of 350 mm long, 43 mm diameter coarse threaded steel sleeve crimped on to the end of the bolt. The dynamic section is a patented sliding anchor mechanism that is pressed on to the bolt below the mixing device. The remainder of the bolt is covered in a polyethylene sleeve to provide a debonding action, which debonds the bolt behind the dynamic section. Under a dynamic condition the bolt is forced through the constriction and elongates. (Varden et al, 2008)

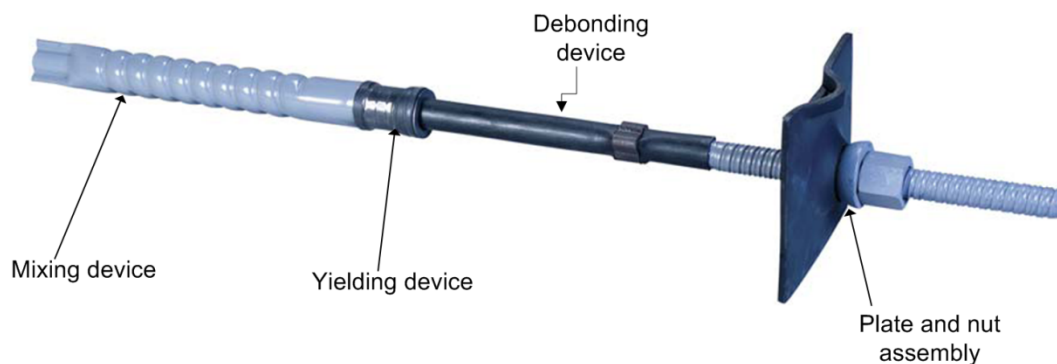
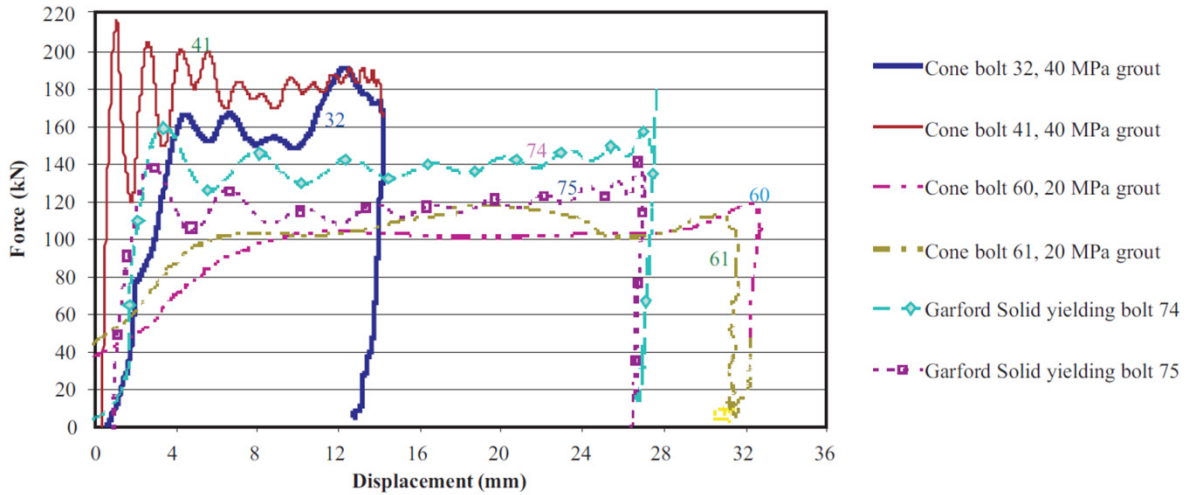
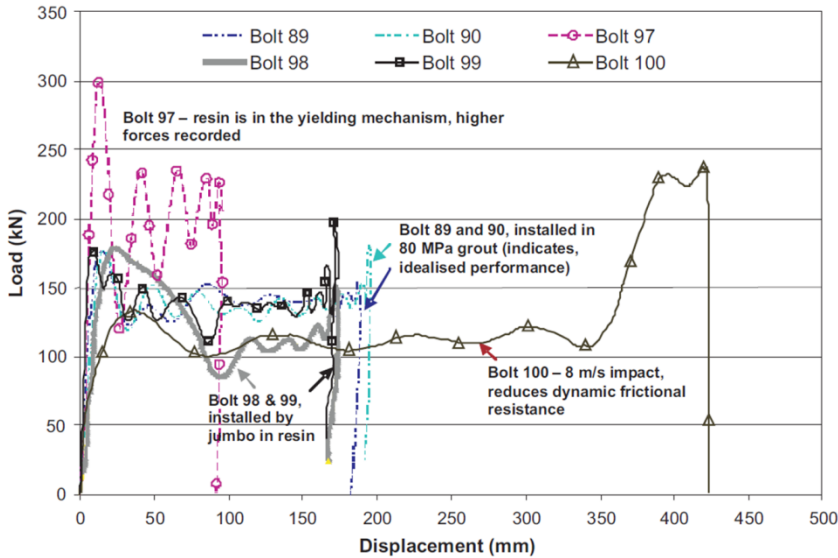


Figure 3-14 The Garford dynamic bolt

The performance of the garford dynamic bolt in a simulated borehole by Varden et al. (2008) is presented in Figure 3-15. It can be noticed that the results are compared with that of cone bolt. Figure 3-18(a) shows the results of version 1 and Figure 3-15(b) shows the results of version 2, where the bolt is modified to achieve more displacement.



a) dynamic force displacement curves, Version 1



b) dynamic force displacement curves- Garford dynamic bolt. Version 2

3-15 Dynamic test results of Garford dynamic bolt (Varden et al, 2008)

### 3.2.6 DSI dynamic bolt

Dywidag systems international, presents a dynamic rock bolt called dynatork bolt shown in Figure 3-16. According to DSI, dynatork bolt is designed with a spiral mixing blade to ensure ultimate mixing of DSI resin in the borehole. This blade design, according to DSI, has a dual propose: to mix the resin properly and provide anchorage for static ground support. The cone is designed to yield and transfer dynamic loads into the resin in rock burst conditions, absorbing the energy through controlled deformation. The kinetic energy is expected to absorb during the ploughing effect of the cone through the resin. The laboratory performance of the dynatork under static and dynamic conditions is shown in Figure 3-17.

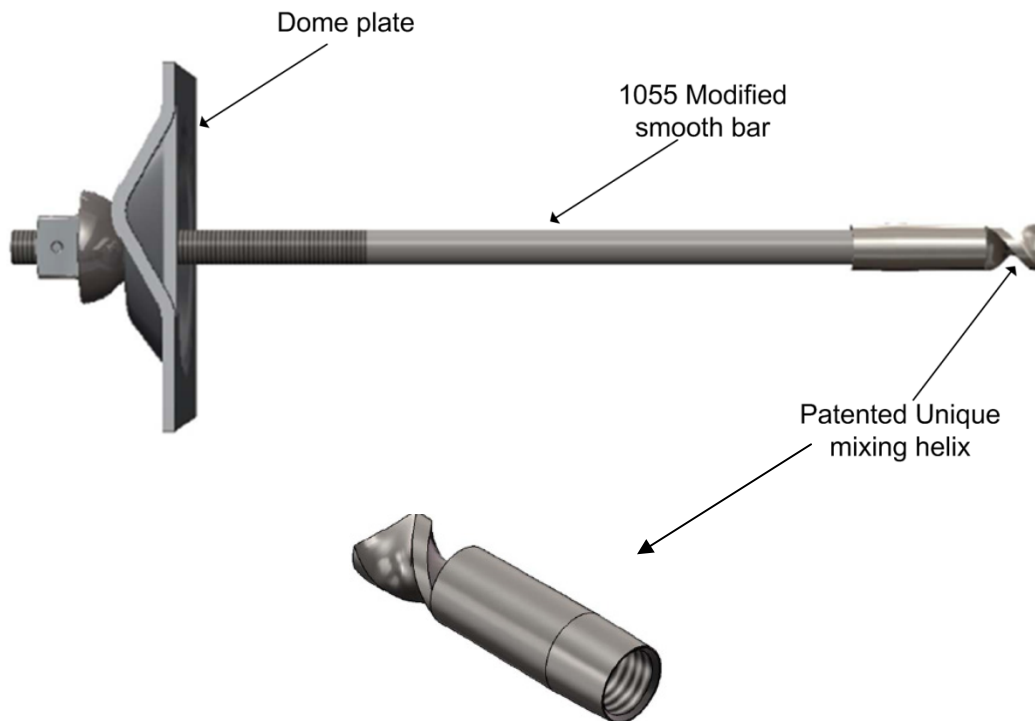
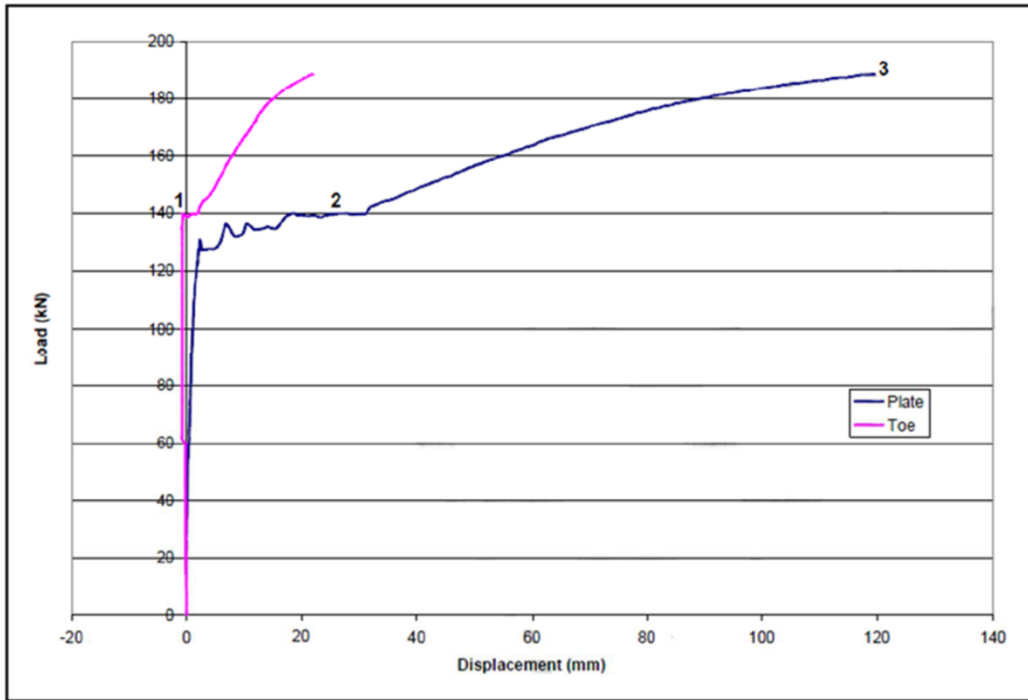
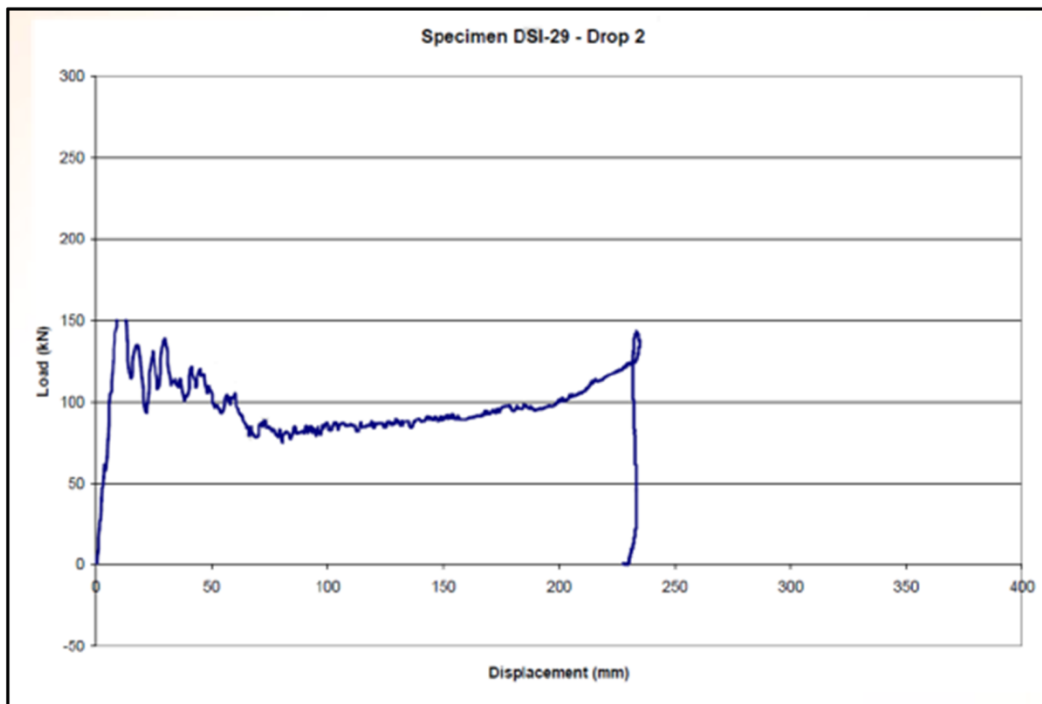


Figure 3-16 DSI dynatork- dynamic bolt (dsiunderground.com)



a) Static results (Holding force of 11tons-17 tons)



b) Dynamic results ( Impact test results at 22.97kJ, drop 2)

Figure 3-17 Static and dynamic laboratory test results of DSI-Dynatork bolt, conducted at CANMET facility (dsiunderground.com)

### 3.2.7 Discussion on current technologies

The performance details of most of the yielding bolts discussed above is given in Li (2011a). According to Li and Doucet (2012), all above mentioned yielding rock bolts accommodate rock dilation and absorb energies via either ploughing of the anchor in the grout (cone bolt and Yield- Lok) or slippage of the bolt shank through the anchor/grout (Garford bolt, and Durabar). A common factor among them is that they are all two-point anchored in boreholes.

Apart from the above mentioned yielding bolts, some Mine specific and unpublished inventions do also exist. Mercier-Langevin (2010) reported a new support element called Hybrid bolt, developed in their LaRonde mine of Agnico-Eagle in Quebec in order to deal with the increasingly difficult ground conditions encountered at depth. This bolt simply consists of a combination of a friction bolt and a rebar. A 1.9m resin grouted rebar is installed inside a 2.0m friction set bolt. The bolt basically acts as a de-bonded rebar, retaining all the best properties of the rebar (high capacity, high resistance to shear) while allowing the bolt to yield (slippage occurs at 12 to 16 tons on average). Stacey *et al.* (1995) reported their test results based on the static tests on the energy absorbing capacity of reinforced shotcrete. The mesh-reinforced shotcrete has sufficient energy-absorbing capacity to contain rockbursts of significant magnitude. CAMIRO (1990-1995) stated from actual observations that both mesh and fibre-reinforced shotcrete can survive ground motions of 1.5-2.0m/sec.

Wojno and Kuijpers (2001), reported a development of yielding cone cable to deal with the excessive shear deformations experienced when mining under extremely high stress conditions. These tendons can yield more than 0.5 m at design forces of 100 kN and 250 kN for cone bolt tendons and 100 kN and 200 kN for cone cable tendons.

Also according to CAMIRO Mining Division (1990-1995), the maximum support limit with the best support systems based on optimal combinations of holding/reinforcing and tough-retaining elements will be limited to energy absorption capacities of roughly 50 KJ/m<sup>2</sup>. In some situations, rockbursts may be so severe that they generate violent ejection of rock despite any reasonable support system (i.e. exceeding 50KJ/m<sup>2</sup>). In these cases the maximum practical support limit is reached and a combination of strategic mine-design measures such as modified distressing must be adopted to alter the conditions leading to rockburst (CAMIRO, 1990-1995). A summary of the current technologies and their application advantages and limitations are given by CANMET-MMSL (2012). It summarizes two major dynamic support mechanisms as ploughing and sliding and support stretching as shown in Figure 3-18.

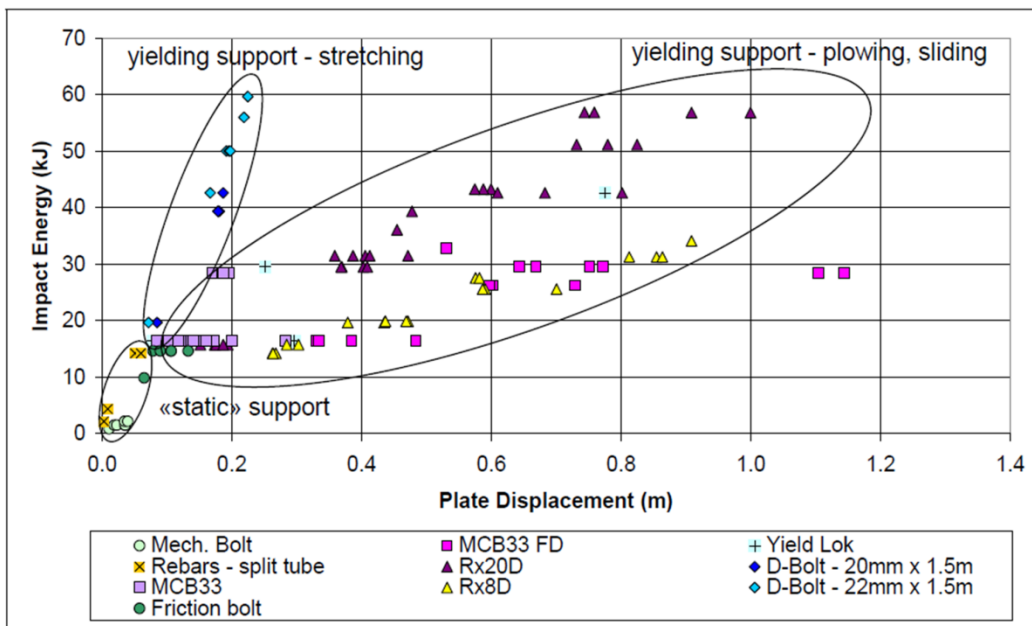


Figure 3-18 Summary of yielding supports tested (CANMET-MMSL, 2012)

As can be seen from the Figure 3-18, except D-bolt all the other yielding support has the ploughing and sliding mechanism, where as the D-Bolt stretches within the anchors during the process of energy

absorption. In Canada, the deep hard rock mines that are burst prone uses cone bolts/ modified cone bolts extensively. Simser et al (2007) gives a field behaviour and failure modes of modified cone bolts at the Craig, LaRonde and Brunswick Mines in Canada and concludes that “the Modified cone bolt has been successfully used in Canada at a number of operations and in a wide range of rock mass conditions”. And also mentions that the seismic energy can be successfully dissipated by using these bolts in combination with strong straps and steel wire mesh. McKenzie (2002), after seeing the performance of the Modified cone bolts, opines that the future of their Big Bell operations mainly dependent on the success of cone bolt installation in both the rehabilitation drives and the new development drives. Yao et al (2009) also reports the successful implementation of modified cone bolts to tackle with the highly stressed burst prone ground in one of their operations in Sudbury. St-Pierre et al. (2009) developed a dynamic model for cone bolt to simulate the sliding action of the cone due to dynamic loads and compared the same with the lab dynamic testing results as shown in Figure 3-19. As can be seen from the Figure, the force elongation curve obtained from experimental tests is in close agreement with the results of the model. The results of displacement and time, Force and time curves also matches with the experimental test results.

It is evident from the above review that, mining industry now has several types of yielding support which utilizes broadly two mechanisms such as ploughing through grout and bolt stretching. They also have considerable displacement capacities. It is also noted that the cone bolt yielding support is being widely used in burst prone ground as a yielding support.

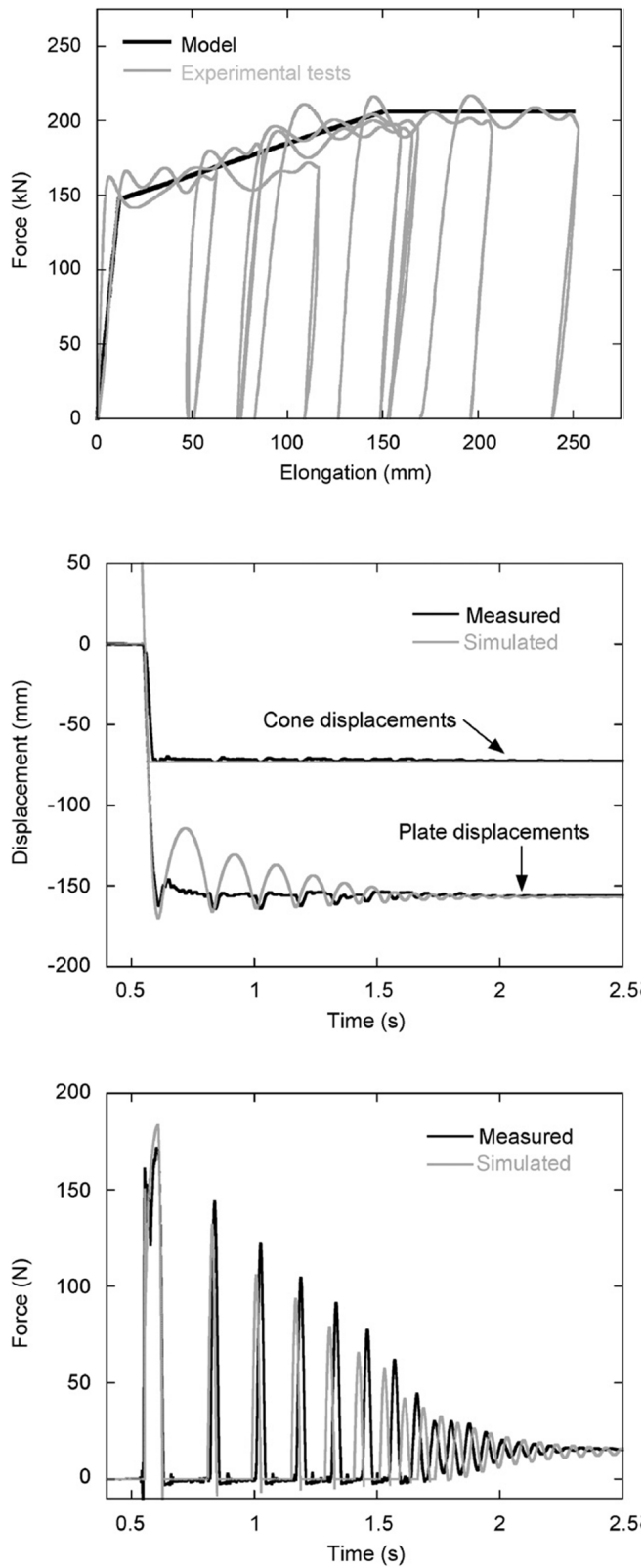


Figure 3-19 Comparison between the measured and simulated responses for cone-bolt under dynamic conditions (St-Pierre et al. 2009)

## **4 Case study**

### **4.1 Introduction**

Haulage drifts in deep hard rock mines are the arteries of the life of the mine. Performance of the drift depends on many factors including the stope sequencing, support system and its distance to the nearby stopes. The actual performance of these support systems influences the stability of the haulage drift. Drift supports are installed in two phases as primary supports and secondary or enhanced supports. Primary supports are installed during the drift development and the secondary or enhanced support systems are installed when the drift openings intersect with other drifts and before nearby mining activity take place, causing multiple openings. Generally the primary supports consist of fully grouted rebars and the secondary or enhanced supports include fully Modified Cone Bolts (MCB), cablebolts and Swellex bolts.

The most influencing factors include the stope sequencing, distance between the haulage drift and the nearby stope, the footwall rock competency and the depth from the surface (Zhang and Mitri, 2006). The orientation of the haulage drift with respect to in situ stress direction also plays an important role in haulage drift stability. Appropriate supports are designed and implemented to have stable drifts in deep underground hard rock mines. Also dynamic or yielding supports are necessary in burst prone areas. The performance of these support systems is most important under various geomining conditions. Typical drift support systems and geomining conditions of case study mine is given in the following section.

## 4.2 Geo mining conditions of Garson Mine

The Garson nickel-copper (Ni-Cu Sulphides) mine is located in Greater Sudbury, Ontario as shown in Figure 4-1. It comprises two ore bodies namely #1 Shear and #4 Shear, that runs 250 feet to the North of #1 Shear. The two ore bodies have a strike length of about 2000 feet, dip about 70 degrees to the south and vary in size and shape. An Olivine Diabase Dyke crosses these two ore bodies near the mid-span on the 5100 level. The dyke is steeply dipping to the west and continues with depth. The footwall typically consists of Norite (NR) and Greenstone (GS) and the hanging wall consists of Metasediments (MTSD) as shown in Figure 4-2. The mine has essentially been in operation for 100 years and has produced 57.2 million tons containing an average grade of 1.33% copper and 1.62% nickel (Vale Feb., 2009). Both transverse and longitudinal stope mining methods are employed. The typical planned stope dimensions are 100x50x40ft (30x15x12 m). The stopes are extracted in two or 3 blasts and then tight filled with a mixture of paste fill and waste rock. Atypical level plan of the case study area is shown in Figure 4-3. The present study is limited to No1 Shear East from 4900L to 5100L.

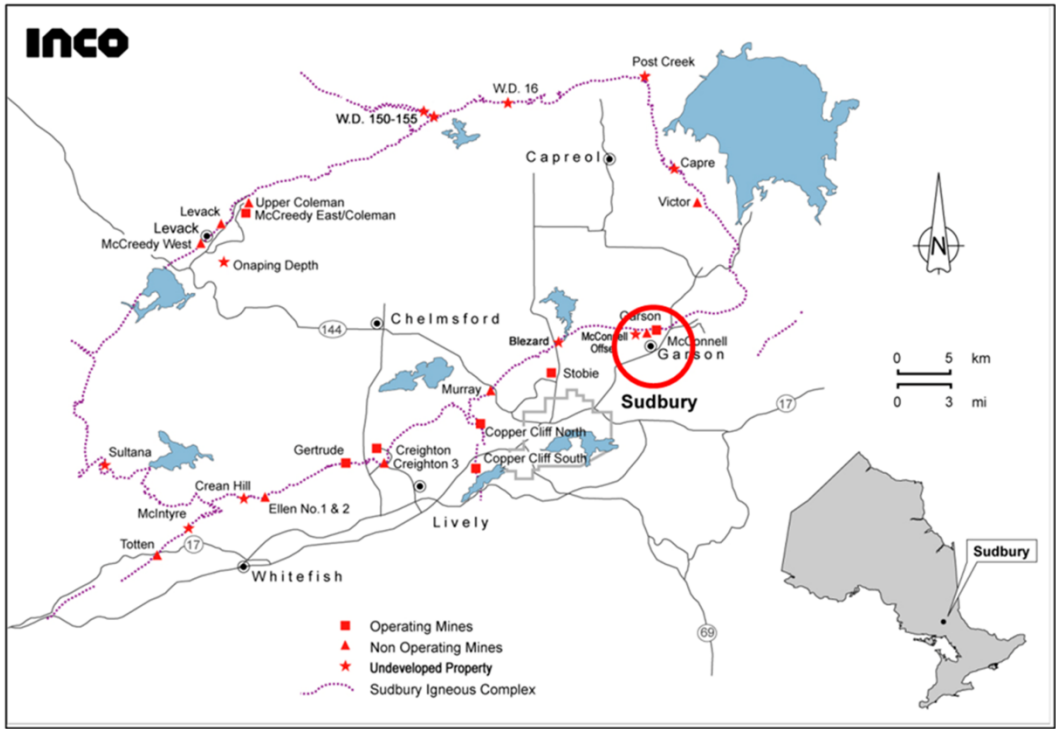


Figure 4-1 Garson Mine location map

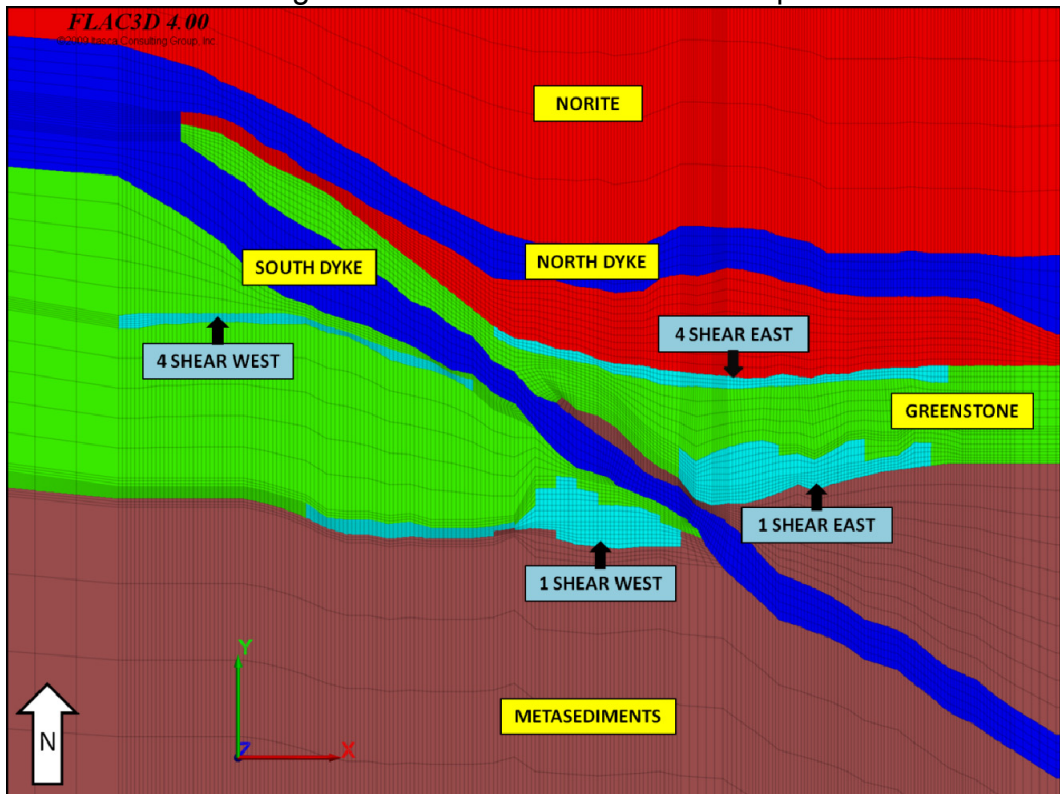


Figure 4-2 Geological units of Garson Mine (Shnorhokian et al, 2013)

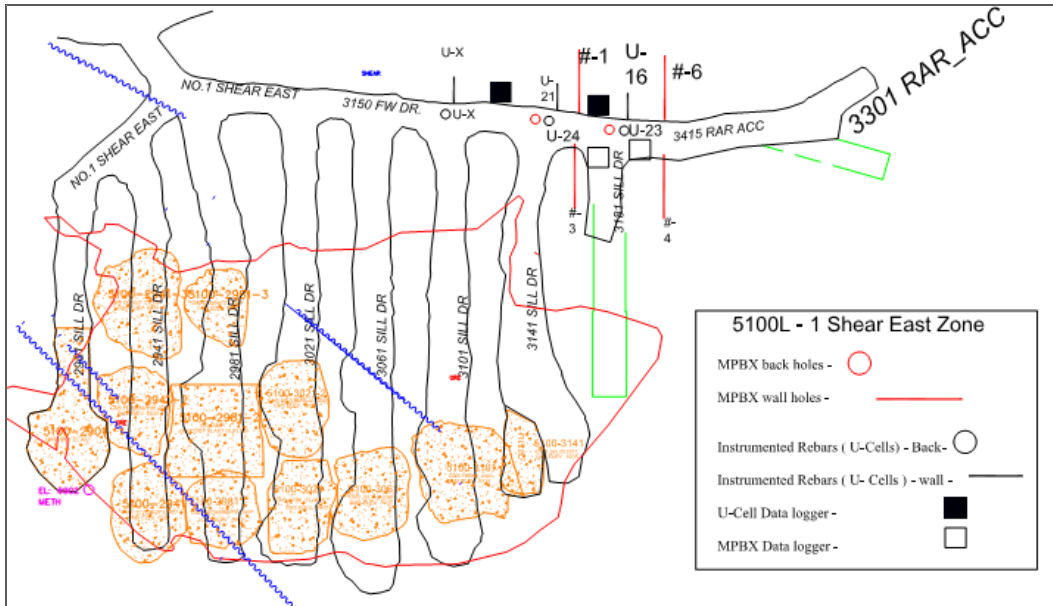


Figure 4-3 Typical level plan of 1 shear east zone of the study area

### 4.3 Drift Support practice at Garson mine

Primary support systems in Canadian mines typically employ 3/4 inch resin grouted rebar in the back and shoulder. In low stress environment, jointed/fractured rock mass for short term openings (2 year life or less), the efficiency of resin grout is not warranted, hence the use of 5/8 inch and 3/4 inch mechanical rock bolts with expansion shell. Typical support length is 6 to 8 feet (1.8 to 2.4 m) for drifts of spans in the range of 4 to 5 m. On the other hand, sidewall support systems employ more ductile support such as Swellex and Split-Sets. These supports offer greater ability to accommodate sidewall deformations due to mining-induced convergence. Typical primary and secondary support systems practiced at Garson mine, where a high horizontal stress causes the instability are shown in Figures 4-4 and 4-5.

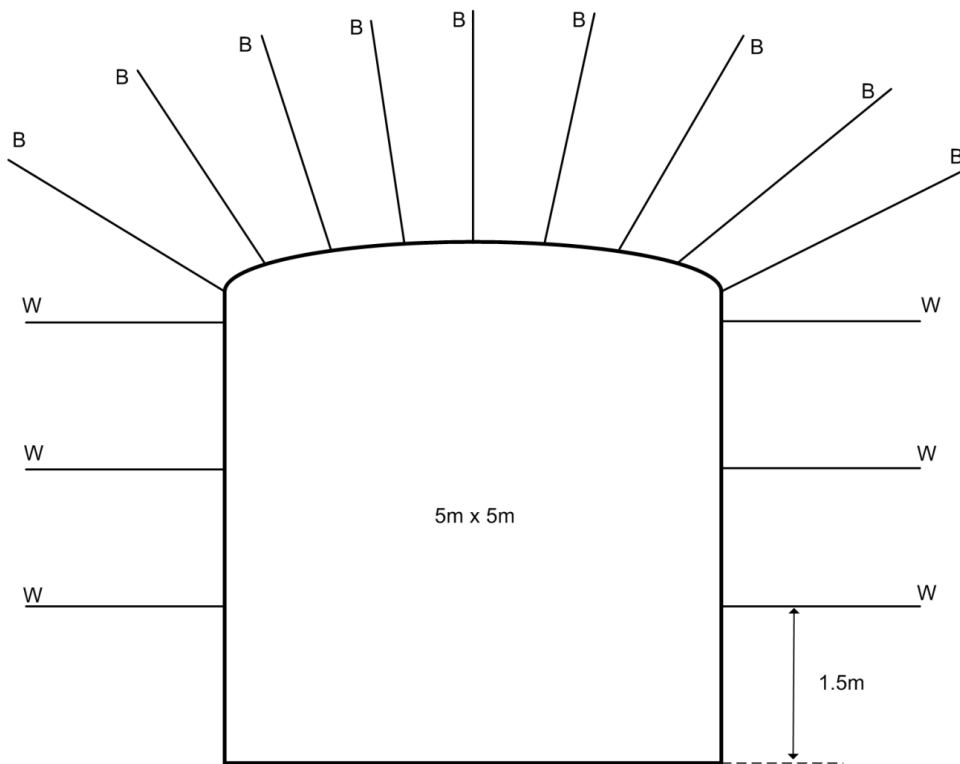


Figure 4-4 Primary support system

Table 4-1 Primary rock support specifications in mine developments(refer to Figure 4-4)

Regular Rock Development	Excavation width < 6m		Excavation width > 6m
	B	1.8m –Rebar	2.4m-Rebar
W	1.8m-Rrebar	1.8m-Rebar	
Development in Ore	B	1.8m-Rrebar	2.4m-Rebar
	W	1.95m FS46 Split-Set	1.95m FS46 Split-Set

As can be seen from figure 4-4, it is evident that the rebar of 6 or 8 ft is the primary support system during the regular rock development. In the ore development the primary support in the sidewall consists of split sets (refer to Table 4-1). The secondary or enhanced support system consists of 8ft long Modified cone bolt(MCB) or MN12 Swellex bolt along with 'O'gage mine mesh as shown in Figure 4-5( refer to Table 4-2). It is understood that the secondary or enhanced support system has the yielding capacity to resist the dynamic loading. This sort of support system

will enhance the haulage drift stability against seismic loads. Apart from this reinforced shotcrete with “0” gage mesh or with steel fibres is also employed to have a stable back and walls in burst prone ground.

Table 4-2 Secondary rock support specifications in mine developments (refer to Figure 4-5)

Secondary support	Type of secondary support	
	SB	2.4m long Modified Cone Bolts ( MCB)
SW	Or MN12 Swellex bolts	

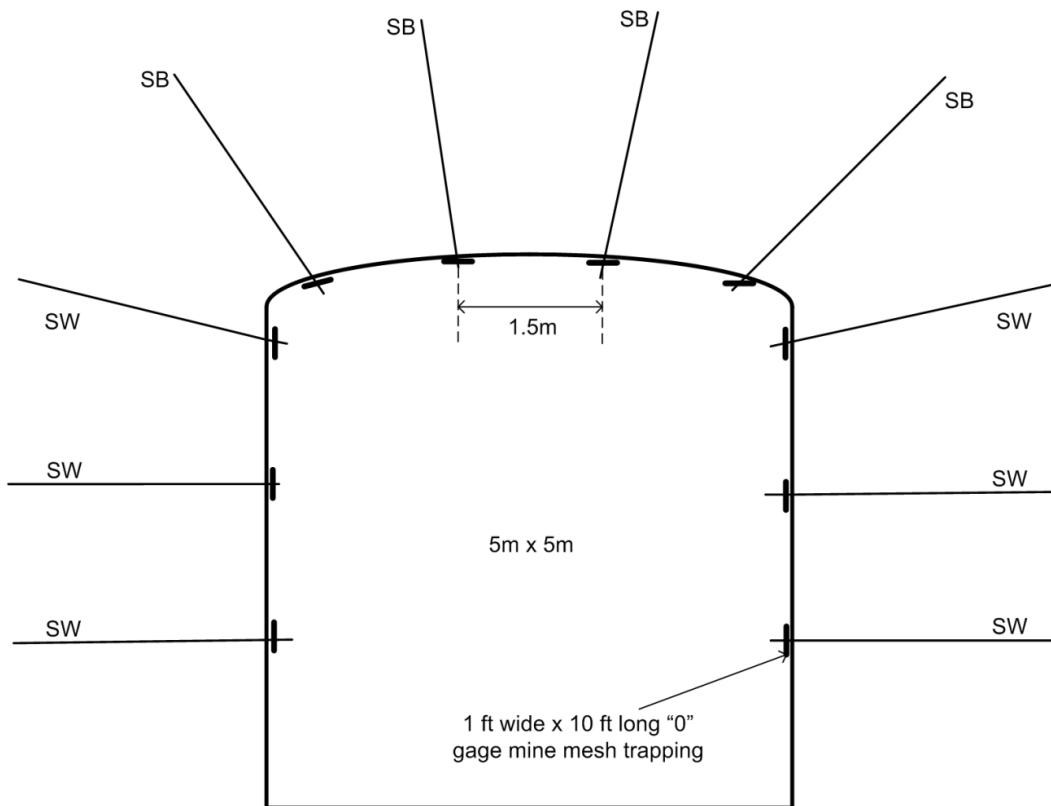
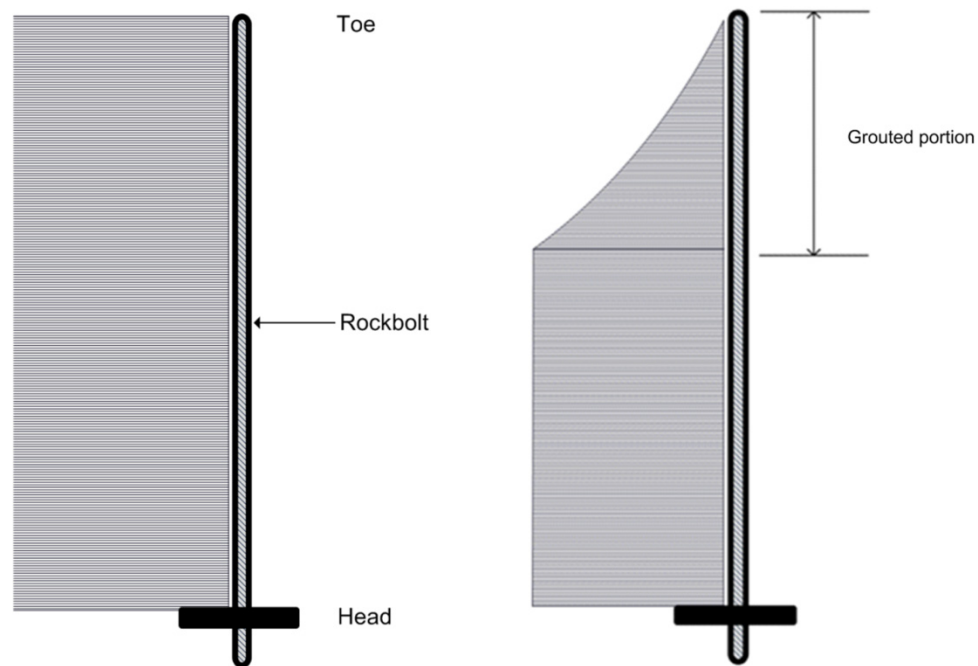


Figure 4-5 Secondary or enhanced support system

#### 4.4 Evaluation of current drift support behavior

It is evident from the above practices that the rock bolt forms the major support element during primary and secondary support system used to reinforce the rock mass. Hence it is important that the behaviour and performance of fully grouted rock bolt be evaluated and accordingly the stability of the haulage drift is estimated. The concepts associated with end-anchored and partially grouted rock bolts are generally well understood. Along the free length of the bolt, the load is constant and equal to the resisting force developed by either a mechanical anchor or a partial section of resin grout as shown in Figure 4-6.



a) Mechanically anchored rock bolt      b) Partially grouted rock bolt  
4-6 Axial load distribution along rock bolt

The case of fully grouted rock bolts is more complex, which probably explains why the majority of recent theoretical studies have been focused on the axial deformation of fully grouted rock bolts in response to a continuous distribution of rock mass convergence (Hyatt & Mitri, 2012).

A conceptual model of the behavior of the fully grouted rebar was presented by Freeman (1978). Many variations of analytical and numerical models of rockbolt behavior have been developed (Mitri and Rajaie, 1990; Tang and Mitri, 2000; Tadolini and Mitri, 2002; Li C, 2009; Martin, Tijani, and Hadj-Hassen, 2011; Deb and Das, 2010; Hyett, Moosavi, and Bawden, 1996).

In a discontinuous rock mass, the load distribution along the bolt will be dominated by discrete rock mass displacements on a limited number of discontinuities (Li C, 2010). A closed form solution to this problem was developed by Hyett, Moosavi, and Bawden (1996) for cablebolts. Numerical models demonstrated that, especially for longer bolts such as fully grouted cable bolts, several peaks in load may occur along the bolt length. Such an effect was observed experimentally by Bjornfot and Stephansson (1984) for long rockbolts in hard, blocky rock at the Kiruna Mine in Sweden. Figure 4-7 illustrates typical axial load distribution along fully grouted rock bolt.

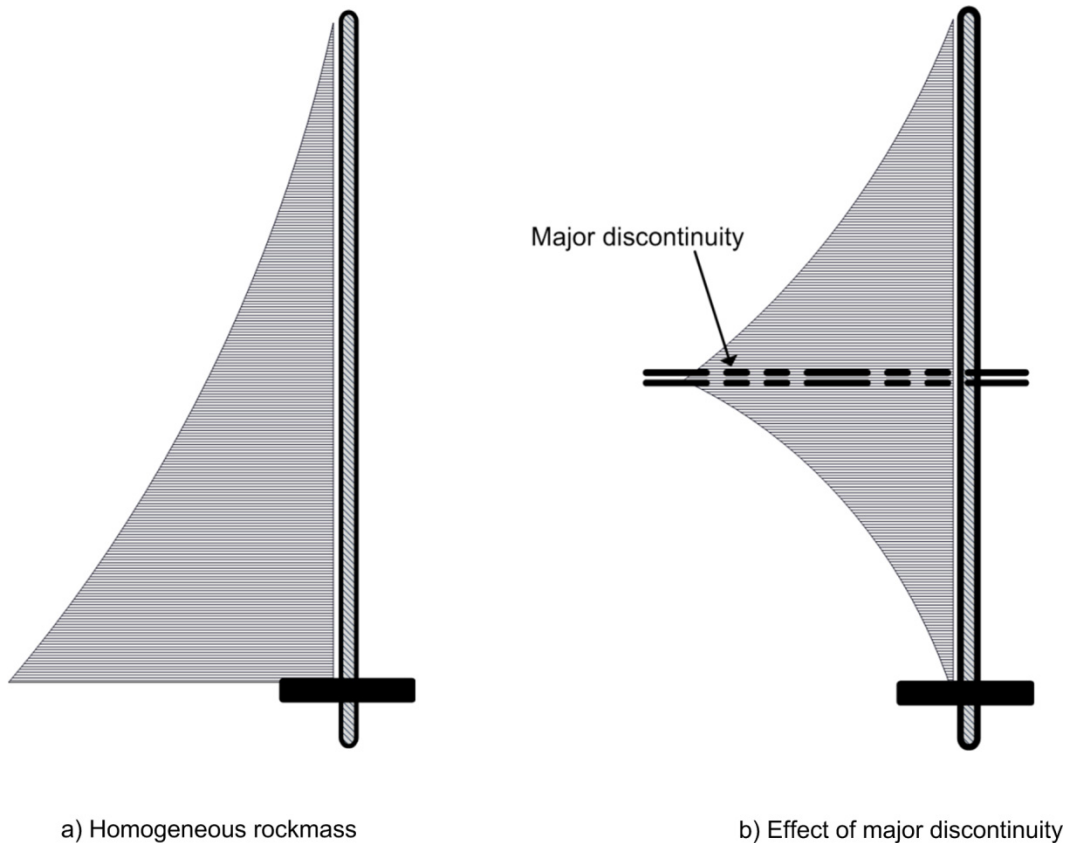


Figure 4-7 Axial load distribution along fully grouted rockbolt

In order to evaluate the behavior of current drift support system consisting of fully grouted rebars and modified cone bolts (MCB) as primary and secondary supports respectively, numerical modeling was conducted using FLAC 2D by simulating the actual mining sequence as practiced in Garson mine. Also to validate the numerical model, instrumentation program for monitoring insitu performance of the rockbolts was performed.

#### 4.5.1 Numerical Modeling – Static analysis

Numerical modeling of the drift support system was performed using the finite difference modeling software FLAC of Itasca. FLAC2D (Fast Lagrangian Analysis of Continua) is a two dimensional explicit finite difference program for engineering mechanics computation, developed by

Dr. Peter Cundall in 1986, originally for geotechnical and mining engineering applications (Itasca, 2011). Since then many versions of the code with new upgrades were made available.

FLAC version 7.0 is used for this study. This program simulates the behavior of soil and rock structures as their yield limits are reached. Containing many special features and facilities such as built-in programming language called FISH and also power full Graphical user interface system. In FLAC, materials are presented by elements or zones which, together, form a grid. This grid can be shaped to fit the geometry of the object to be modeled. Each element is then given a constitutive model based on which it responds to the applied forces or boundary restraints. As the stresses and forces are initialized within the modeled structure, the FLAC calculation sequence is started; the equations of motion are invoked to derive the velocities and displacements from applied stresses and forces. The velocities are then used to calculate the strain rates. The new stresses are finally derived from strain rates based on the prescribed stress/strain law (constitutive model) in the elements (Itasca, 2011). This cycle is then repeated until the initially applied forces are approaching zero, i.e. the model reaches the equilibrium. Figure 4-8 simply shows the basic calculation cycle in FLAC

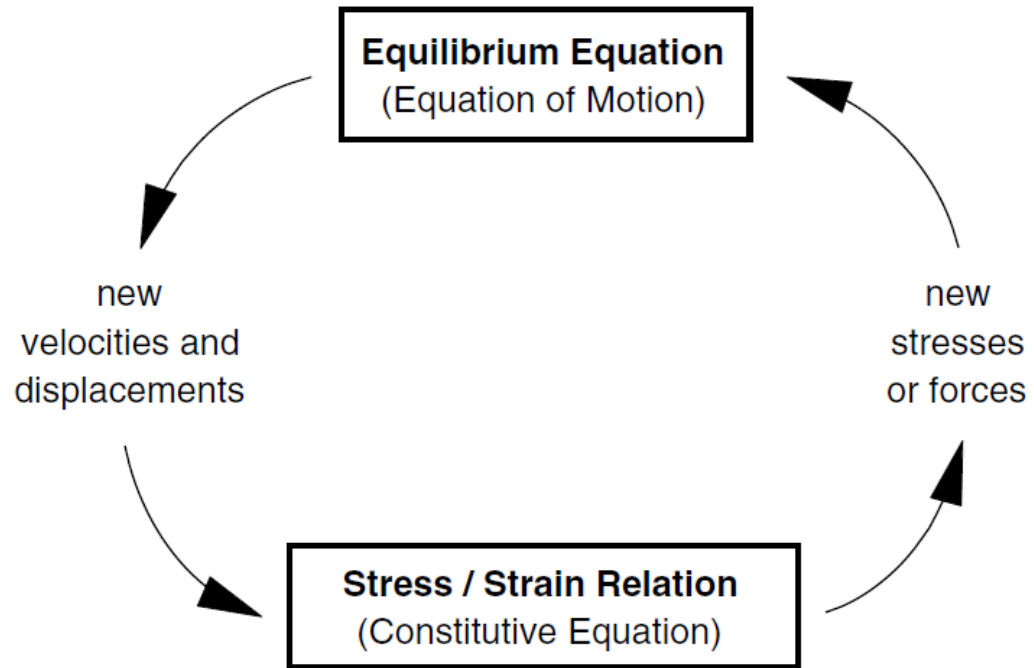


Figure 4-8 Basic explicit calculation process in FLAC (Itasca, 2011)

#### 4.5.2 Mining sequence simulation

A multi-stage simulation of mine-and-fill sequence in the vicinity of the haulage drift is conducted to examine the performance of the fully grouted rock bolts as drift support system. Mining sequences are simulated in two directions: from lower to upper levels and from hanging wall to footwall in retreat. This mining sequence is as practiced in the case study mine. Accordingly the geometry of the conceptual model is built in FLAC. The model geometry assuming the vertical Orebody is illustrated in Figure 4-9.

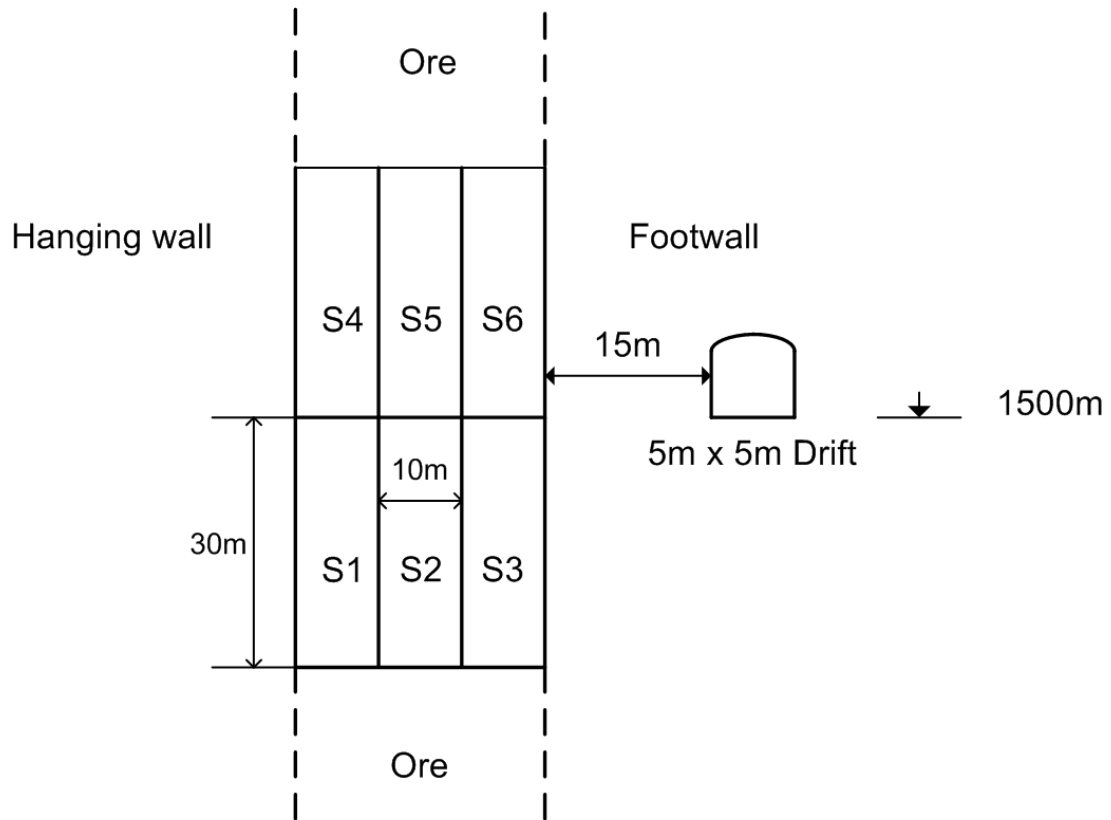


Figure 4-9 Model geometry with drift

Two numerical models were developed in this study. The first (Model 1) simulates the primary support system of 20mm fully grouted rebars as shown in Figure 4-10. The second (Model 2) simulates both the primary and secondary support system as shown in figure 4-11.

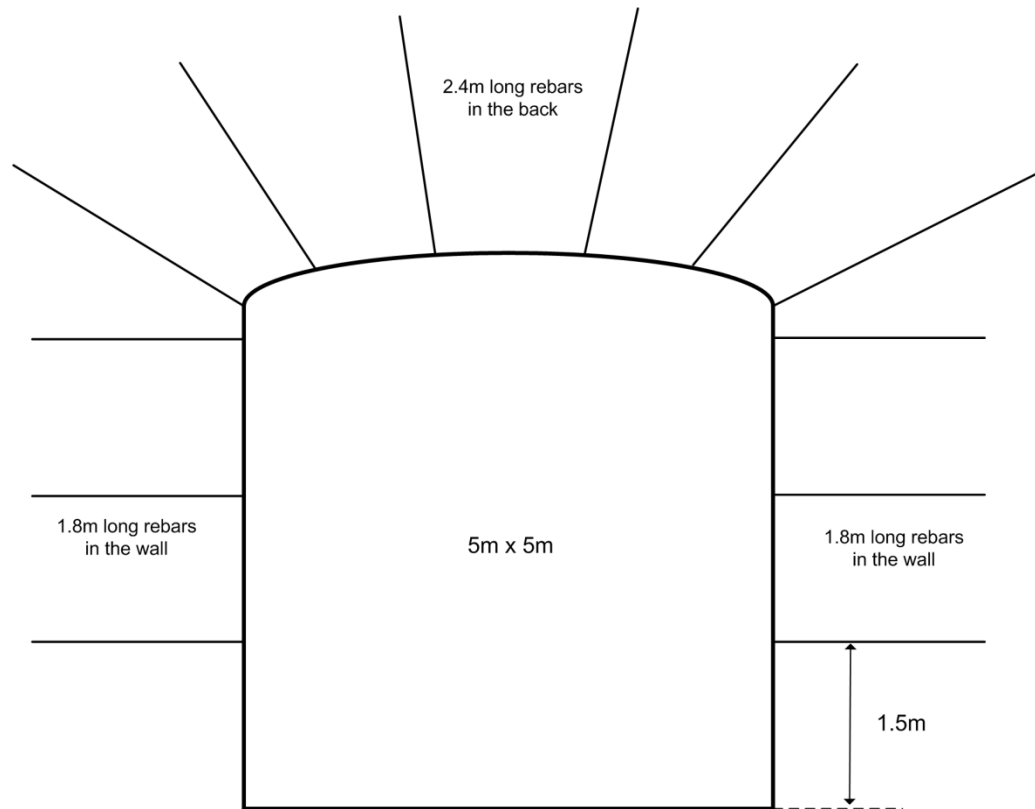


Figure 4-10 Primary support system of fully grouted rebar: Model 1

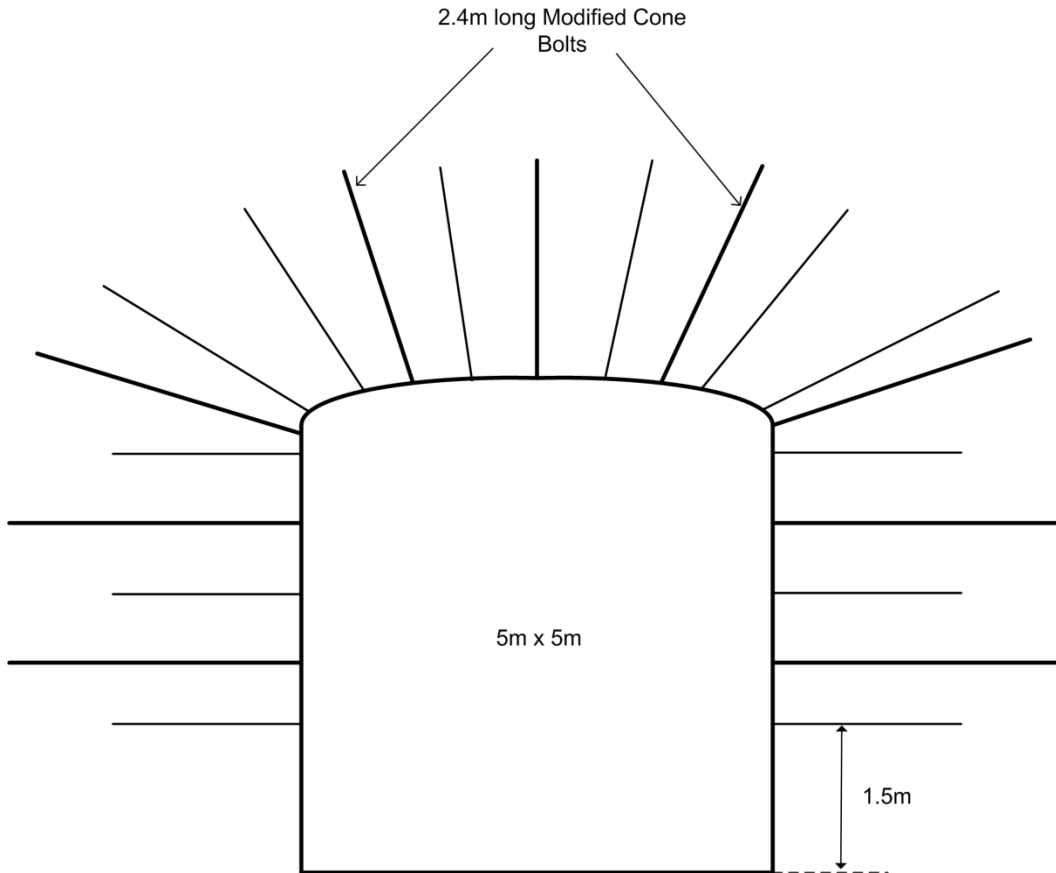


Figure 4-11 Primary and secondary support system: Model 2

Three rock units are present in the modeling area namely footwall, orebody and the hanging wall rocks. Accordingly the model is treated with the properties of these three rock units. The mechanical properties of the rock masses in the model, as well as those of the mine backfill, are presented in Table 4-3. All rocks are treated as Mohr-Coulomb elastoplastic materials. The modeling technique of rock support elements is based on the assumption that the rock support is attached to the rock mass through a set of continuous shear springs representing the shear bond stiffness of the rock-grout interface (Tang et al, 2000) as shown in Figure 4-12.

Table 4-3 Rock mass properties (Itasca, 2009)

Property	Hanging	Ore	Foot wall	Backfill
Density ( $\text{Kg/m}^3$ )	2782	4531	2916	2000
E (GPa)	25	20	65	0.1
Poisson's ratio	0.24	0.22	0.23	0.3
Cohesion (MPa)	4.8	10.2	5.7	1.0
Tensile strength(	0.11	0.31	0.51	0.01
Friction angle( $^\circ$ )	38	43	55	30

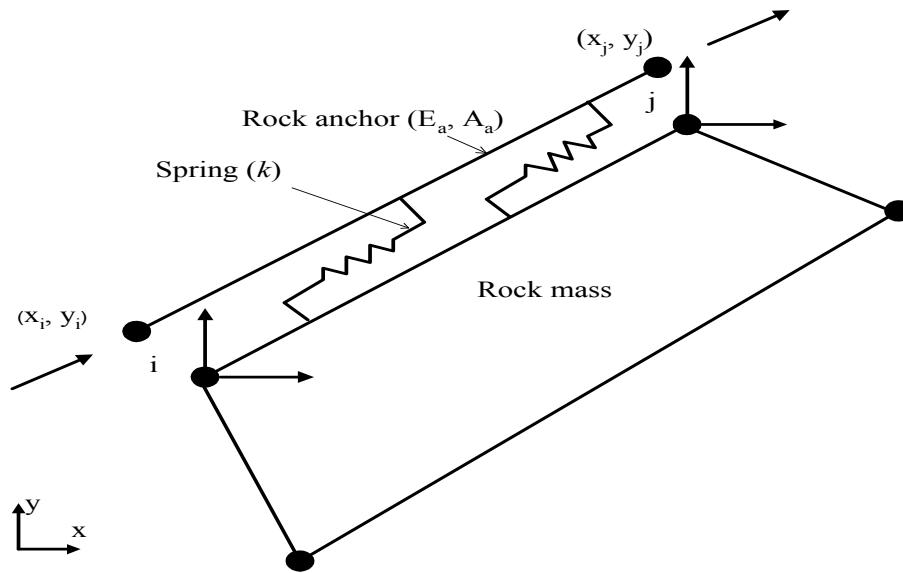


Figure 4-12 Basic model of rockbolt element (Tang et al. 2000)

### 4.5.3 Structural elements in FLAC

The structural elements available in FLAC are briefly discussed in this section. It is well known fact that geomechanical analysis and design is the use of structural support to stabilize a rock or soil mass. Structures of arbitrary geometry and properties, and their interaction with a rock or soil mass, may be modeled with *FLAC (Itasca, 2011)*. Generic concepts such as geometry specification, linkage of elements to the grid and to each other, options for specifying end conditions, and specification of properties are discussed. Each type of structural element is briefly described. In case of rockbolt element, a description of the numerical formulation and the properties required are also provided.

Seven forms of structural supports may be specified in FLAC as described below (verbatim from (Itasca, 2011)):

- **Beam Elements** – Beam elements are two-dimensional elements with three degrees of freedom ( $x$ -translation,  $y$ -translation and rotation) at each end node. Beam elements can be joined together with one another and/or the grid. Beam elements are used to represent a structural member, including effects of bending resistance and limited bending moments. Tensile and compressive yield strength limits can also be specified. Beams may be used to model a wide variety of supports, such as support struts in an open-cut excavation and yielding arches in a tunnel. Interface elements can be attached on both sides of beam elements in order to simulate the frictional interaction of a foundation wall with a soil or rock. Beam elements attached to sub-grids via interface elements can also simulate the effect of geotextiles.
- **Liner Elements** – Liner elements, like beam elements, are two-dimensional elements with three degrees of freedom ( $x$ -translation,

y-translation and rotation) at each end node, and these elements can be joined together with one another and/or the grid. Liner elements are also used to represent a structural member in which bending resistance, limited bending moments and yield strengths are important. The primary difference between liner elements and beam elements is that liner elements include bending stresses to check for yielding, whereas beam elements only base the yielding criterion on axial thrust. Liner elements are recommended for modeling tunnel linings, such as concrete or shotcrete liners.

- **Cable Elements** – Cable elements are one-dimensional axial elements that may be anchored at a specific point in the grid (point-anchored), or grouted so that the cable element develops forces along its length as the grid deforms. Cable elements can yield in tension or compression, but they cannot sustain a bending moment. If desired, cable elements may be initially pretensioned. Cable elements are used to model a wide variety of supports for which tensile capacity is important, including rockbolts, cable bolts and tiebacks.
- **Pile Elements** – Pile elements are two-dimensional elements that can transfer normal and shear forces and bending moments to the grid. Piles offer the combined features of beams and cables. Shear forces act parallel to the element, and normal forces perpendicular to the element. The three-dimensional effect of the pile interaction with the grid can be simulated. A user-defined *FISH* function describing the load versus deformation at the pile/medium interface normal to the pile can also be specified. The element does not yield axially, but plastic hinges can develop. Pile elements are specifically designed to represent the behavior of foundation piles.
- **Strip Elements** – Strip elements represent the behavior of thin reinforcing strips placed in layers within a soil embankment to provide structural support. The strip element is similar to the

rockbolt element, in that strips can yield in tension or compression, and a tensile failure strain limit can be defined. Strips cannot sustain a bending moment. The shear behavior at the strip/soil interface is defined by a nonlinear shear failure envelope that varies as a function of a user-defined transition confining pressure. Strip elements are designed to be used in the simulation of reinforced earth retaining walls.

- **Support Members** – Support members are intended to model hydraulic props, wooden props or wooden packs. In its simplest form, a support member is a spring connected between two boundaries. The spring may be linear, or it may obey an arbitrary relation between axial force and axial displacement, as prescribed from a table of values. The support member has no independent degrees of freedom: it simply imposes forces on the boundaries to which it is connected. A support member may also have a width associated with it. In this case, it behaves as if it were composed of several parallel members spread out over the specified width.
- **Rockbolt Elements** – Rockbolt elements, like pile elements, are two-dimensional elements that can transfer normal and shear forces and bending moments to the grid. Rockbolt elements have the same features as pile elements. In addition, rockbolt elements can account for (1) the effect of changes in confining stress around the reinforcement; (2) the strain-softening behavior of the material between the element and the grid material; and (3) the tensile rupture of the element. Rockbolt elements are well-suited to represent rock reinforcement in which nonlinear effects of confinement, grout or resin bonding, or tensile rupture are important.

In all cases, the commands necessary to define the structure(s) are quite simple, but they invoke a very powerful and flexible structural logic.

This structural logic is developed with the same finite-difference logic as the rest of the code (as opposed to a matrix-solution approach), allowing the structure to accommodate large displacements and to be applied for dynamic as well as static analysis. The geometries of all structural elements are defined by their endpoints. The user defines the endpoints for beams, liners, cables, piles, rockbolts, and strips, whereas the endpoints for support elements are found automatically by *FLAC*.

In order for beam or liner elements to interact with the model grid, they must be explicitly linked to the grid. Cable, pile, rockbolt, and strip elements can interact with the grid via the shear coupling springs (and normal coupling springs in the case of a pile or rockbolt). Elastic stiffness properties and cohesive and stress-dependent frictional properties describe the interaction between the elements and the grid. If all the parameters are zero, these elements will not interact with the grid. If a cable, pile, rockbolt or strip node is placed with the **grid** keyword, then it will be rigidly connected to that grid point, and the springs will have no effect at that point.

**Rockbolt element formulation (Itasca, 2011):** The rockbolt element is based on the pile element, with axial and bending behavior. The connection to the grid, in both the normal and shear directions, is via coupling springs, as described in Figure 4-12. The rockbolt element may yield in the axial direction in both tension and compression (**yield** and **ycomp**). Rockbolt breakage is simulated based upon a user-defined tensile failure strain limit (**tfstrain**). A strain measure, based on adding the axial and bending plastic strains, is evaluated at each rockbolt node. The axial plastic strain,  $\varepsilon_{pl}^{ax}$ , is accumulated based on the average strain of rockbolt element segments using the node. The bending plastic strain is averaged over the rockbolt and then accumulated. The total plastic tensile strain,  $\varepsilon_{pl}$ , is then calculated by

$$\epsilon_{pl} = \sum \epsilon_{pl}^{ax} + \sum \frac{d}{2} \frac{\theta_{pl}}{L} \quad (4.1)$$

Where  $d$  = rockbolt diameter;

$L$  = rockbolt segment length; and

$\theta$  = average angular rotation over the rockbolt.

If this strain exceeds the limit **tfstrain**(tensile failure strain), the forces and moment in this rockbolt segment are set to zero, and the rockbolt is assumed to have failed.

#### 4.5.4 Analysis and results

Primary supports with fully grouted rebars are installed during the haulage drift development, and the sequencing of the nearby mining commenced subsequently. Rebar mechanical properties are presented in Table 4-4. As mining activities continue with primary support in place, the mining-induced axial loads are obtained.

Table 4-4 Rebar mechanical and grout interface properties

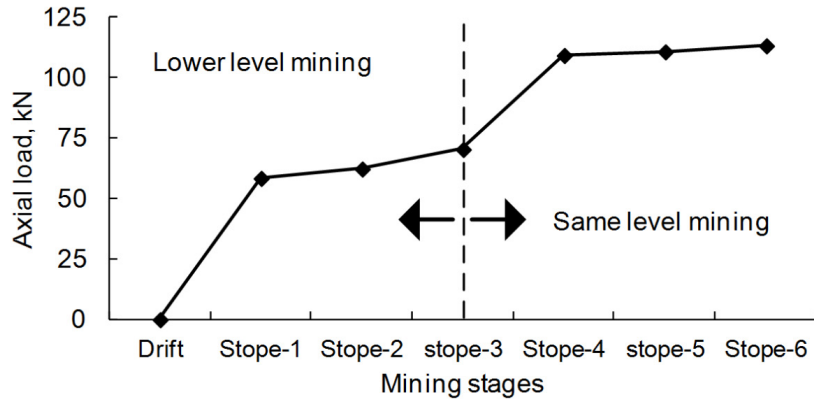
Property	Value
E (GPa)	200
Diameter (mm)	19
Yield load (kN)	125
Perimeter (m)	0.059
Tensile strain	0.09
Shear bond	4e8(rebar)/4e9(MCB)
Normal bond	4e11

As mentioned already the mining sequence was from hanging wall to footwall and from lower to upper levels. Also a multi-stage simulation of mine-and-fill sequence in the vicinity of the haulage drift was conducted to examine the performance of the fully grouted rock bolts. The analysis is presented in terms of maximum axial load in the rock bolt after each

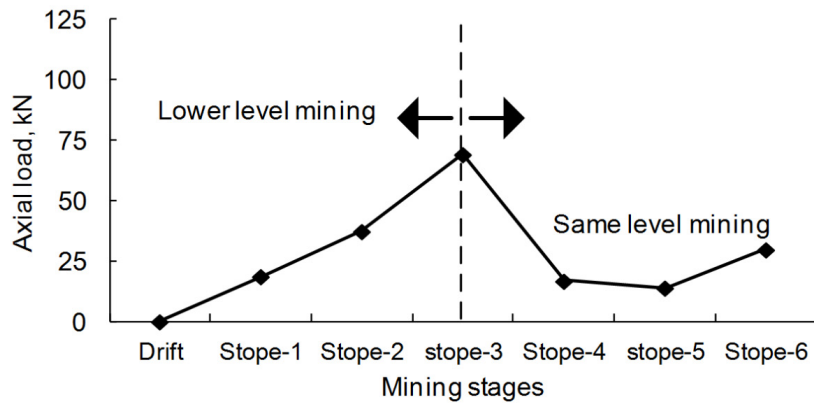
mining step in the drift north wall (NW), the south wall-towards the ore body-(SW) and the drift back. Figure 4-13 shows the maximum axial loads at the head of the primary supports (rebars) for various mining stages from both walls and the back of the drift for model- 1.

It can be observed from figure 4-13, that the support behavior of NW is different from the SW and the back. The axial load on rebars in the NW continues to increase as the mining progressed and reached almost towards the yield capacity of the rebar which is 125kN (Figure 4-13a). Where as in the case of SW and Back, the axial load increases till the end of lower level mining (stope1 to 3). The bolts then start to relax once the same level mining begins. Also the magnitude of axial load is higher in case of NW supports than in the other two cases. The maximum axial load in SW supports at the end of the lower level mining is 75kN (figure 2-8b) and it is 50kN for the supports in the back of the drifts (Figure 4-13c). It is to be noted that the pretension load at installation is not included in these results. Thus, the estimated maximum loads should be further increased by the amount of pretension load at installation, which is typically 10-20 kN.

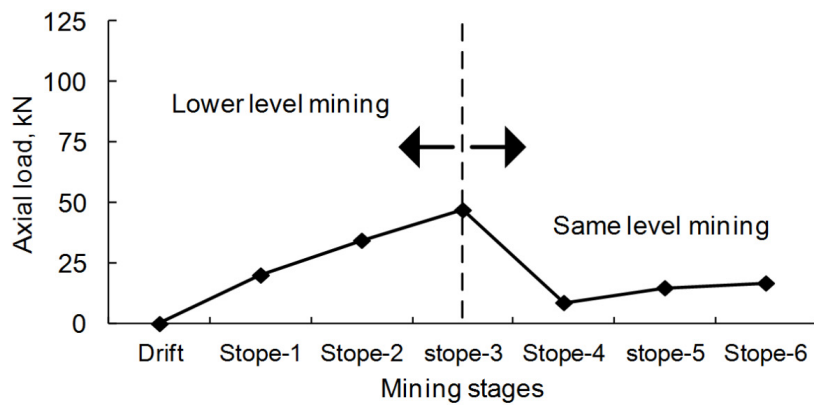
It can thus be calculated that the 125kN capacity of the primary support is likely to be exceeded during same level mining ( $115\text{kN} + \text{Pretension load}$ ); hence the need for enhanced support system. In Model-2, both primary and secondary supports are simulated at the same time to compare the behavior of the drift support with respect to the mining sequence. The computed axial loads of both primary and secondary supports are shown in Figure 4-14



a) Axial loads in North wall rebars

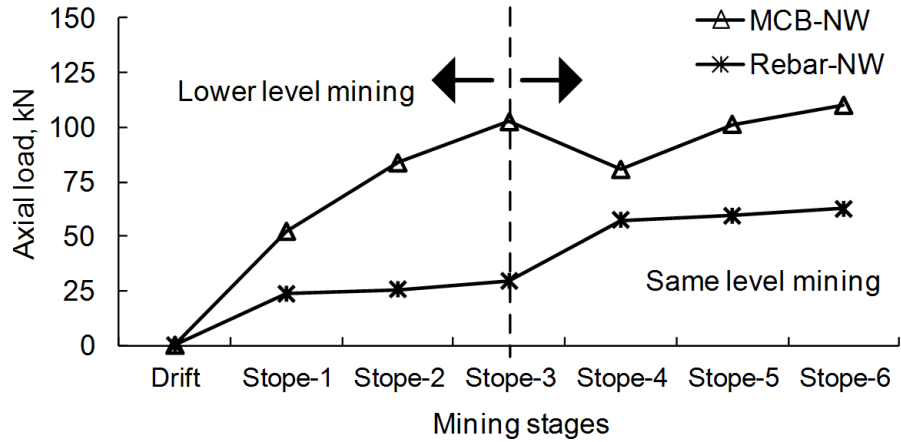


b) Axial loads in South wall rebars

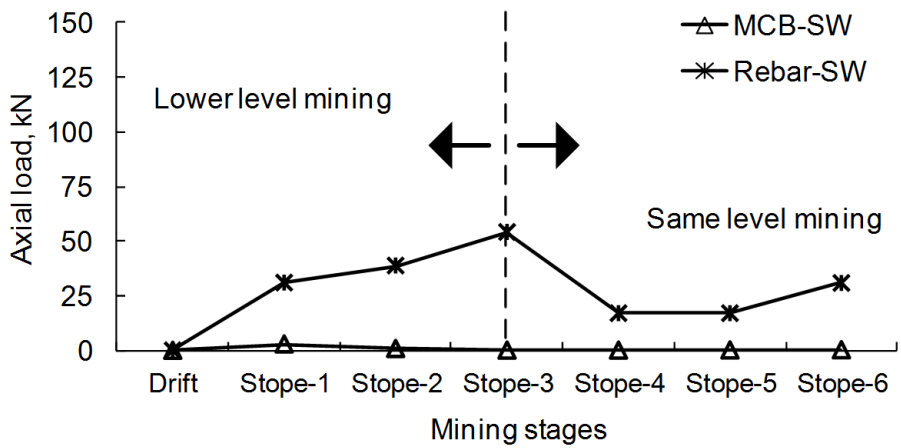


c) Axial loads in drift back rebars

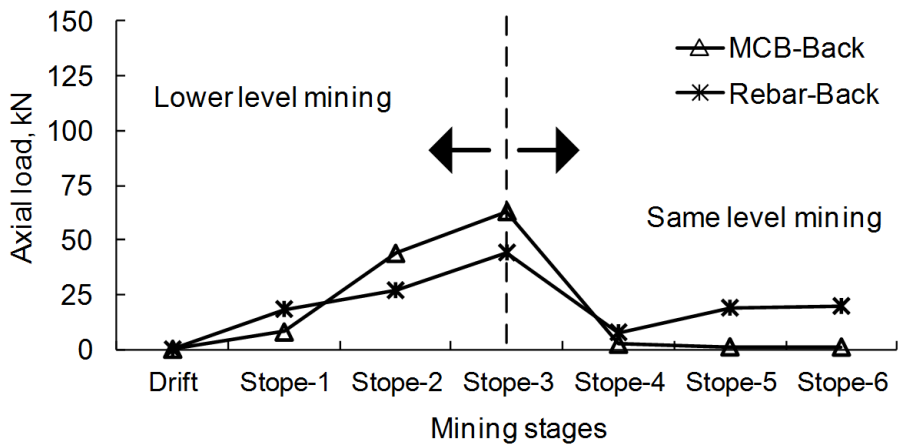
Figure 4-13 Maximum axial loads on primary supports during different mining stages – Model 1



a) Axial loads in North wall, rebars and MCB



b) Axial loads in South wall, rebars and MCB



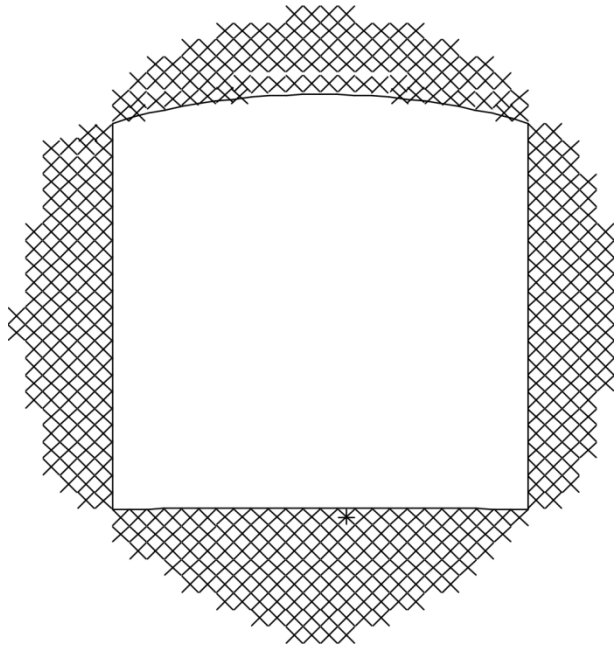
c) Axial loads in drift back, rebars and MCB

4-14 Maximum axial loads on primary supports during different mining stages – Model 2

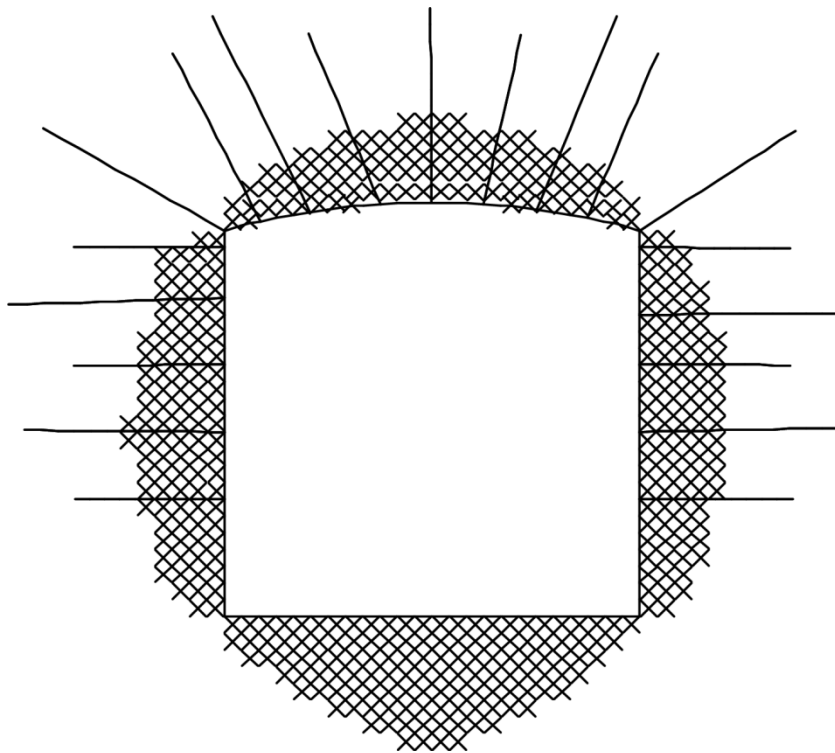
As can be observed from the results as shown in Figure 4-14(a,b,c), that the axial load on rebars is shared by the secondary supports and none of the primary supports yielded. Although the loads have been shared by secondary supports, the behavior of the rebars doesn't seem to be changed even in combination with the secondary supports i.e the influence of the same level mining on the drift support system is still evident. On the other hand the secondary supports also follow the trend of primary supports, though in this case they are highly loaded and shared the load of rebars. Also secondary supports (in the form of MCBs) have still some capacity to take even more loads in any adverse ground conditions.

It can also be observed that in general the secondary supports in the form of MCBs are necessary in case of drift back and SW to take care of the dynamic event, and in case of NW the secondary supports in the form of MCB is necessary to avoid the yielding of primary supports before the same level mining begins and also to provide the yielding supports for countering the dynamic conditions. It can also be observed that the secondary supports should be in place before mining the same level stopes, particularly in the case of NW so as to avoid the yielding of the primary supports already in place.

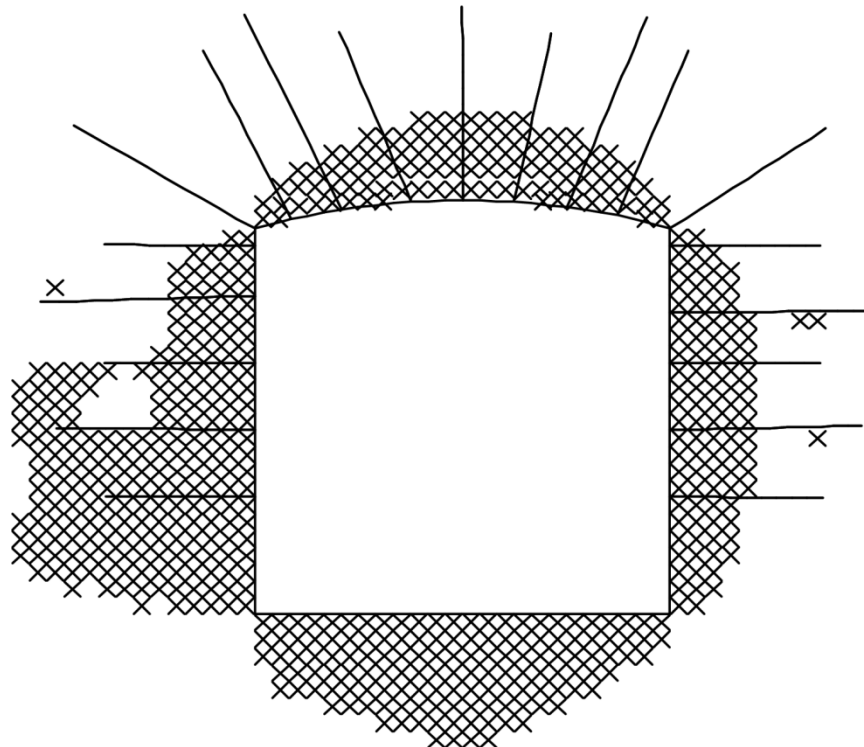
The yielding around the drift during various stages of mining is shown in Figure 4-15. The progression of yielding zone around the drift with respect to mining can be observed from this figure. It is worth noting that after lower level mining, the yielding zone extends beyond the bolting horizon (Fig 4-15(e)), on South Wall towards ore body and hence, the bolts started to relax in South wall.



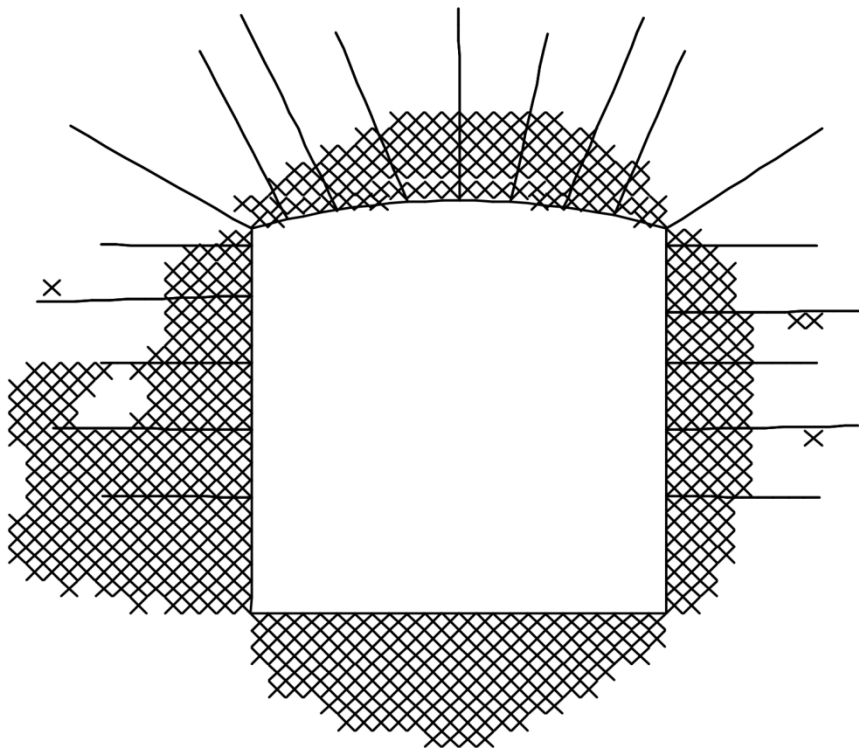
a) After drift



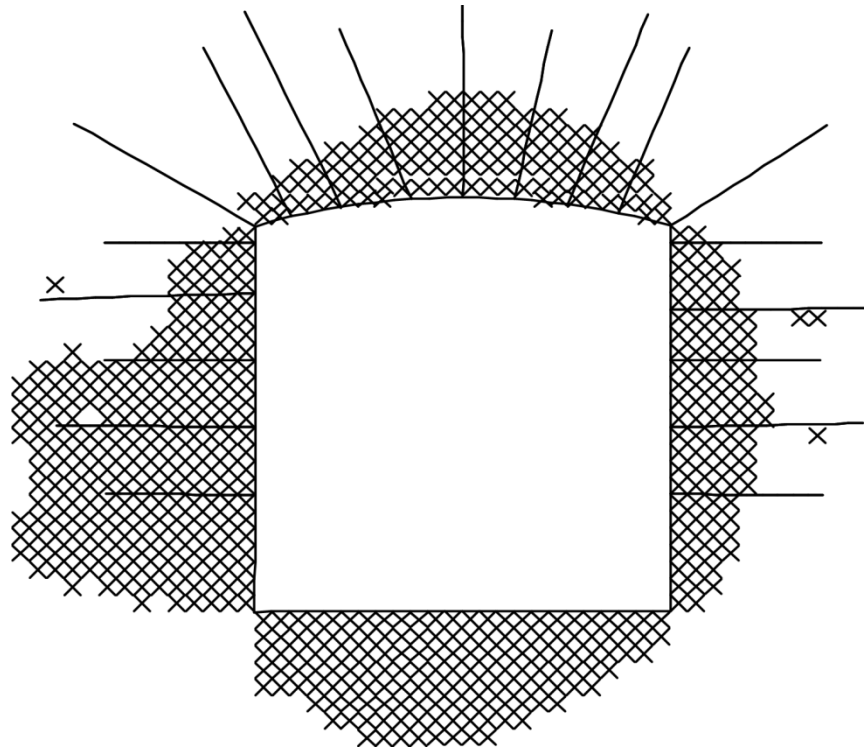
b) After installation of bolts



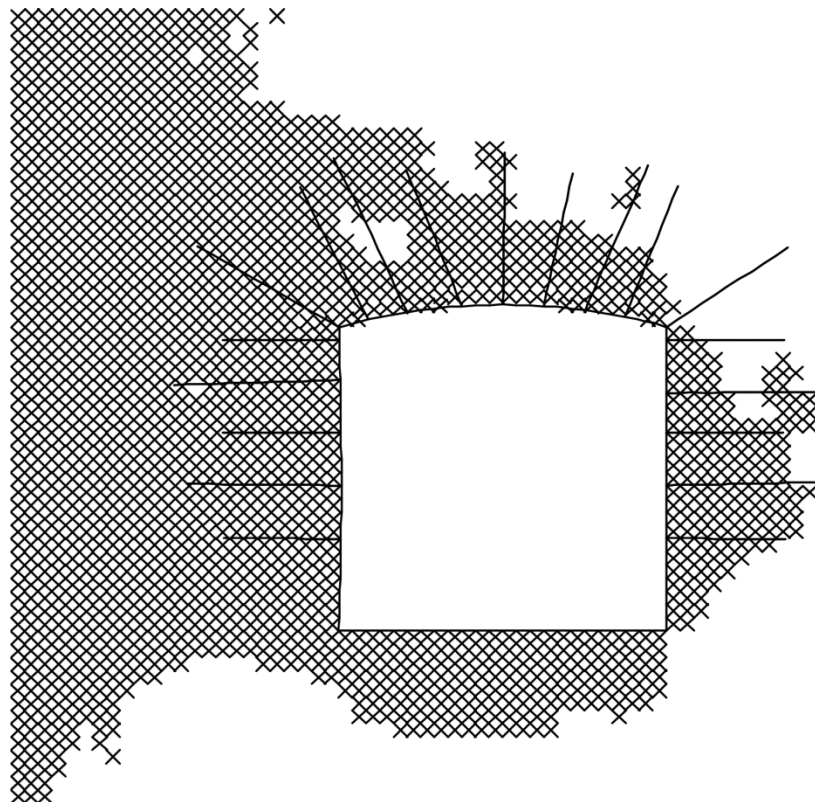
c) after Stope-1



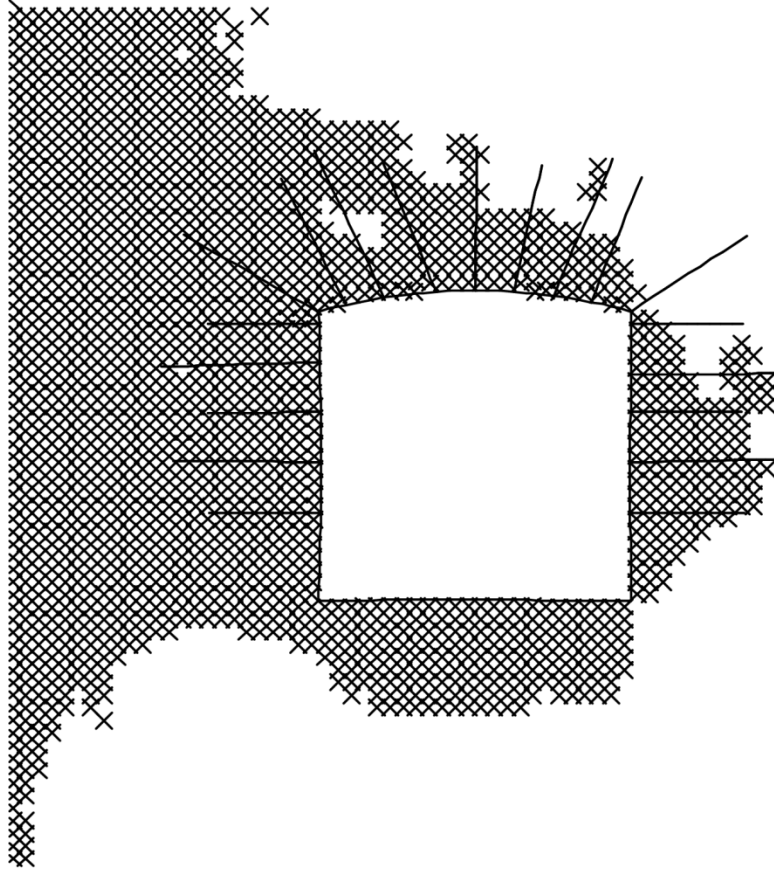
d) after Stope-2



e) after Stope-3 ( end of lower level mining)



f) after Stope-4 ( same level mining begins)



g) after Stope -5

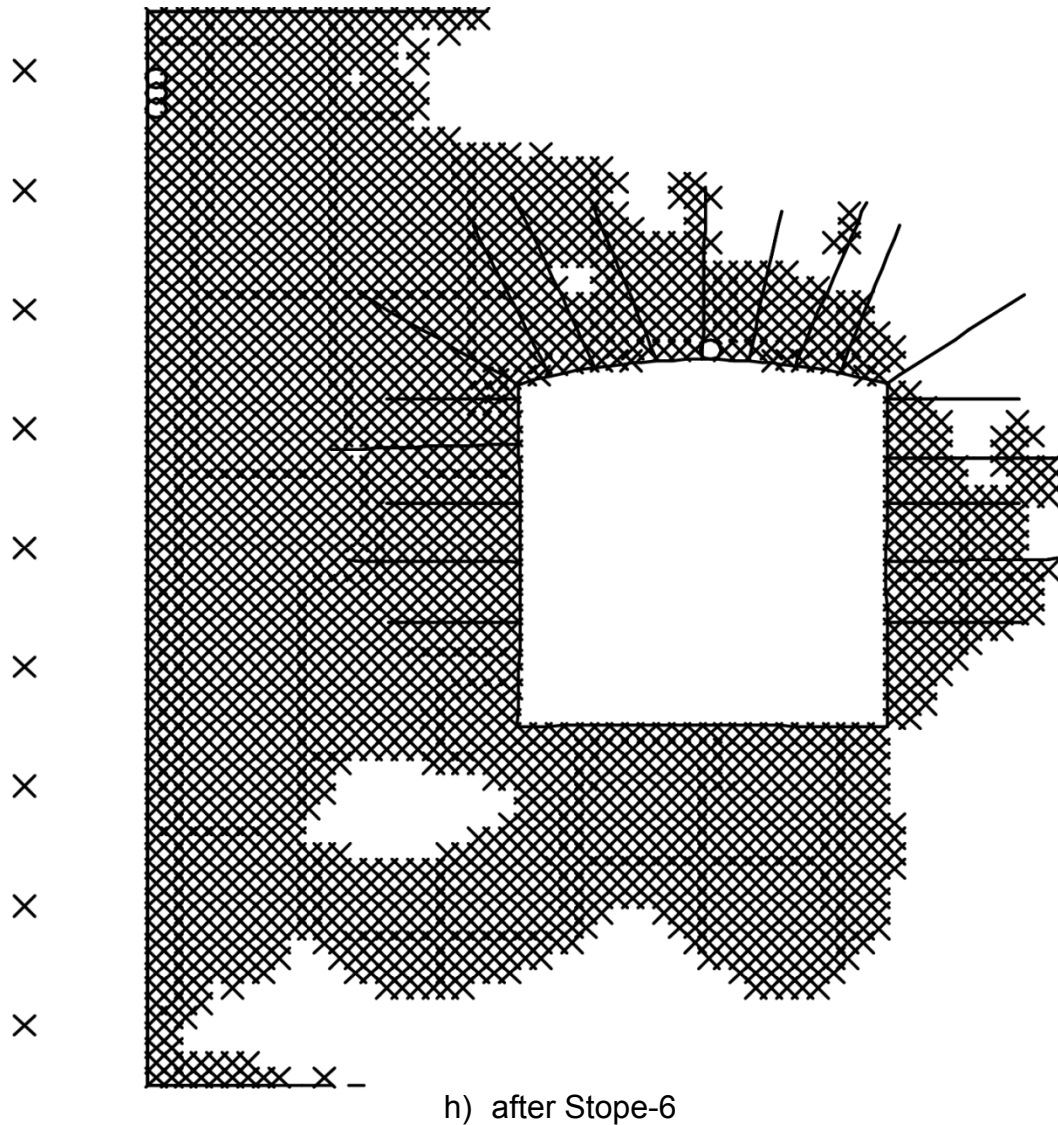


Figure 4-15 Extent of rock mass yielding around the drift

#### 4.5.5 Load distribution along the fully grouted rebar

As already mentioned in the earlier sections the behavior of the fully grouted rebar is complex. With this in view it was decided to examine the load distribution along the fully grouted rebar by simulating the same as a drift primary support. Also it will form the basis for selecting the appropriate load monitoring device to monitor the in situ performance of the fully grouted rebar. All the numerical modeling conditions are same as those used for the above results except that only the rebars were

examined in this analysis for their load distribution along the length. It can be seen from figure 4-16, that the maximum axial load is at the head of the bolt. Also, it was found that the maximum load shifts further inside of the bolt, once the bolt load exceeds the yield load at the head of the bolt. In case of MCB the distribution of axial load along the length of the bolt is shown in figure 4-17. It can be observed from this figure that the load distribution along the de-bonded length follows the trend of end anchor or mechanical bolt and the rest of the length (high strength resin grouted length) behaves like the fully grouted rebar.

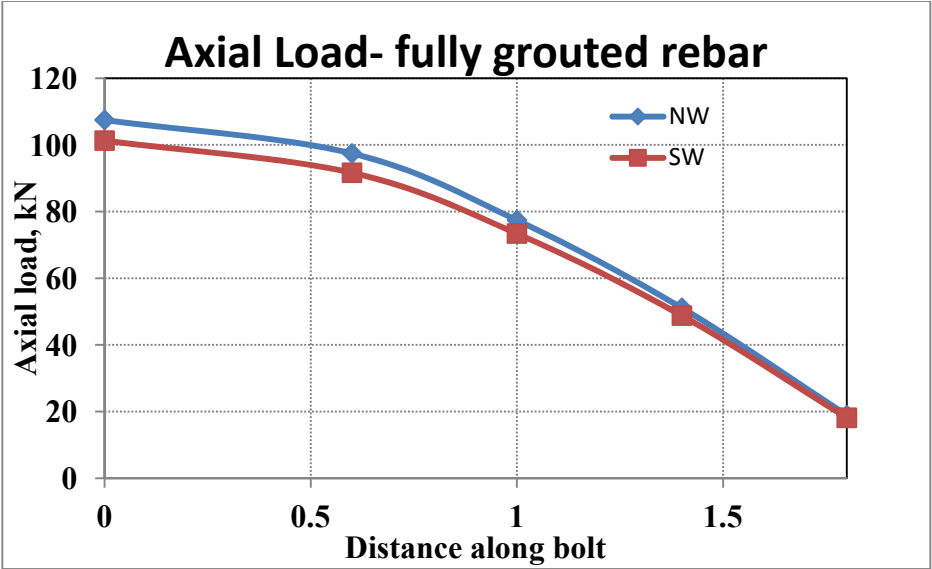


Figure 4-16 Axial load distribution along fully grouted rebar

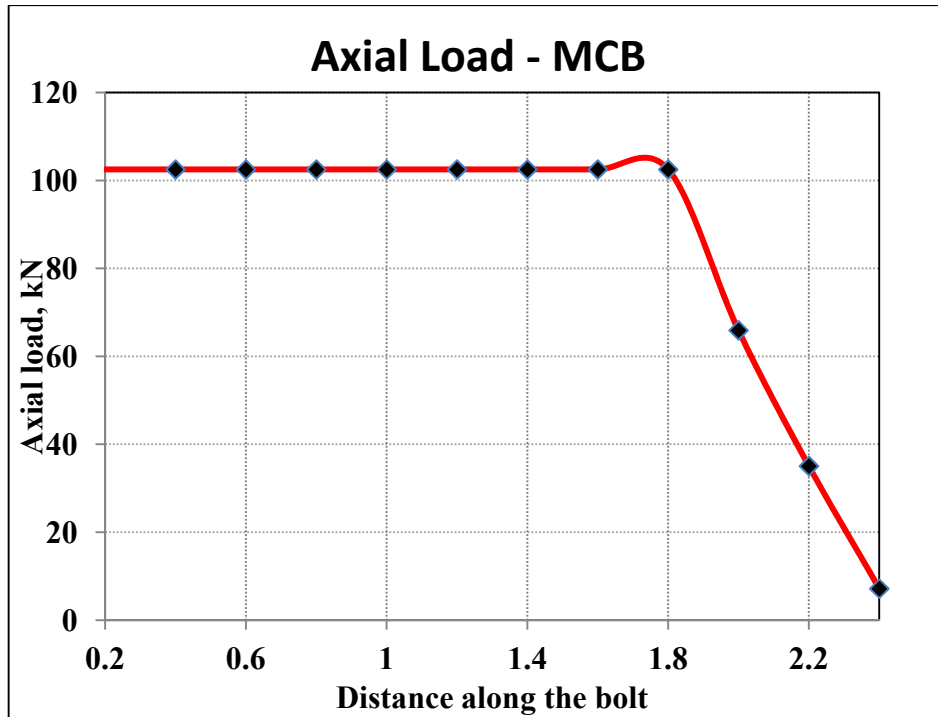


Figure 4-17 Axial load distribution along fully grouted MCB

#### 4.5.6 Parametric study

Two parametric studies were conducted as part of this project. One analysis was devoted to the effect of drift support performance while varying the modulus of the footwall rock mass and is done using FLAC. Another parametric study was also conducted by Wei (2010), in which the parameters of in situ stress ratio and the distance between the drift and nearby stopes were varied to examine the stability of the drift using Phse2 software. Parametric study conducted in FLAC was to examine the effect of footwall rock elastic modulus on the behavior of drift support system. In this analysis, the elastic modulus “E” of the footwall rock is varied while keeping all other properties same as in earlier analysis.

The various values of “E” used in this analysis are 40GPa, 50GPa, 65GPa and 100GPa. The value of 65 GPa is the original tested value, which is used in all other models. The main purpose of this analysis was to understand the behavior of the drift primary support system under

various stiffness of the rock mass in which it is placed. The results obtained for NW is shown in figure 4-18.

It can be observed from this that stiffer the rock mass, the lesser the loads which are imposed on to the supports. It can also be observed that the axial load on to the supports doesn't seem to vary for the rock mass having modulus between 40GPa and 50GPa. It suggests that modulus variation of 10GPa doesn't create any drastic changes in imposing the axial loads in support system. On the other hand, it was also observed that, if the footwall rock mass modulus is less than 40GPa, then the existing primary support system cannot sustain the collapse of the drift.

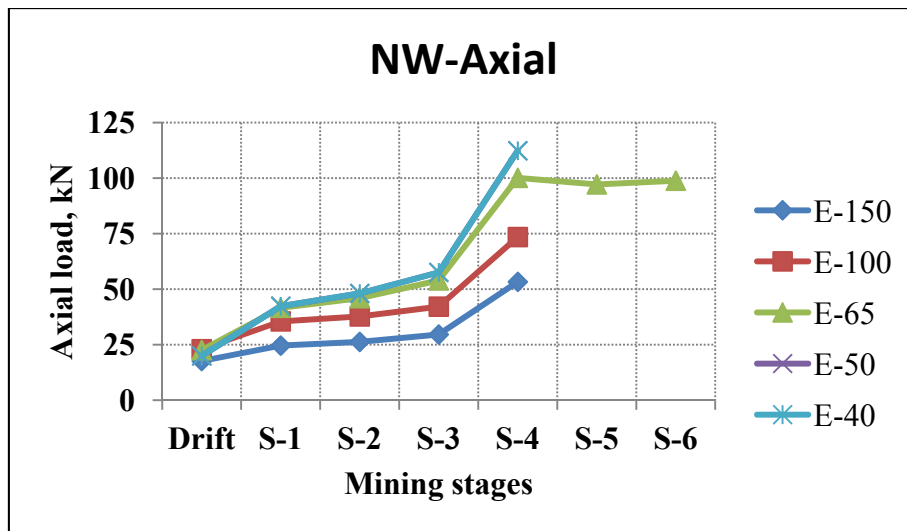


Figure 4-18 Axial loads with various rockmass modulus in primary supports

## **5 Model Calibration**

### **5.1 Introduction**

In order to have the confidence in the numerical model results, an instrumentation program was planned and implemented to calibrate the numerical model in terms of axial loads on the rockbolts and the wall deformations. Detailed description of the instrumentation program and the summary of the results are presented in this section. The comparison of predicted and the measured bolt axial loads are presented in this section. The rockbolts were instrumented with bolt load cells commercially known as “U-cells” to monitor the axial loads at the head of the bolt in three levels of # 1 Shear east. The maximum axial loads measured from the instruments in NW, SW and in the back are selected to compare with that of analytical results and presented in the following sections.

As part of the footwall study in # 1 Shear East from 4900 L to 5100L of Garson mine, rock mechanics instrumentation system such as Multi point bore hole extensor meters (MPBX), U-Cells and SMART cables was planned and installed. The data from these instruments were collected at regular intervals and analyzed. This section presents the details of the instrumentation program and the up to date analysis of the data from MPBX and U-Cells.

The main purpose of this instrumentation program was to monitor the in situ performance of the drift support system (rockbolts) and deformations around the drift under study. With this in mind MPBX were selected and installed for deformation monitoring in the walls and the back of the drift. For in situ monitoring of bolt axial load, a new instrument called U-cell was selected and installed. It is general and well proven that the MPBX is the best option for monitoring deformations. But the regular

practice of load monitoring is with the conventional anchor load cells (Figure 5-1), which has the following disadvantages (Mitri, 2011).

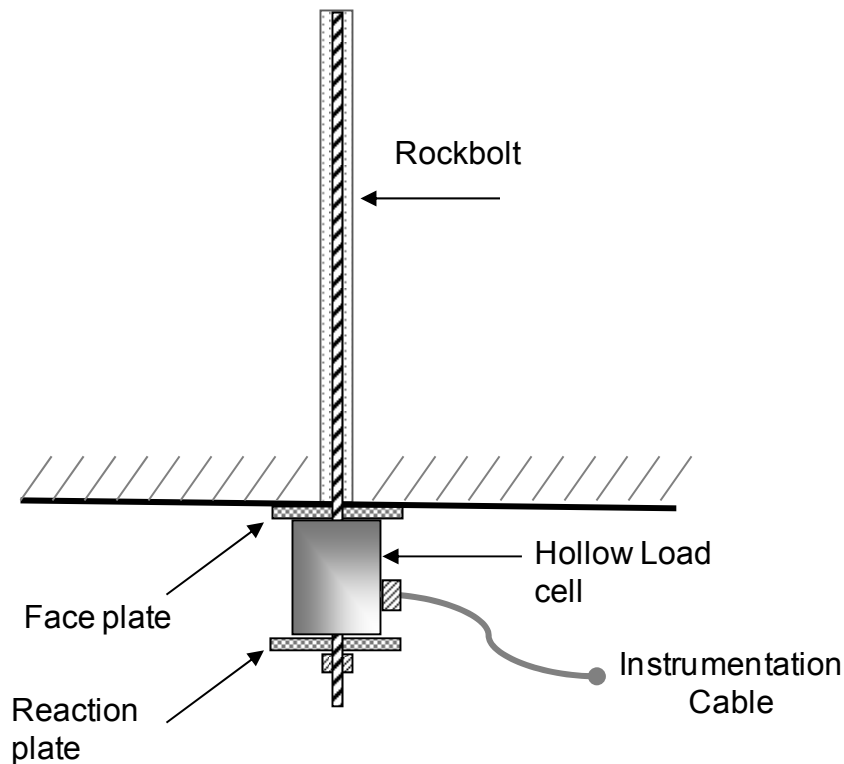


Figure 5-1 Conventional hollow load cell

- The vibrating wire strain gauge often breaks prematurely as it reaches its limit of 2500 to 3000  $\mu\epsilon$ , which is often not enough to ensure the measurement of the bolt yield load.
- The face and reaction plates must be placed perpendicular to the bolt to capture the correct force, which is not always possible in mining applications.
- The hollow load cell reduces the headroom of the gate road by at least 15 cm.
- Surface preparation is often required to make sure that the plates are parallel.

The new bolt load cell commercially known as, U-cell is used in this project to overcome the above and to get the other advantages those U-cell possess. A brief detail of the U-cell is given in the following section.

## 5.2 U-cell

The U-cell technique is applicable to virtually any type of rock anchor, such as mechanical rock bolt, cone bolt, grouted rebar, and forged head bolt. Detailed description and working of the U-cell is given elsewhere (Mitri, 2011; Hyatt and Mitri, 2012, Mitri et al, 2012). The U-cell (Figure 5-2) is a steel coupler attached to a rockbolt prior to installation that can measure the axial load at the head of the bolt. As already mentioned the maximum load in a fully grouted rebar is expected at the head of the rebar, so use of U-cell for monitoring the axial loads is appropriate and justified.

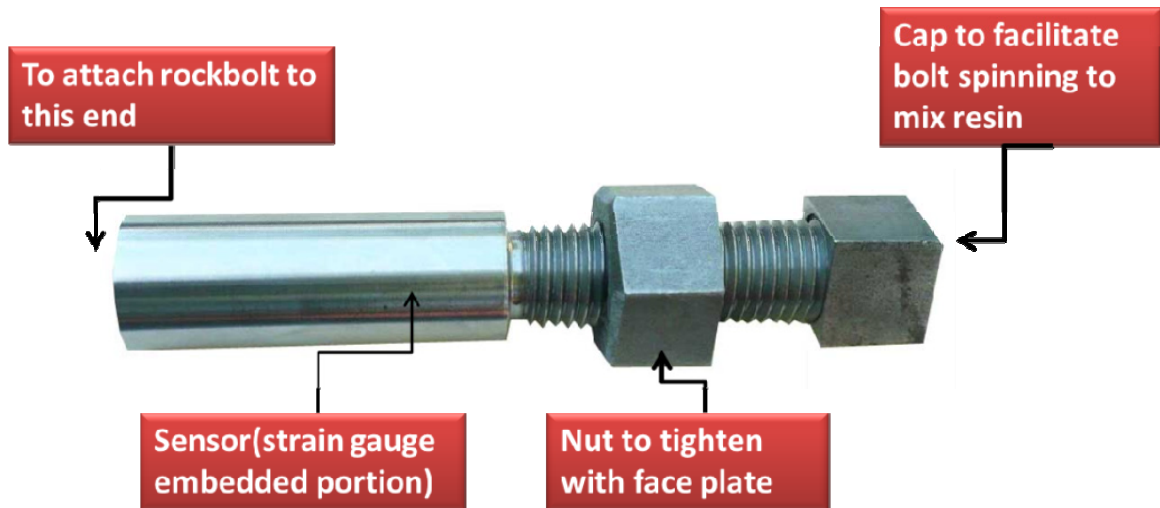


Figure 5-2 The U-cell, typical dia 31mm for 16mm or 19mm rockbolts, and 35mm dia for 22mm rockbolts

If the axial strain ( $\varepsilon$ ) in the U-cell is known, it is possible to calculate the axial load,  $F$  as follows:

$$F = \varepsilon \cdot E \cdot A \quad (5-1)$$

Where  $\varepsilon$  is the axial strain measured by the strain gauge embedded in the U-cell,  $A$  is the cross-sectional area of the U-cell where the strain gauge is located, and  $E$  is the modulus of elasticity of the steel from which the U-cell is manufactured. The underlying concept of the U-cell technology is to monitor the axial load,  $F$ , at the head of the bolt. In practice, the U-cell strain readings ( $R$ ) must be referenced to an initial unloaded state ( $R_0$ ), usually measured immediately prior to installation:

$$\varepsilon = f(R - R_0) \quad (5-2)$$

Referring to Equations (5-1) and (5-2), the axial load,  $F$  can be written as

$$F = f((R - R_0) \cdot A \cdot E) \quad (5-3)$$

An on-board digital interface unit for the U-cell performs the following tasks:

- i. zeroing the reading prior to installation by saving the offset into memory (Equation 3)
- ii. applying the temperature compensation

As a result, an accurate load reading can be directly displayed to personnel working in the vicinity of the instrumented rock bolt. The hand held readout unit and the new generation U-cells are shown in Figure 5-3.



Figure 5-3 The U-cell portable readout unit and the new generation U-cells

The U-cell is calibrated in laboratory with the designated data acquisition system which will be used in the field. The typical calibration sheet with the designated readout is shown in Figure 5-4 and the typical installation of U-cell in the field is shown in Figure 5-5.

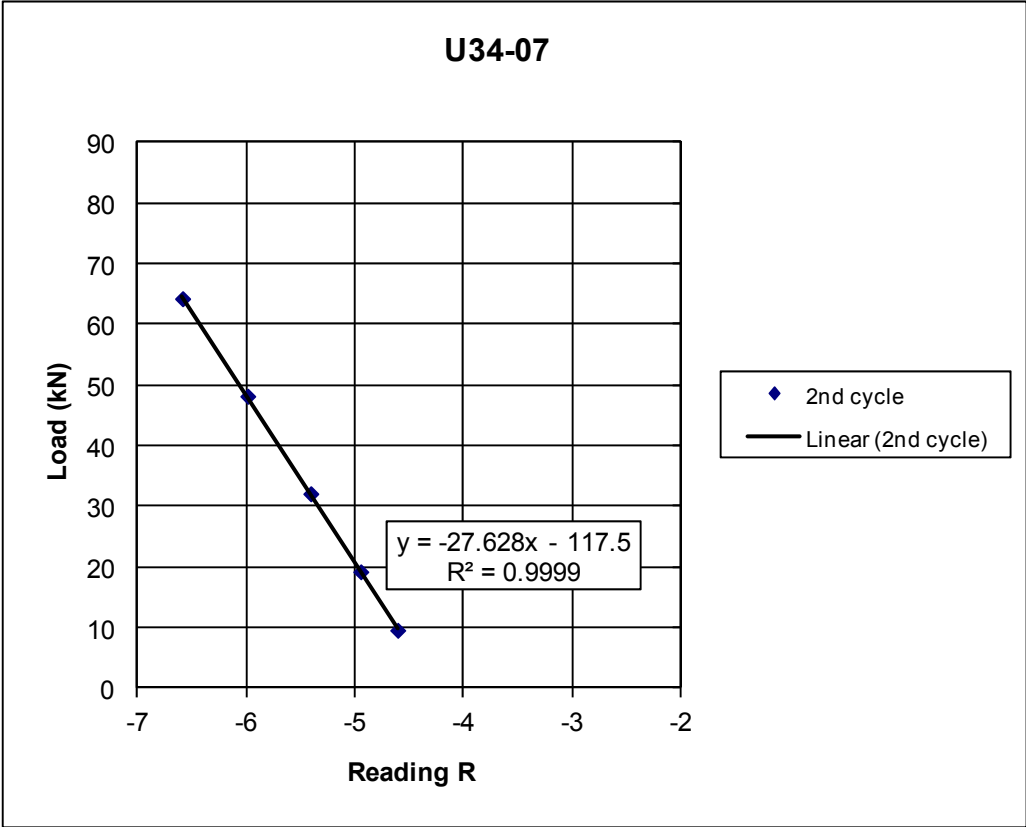


Figure 5-4 Typical calibration of U-cell in the lab



Figure5-5 Typical field installation of U-cell in a fully grouted rebar

### **5.3 Instrumentation program**

#### **5.3.1 No 1 Shear east – 4900 level**

As mentioned already, the study area is concentrated from 4900L to 5100L within No.1 Shear East. The details of the instruments planned, installed and their status in 4900L, 1 shear east is given in Table 5-1. Also the location of the particular instrument is shown in Figure 5-5. As can be seen from Table 5-1, to monitor the deformations from the wall as well as the back, five MPBX were planned and three of them were installed during September 2010 and the initial readings were taken. During the next visit in January 2011, all three instruments were found damaged due to movement of machines and mining operation. Due to this reason, there is no data to observe the mining induced deformations from this area. Efforts were made to revive these instruments, since it is only the lead cable that got cut but could not be successful. Three more MPBX were subsequently installed in place of those damaged during March 2012 and the monitoring is continued.

Table 5-1 Details of instruments at 1 Sh East 4900 level

Location		Wall/ Back	Instr ID	Instr Type	Date Installed	Remarks
Level	Zone					
4900	1SHE	Wall	4900/1SE-MPBX-W11	MPBX	9/23/2010	Damaged reinstalled on 12/21/2011
4900	1SHE	Wall	4900/1SE-MPBX-W12	MPBX	9/23/2010	“
4900	1SHE	Back	4900/1SE-MPBX-B13	MPBX	9/23/2010	“
4900	1SHE	Back	4900/1SE-Ucell-B3	U-Cell	20/10/2011	
4900	1SHE	Back	4900/1SE-Ucell-B22	U-Cell	20/10/2011	
4900	1SHE	Wall	4900/1SE-Ucell-W4	U-Cell	20/10/2011	
4900	1SHE	Wall	4900/1SE-Ucell-W2	U-Cell	20/10/2011	
4900	1SHE	Wall	4900/1SE-Ucell-W19	U-Cell	20/10/2011	
4900	1SHE	Wall	4900/1SE-Ucell-W14	U-Cell	20/10/2011	Rejected due to bad Installation

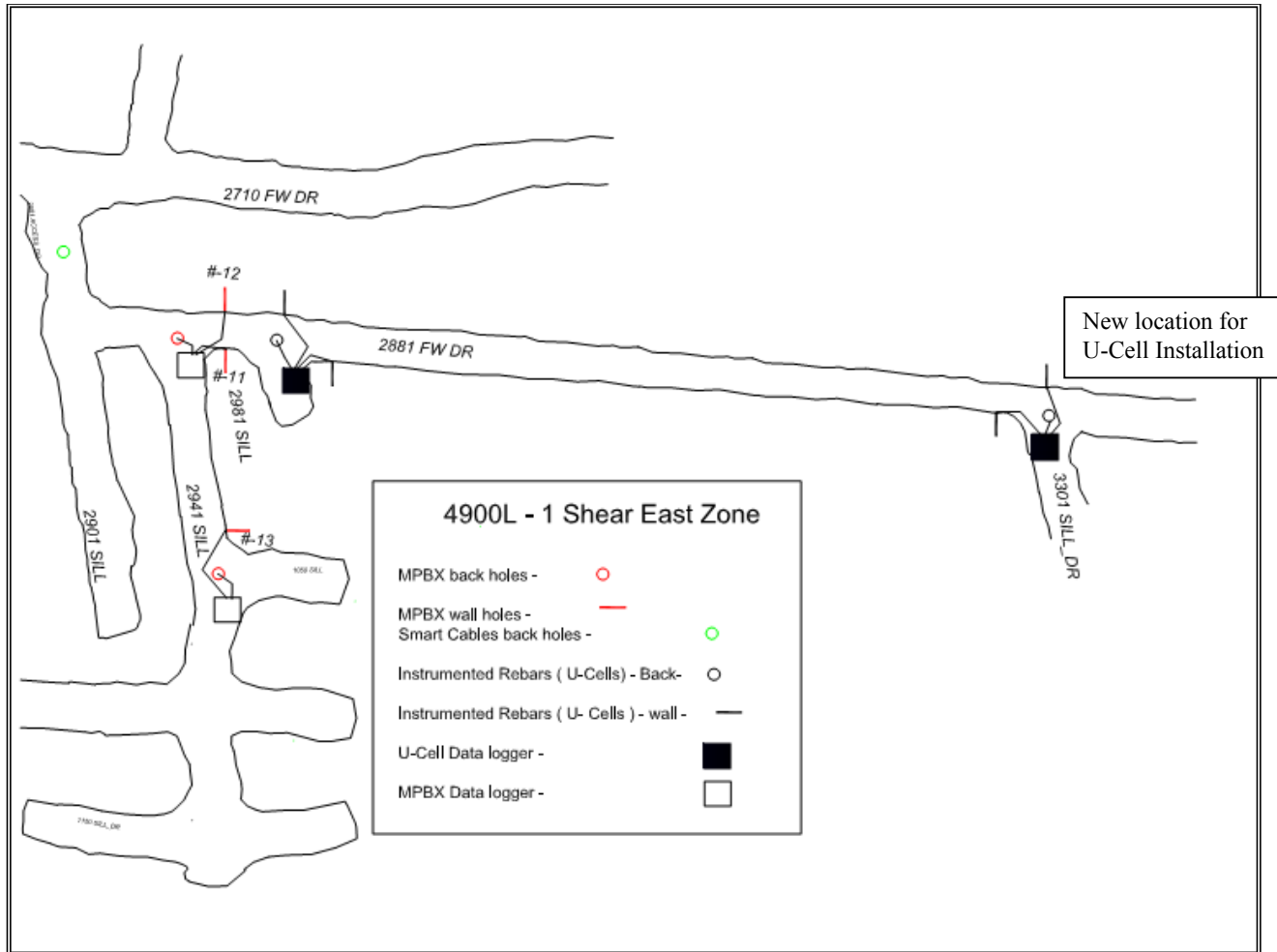


Figure 5-6 Plan showing the location of instruments, 4900level-1 SHE

### 5.3.1 No 1 Shear east – 5000 level

The details of the instruments planned, installed in 5000 level of 1Sh east and their status is given in Table 5-2. Also the location of the particular instrument is shown in Figure 5-7.

Table 5-2 Details of instruments at 1 Sh East 5000 level

Location		Wall/ Back	Instr ID	Instr Type	Date Installed	Remarks
Level	Zone					
5000	1SHE	Wall	5000/1SE-MPBX-W7	MPBX	9/23/2010	
5000	1SHE	Wall	5000/1SE-MPBX-W10	MPBX	9/23/2010	
5000	1SHE	Back	5000/1SE-MPBX-B8	MPBX	9/23/2010	
5000	1SHE	Back	5000/1SE-Ucell-B7	U-Cell	16/03/2011	
5000	1SHE	Back	5000/1SE-Ucell-B10	U-Cell	16/03/2011	
5000	1SHE	Back	5000/1SE-Ucell-B11	U-Cell	16/03/2011	
5000	1SHE	Wall	5000/1SE-Ucell-W5	U-Cell	16/03/2011	
5000	1SHE	Wall	5000/1SE-Ucell-W6	U-Cell	16/03/2011	
5000	1SHE	Wall	5000/1SE-Ucell-W12	U-Cell	16/03/2011	

As can be seen from the Table 5-2, to monitor the deformations from the wall as well as the back, five MPBX were planned and three of them were installed during September 2010 and the initial readings were taken. Regular monitoring of these instruments are carried out using both manual and data loggers. Also six U-Cells were planned and installed on the rebar to monitor the load on the support system during March 2011. Initially manual readings using hand held readout unit were taken for U-cells and later they were connected to dataloggers.

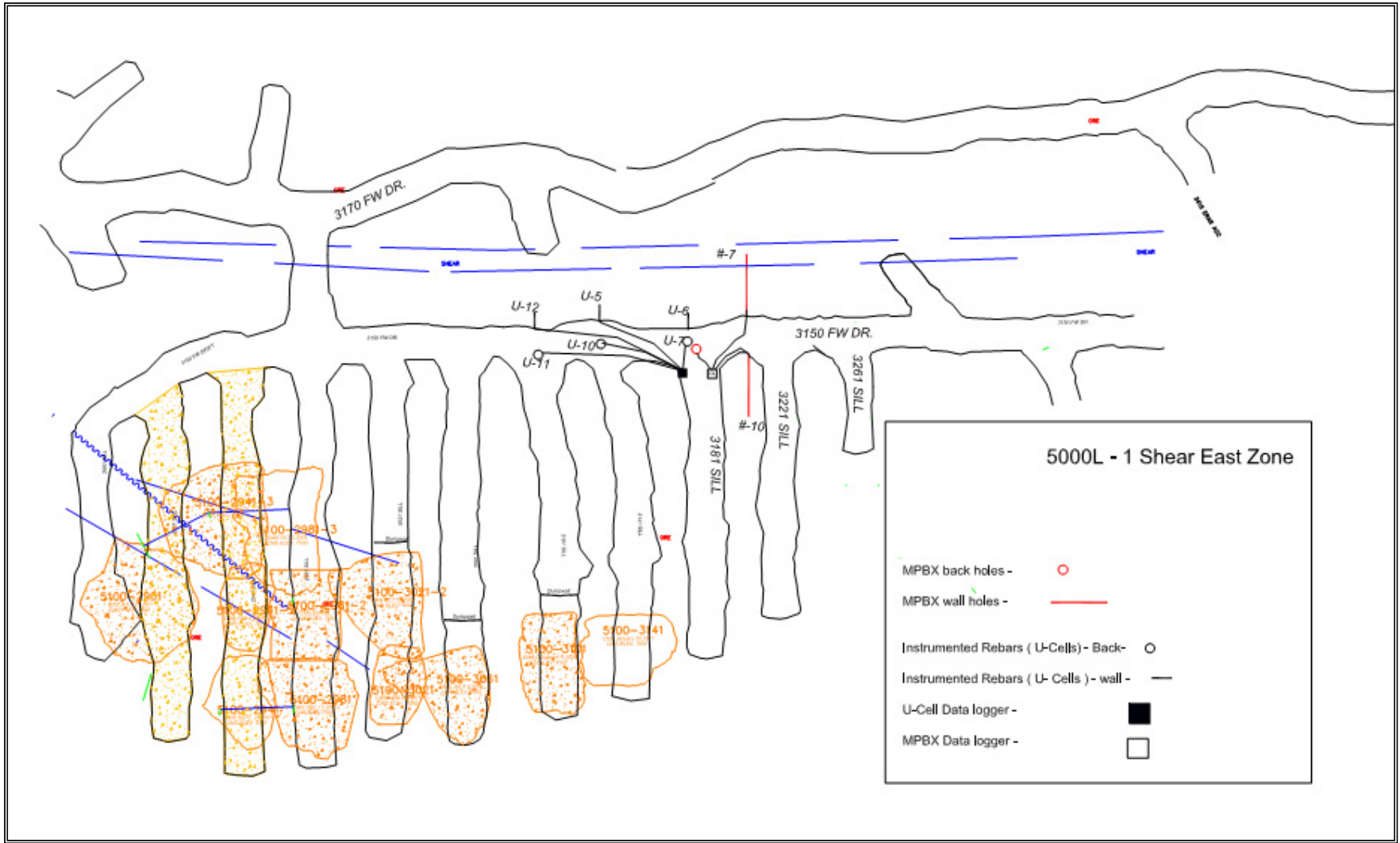


Figure 5-7 Plan showing the location of instruments, 5000 level-1 SHE

### 5.3.2 No 1 Shear east – 5100 level

The details of the instruments planned, installed and their status is given in Table 2-6. Also the location of the particular instrument is shown in Figure 5-8.

Table 5-3 Details of instruments at 1 SH E – 5100 level

Location		Wall/ Back	Instr ID	Instr Type	Date Installed	Remarks
Level	Zone					
5100	1SHE	Wall	5100/1SE-MPBX-W6	MPBX	9/23/2010	
5100	1SHE	Wall	5100/1SE-MPBX-W4	MPBX	9/23/2010	
5100	1SHE	Wall	5100/1SE-MPBX-W1	MPBX	9/23/2010	
5100	1SHE	Wall	5100/1SE-MPBX-W3	MPBX	9/23/2010	
5100	1SHE	Back	5100/1SE-MPBX-B5	MPBX	9/23/2010	
5100	1SHE	Back	5100/1SE-MPBX-B2	MPBX	9/23/2010	
5100	1SHE	Wall	5100/1SE-Ucell-W16	U-Cell	27/01/2011	
5100	1SHE	Wall	5100/1SE-Ucell-W21	U-Cell	27/01/2011	
5100	1SHE	Wall	5100/1SE-Ucell-WX	U-Cell	27/01/2011	Rejected
5100	1SHE	Back	5100/1SE-Ucell-BX	U-Cell	27/01/2011	Rejected

As can be seen from Table 5-3, to monitor the deformations from the wall as well as the back, Six MPBX were planned and installed during September 2010 and the initial readings were taken. Regular monitoring of these instruments and the data

analysis are carried out. Also six numbers of U-Cells were planned and installed on the rebar to monitor the load on the support system during January 2011. Initially due to problem in reaching the instrument, readings from only U-16 and U-12 were taken manually, as the other locations are not approachable. At a later stage all these instruments are hooked to the data logger.

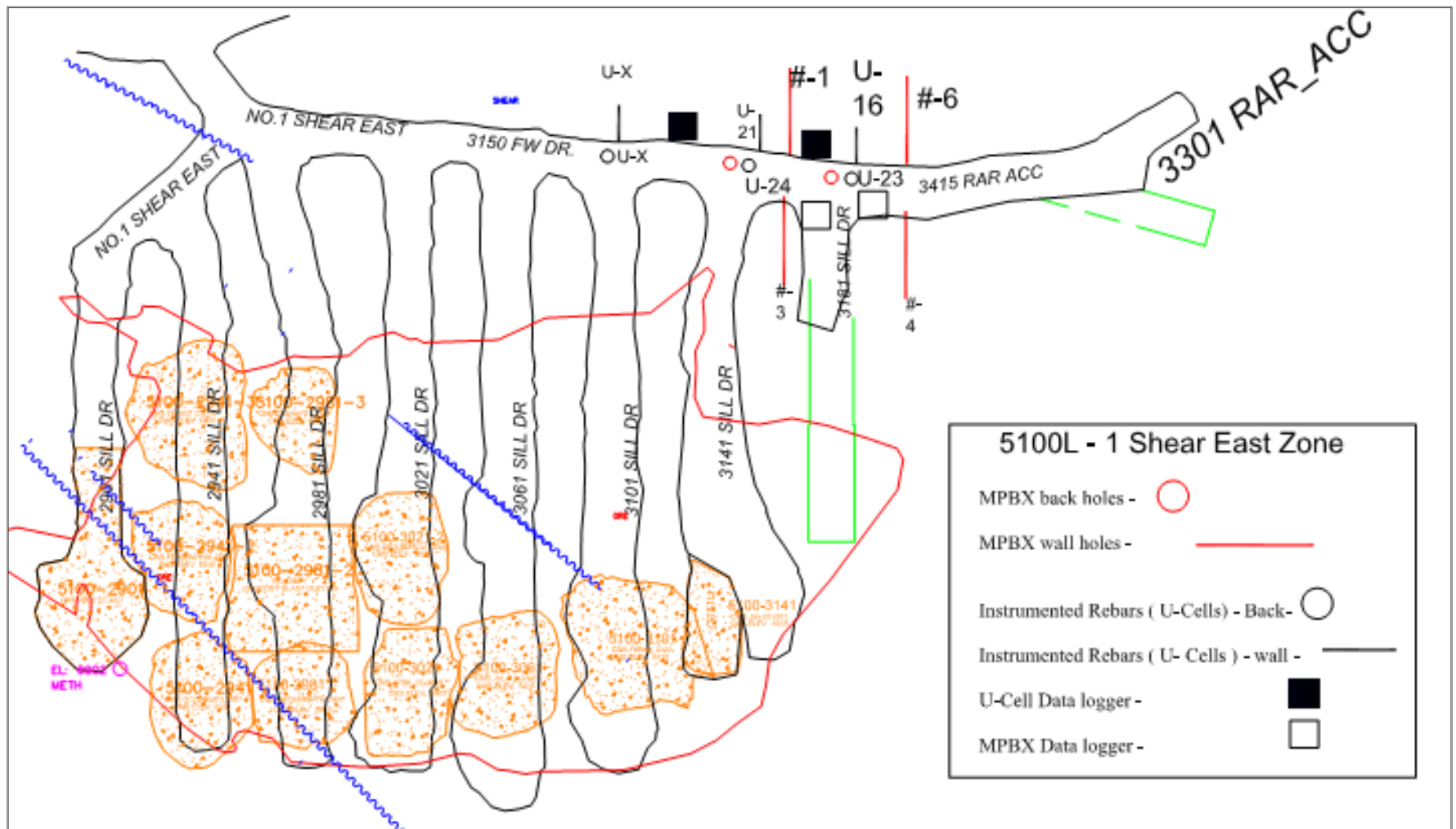


Figure 5-8 Plan showing the location of instruments, 5100 level-1 SHE

### **5.3.3 Summary of instrumentation results**

A summary of the instrumentation data analysis up to date is given in the following sections. Basically two parameters such as deformation around the drift and axial load on the fully grouted rebars/MCB were measured in the study area. The instrumentation plan and the type of instruments installed in all the three levels were given already in the earlier sections.

#### **5.3.3.1 Axial loads**

Twenty U-cells were installed on three mine levels of the case study area to monitor the axial load on the rock bolts in response to the nearby mining. The U-cells were installed both on fully grouted rebars and on modified cone bolts (MCB). All the U-cells were installed in the footwall drift walls, and the back. The initial loads on the bolt head measured immediately after installation are presented in Table 5-4. It is interesting to note the wide variation of bolt pretension load at installation. These vary from 7.9 kN to 58.0 kN with an average of 20.3kN, while a pretension load of 10-20 kN is considered adequate. Higher loads of more than 40 kN should be avoided as these will reduce the “remaining” capacity of the bolt (Raju et al. 2012)

The summary of maximum axial loads measured by U-cells installed on to the fully grouted rebars is given in Table 5-5. U-cells were being monitored regularly using both manual read out unit and also with data loggers. In case of 5100L maximum axial load measured in the NW is about 111kN before the U-cell in this location was damaged due to mining operations. It was about 60kN in the back. At this time the same level mining was already started.

Table 5-4 Initial loads on rockbolts, soon after installation

U-Cell ID	Rock support	Mine Level(ft)	Location	Load (kN)
2	MCB	4900	South Wall	9.1
4	MCB	4900	North Wall	16.2
14	MCB	4900	South Wall	18.0
19	MCB	4900	North Wall	19.9
3	MCB	4900	Back	9.6
22	MCB	4900	Back	24.0
5	Rebar	5000	North Wall	14.0
6	Rebar	5000	North Wall	26.0
12	Rebar	5000	North Wall	17.0
7	Rebar	5000	Back	18.4
10	Rebar	5000	Back	9.0
11	Rebar	5000	Back	21.0
16	Rebar	5100	North Wall	7.9
21	Rebar	5100	North Wall	72.4*
23	Rebar	5100	Back	36.1
24	Rebar	5100	Back	58.5
Average				20.3
Standard deviation				12.9

(\* load after three months of installation)

Table 5-5 Axial loads on rebars by in situ measurements (kN)

Location	5100 level	5000level	4900level
Back	60	68	10
South Wall	-	-	58
North Wall	111	107	100

In the case of 5100L maximum axial load measured in the NW is was about 111kN before the U-cell in this location got damaged due to mining operations. It is about 60kN in the back.

In the case of 5000L, the maximum axial load in the back is 68kN and in the NW it is 107kN. It is to be noted here that the mining is still not reached near to the location of instruments. However in the case of 5100L mining reached near the instruments and instruments got damaged as well due to mining. In view of this more axial loads can be expected from the instruments of 5000L. In case of 4900L maximum axial load is 100kN in the NW, 58kN in the SW and 10kN in the back.

As can be seen from the Table 5-5, rebars in the North wall of the drift experiencing higher axial loads than that of the South wall and back. It is worth noting here that some of the U-cell instruments got damaged due to the mining operations. As explained in the modeling results, the axial loads reach maximum and yield once the same level mining begins. At the time of writing this thesis, monitoring of some of the instruments is still under way in 4900L 1 shear east.

Comparisons of computed and measured axial loads are presented in Table 5-6. Maximum axial loads for North wall, South wall and back along with average pretension loads are presented. It can be noted that,

as expected in the numerical model, North wall rockbolts are carrying higher loads than the south wall and back rockbolts. Accounting for the pretension loads in the computed loads improves the correlation between the computed and the measured results.

Table 5-6 Comparison of computed and measured axial loads (kN)

Location	level	Computed	Measured	Pretension load	Computed (including pretension)	Computed-to-measured ratio
Back	5000	49	68	9	58	0.85
South Wall	4900	69	58	9.1	78.1	1.35
North Wall	5100	113	111	7.9	120.9	1.09

### Deformations

The maximum deformations measured from 5100L of I shear east is given in Table 5-7. The typical graph showing the deformation pattern from both North wall and south wall is shown in Figure 5-9 and Figure 5-10.

Table 5-7 Summary of deformation in 5100L

5100 Level		
Location	Max, mm	Min,mm
Back	1.01	0
South Wall	34.31(SW-pillar nose)	0.31
North Wall	10.98	-

It can be seen from the Table 5-7 that the maximum deformations measured is in the order of 34.31mm in case of South wall and in case of

North wall it is 11.00mm. Also it can be seen from the Figures 5-9 and 5-10, that the maximum relative deformation with respect to toe at 10m is at the surface of the wall. This can be evidenced from the Figure 5-11, where the location of the South wall MPBX is situated. Further the sudden raise of the deformation in Figures 5-9&5-10 is attributed to the production blasts in the nearby stopes. This was confirmed and reported by Lindsay (2012). The instruments at both the locations were damaged as the mining approached nearby in September 2012. Also Abdellah et al (2012) confirmed that the field deformation observations are in good agreement with estimated deformations from his FLAC3D model of the same area.

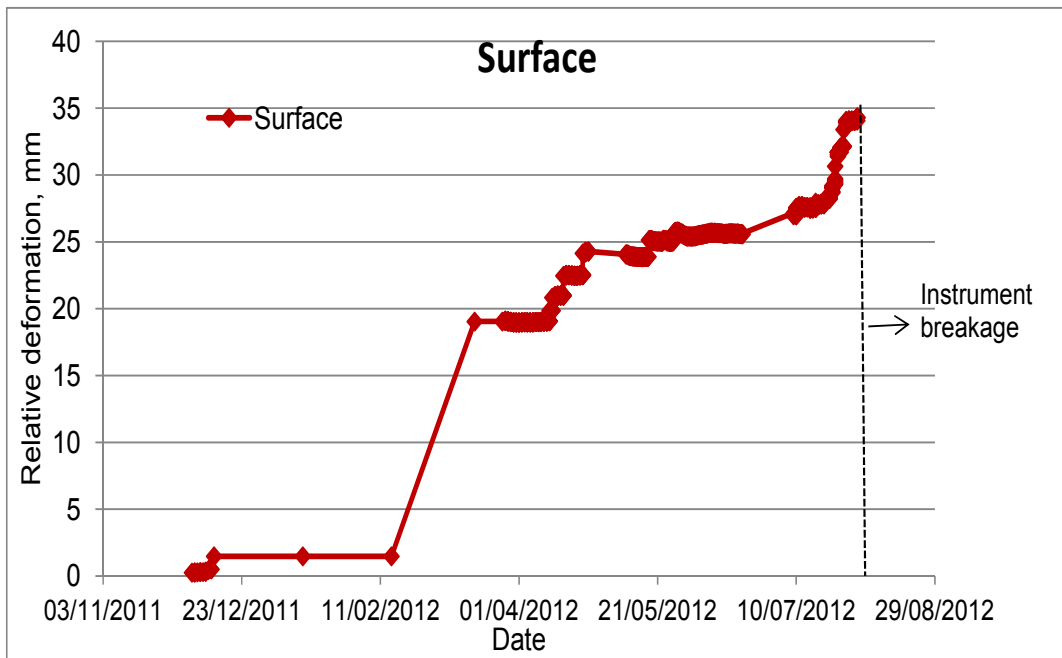


Figure 5-9 Relative surface deformation with respect to toe at 10m - MPBX - ID-4-5100L-SW-Pillar

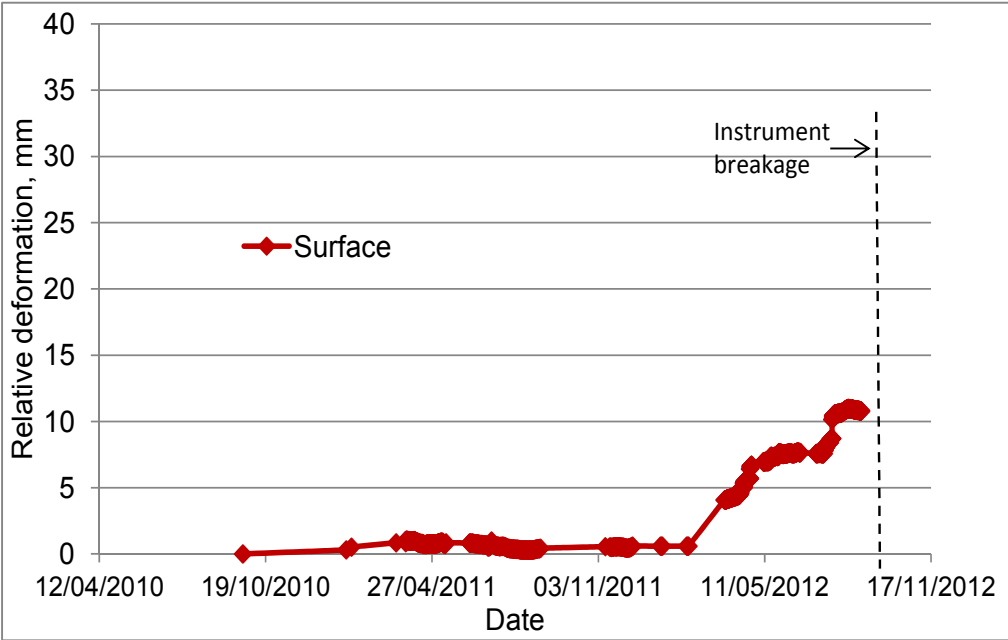


Figure 5-10 Relative surface deformation with respect to toe at 10m -  
MPBX-ID-6-5100L- NW



a) Surface rock damage at MPBX location



b) Rock fracture near the MPBX location

Figure 5-11 Wall damage that caused high surface deformations at 5100L-SW pillar nose bet 3181 sill and 3221 sill

## 6 Dynamic Modeling of Drift Performance

### 6.1 Introduction

This Chapter presents preliminary dynamic analysis of drift performance. The modeling set up, boundary conditions, and the modeling procedure is explained in the following sections followed by the dynamic analysis of drift performance. Numerical modeling solution for dynamic analysis is reported by many authors (e.g Clough and Penzen, 1975). Dynamic analysis option in FLAC 2D enables the dynamic modeling of underground openings, Slopes and other civil engineering structures subjected to seismic activity. In FLAC2D, the calculations are based on the explicit finite difference scheme to solve the full equations of motion, using lumped grid-point masses derived from the real density of surrounding zones. With the dynamic analysis option the capability of FLAC expands to a range of dynamic problems such as earthquake engineering, seismology and mine rockbursts (Itasca, 2011).

Conducting a dynamic analysis is often very complicated and requires a systematic approach to set up the dynamic model and requires considerable amount of insight in to its interpretation. FLAC manual on dynamic analysis recommends following procedure for conducting dynamic numerical analysis with FLAC.

- Ensure that the model conditions satisfy the requirements for accurate wave transmission.
- Specify appropriate mechanical damping, representative of the problem materials and input frequency range.
- Apply dynamic loading and boundary conditions with a time history
- Set up facilities to monitor the dynamic response of the model

Fully non-linear analysis method is used in FLAC. An overview of practical applications of different methods with non linear methods of dynamic analysis is given by Byrne et al. (2006).

### **6.1.1 Dynamic Modeling Setup**

Following features must be considered for a dynamic analysis:

- Boundary conditions
- Dynamic loading
- Wave transmission through the model
- Damping

### **6.1.2 Boundary Conditions**

In FLAC, a region of material subjected to external and/or internal dynamic loading, is modeled by applying a dynamic boundary condition. This boundary condition can be specified either at the model boundary or at internal grid points. To avoid wave reflections at model boundaries, either quiet (viscous), free-field boundary conditions are set. In addition to these two boundary conditions, three-dimensional radiation-damping boundary condition is also available in FLAC. In the present analysis, quiet boundary conditions were specified for the analysis and are described in the following section.

#### **6.1.2.1 Quiet Boundary Conditions**

The modeling of geomechanics problems involves media which, at the scale of the analysis are better represented as unbounded (Itasca, 2011). Also the manual on dynamic analysis of FLAC code explains that the deep underground excavations are normally assumed to be surrounded by an infinite medium, while surface and near surface structures are assumed to lie on a half-space. Numerical methods relying on the discretization of a finite region of space require that appropriate conditions be enforced at the artificial numerical boundaries. In static

analysis, fixed or elastic boundaries can be realistically placed at some distance from the region of interest and the fixed boundary effects vanishes at some particular distance, however in dynamic analysis the same boundaries may reflect the dynamic waves, increasing the magnitude of vibrations. The use of larger model boundaries would minimize this problem as the material damping will absorb most of the energy reflected from far boundaries. Figure 6-1 shows the quiet boundaries around the model with internal dynamic loading.

Another option to overcome this wave reflection at boundaries, is to use quiet(absorbing) boundaries(Itasca, 2011). Many formulations have been presented for modeling quiet boundaries (e.g,Lysmer and Kuhlemeyer 1969).

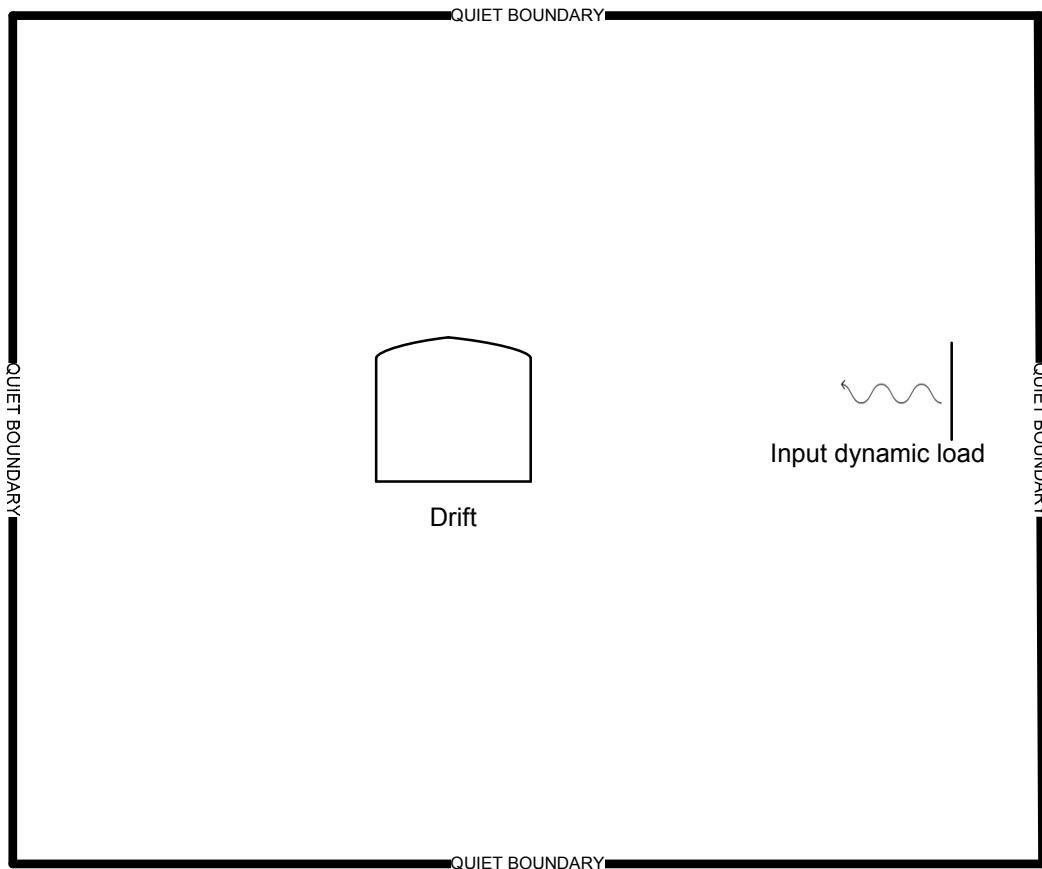


Figure 6-1 Quiet boundary conditions

### 6.1.3 Application of Dynamic Input

In *FLAC*, the dynamic input can be applied in one of four ways:

- (a) an acceleration history;
- (b) a velocity history;
- (c) a stress (or pressure) history; or
- (d) a force history.

Dynamic input is usually applied to the model boundaries with the **APPLY** command. Accelerations, velocities and forces can also be applied to interior grid points by using the **INTERIOR** command. Note that the free-field boundary is not required if the only dynamic source is within the model. The history function for the input is treated as a multiplier on the value specified with the **APPLY** or **INTERIOR** command. The history multiplier is assigned with the **hist** keyword and can be in one of three forms:

- a table defined by the **TABLE** command;
- a history defined by the **HISTORY** command; or
- a *FISH* function.

With **TABLE** input, the multiplier values and corresponding time values are entered as individual pairs of numbers in the specified table; the first number of each pair is assumed to be a value of dynamic time. The time intervals between successive table entries need not be the same for all entries. Note that the use of tables to provide dynamic multipliers can be quite inefficient compared to the other two options. When using the **HISTORY** command to derive the history multiplier, the values stored in the specified history are assumed to be spaced at constant intervals of

dynamic time. The interval is contained in the data file that is input with the **HISTORY read** command and associated with a particular history number. If a **FISH** function is used to provide the multiplier, the function must access dynamic time within the function, using the *FLAC* scalar variable **dytime**, and compute a multiplier value that corresponds to this time.

Dynamic loading derived from a *FISH* function is used in this analysis. Dynamic input can be applied either in the *x*- or *y*-direction corresponding to the *xy*-axes for the model, or in the normal and shear directions to the model boundary. Certain boundary conditions cannot be mixed at the same boundary segment (Itasca, 2011). One restriction when applying velocity or acceleration input to model boundaries is that these boundary conditions cannot be applied along the same boundary as a quiet (viscous) boundary condition because the effect of the quiet boundary would be nullified (Itasca, 2011)

A velocity wave may be converted to a stress wave using the formula

$$\sigma_n = 2(\rho C_p) v_n \quad (6.1)$$

or

$$\sigma_s = 2(\rho C_s) v_s \quad (6.2)$$

Where  $\sigma_n$  = applied normal stress;

$\sigma_s$  = applied shear stress;

$\rho$  = mass density;

$C_p$  = speed of *p*-wave propagation through medium;

$C_s$  = speed of *s*-wave propagation through medium;

$v_n$  = input normal particle velocity; and

$v_s$  = input shear particle velocity.

As mentioned already, dynamic input in the form of velocity wave derived from a FISH function is applied within the model boundary at a distance of 80m ( assuming that majority of the rockbursts are originating around the dyke, which is approximately 80m away from the drift in the case study area) from the drift opening as shown in Figure 6-2. The applied input dynamic load is varied so as to see the effect of the applied dynamic load at the drift opening surfaces.

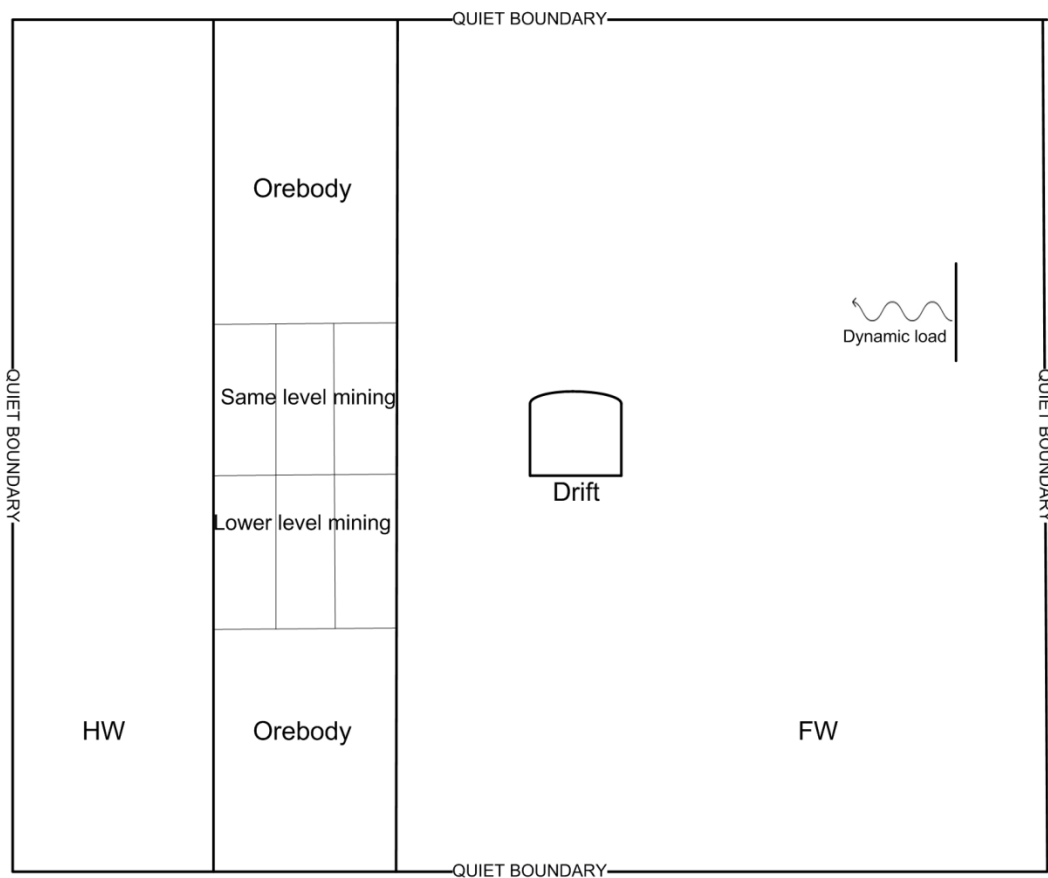


Figure 6-2 Model geometry with input loading and boundary conditions for dynamic modeling

### 6.1.3.1 Wave transmission through model

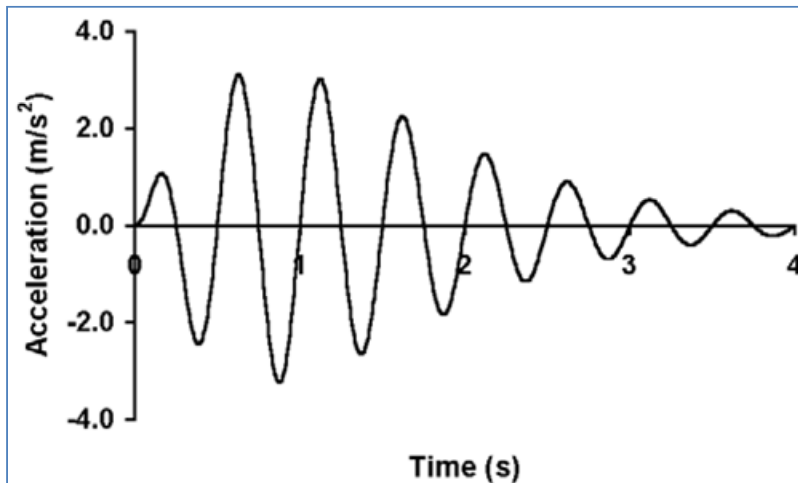
For the accurate representation of wave transmission through a model, the spatial element size,  $\Delta l$ , must be smaller than 1/10 or 1/8 of

the wave length associated with highest frequency component of the input wave ( Itasca, 2011).

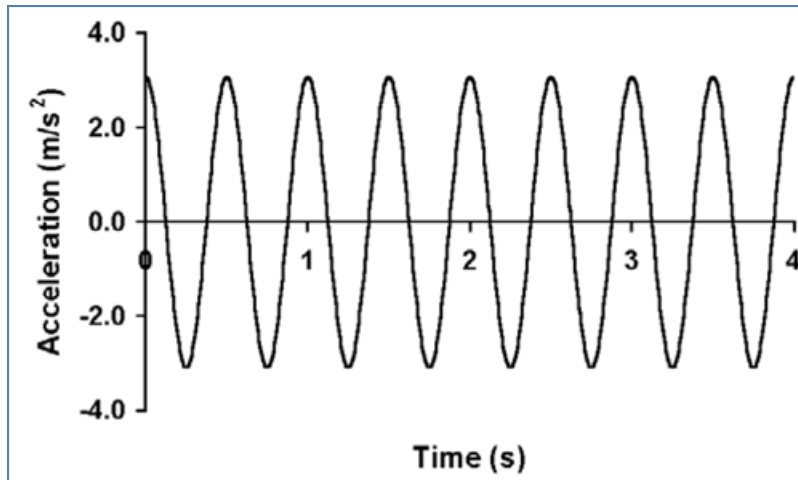
$$\Delta l \leq \frac{\lambda}{10} \quad (6.3)$$

Where  $\lambda$  is the wave length

Two types of waves as a sinus function can be applied as a dynamic load. Increasing-diminishing wave and constant amplitude wave are the two types of waves as shown in Figure 6-3. Genis and Gercek(2003), showed that the effect of both types of wave are not significantly different after comparing the effect of two types of waves as dynamic input load on underground drift due to earth quake. Also the same authors suggest that instead of actual seismic records, simplified wave types with equivalent features can be used to study the effect of dynamic loadings.



a) Sinusoidal function with an increasing-diminishing amplitude



a) The sinusoidal function with constant amplitude

Figure 6-3 Two types of waves for dynamic loading (Genis and Gercek, 2003)

#### 6.1.4 Mechanical damping

The region of the material within the model geometry, when subjected to dynamic loading, should reproduce in magnitude and form the energy losses in the natural system. This is achieved by the damping in dynamic numerical analysis. However in soil and rock, natural damping is mainly hysteric i.e .independent of frequency ( Itasca, 2011). According to the FLAC dynamic manual, 2011, Rayleigh damping is commonly used to provide damping that is approximately frequency-independent over a restricted range of frequencies. Another damping option available in FLAC is known as “hysteric damping”. For routine engineering design, FLAC recommends to use an approximate representation of cyclic energy dissipation, particularly when using simple plasticity models such as Mohr-Coulomb and the choice is between the Rayleigh damping and hysteric damping. Guidelines for selecting damping parameters are given in the FLAC manual. For geological materials, damping commonly falls in the range of 2 to 5 % of critical; for structural systems, 2 to 10% is representative (Biggs, 1964). According to Saharan (2004), inherently, rock is a good damper itself. Further damping is provided by energy

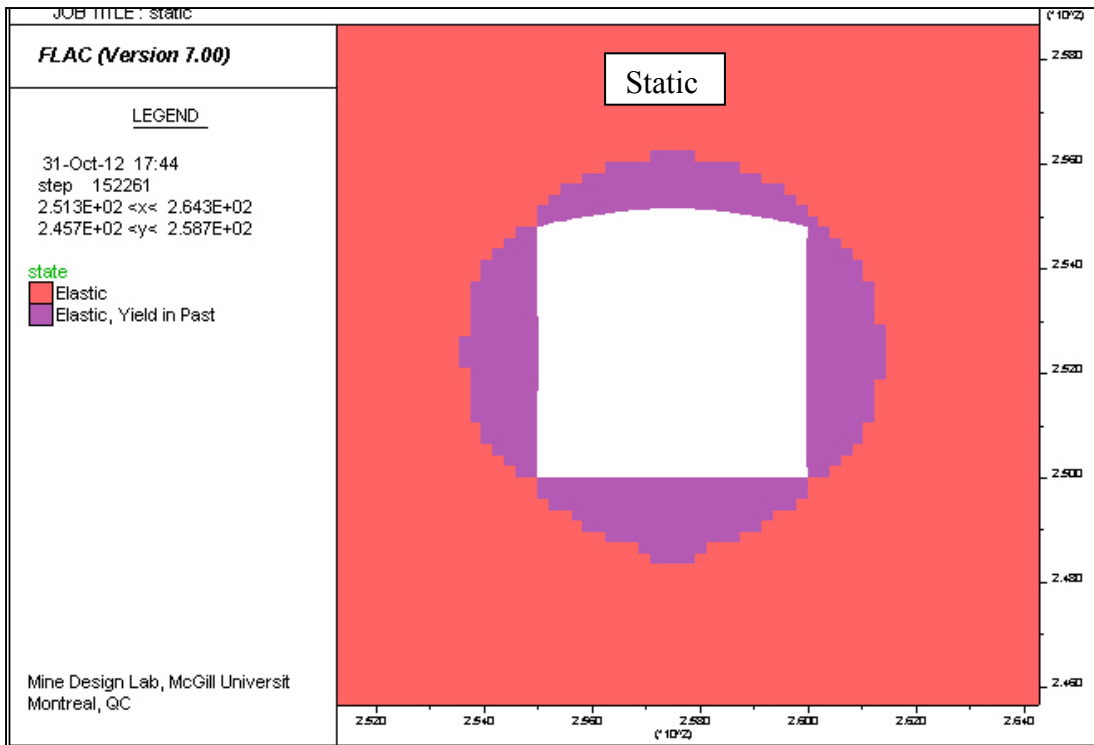
consumed in the fracturing process (numerically, in plasticity) during wave propagation. The numerical model should reflect such typical damping characteristics. Also, damping in natural material is hysteretic, so he cautions that, monotonic damping should be avoided to negate the possibility of over damping.

## **6.2 Dynamic analysis**

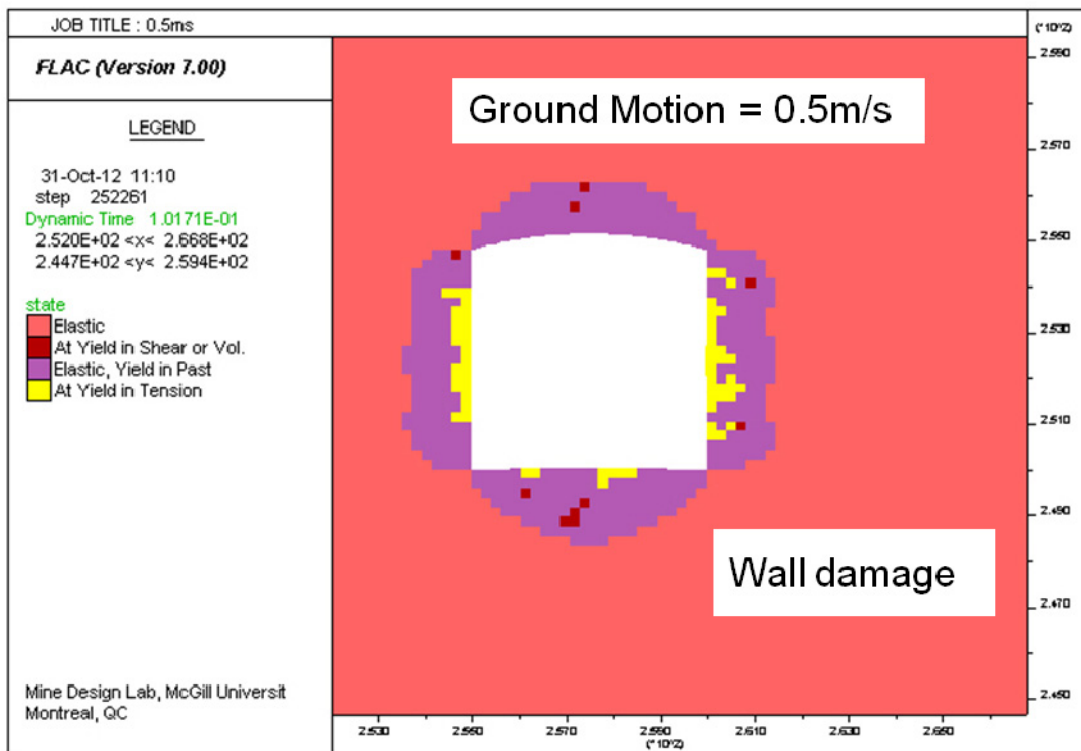
The performance of drift support system in the regions of seismic activity is important not only under static conditions but also during seismic events. The behavior of drift support system under dynamic loading should be considered for effective selection and design of the supports under dynamic conditions. This section presents the results of a preliminary dynamic analysis of the effect of dynamic loading on the performance of drift supports (rockbolts) using finite difference numerical modeling code, FLAC2D. The same model geometry used in static analysis (chapter 4) is used for this analysis. The effect of seismic wave peak particle velocity on the drift support system is examined. Wall damage, extent of yield axial loads induced in the supports (rockbolts) and displacement conditions around the drift is used to determine the effect of dynamic loads on the drift support system.

### **6.2.1 Dynamic performance of drift without support**

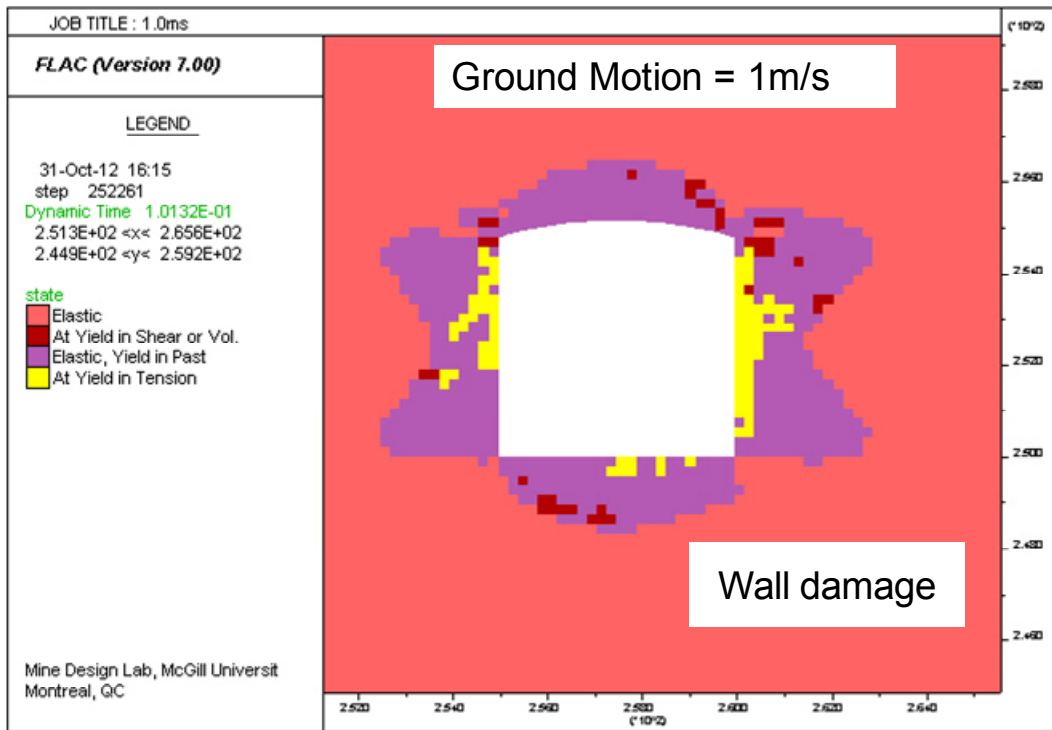
The effect of seismic wave peak particle velocity on the drift stability was examined in this case. Various magnitudes of velocity as a dynamic load are applied far from the drift to simulate the rock burst that is occurring near the dyke. The performance of the stability of the drift under the above dynamic situations is presented in Figure 6-4



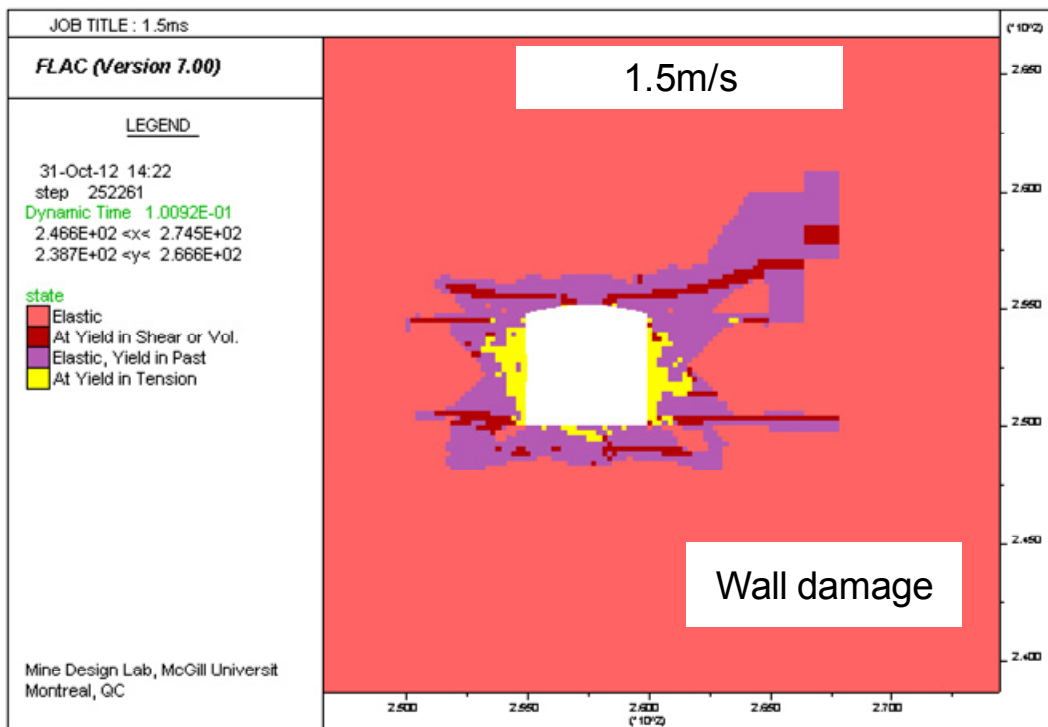
a) Rock mass yielding around the drift during static analysis( no wall damage)



b) Rock mass yielding and wall damage with 0.5m/s PPV



c) Rock mass yielding and wall damage with 1.0m/s PPV



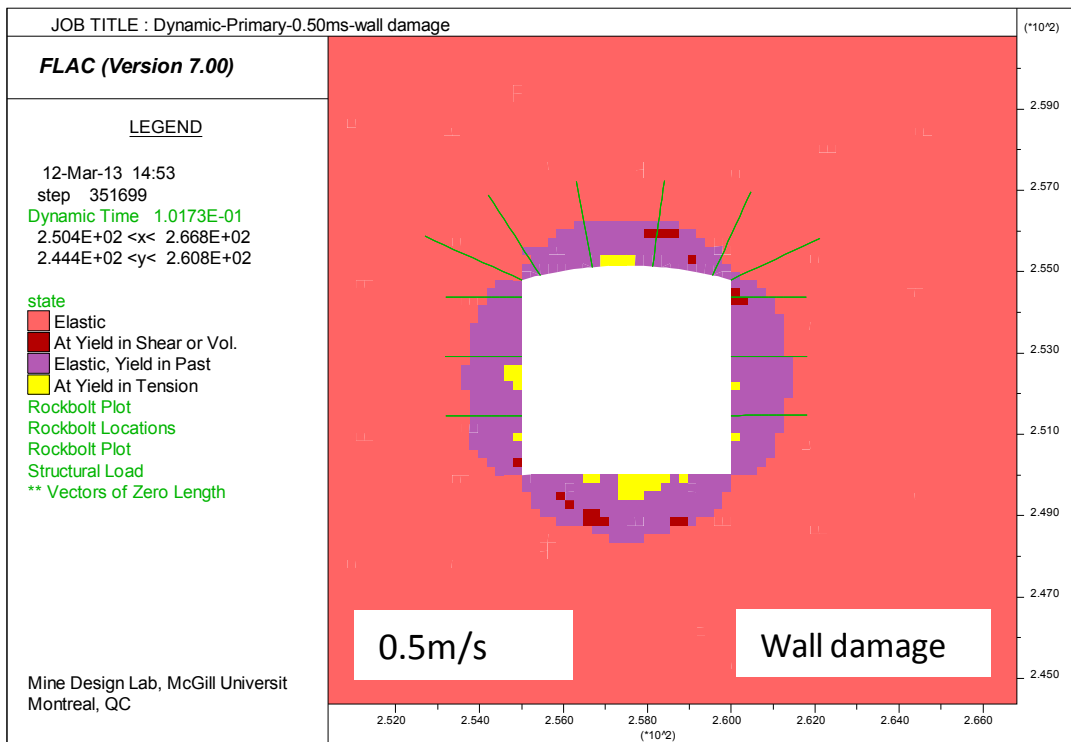
d) Rock mass yielding and wall damage with 1.5m/s PPV

Figure 6-4 Drift behaviour under dynamic loading without supports and no mining

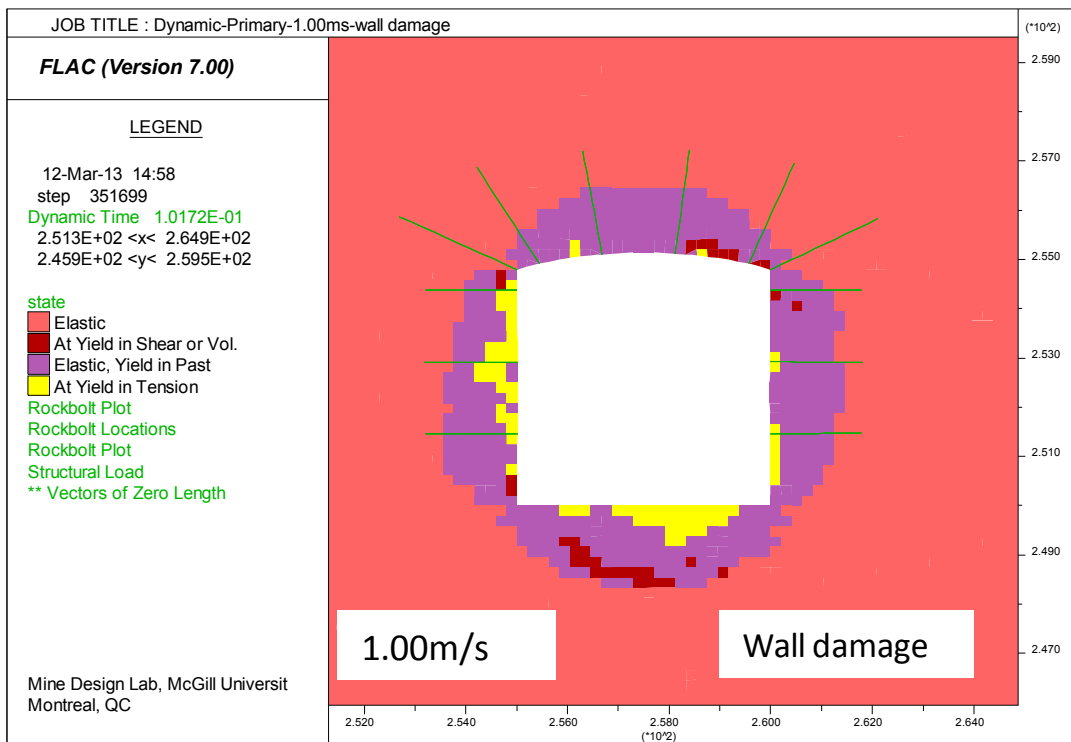
As can be seen from Figure 6-4, the wall damage due to tension is progressing as the ground motion increases. Damage due to tension, however is not significant in the back of the drift, where as the shear failure can be observed in the back particularly at the higher ground motion levels. On the other hand extent of rock mass yielding around the drift is uniform for lower levels of ground motion. The same is not uniform for higher levels of ground motion and in that case it extends more towards the source of the seismic event.

### **6.2.2 Dynamic performance of drift primary support**

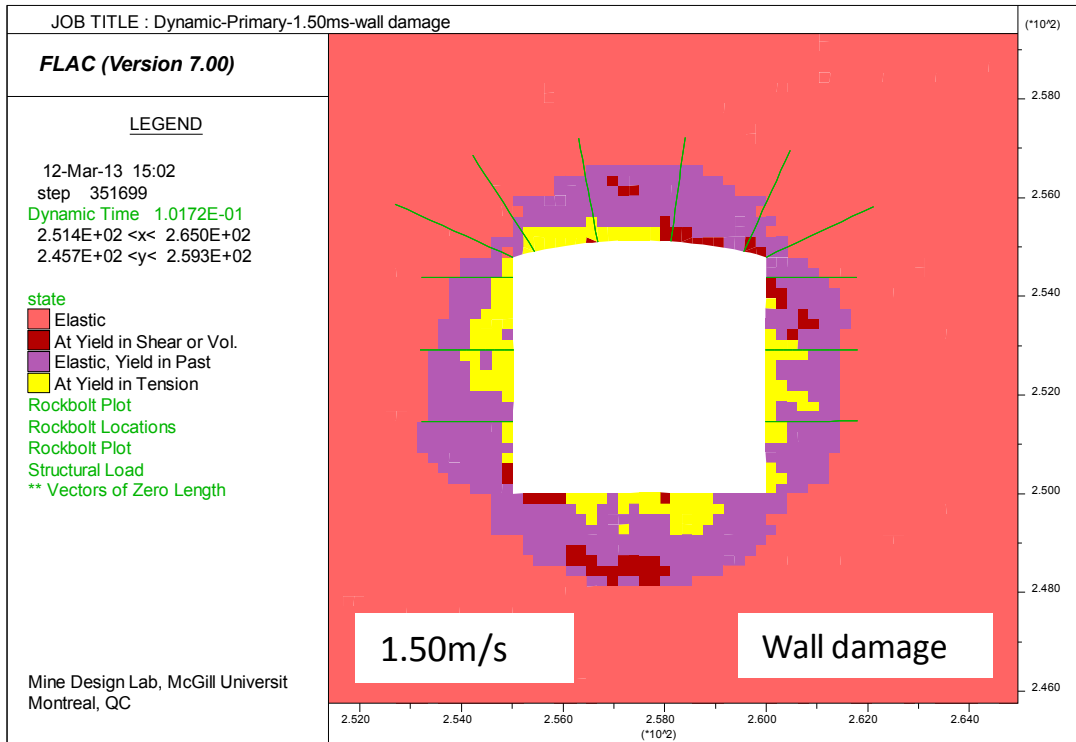
The performance of the drift primary support was examined by subjecting the drift to a dynamic loading as explained in previous section. The drift behavior in terms of wall damage and extent of yielding due to various levels of ground motion without any stope sequencing is shown in Figure 6-5. The results show that with the primary supports in place, yielding of the rock mass is uniform around the drift until the ground motion level of 2.0m/s. At 1.5m/s of ground motion, the rock mass yields beyond the bolting horizon in both North and South walls of the drift. On the drift back (right corner), yielding does not reaches beyond the bolting horizon and the rebars here still experience higher axial loads.



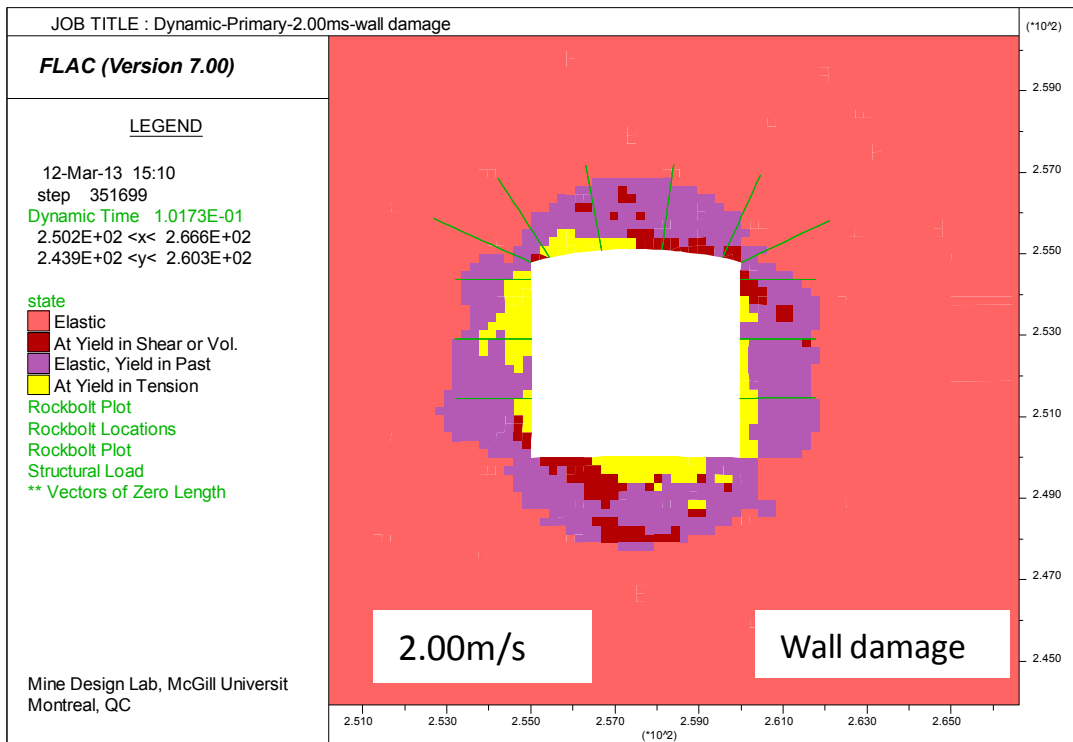
a) Rock mass yielding and wall damage with 0.5m/s PPV with primary supports



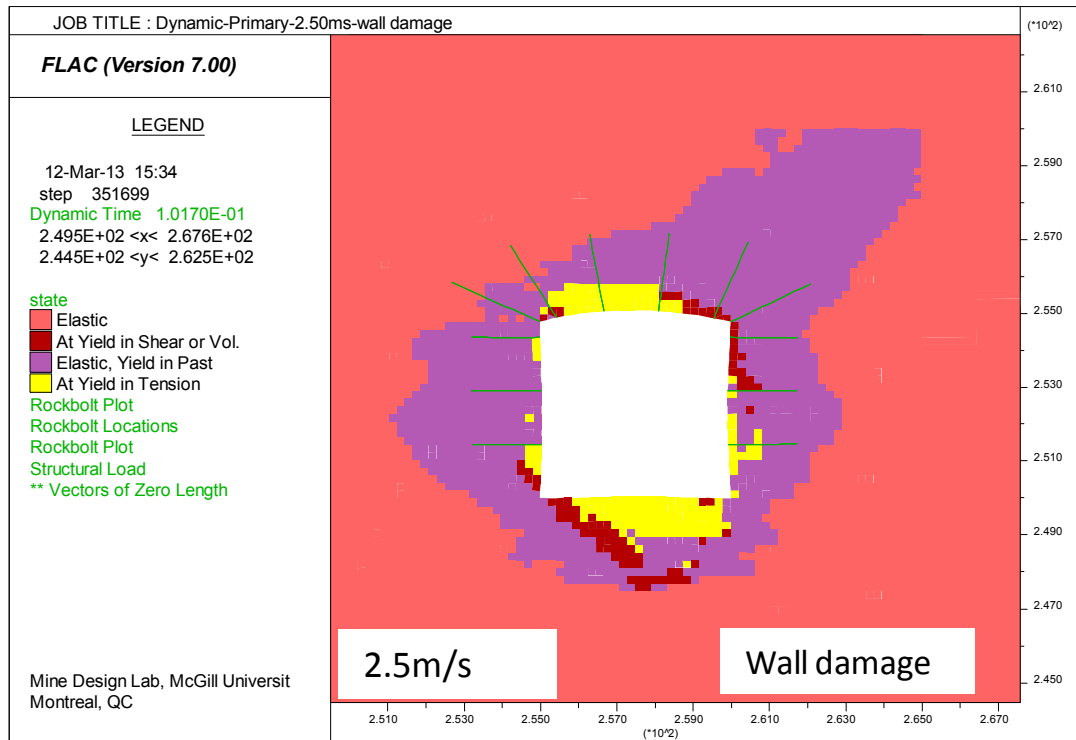
b) Rock mass yielding and wall damage with 1.0m/s PPV with primary supports



c) Rock mass yielding and wall damage with 1.5m/s PPV with primary supports



d) Rock mass yielding and wall damage with 2.0m/s PPV with primary supports



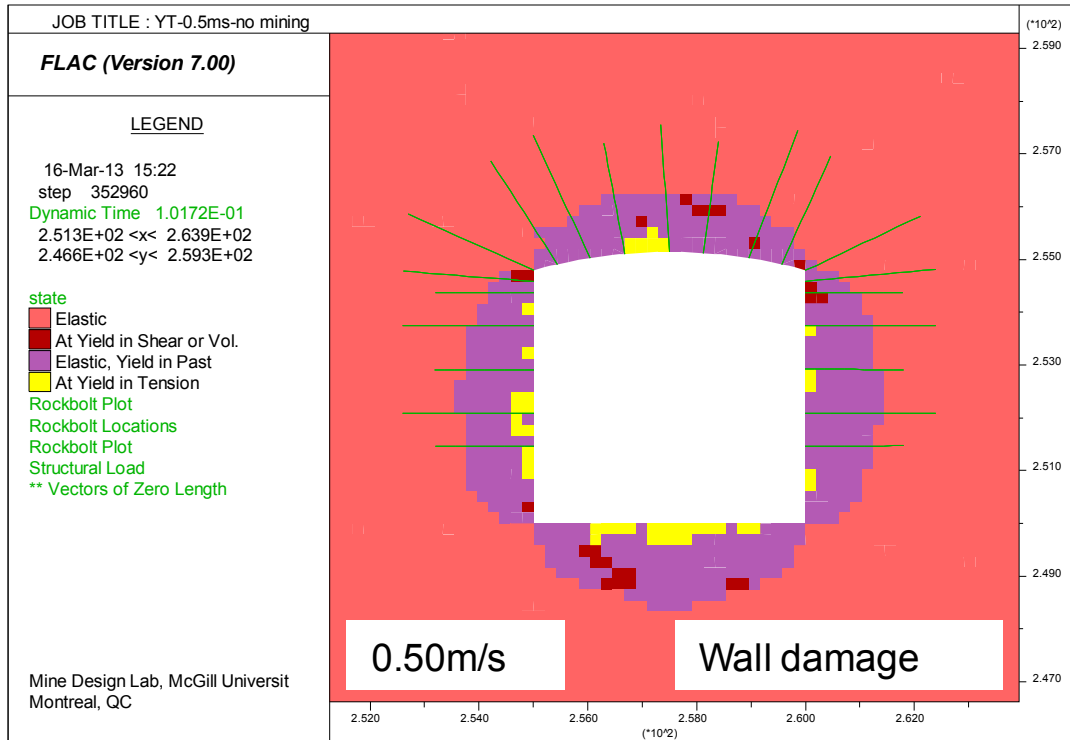
e) Rock mass yielding and wall damage with 2.5m/s PPV with primary supports

Figure 6-5 Drift behavior under dynamic loading with primary supports

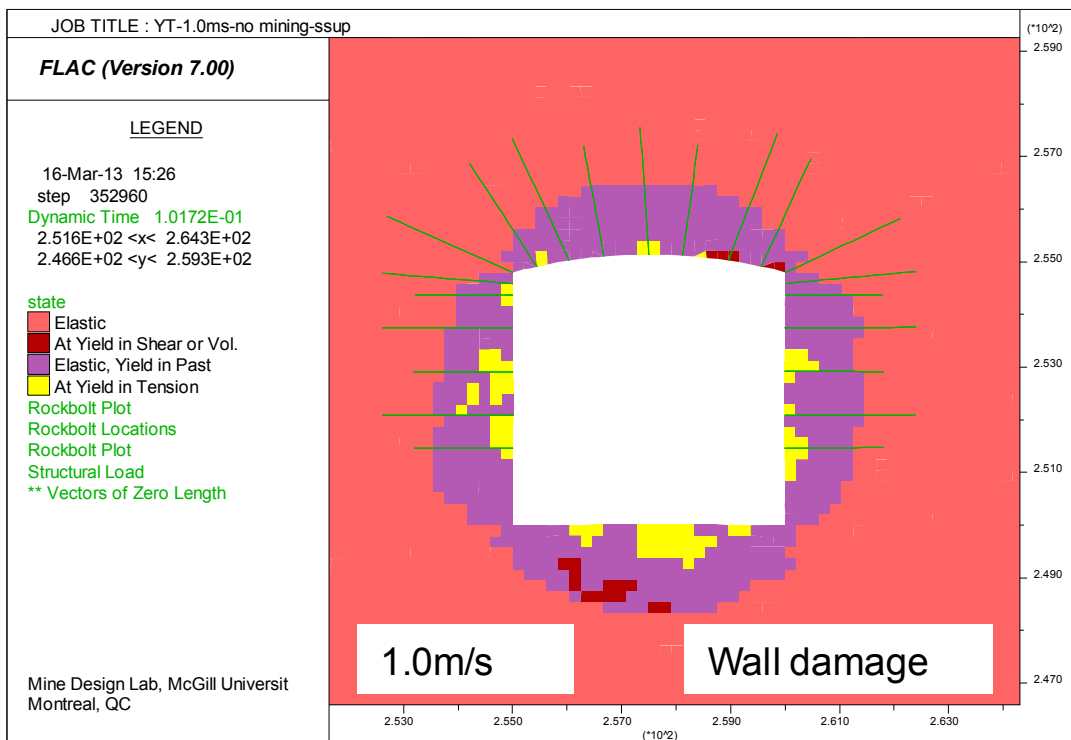
It is only beyond the ground motion level of 2.0m/s, that yielding extends well beyond the bolting horizon of all the three faces of the drift.

### 6.2.3 Dynamic performance of drift secondary support

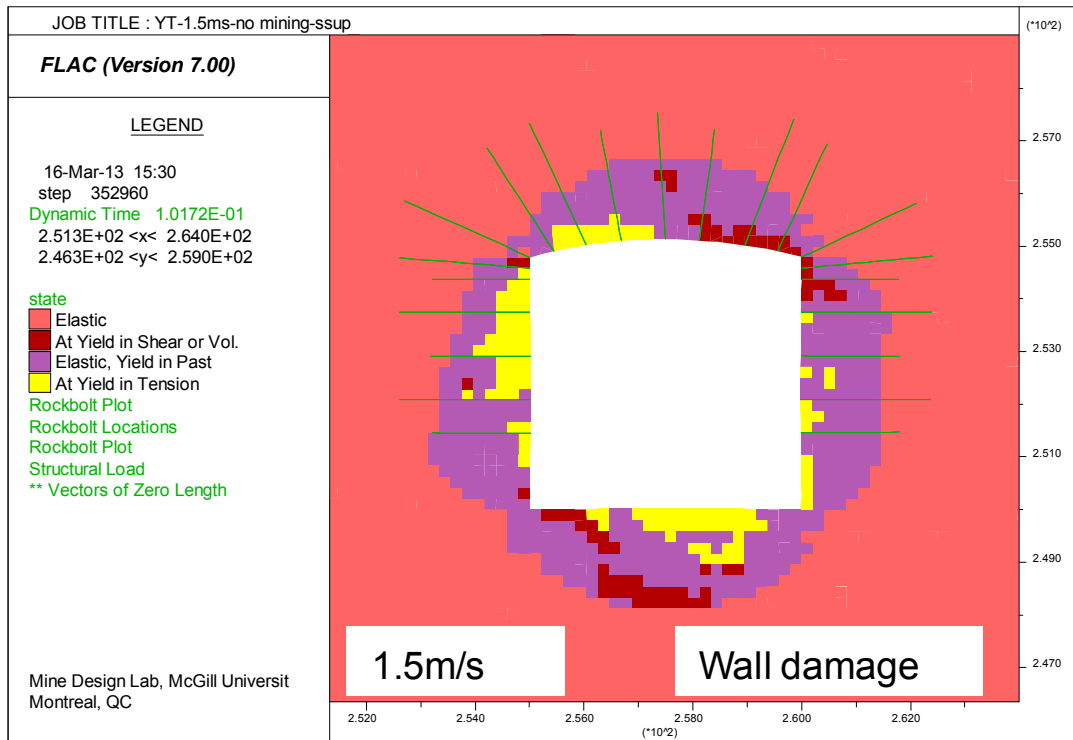
The performance of the drift after secondary or enhanced support system is examined by subjecting the drift to a dynamic loading as explained in previous section. The drift behavior in terms of wall damage and extent of yielding due to various levels of ground motion without any stope sequencing is shown in Figure 6-6.



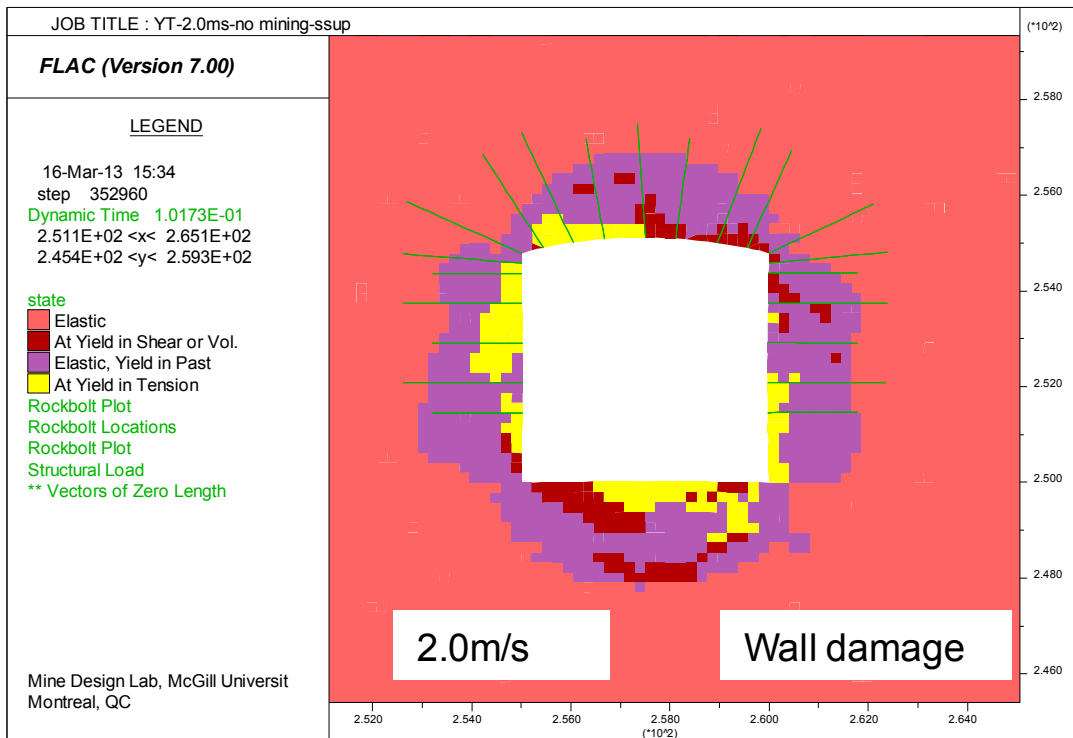
a) Rock mass yielding and wall damage with 0.5m/s PPV with primary and secondary supports



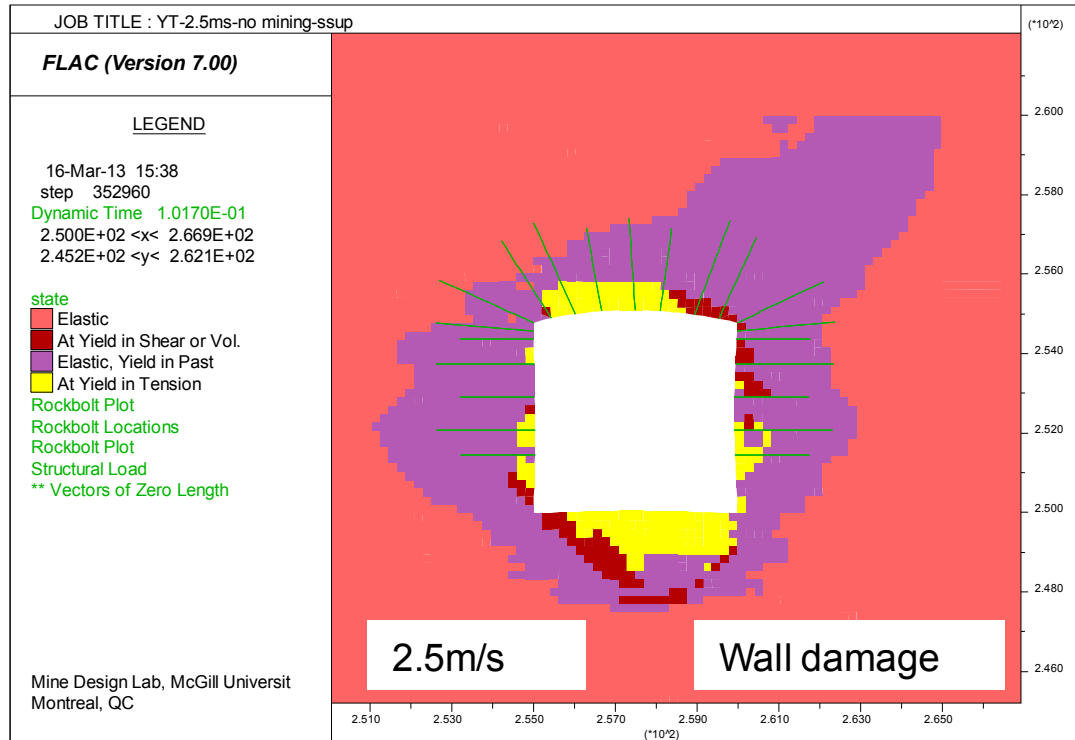
b) Rock mass yielding and wall damage with 1.0m/s PPV with primary and secondary supports



c) Rock mass yielding and wall damage with 1.5m/s PPV with primary and secondary supports



d) Rock mass yielding and wall damage with 2.0m/s PPV with primary and secondary supports



e) Rock mass yielding and wall damage with 2.5m/s PPV with primary and secondary supports

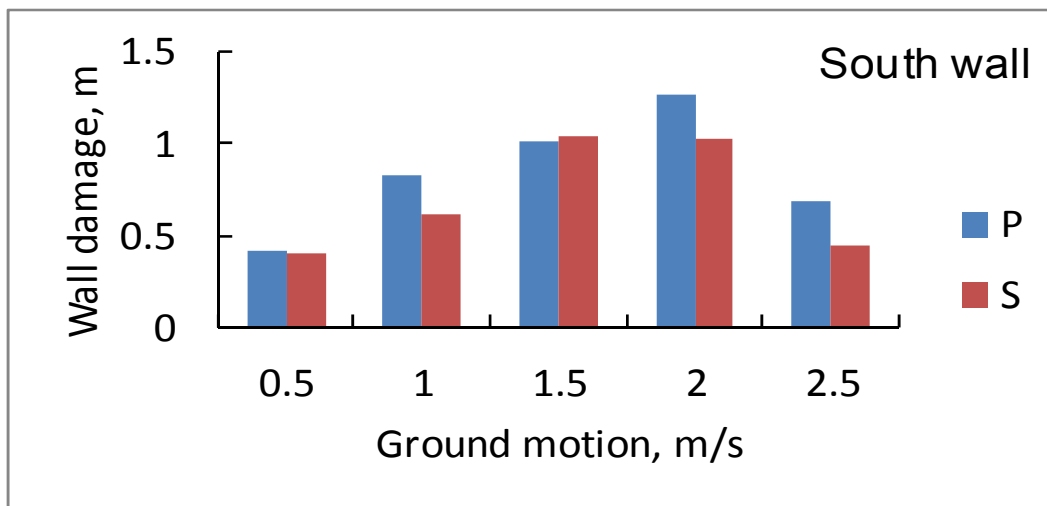
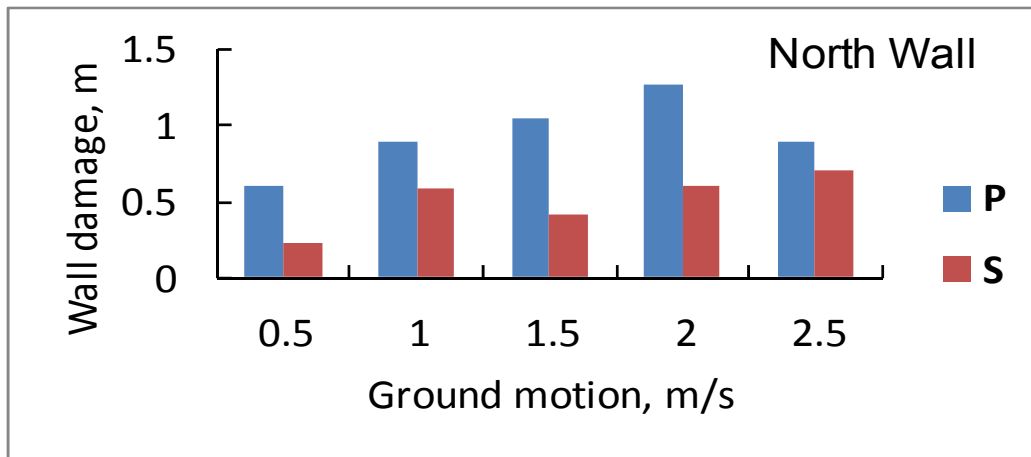
Figure 6-6 Drift behavior with primary and secondary support without mining sequence under dynamic condition

It can be observed from Figure 6-6 that, with the secondary supports, yielding of the rock mass is uniform around the drift until the ground motion level of 2.0m/s and never reaches beyond the secondary supports. The wall damage also largely contained when compared to the drift wall damage with only primary supports. The rock mass yields beyond the bolting horizon on both North and South walls of the drift only after the high ground motion level of 2.5m/s. On the drift back(left corner), yielding doesn't go beyond the bolting horizon even after this high ground motion and the rockbolts here still experience higher axial loads.

#### 6.2.4 Summary of yielding and wall damage

The summary of rock mass yielding and wall damage around the drift during dynamic analysis is presented in this section. The rock mas

yielding and the wall damage around drift with primary and secondary supports without any mining sequence for various ground motion levels is shown in Figure 6-7 and Figure 6-8. The drift wall damage progress with increasing levels of ground motion. Secondary supports seem to be restricting the wall damage particularly in North wall. Also it is found that the wall damage is not following any trend particularly after 1.5m/s of ground motion. On the other hand the rock mass yielding is not affected by the secondary supports under dynamic loading. However it can be seen from the Figure 6-8, that the secondary supports are able to restrict the rock mass yielding in the drift back to some extent.



P - Primary Supports  
 S- Primary & Secondary Supports

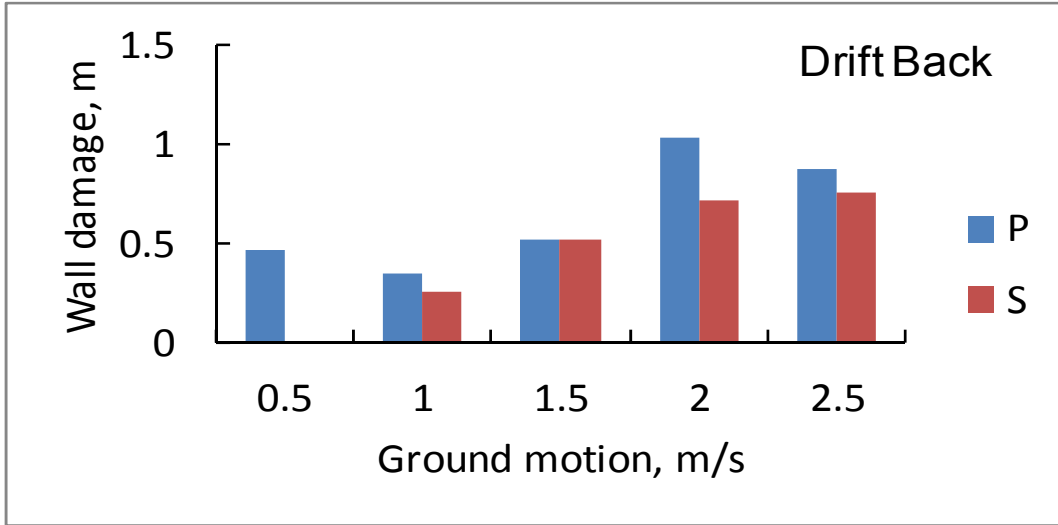
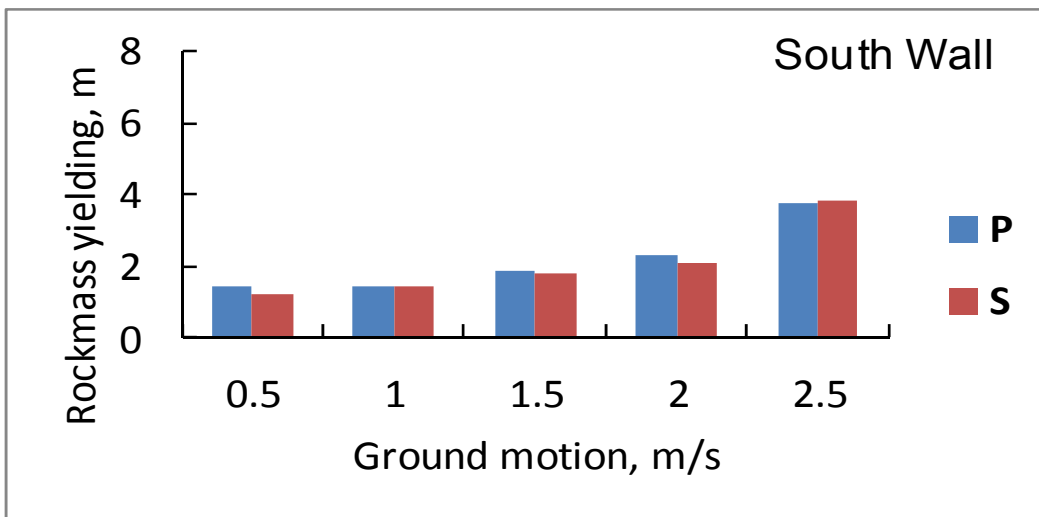
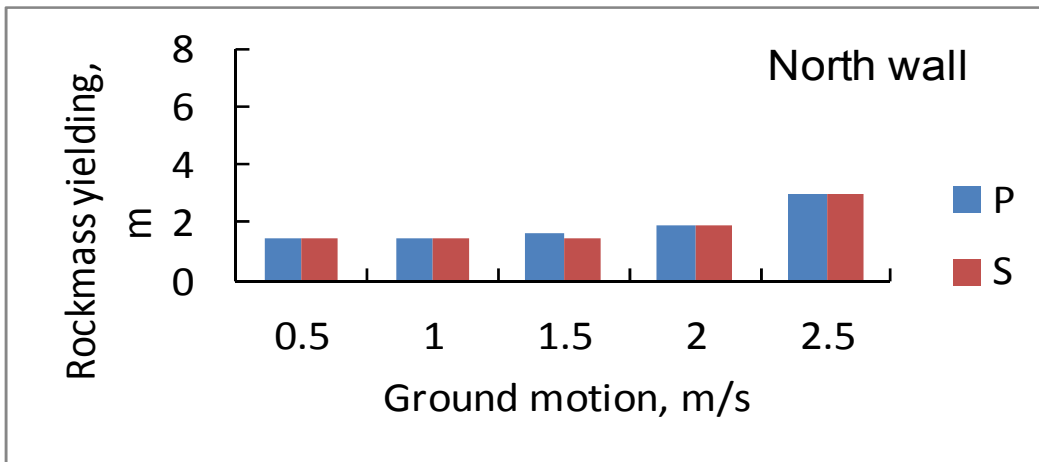


Figure 6-7 Wall damage around the drift faces – without mining



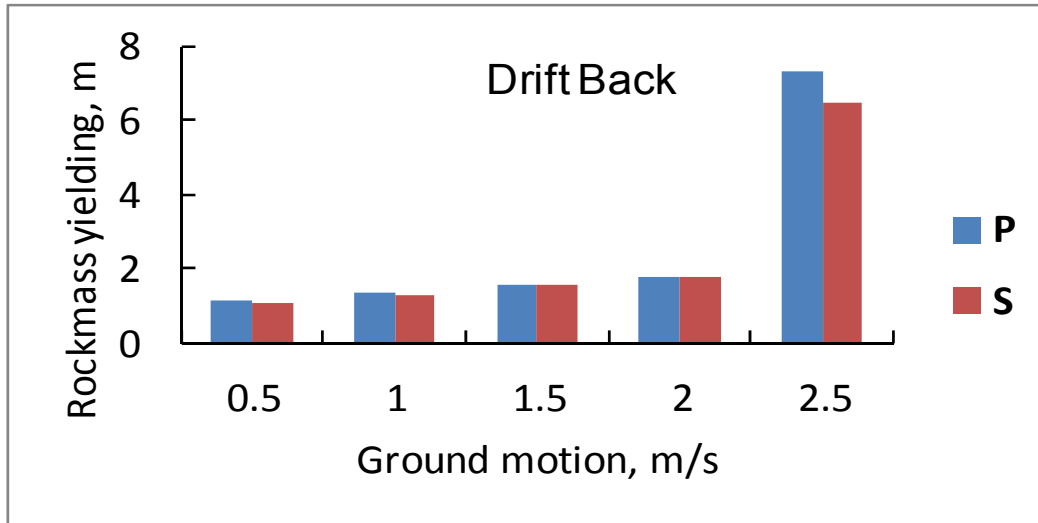


Figure 6-8 Rock mass yielding around the drift – without mining

### 6.2.5 Summary of bolt axial loads

In this section the axial load induced in rock bolts during dynamic event is examined. The drift with primary and with both primary and secondary supports is subjected to various levels of ground motion velocity. Material properties of the rock mass material and the rockbolt properties are the same as those used in the static analysis presented in Chapter-4. Summary of the results in terms of axial loads for the case of primary supports without any mining sequence under various levels of ground motion is shown in Figure 6-9. It can be observed from the figure that the rebars in the North wall and South wall are lightly loaded for the low level of ground motion(0.5m/s), where as the rebars in the back are taking more loads as the yielding not reached beyond the rebars here. For the higher levels of ground motion the rebars in the walls are seem to be completely relaxed as the rock mass yielding reaches beyond the bolting horizon and also the walls experience the damage due to tension under the dynamic event. The rebars in the back, particularly in the corners continue to take loads as the rock mass yielding doesn't cross the point of minimum anchorage length.

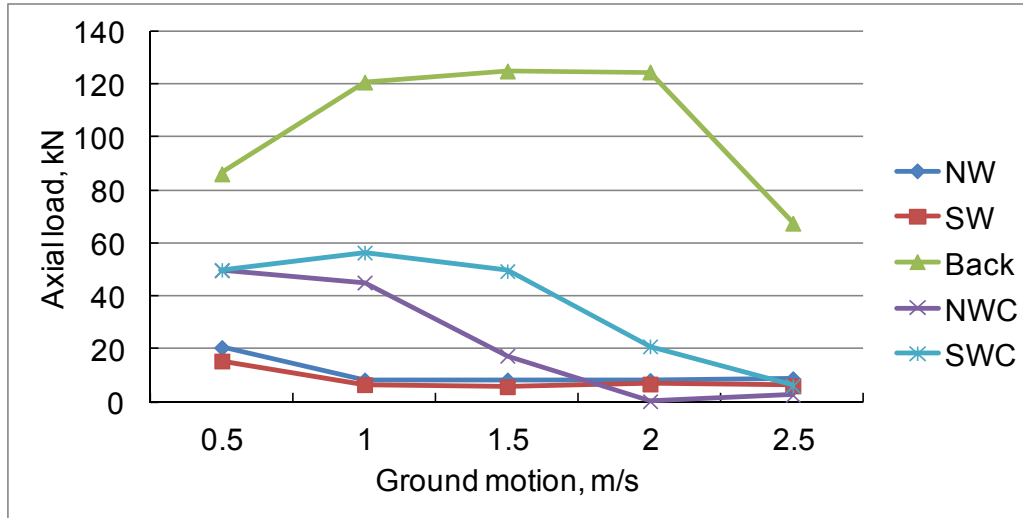


Figure 6-9 Axial loads on primary supports under dynamic condition

Summary of the results in terms of axial loads for the case of primary and secondary supports without any mining sequence under various levels of ground motion is shown in Figure 6-10. It can be observed from the figure that the rebars in the North wall and South wall are lightly loaded for the low level of ground motion (0.5 m/s), whereas the rebars in the back are taking more loads as the yielding not reached beyond the rebars here. For the higher levels of ground motion the rebars in the walls seem to be completely relaxed as the rockmass yielding reaches beyond the bolting horizon and also the walls experience the damage due to tension under the dynamic event. The rebars in the back, particularly in the corners are continued to take loads as the rockmass yielding does not cross the point of minimum anchorage length.

Secondary support in the back (let corner) is reaching to its yield at high ground motion levels of 2.5 m/s. Since the mining sequence is not simulated in this case, the combination of primary and secondary support system seems to withstand the axial loads up to 2.0 m/s ground motion levels. Also both the primary and secondary supports are lightly loaded below the ground motion levels of 2.0 m/s after which the supports in the walls relaxed and part of the supports in the back are reach their capacity while the other part is relaxing.

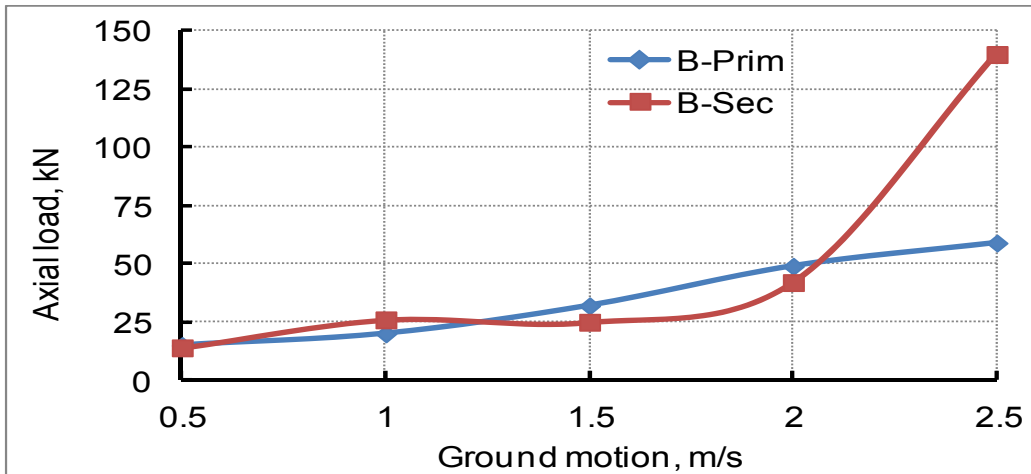
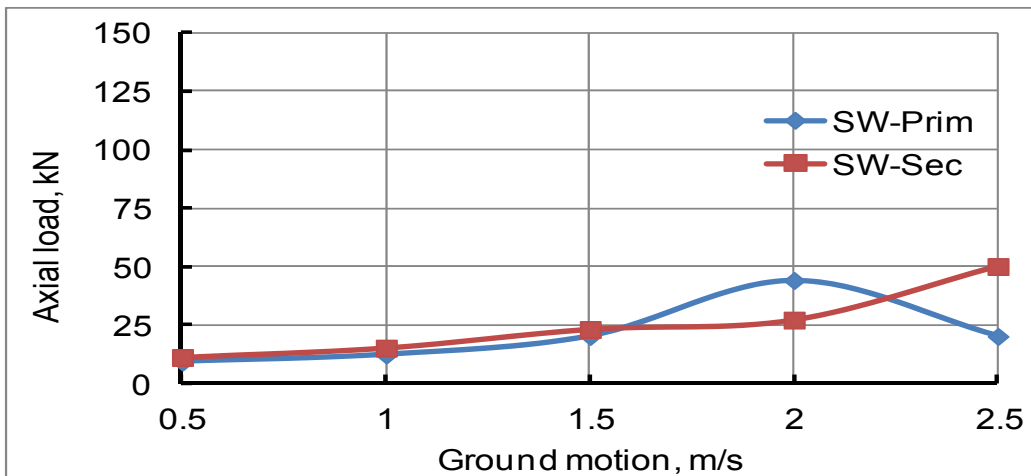
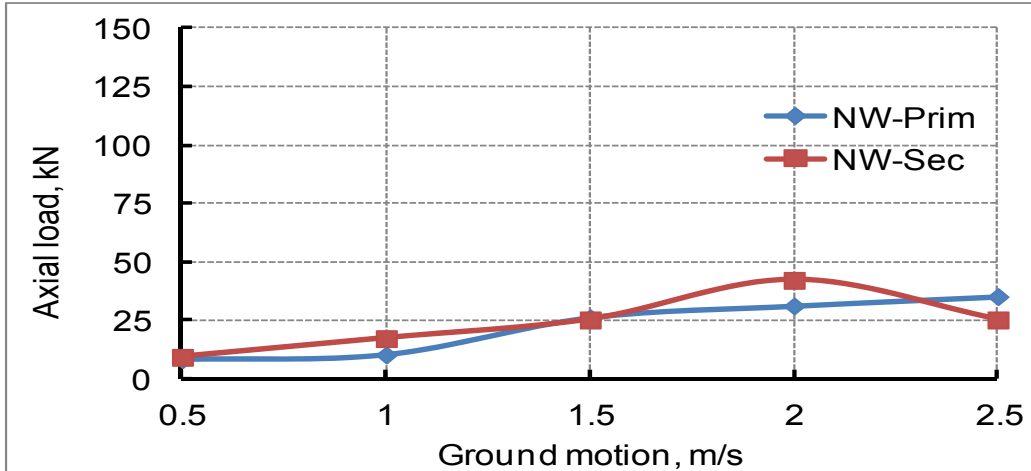
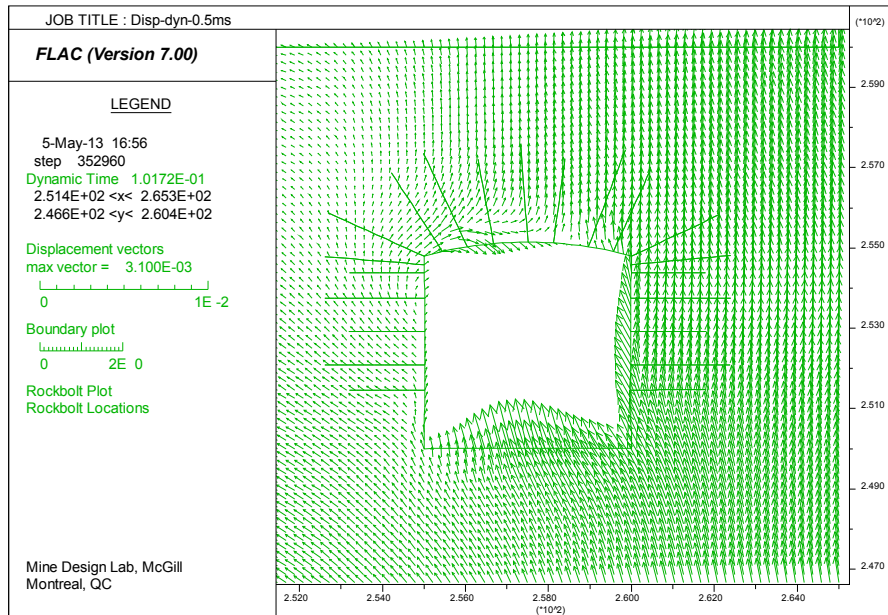


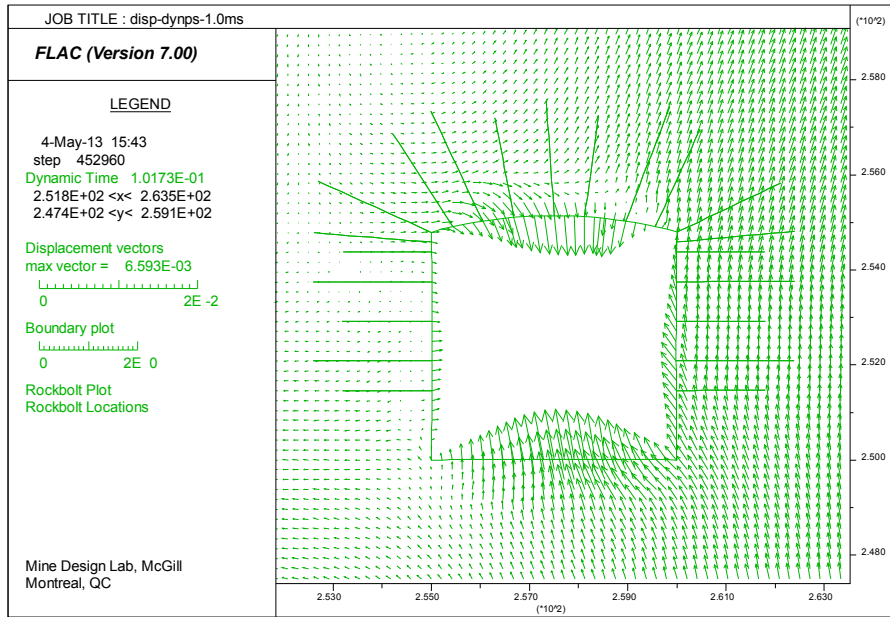
Figure 6-10 Axial loads on primary and secondary supports under dynamic condition – No mining sequence

## 6.2.6 Drift wall displacements

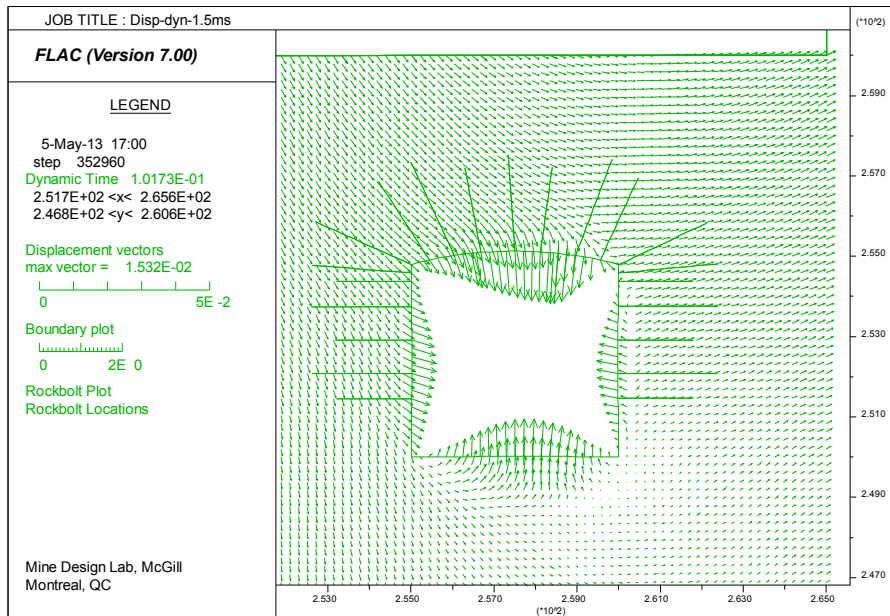
Displacements around the drift opening due to dynamic loading are presented in this section. Result of displacement vectors around drift opening as obtained from the dynamic modeling is shown in Figure 6-11. As can be seen from the figure that displacement for different levels of ground motion is presented. The same results were plotted against peak particle velocity and presented in Figure 6-12. As can be seen from the figure that the displacements around the drift are restricted to below 20mm up to peak particle velocity of 1.5m/s. Beyond 1.5m/s, displacements are increased sharply and reaches to 89.6mm at the peak particle velocity of 2.5m/s. However it is to be noted here, that these displacements does not include any static deformations caused by mining induced stresses.



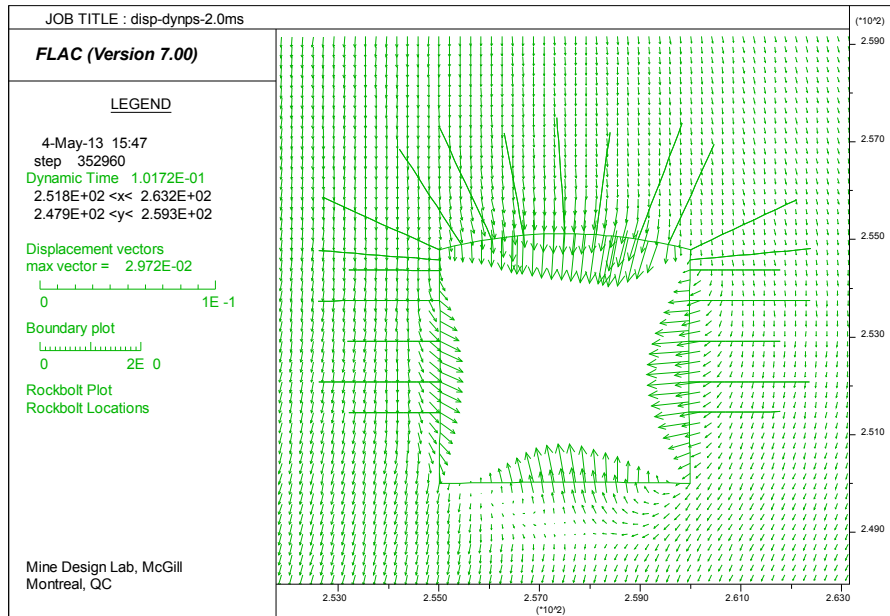
a) Displacements for PPV of 0.5 m/s



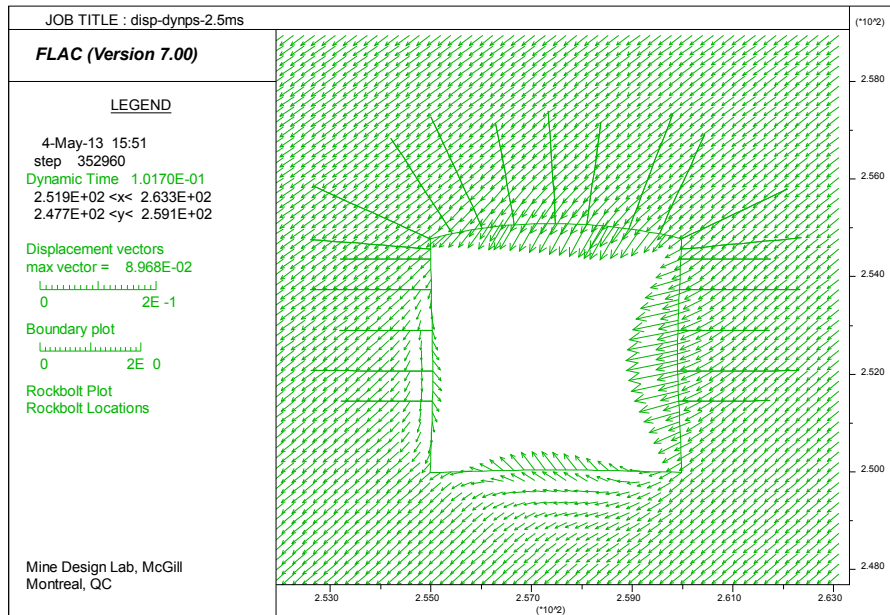
b) Displacements for PPV of 1.0 m/s



c) Displacements for PPV of 1.5 m/s



d) Displacements for PPV of 2.0 m/s



e) Displacements for PPV of 2.5 m/s

Figure 6-11 Displacements around drift opening due to dynamic load

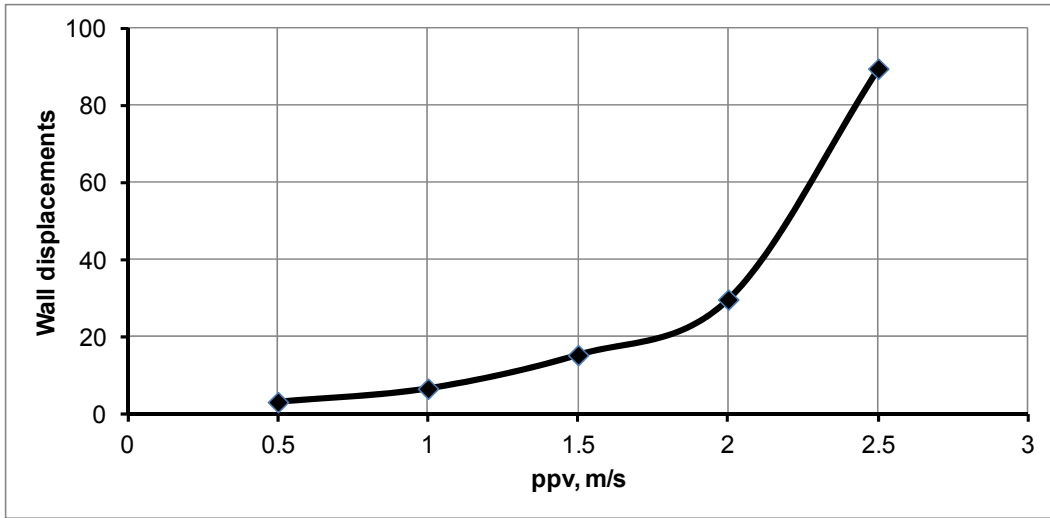


Figure 6-12 Displacements around drift opening plotted against PPV

## 7 Dynamic Rock Support Selection/Design Methodology

### 7.1 General

Mines experiencing high stress conditions are on the rise, as the mining depth is increasing. These high stress conditions lead rockburst which then requires dynamic rock supports with the need of dynamic support increasing, there are now several dynamic rock supports available. However, the task of selecting the appropriate dynamic ground support for the appropriate location is complex. It must contend with many factors related to the complexities of seismic event mechanisms; the varying susceptibility of excavations to damage, the different damage mechanisms, the complex behaviour of ground support schemes, and the imprecise nature of much of the available data (Mikula, 2012).

The main requirements of the dynamic supports can be described by an energy absorption capacity, a displacement or elongation capacity, and a load capacity. The design methodology should consider the demands of a particular opening that is subjected to dynamic loads. Mikula(2012) presents three broad approaches to the design problem.

Mechanistic approach – defines equations that mimic the expected behaviour mechanism

Numerical approach – constructs sufficiently detailed simulation models

Empirical approach – collects site data and interprets behaviour.

The fundamental methodology in the above approaches has the following components:

(1) Expected seismic event locations and source parameters must be defined. This is necessary to have an idea of the nature and character of

the expected dynamic disturbance sources. This is often based on interpretation of historical data collected by a seismic monitoring system, but should also take into account the potential occurrence of rogue(outside of known history expectations) fault slip events on major structures.

(2) A ground motion relationship for the mine must be defined. This is necessary to define how dynamic disturbances will propagate through the mine, and how vibrations will affect openings. Usually this is done by relating PPV, distance, and event magnitude. PPV is widely used as an input parameter for seismic calculations.

## **7.2 Current design methods**

Ortlep (1992) presented an engineering approach for design of support for the containment of rockburst damage in tunnels. While presenting this approach he mentions “considering the modes of failure and the vast amount of energy available at source will show that there is no economically practical way to oppose rockburst damage by simply increasing the strength of the support”. He continues referring the work of Jager et al. (1990) to support this argument. In his design rational, he considers energy, tendons, the cladding elements and extent of yield (of the support) as four important steps.

In his approach, Ortlep suggests that, when a damaging seismic event occurs, it is more important to understand kinetic energy behavior rather than stresses and strengths which are static concepts.

Ortlepp (1992) presented an application of this design principle for the ejection of a single block. The conclusions he reaches are noteworthy. Ortlepp’s conclusions reinforce the rationale behind the proposed dynamic rock support design methodology in this thesis, and are paraphrased below (Ortlepp, 1992).

- Powerful numerical methods are now available to aid analysis of complicated situations that are encountered in rock engineering, particularly when dynamic failure of underground structures occurs. Twenty years ago he stated “it is still impossible to use these realistically in any formal design method because of difficulties in defining the structure, estimating the transient loads and modeling the damage mechanism. For the same reasons, the classical engineering design procedures cannot be used in a strict way”.
- It is neither practical nor economically possible to contain severe rockburst damage by increasing the strength of the tunnel support.
- Yieldability in the design is essential to prevent support components being broken by rockbursts.
- Ejection velocity imposed on the rock walls by the seismic wave is the single most important determinant of damage intensity in a tunnel.(combined seismological and rock engineering research is urgently needed to establish how ground motion parameters in the seismic wave translates in to ejection velocity).
- Energy considerations, rather than stress and strength calculations, should form the basis for the design of a tunnel support system and its elements.
- Ejection velocities of the order of 10m/s and higher can result from seismic events of moderate magnitude.
- Such velocities will cause severe damage in tunnels reinforced with conventionally active support even if they are heavily supported.
- Using the energy approach, yielding support systems based on presently available components, can be designed to withstand these velocities and can contain the damage that would otherwise occur as a result of even very large seismic events.
- The effectiveness of these yielding systems can realistically be demonstrated by means of controlled blasting tests. Suggestions for testing for this purpose are given by Ortlepp (1992).

CAMIRO Mining Division (1990-1995) in their Canadian rockburst research program presented the significant findings on rockburst support systems from various other aspects of rockburst. Three distinct mechanisms that are involved in most of the damage caused by rockbursts in Canadian mines have been identified. The following are listed in order of priority.

- Sudden volume expansion or bulking of the rock due to fracturing of the rock mass around an excavation. The significance of assessing the amount of bulking and controlling the bulking process has not been recognized before. Rock mass bulking is a major cause of damage to support in burst-prone ground. It is now evident that it accounts for a substantial amount of the damage that is observed in Canadian mines.
- Rock falls (or fall of ground), which have been induced by seismic shaking, are the second most common cause of damage in Canadian burst-prone ground
- Ejection of rock due to energy transfer from a remote seismic source may be a major cause of damage in deep South African mines, but is far less common in rockburst prone Canadian mines.

It is worth noting that this study implies that ***the first step in dealing with support selection for burst prone conditions is to estimate the type of damage mechanism involved and the likely severity of the resulting damage. Also it is useful to understand the conditions that lead to or trigger a rockburst.*** Additionally, for the purpose of support selection, a primary goal is to assess the anticipated thickness of the rock that could be involved in the damage process. In the process of rock support design for the burst prone ground, three levels of rockburst damage severity are defined by this study. Damage level

determination is based on observations of previous damage, where such observations are available, plus the analytical methods. The three levels of damage are:

- Minor damage
- Moderate damage
- Major damage

The damage severity is estimated

- By observations from previous rockbursts
- Rock stress-to-strength ratio
- Peak particle velocity

The support functions (consisting of reinforcing, retaining and holding) will be required in varying proportions due to rockburst conditions depending on the specific damage mechanisms and severity of a particular situation. As the severity of rockburst damage increases, the support system will not be able to prevent initiation of the damage mechanism. An appropriate support system must be able to survive the displacements associated with the rockburst and remain functional after the rockburst to hold and retain any broken rock.

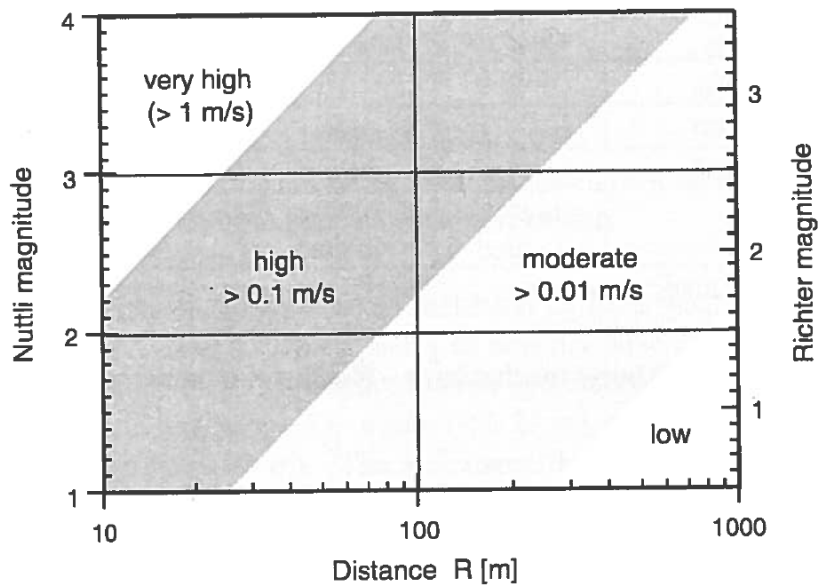
Under situations that involve violent rock ejection the support must also be able to absorb kinetic energy in the ejected material. Accordingly the rock support design approach consists of the following four important steps.

- Rockburst hazard assessment
- Estimating of demand on support
- Determination of support system capacity
- Selection of most appropriate support system by fitting support capacity to anticipated demand

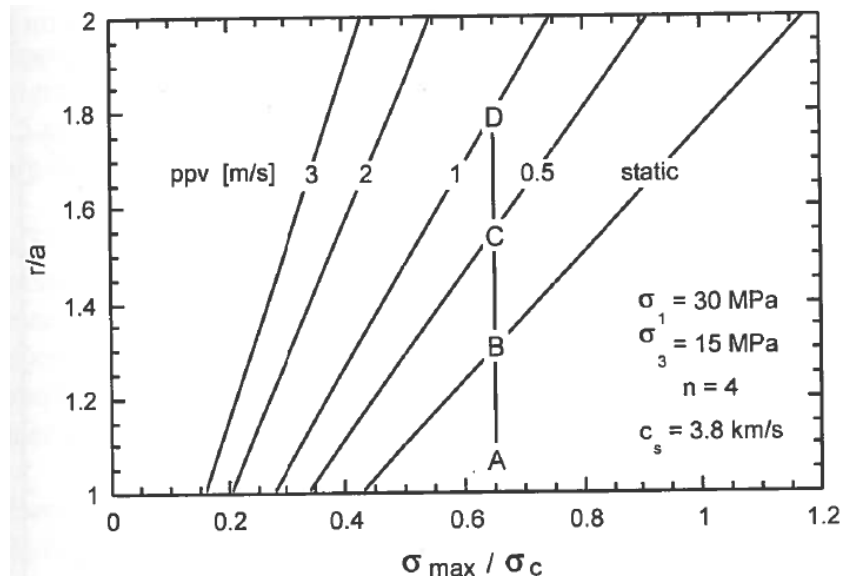
A typical detail design sequence under the above four steps would include steps such as:

- Determine whether rockburst damage is expected due to remote seismic event, or due to self-initiated fracturing of the rock mass around the excavation.
- Assess the seismic hazard and determine the anticipated ground motion intensity in the support design sector if damage is triggered by remote events.
- If possible, based on previous observations, anticipated ground motions and with charts provided, will evaluate which rockburst damage mechanism is likely to dominate in the target area. Evaluate which rockburst damage mechanism is likely to cause damage in the target area. This should be based on previous observations, anticipated ground motions, and with charts provided.
- Estimate the severity of the anticipated rockburst damage, that is, the mass of rock potentially involved in the failure process.
- Determine the load, displacement, or energy demand on the support for the dominant rockburst damage mechanism, if known. If not, evaluate support demand for each mechanism separately.
- Evaluate whether support can be designed to prevent the initiation of damage or whether the support must be designed to control the failure process.
- Select support elements and combine them to create a support system with the desired support characteristics.

Various charts and tables (for example: as shown in Figure 7-1 and Table 7-1) have been provided for performing most of the above steps in the design to finally select an appropriate support system for the particular condition.



a) Anticipated levels of ground motion under typical conditions



b) Maximum radius of failure under dynamic loading conditions

Figure 7-1 Example of various charts provided for aiding the design process in CRRP, 1990-1995(CAMIRO-Mining Division (1990-95))

Table 7-1 Rockburst damage mechanisms and nature of the anticipated damage (CAMIRO-Mining Division, 1990-95)

Damage mechanism	Damage severity	Cause of rockburst damage	Thickness(m)	Weight (kN/m <sup>2</sup> )	Closure, mm	Ve (m/s)	Energy (kJ/m <sup>2</sup> )
Bulking without ejection	Minor	Highly stressed rock	<0.25	<7	15	<1.5	Not critical
	Moderate	With little excess	<0.75	<20	30	<1.5	Not critical
	Major	Stored strain energy	<1.5	<50	60	<1.5	Not critical
Bulking causing ejection	Minor	Highly stressed rock	<0.25	<7	50	1.5 to 3	Not critical
	Moderate	With significant	<0.75	<20	150	1.5 to 3	2 to 10
	Major	Excess strain energy	<1.5	<50	300	1.5 to 3	5 to 25
Ejection by remote seismic event	Minor	Seismic energy transferred to jointed or broken rock	<0.25	<7	<150	>3	3 to 10
	Moderate		<0.75	<20	<300	>3	10 to 20
	Major		<1.5	,50	>300	>3	20 to 50
Rock fall	Minor	Inadequate strength, forces increased	<0.25	<7g/(a+g)	na	na	Na
	Moderate		<0.75	<20g/(a+g)	na	na	Na
	Major	By seismic acceleration	<1.5	<50g/(a+g)	na	na	na

Mikula (2012) documented progress on development of a site-specific empirical charting approach to dynamic ground support selection. Mikula and Lee (2007) developed a chart several years ago to assist the mining of the ROB5 ore body at Mt Charlotte Mine, followed by charts for Argo Mine and the Long-Victor Complex, with each revision expanding the knowledge base (Mikula, 2012). In this paper he presents the context and application of an empirical chart concept. Mikula demonstrates that it is well within the capability of a mine site to collect the required data and construct an empirical model of their site. This conclusion is based on the work that was in progress at Long-Victor Mine. Also, he warns that there is no guarantee that the findings are generic across mine sites – this is yet to be verified by independent application to numerous other mine datasets.

In the methodology, Mikula considers the following components:

- Define expected seismic event locations and source parameters. It is necessary to have some idea of the nature and character of the expected dynamic disturbance sources. This often is based on interpretation of historical data collected by a seismic monitoring system, but should also take into account the potential occurrence of rogue, i.e. outside of known history expectations, fault slip events on major structures.
- Define a ground motion relationship for the mine. It is necessary to have a way of defining how a dynamic disturbance will propagate around the mine and how the vibrations will affect openings. Usually this is done by relating PPV, distance, and event magnitude. PPV is widely used as an input parameter for seismic calculations. However, it is possible that PPV may not be the best parameter to use, or even a suitable parameter, or that other input parameters should also be included. PPV is used in the empirical charts here for lack of a better alternative.
- Define damage criteria. This is a statement of what level of dynamic vibrational disturbance will cause the worst-case extent of damage to rock and ground support. This sounds simple but is not, because the support scheme interacts with the rock to influence both scheme damage and rock mass damage.
- Define a specification for guide selection of a scheme that would survive the dynamic condition.

The empirical charting process methodology, he adopted for each data point includes:

- Review site records of the larger seismic events and associated damage.
- Compile a spreadsheet of relevant seismic data.
- Estimate the distance from event source to damage site. Estimate the incoming PPV at the support location due to the seismic event. Often

for the datasets, this was judged to be near-field PPV, unless certain that it was far-field.

- Identify the ground support scheme installed at each damage site.
- Estimate the mobilised energy dissipation capacity and load capacity of the scheme using estimates of sliding, elongation, and bulking distances for each component.
- Create charts of PPV versus scheme capacities. Some data points appear on multiple charts. To be conservative, if damage at a location was variable, only the worst-rated damage was plotted.

Mikula(2012), while presenting the empirical charting method, draws following conclusions.

- This work has developed an empirical chart system which fulfils the practical requirement to provide a sufficient engineered dynamic support selection method.
- It does this by providing conservative guidelines which reflect all the observed variability as defined for the mine site.
- If the past observed seismic history is sufficient, and is a valid representation of future history, then the method can be used for forward planning and design. Yet, it is always essential to verify in the construction period that the estimates and assumptions made in the design period are valid.
- As the charts depend on the past history and variability of the Long-Victor Complex, they are not portable to another mine. Attempting to do so is not valid unless it can be demonstrated otherwise

Yao et al. (2009) applied site specific innovative methods successfully for designing the dynamic rock support for the burst-prone areas in Vale's Copper Cliff North Mine in Sudbury operations. The approach adopted here was risk based approach to design highly yielding

support to sustain future seismic impact after gaining experience from the major rockburst. A risk rating system to determine where enhanced support system is required was evolved by taking the following six parameters in to consideration and then assigning numerical rating to the parameters.

- Historic Seismic data of the area
- Ground condition
- Efficacy of the existing ground support
- Deteriorated infrastructures in the proximity
- Anticipated mining induced stress
- Other geological structures in the proximity

The total risk rating will be arrived after summing up the individual ratings. The threshold rating of the risk is established after back analysis of number of areas within the mine. If the total risk rating crosses this threshold rating, then enhanced support is required in the form of yielding supports in that area. Also the type of enhanced support is determined using the five step methodology. Typical burst prone area supported using this methodology is shown in Figure 7-2.



Figure 7-2 Enhanced supports installed in burst prone area (Yao et al, 2009)

### 7.3 Summary of existing methods

Review of the existing methods for design of dynamic rock supports, provides a better understanding of the problem. All the methods express that the analysis of the dynamic event to estimate the required parameters for design of support is complex. All the authors when presenting the concerned methods agree that the most important aspect in design of dynamic rock support is to estimate the wall damage due to the incoming seismic event and then the ejection velocity. Also there is a general agreement on the essential requirements in a dynamic support i.e. the energy capacity, the displacement capacity and the load capacity.

The energy that was ejected by a rock block due to seismic event can only be estimated, when we know the extent of the damage suffered

by the faces of particular opening due to the seismic event. Needless to mention that damage severity depends on intensity of the seismic event, the rock mass properties, and the support efficacy. Also it was observed from the existing methodologies, that particular mines should have suffered from rockbursts already. This forms the database for the future design by establishing a seismic activity centre. All the methods discussed above estimate the important criteria such as the wall damage, ejection velocity and displacements empirically and some of them are site specific. In the following section, the proposed methodology will be introduced where by the important criteria for dynamic rock support design is estimated through dynamic numerical modeling of the underground opening prone to rockbursts.

## **7.4 Proposed methodology for design of dynamic rock supports**

### **7.4.1 General**

The complexity of containment of the rockburst damage is discussed already in previous sections. This includes difficulties of determining and understanding various unknowns, which are important in facilitating the better design process. Literature review in general and on existing design methods reveals that the following criteria are crucial for dynamic rock support design.

- Location and extent of damage
- Ejection velocity
- Energy capacity
- Displacement and load capacity

Kaiser, (1993), attributes damage to three factors: fault slip, ground failure, and shaking. The latter acknowledges that repeated and lasting shaking with strong energy content may cause more damage than a single high ppa or ppv pulse. Most of the data needed for detailed analysis of damage is often not obtainable and the need for empirical damage models is considered to be first and crucial step in any seismic design (Kaiser, 1993). Almost 25 years back St.Jhon and Zahrah(1987), realised that the relatively sophisticated methods for modeling the dynamic response of underground openings are available, however they concluded that it is best to start with a simple empirical method followed by a rigorous analysis to justify it. Although the overall design of empirical methods consist of only a few steps, the detailed steps involved in the design process are more complex, thus requiring various iterations and comparisons of alternatives. Further, these methods require the database of similar events in that area, which means that the area should have suffered from damages before for the future design.

All the authors( Ortlepp(1992), Kaiser(1993), CRRP(1990-95), McGarr(1997), Varden et al (2008), Mikula( 2012)) emphasise the fact that the energy capacity of the dynamic rock support be designed on the basis of the ejection velocity of the rock block due to the seismic event. The ejection velocity and the site effect factors are discussed below.

### **Ejection velocity**

Ortlepp (1992) presented evidence indicating, wall rock ejection velocities associated with rock bursts of the order of 10 m/s and greater. The Canadian rockburst research program (CRRP: 1990-1995), deals with depth on rockburst ejection velocity and explains that rock may fail in a stable or controlled manner without rock ejection during a rockburst, meaning that the fractured rock deforms in to the opening without gaining much velocity. On the other hand, the rock may fail in an unstable manner,

generating high ejection velocities. The difference between these two situations is the rate of deformation or the ejection velocity. The latter situation is encountered when the loading system is relatively soft and the stored strain energy around the failing rock annulus cannot be dissipated during the failure process or by the rock support. For design, it is therefore necessary to estimate the anticipated rock ejection velocity. Also this work reports the work of Yi and Kaiser (1993), where they suggested, based on analytical considerations, that the ejection velocity would seldom exceed the ground motion ( $V_e \leq ppv$ ). For rock ejection associated with stress-induced fracturing and the associated release of excess stored energy, the amount of energy available to eject rock depends on the brittleness of the rock mass, i.e., the post peak stiffness of the failing rock, and the stiffness of the loading system, which is very difficult to determine in practice. Hence, it is often necessary to assess the anticipated ejection velocity based on field observations.

Also, the work of Yi and Kaiser (1993) as presented in the CRRP (1990-95) says under special conditions the ejection velocity could approach twice the peak particle velocity when wave reflections occur. However, it says that wave reflection is only possible when the wavelength of the stress wave is much smaller than the opening size, implying a very high frequency. Moreover, as per Yi and Kaiser (1993), ejection velocities greater than the peak particle velocity are only possible if the ejected blocks are very small. As a practical consequence, rockburst damage resulting from rock ejected at twice the peak particle velocity is unlikely and would only occur for very small blocks in a drift located very close to the source of a seismic event.

For engineering purposes, when rock ejection damage is expected, CRRP (1990-95) suggests that, the ejection velocity may be conservatively set equal to the peak particle velocity at the opening. The paper also warns that this assumption ignores the beneficial effects arising from

frictional resistance between ejected and stable blocks, which is meaningful for flat walls but for arched backs and curved walls the same may be too conservative. Considering this fact CRRP (1990-95) introduces an ejection velocity adjustment factor as shown in equation 7.1 to account for the influence of curved walls or backs.

$$V_e = n.PPV \quad (7.1)$$

Where

$n < 1$  for low frequency waves and

$1 < n < 4$  for conditions with energy transfer

McGarr (1997) presented a mechanism for high wall-rock velocities in rockbursts. He presented the possibilities of high wall rock velocities in terms of the available energy for this process, as how much energy is available at the free surface of an excavation to be converted in to the kinetic energy of an ejected fragment of side wall rock. He shows this with the evidence of specific mechanism of slab buckling as shown in Figure 7-3, as this mechanism of slab buckling seems to be ever present in excavations at depth as shown in Figure 7-4

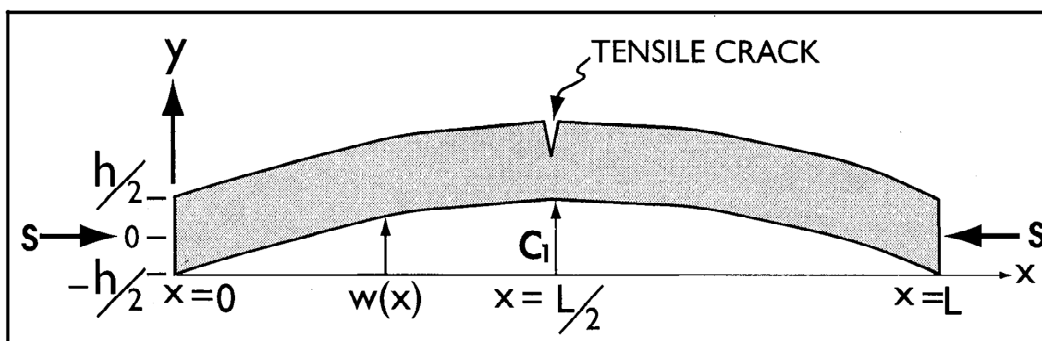


Figure 7-3 Configuration of slab thickness and dimension loaded by stress ( McGarr, 1997)

McGarr (1997) after presenting the mechanism concludes that the buckling of slabs in the sidewalls of tunnels is a common manifestation of rockburst damage. The analysis of such slab flexure and failure implies peak wall-rock velocities  $v$  that depend on a just few rock properties, and in particular,  $v$  is about 26 m/s as estimated from equation he presented. The results of the slab buckling analysis are compatible with both the observations of high wall rock velocities reviewed by Ortlepp(1993) as well as his suggestion that these phenomena are distinct from the causative mine tremor, for which near-fault ground velocities are unlikely to exceed several m/s.

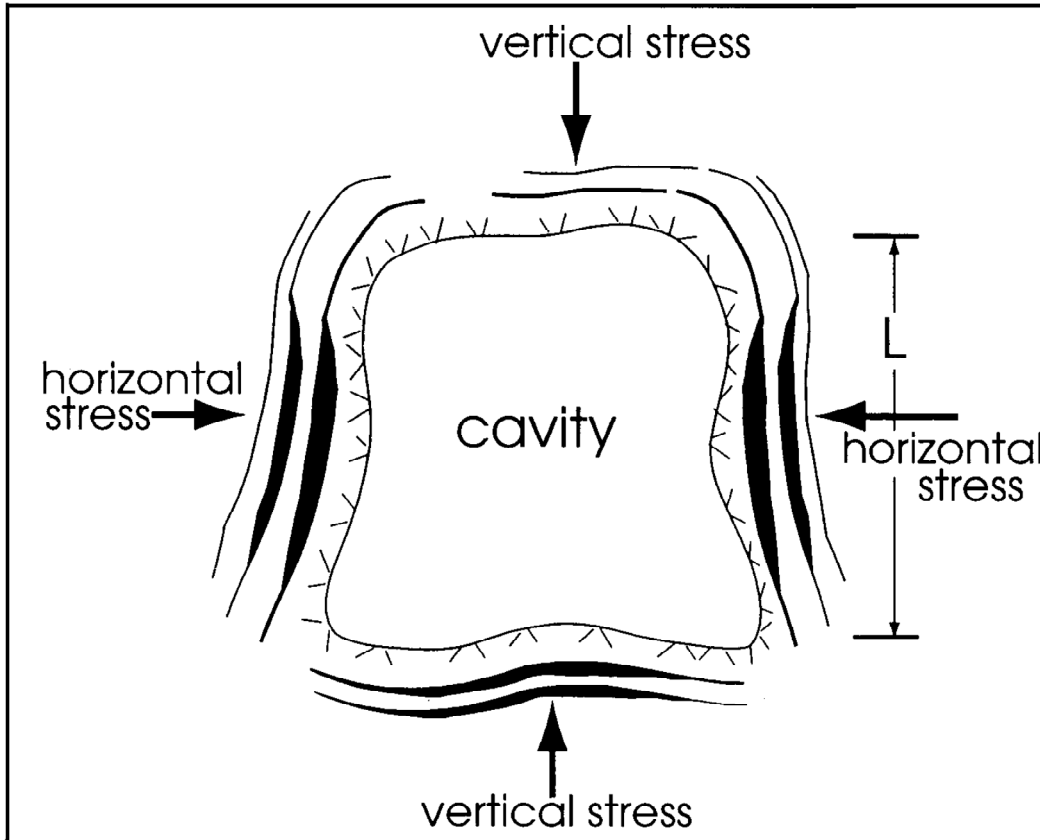


Figure 7-4 Slab formation around underground excavation, after MUHLHAUS, 1993(McGarr, 1997)

Mikula (2012), reports that the ejection PPV is defined as the PPV of a point on the surface of the excavation during the dynamic event and it is definitely not the same as the incoming PPV. The incoming PPV is a dynamic stress wave which only excites or attacks the rock mass, and initiates a cascade of phenomena that may lead to damage. The nature of the failure, or of the damage mechanism, then generates the ejection PPV as a by product. The ejection PPV is what is felt by the ground support scheme. For a local strain burst, i.e. not initiated by a remote event vibration, there is zero incoming PPV, because the burst is the source, and being at the edge of the excavation, it generates its own ejection PPV.

As proposed in CRRP (1990-95), Mikula (2012) also states that a site effect factor is sometimes applied as a multiplier to the incoming PPV to approximate the ejection PPV. He gives an example for instance, the

site effect typical for Western Australian hard rock mines has been quoted as about 2 (Heal, 2007). Quoting his experience at Long-Victor Mine suggests that an average site effect factor of 3 may be typical there. This effect is poorly understood, but amplification of the ground motion by a factor of up to 10 times is considered possible (Milev and Spottiswood, 2005). In reality, the site effect is a variable, not a constant, frequency dependent, and depends on numerous factors. Without measurement, no one knows what it is or was in any particular instance. Sensors (geophones and accelerometers) that are positioned in the solid rock mass register the incoming PPV, and do not experience the site effect.

Varden et al. (2008), while designing the dynamic supports for a case in Australia, assessed potential ejection velocity ranging from 0.5 m/s to 5 m/s. He adopted these ejection velocity values as they are considered to be within the range of current industry design practice. And he the energy demand per bolt was calculated from the resultant kinetic and potential energy requirement to stabilise the mass acting on each bolt from Li et al (2004).

#### **7.4.2 Proposed methodology**

After reviewing the current methodologies for dynamic rock support design and gaining the understanding of the important factors that are crucial for design, a new methodology is proposed in this work for design of dynamic supports that is based on dynamic numerical modeling. As discussed already in previous sections, determining the location and extent of wall damage due to seismic event is crucial in dynamic rock support design. Because the kinetic energy that needs to be absorbed by the designed support is calculated after estimating the damage and ejection velocities, and all the existing methods are based on estimating these crucial factors empirically and explained that the difficulties involved in estimating and are complex. Moreover, a detailed well documented previous data base is a must for evaluating these parameters.

The proposed methodology in this work recognizes the importance of factors such as wall damage and ejection velocity being based on dynamic numerical modeling of the underground opening, which is prone to rockbursts and need to be supported with yielding supports to contain the damage. The wall damage and the ppv at the surface of the opening can be estimated by dynamic numerical modeling of a particular opening in question by subjecting the excavation to the seismic loads. In the proposed methodology, FLAC2D with a dynamic option is used to conduct the dynamic analysis. The model geometry, model boundary conditions and the results of the dynamic modeling with and without supports is presented already in Chapter 6. Here only a few of the results obtained in Chapter 6 will be taken as an example to estimate the wall damage and ppv to be used in the methodology to select/design dynamic rock support. The steps involved in the proposed methodology include the following.

- Rationalise the support system( pattern, length, type etc)
- Perform dynamic numerical modeling of the area
- Predict extent and location of wall damage, displacements
- Estimate support energy, and displacement requirements and select appropriate dynamic support based on this
- Validate by field in situ monitoring

Since, the mining industry now is provided with several dynamic support systems, presented in Chapter 3 are available in the market, one can rationalise the support system by selecting the appropriate support system for the particular condition, if it satisfy the dynamic conditions compared with the design procedure mentioned above. The dynamic analysis results can provide with the location and extent of the wall damage, PPV at the surface of the opening and the displacements. With all these inputs ejection velocity and then kinetic energy that needs to be absorbed by the support system can be estimated. The results of dynamic model, in terms of wall damage for various levels of ground motion with

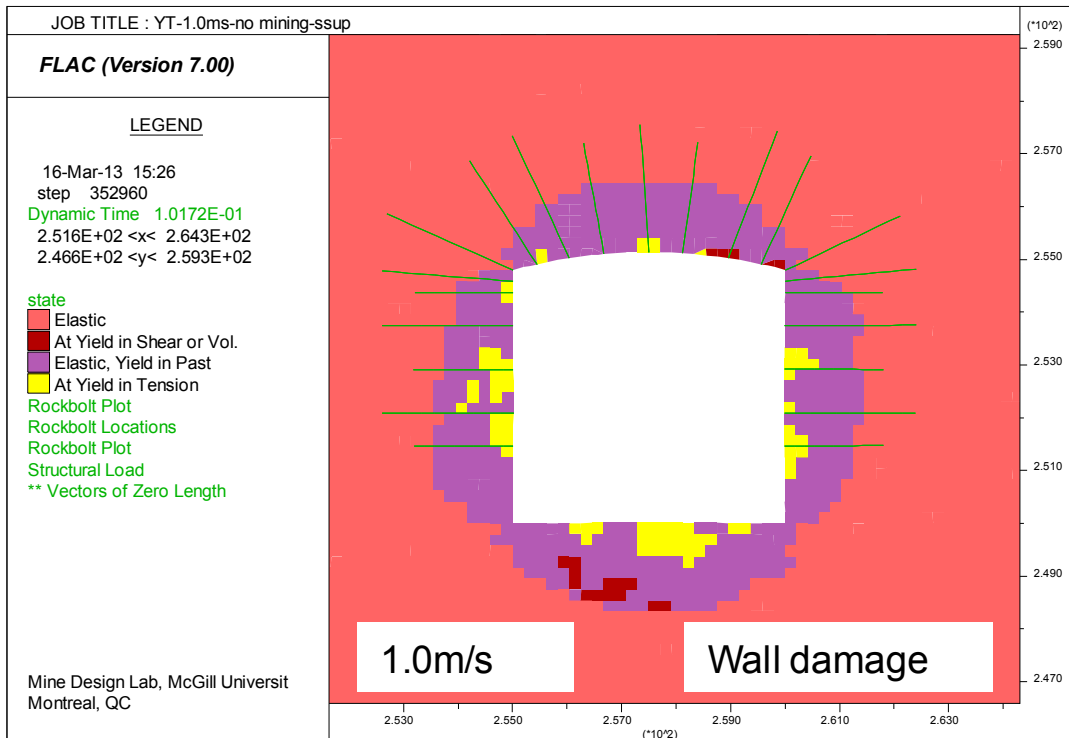
primary and secondary supports before commencing any mining sequence is shown in Figure 7-5. From these results we can estimate the thickness of wall damage and kinetic energy as in the following discussion.

In the case presented below is for the drift with primary and secondary support and the effect of seismic wave peak particle velocity on the drift stability was examined in this case. Various magnitudes of velocity as a dynamic load were applied far from the drift to simulate the seismic event that is occurring near the dyke as explained in Chapter 6. The peak particle velocity at the surface of the drift opening is monitored and will be used this as a ppv for calculating the kinetic energy released during the event as an example.

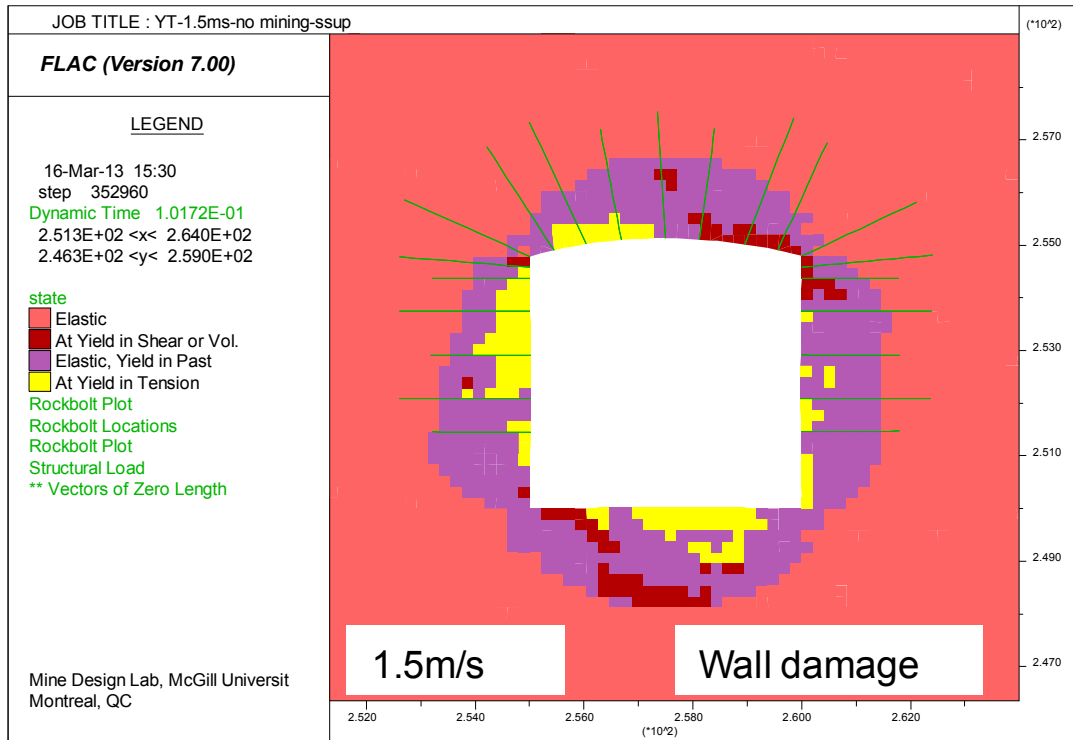
The proposed methodology for design of dynamic rock supports in the form of flow chart involving all the design steps is shown in Figure 7-6, followed by an illustration of calculating the kinetic energy from the results of dynamic analysis from Figure 7-7 is presented. The results shown in Figure 7-7 are used here to present as an example of explaining the damage and PPV to calculate the kinetic energy.



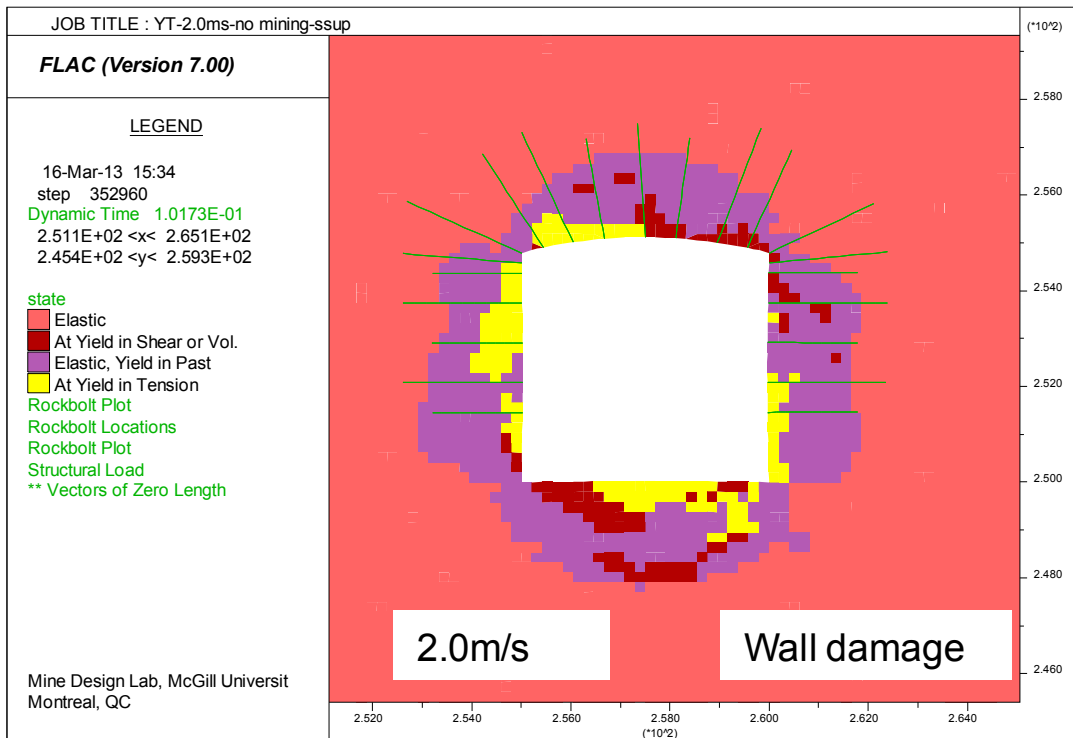
a) Wall damage around the drift for 0.5m/s PPV at the drift boundary



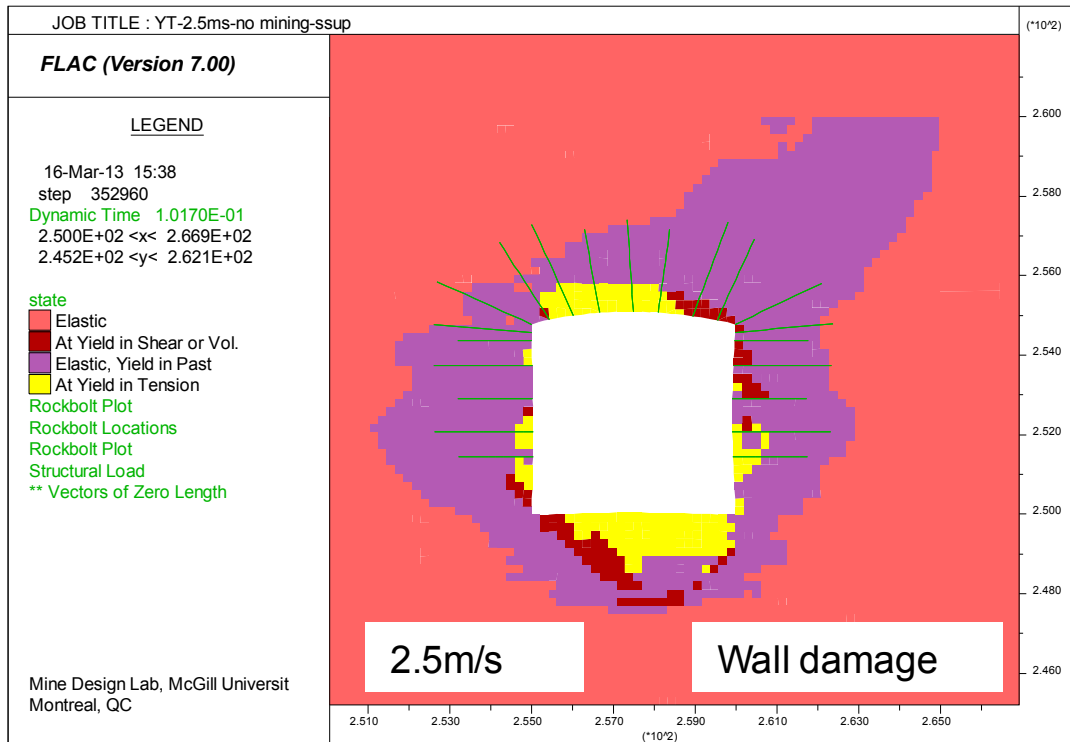
b) Wall damage around the drift for 1.0m/s PPV at the drift boundary



c) Wall damage around the drift for 1.5m/s PPV at the drift boundary



d) Wall damage around the drift for 2.0m/s PPV at the drift boundary



e) Wall damage around the drift for 2.5m/s PPV at the drift boundary

Figure 7-5 Wall damage around the drift with primary and secondary support for various levels of PPV due to seismic event

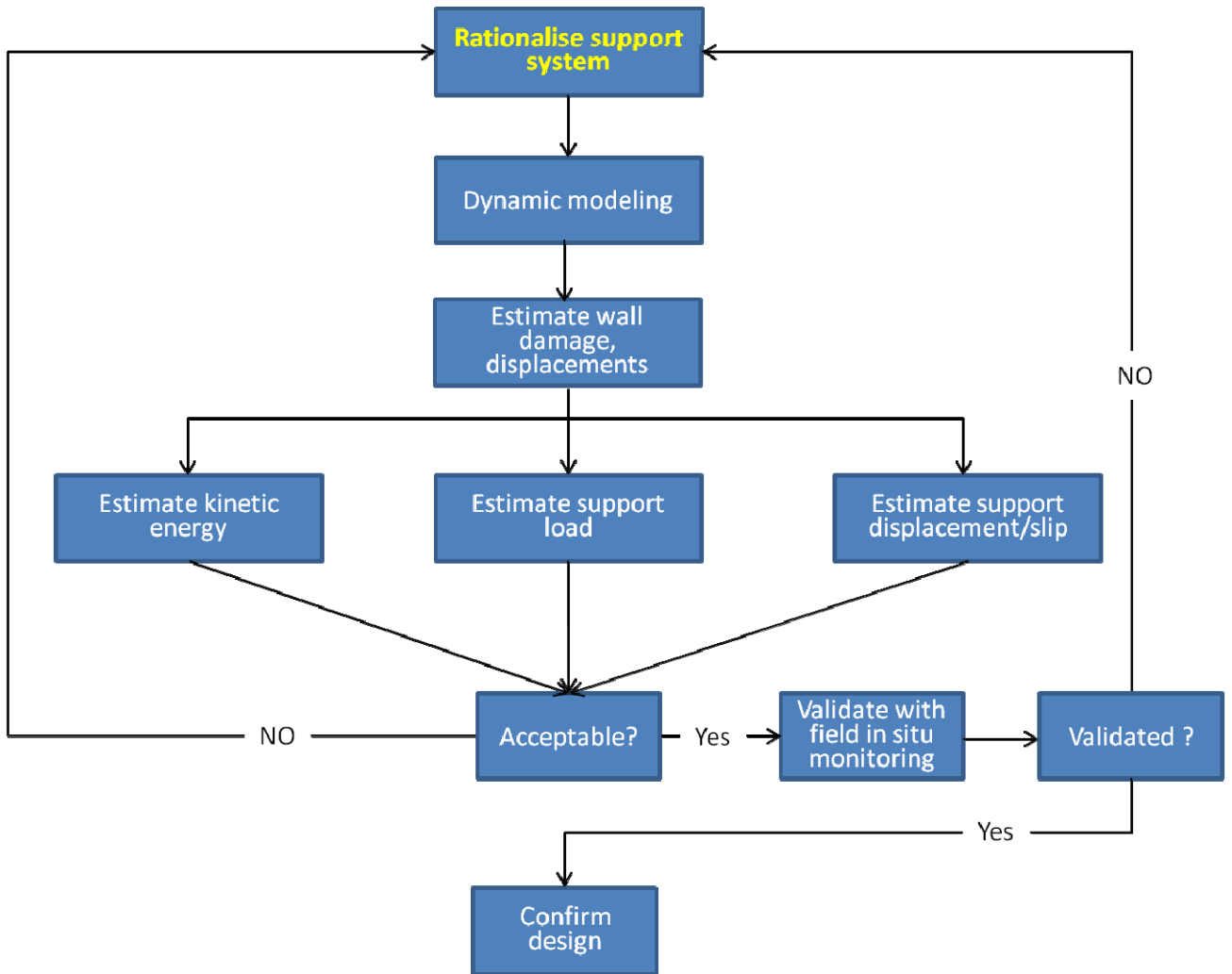


Figure 7-6 Flow chart of proposed design methodology for dynamic rock support design

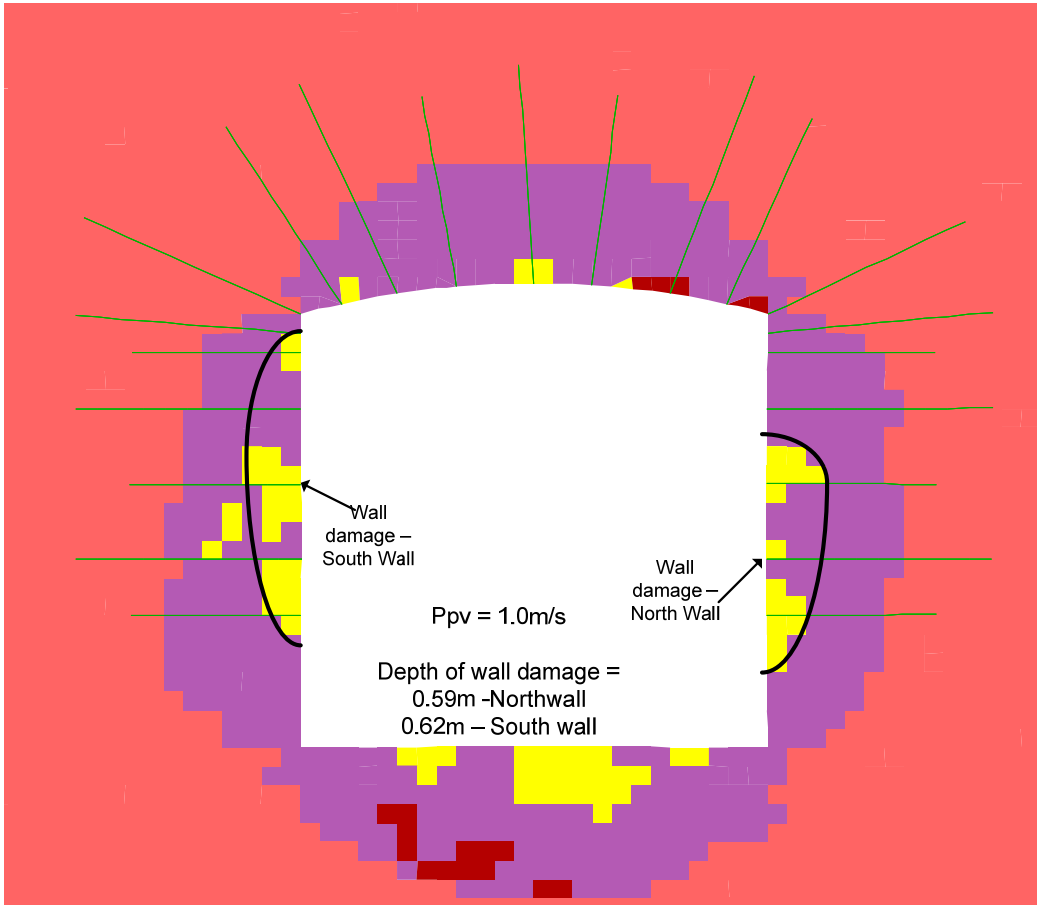


Figure 7-7 Wall damage around drift due to 1.5m/s ppv at the surface of the wall

In the Figure 7-7, PPV measured at the wall surface of the drift opening is 1.0 m/s and the depth of the wall damage is 0.59m on the North wall side of the drift and 0.62 on the south wall side, It can also be observed that the shear failure at the right side of the back of the drift. Considering for instance, that the PPV at the wall surface of the drift due to seismic event is equal to the ejection velocity of the damaged rock block, the kinetic energy of the ejected rock block can be calculated as below.

$$\text{Kinetic Energy (K}_e\text{)} = \frac{1}{2}mv^2$$

7.2

Where

$M$  = mass of the rock block

$V$  = Ppv or ejection velocity

Considering the above damage values of

Thickness of the damage = 0.59m (North Wall)

Density of the rock = 26kN/m<sup>3</sup>

Then the mass ( $m$ ) = unit area (m<sup>2</sup>) x rock density x average thickness of  
the ejected block = 1 x 26 x 0.59

$$= 15.34$$

Therefore  $K_e = 0.5 \times 15.34 \times 1^2$

$$= 7.67 \text{ kJ/m}^2$$

Considering the energy absorbing capacity of

Modified cone bolt (MCB) = 16 kJ (from Chapter 3)

Then the required bolt density to absorb the above energy = 7.67/16

$$\text{Bolt density (bolts/m}^2\text{) required} = 0.47$$

A square pattern of 1.5m x 1.5m is required to efficiently tackle the dynamic event in this case.

The displacement capacity required for the dynamic support for the above condition can also be estimated from the same dynamic modeling. The results of displacements due to dynamic loading are already presented in Chapter 6. However the displacements presented in Chapter

6 is only due to dynamic loading and hence doesn't include mining induced displacements. It should be noted that these mining induced displacements (pseudo dynamic) must be taken in to account, when deciding on the displacement requirements while selecting the dynamic rock support. Also the location and extent of the damage is not similar all around the drift. This way the dynamic supports can be designed according to the location and extent of wall damage as the dynamic supports are not required all over the mine and also the density of the dynamic supports required may not be the same around the drift opening. The complete methodology for selecting dynamic support in the form of flow chart involving all the design steps in the proposed methodology is already shown in Figure 7-6

Saharan et al.(2006), in a state-of-the art review on rock fracturing by explosive energy, presents the work of Brinkmann et al.(1987), about estimated peak particle velocity(PPV) at which the damage to the rock mass begins as shown in Figure 7-8. As can be seen from the figure that for the ppv of less than 50mm/s, the surface damage to rock can be avoided, fall of already loose rock can be expected between a PPV of 50mm/s to 100mm/s. Fall of rock in unlined tunnels can be expected at ppv levels of 300mm/s, where as new crack formation in rocks can be seen at 600mm/s (0.6m/s). A damage initiation range to intact hard rock can be attributed to the PPV range between 700mm/s to 1000mm/s.

The dynamic modeling results in this work for wall rock damage due to various peak particle velocities are shown in Table 7-2 and shown plotted in Figure 7-9. It can be observed from both these table and figures that the drift wall damage initiates at peak particle velocity of 0.3m/s. although the damage is concentrated to very small area up to 0.5m/s, the extent of damage remains almost the same. The damage increases in magnitude and also spreads to larger area when the peak particle velocity is 0.7m/s and more.

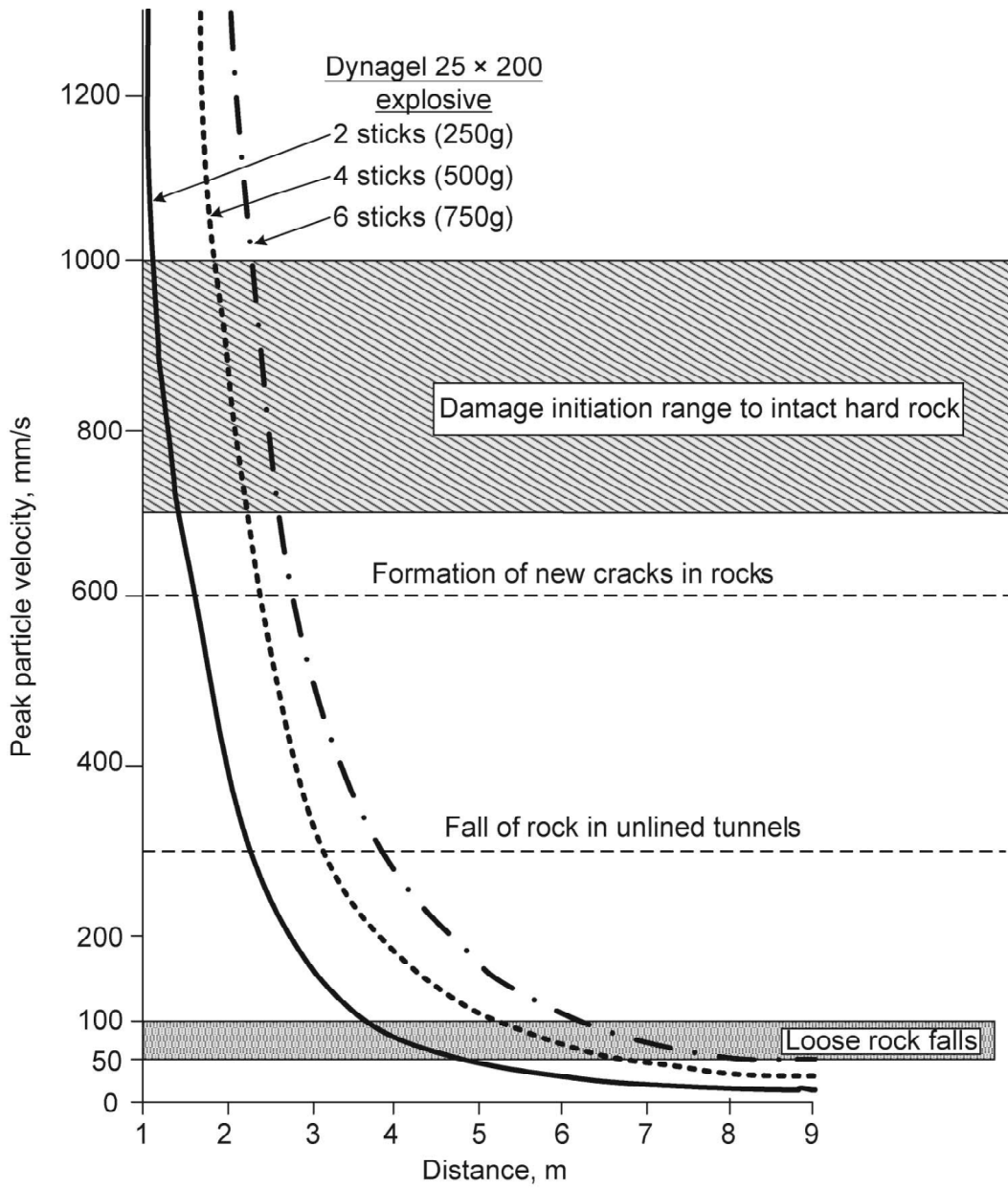


Figure 7-8 Reported damage threshold w.r.t peak particle velocity by Brinkmann et al.1987 (Saharan et al. 2006)

Table 7-2 Drift wall damage for various levels of PPV due to dynamic load

PPV, m/s	Wall damage(North wall)	Remarks
0.3	0.2	Damage confined to very small area
0.5	0.22	Damage confined to very small area
0.7	0.31	Damage starts spreading to wider area
0.9	0.55	
1.0	0.59	
1.5	0.71	
2.0	0.6	Damage due to shear at the wall corners reduces tensile damage
2.5	0.70	Damage due to shear at the wall corners reduces tensile damage

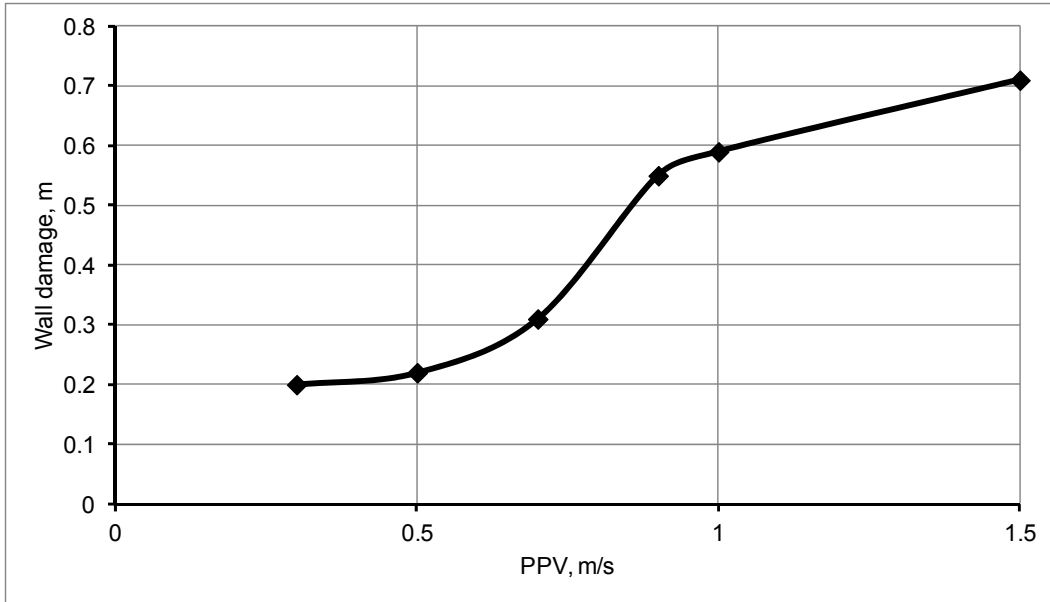


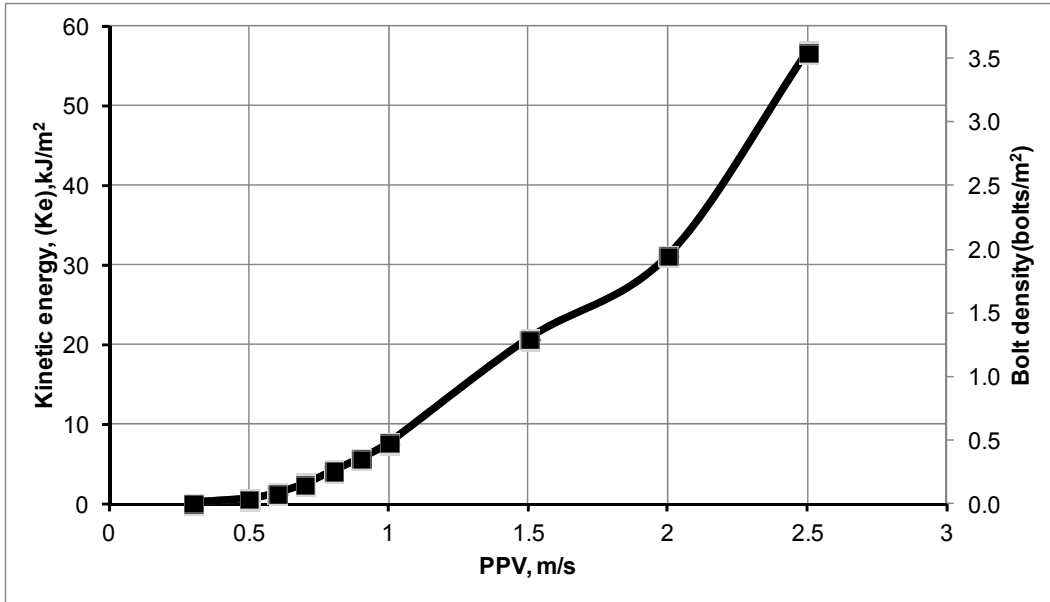
Figure 7-9 Wall damage due to various peak particle velocity

It can be observed from the Figure 7-9, that the wall damage increase sharply when the peak particle velocity at the drift boundary is 0.7m/s and more. At 1.5m/s the wall damage reach to 0.7m and covers the considerable area of the drift wall. Table 7-3 presents the kinetic energy corresponding to the PPV and the wall damage (North wall damage in this case). While Figure 7-10 presents the kinetic energy(taking in to account the wall damage due to corresponding PPV), Peak particle velocity and the required bolt density to effectively support the area to absorb the energy due to dynamic event. As can be seen the energy that is released due to the ejection of the rock block is not very significant up to the peak particle velocity of 0.7m/s with the corresponding wall damage. On the other hand the peak particle velocity of 1.0m/s with the extent of wall damage of 0.59m, the resultant energy is  $7.67\text{kJ/m}^2$ , which means that a square pattern of  $1.5 \times 1.5$  m of cone bolts having 16kJ of energy absorption capacity is required to support this area. Also, the dynamic supports are installed always in conjunction with the mesh reinforced shotcrete, which also have considerable amount of energy absorbing capacity.

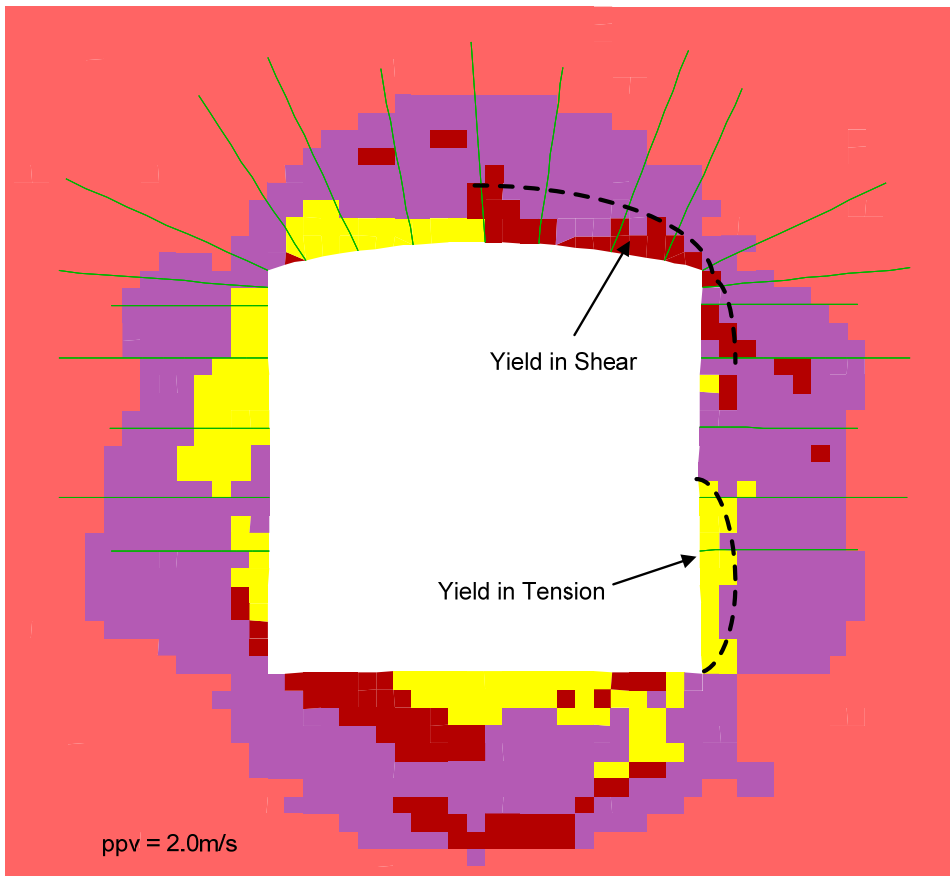
At higher levels of ground motion, such as beyond 1.5 m/s, the energy demand on dynamic support increase substantially and reaches to more than 50kJ/m<sup>2</sup>, which according to Kaiser, 1993 and CRRP(1990-95), is impossible to support economically with the existing methods and thus they called it as Maximum Possible Support Limit(MPSL).

Table 7-3 Kinetic Energy w.r.t peak particle velocity and the associated wall damage

PPV, m/s	Wall damage(North wall)	Kinetic Energy(K <sub>e</sub> ), kJ/m <sup>2</sup>
0.3	0.2	0.23
0.5	0.22	0.71
0.7	0.31	2.54
0.9	0.55	5.79
1.0	0.59	7.67
1.5	0.71	20.76
2.0	0.6	31.2
2.5	0.70	56.87



7-10 Kinetic energy, PPV and corresponding bolt density (based on bolt energy capacity of 16kJ)



7-11 Shear failure at higher levels of peak particle velocities

The shear damage at higher peak particle velocity can be seen from Figure 7-11. It is worth noting here that the shear failure occurring in some parts of the drift opening during a dynamic event. The performance of dynamic supports under such conditions can not be as expected. The details of working of the dynamic supports are presented in Chapter 3. Load deformation curves, under dynamic loading presented, pertains to pure axial loading. No doubt that, the dynamic bolts such as cone bolts performed well under dynamic event in many cases, as shown in Figure 7-12.(e.g. Mckenzie (2002), Simser et al.(2007), Yao et al. (2009)). The apprehension expressed here, based on the dynamic numerical modeling, is when there is a high shear failure in part of the drift opening due to higher peak particle velocities, the dynamic action of yielding of the dynamic support may not be possible and hence the dynamic support will fail in the same manner as the grouted rebar. Field observations of rockbolt failure by shear is reported by many authors (e.g, Simser(2007),Li (2010). Figure 7-13 shows the field observations of rockbolt failure by Li (2010).

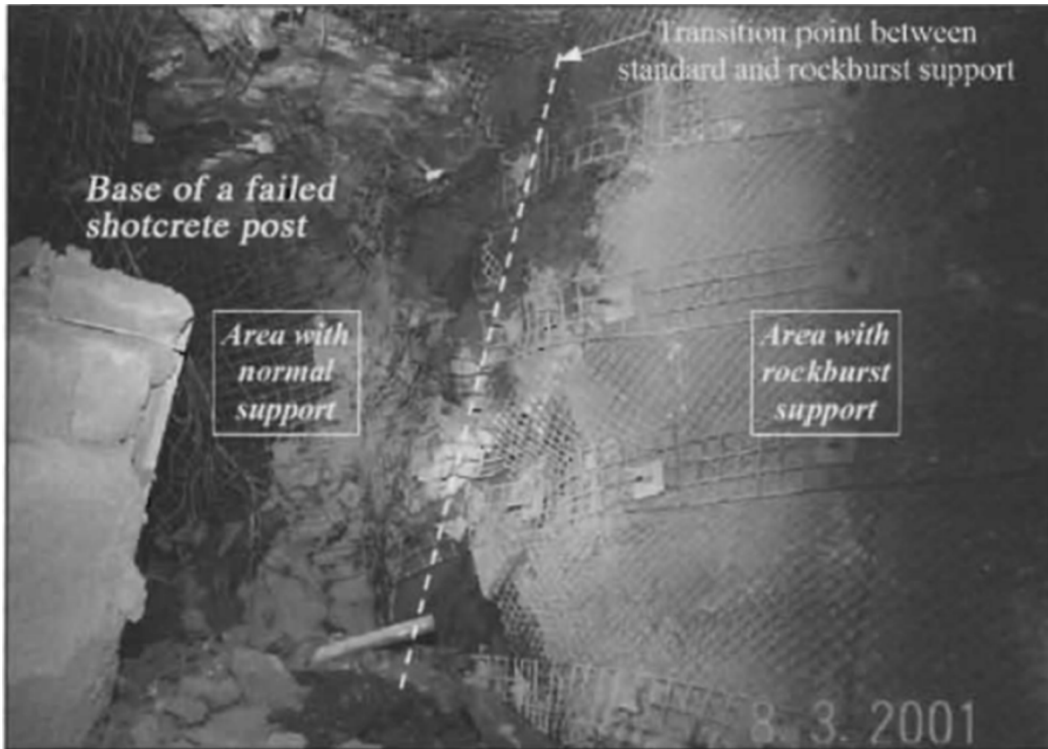


Figure 7-12 Effect of dynamic rock supports, cone bolts in this case ( Simser et al. 2007)

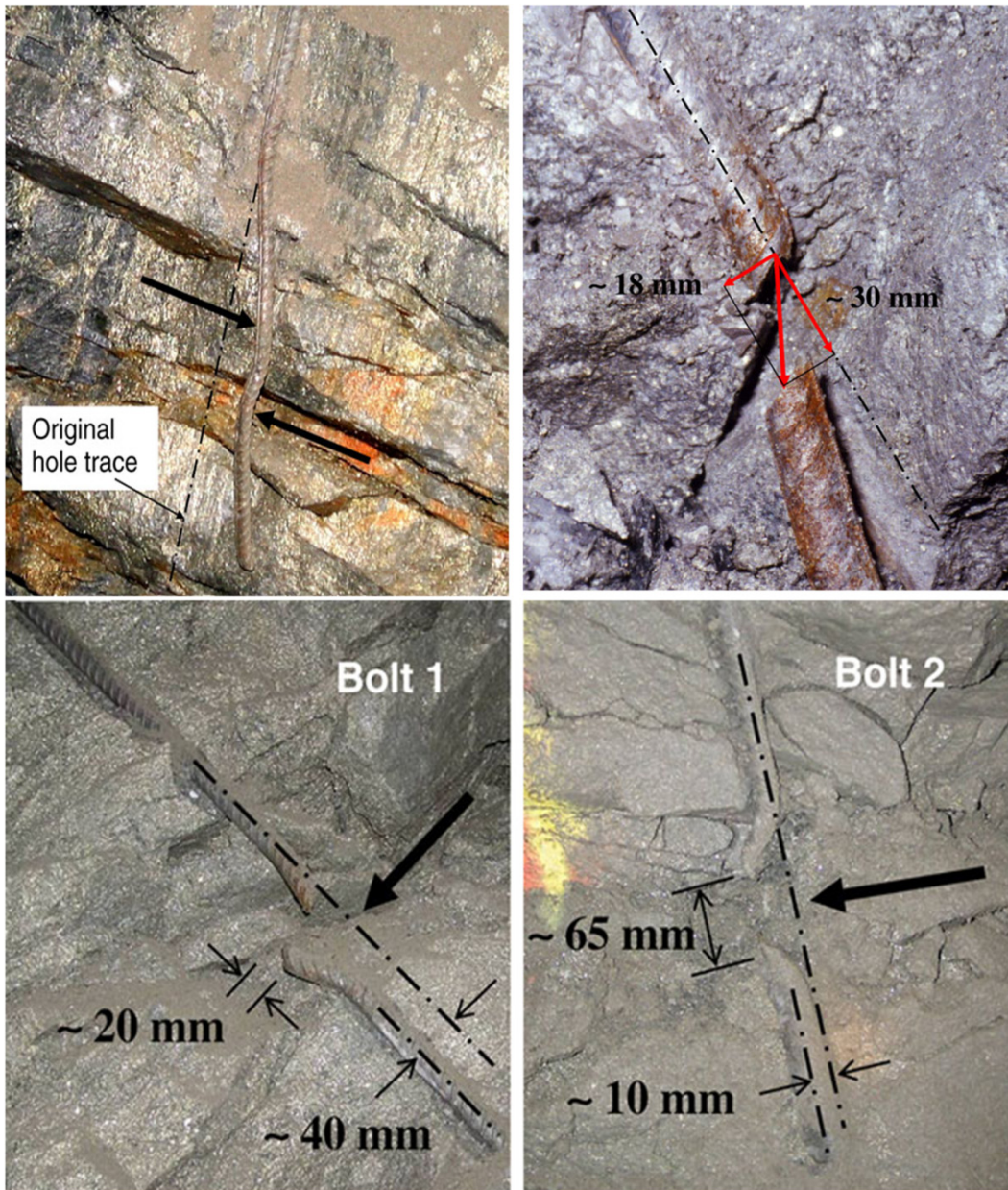
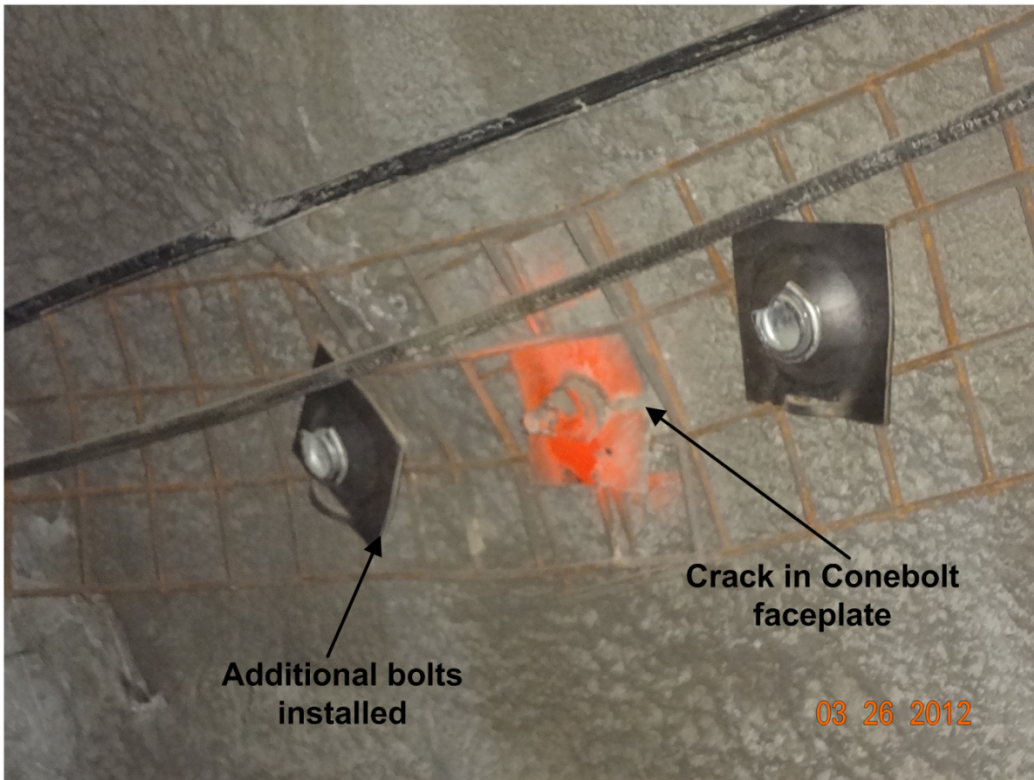


Figure 7-13 Field observation of rockbolt failure ( C.C.Li, 2010)

Rockbolt failure particularly the cone-bolt failure under high shear stress is also observed by the author from the case study mine. Figure 7-14 shows pictures of cracking of cone-bolt face plate and the crack and spalling in the walls of drift and sill openings. It can be observed from these figures, that the cone-bolt is not seem to yield due to shear failure of the rock and hence the face plate is being cracked. Some more pictures of field observation are given appendix A-2.



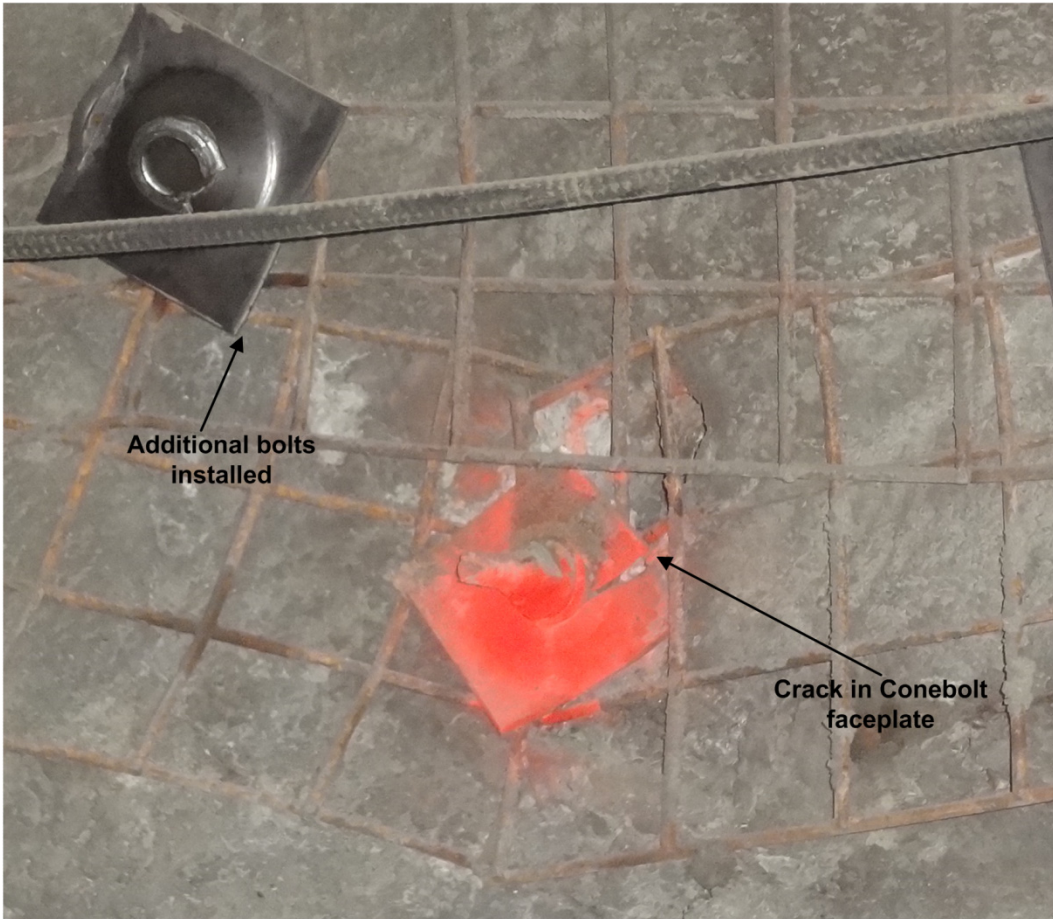


Figure 7-14 Field observation of conebolt failure in shear from the case study mine

## 8 Conclusions and Suggestions for Future research

### 8.1 Case study numerical modeling

In this research ground support analysis of footwall haulage drift is performed, where two numerical models are developed to examine the mining induced loads on primary and secondary support system with respect to mining activities. Based on the results of the numerical modeling and instrumentation following conclusions can be drawn.

- Two numerical models are developed to examine the mining-induced loads on primary and enhanced support systems with respect to mining activities. Modeled primary supports are  $\frac{3}{4}$  inch grade 60 rebars and modeled enhanced supports are Modified Cone Bolts (MCB). The drift behaviour under static and dynamic conditions is examined.
- All numerical models show that the maximum bolt axial load occurs at the bolt head suggesting the use of the load cells at the bolt head is adequate for capturing the maximum load.
- It appears that the same-level mining is more critical than lower-level mining in terms of induced axial loads on the rock supports.
- The increase in load on the bolt head is more immediate in the north wall after same-level mining begins, whereas in the case of the south wall and drift back, the bolt load relaxes during same-level mining suggesting the formation of an extensive yield (relaxation) zone between the drift and the orebody.

- The installation of enhanced supports greatly improves the stability of the drift by sharing the loads of primary supports, which are otherwise yielding as soon as same-level mining begins.
- A new load cell called U-cell is installed in the field to measure the rockbolt load at the head of the bolt for both rebars and MCB.
- It appears from in-situ measurements that the average rockbolt pretension load is 20 kN
- The results of the numerical models are found to be in good agreement with monitored loads as obtained from the U-Cells.

## **8.2 Dynamic modeling**

In another model, dynamic analysis is conducted to evaluate the performance of the drift when subjected to seismic loads. The far and near field effect on the drift with or without support is also examined. Further it is intended to estimate the location and extent of the wall damage due to various levels of ground motion when subjected to seismic loads. Major conclusions drawn from this analysis is as follows

- Dynamic analysis is conducted to evaluate the performance of the drift when subjected to seismic waves. The far and near field effect on the drift with or without support are examined.
- The location and extent of the wall damage due to various levels of ground motion when subjected to seismic loads are estimated. The range of applied seismic wave velocities is 0.5 to 2.5 m/s and found that beyond 1.0m/s the wall damage increases sharply
- Enhanced supports appear to be restricting the wall damage particularly in north wall.

- It is observed that the rebars in the north wall and south wall are lightly loaded for a ground motion of 0.5m/s at the drift, whereas the rebars in the back take more loads as yielding does not reached beyond the rebars anchorage limit. Mining sequence is not simulated in this case, thus, the combination of primary and secondary support system is strongly recommended.
- A simple methodology for the rationalization of drift dynamic rock support system in burst-prone environment is developed on the basis of dynamic modeling and energy considerations.

Displacements around drift opening due to dynamic loading are also presented in this work. Under the dynamic loading conditions, wall displacements are restricted to below 20mm for the peak particle velocity of 1.5 m/s. at higher levels of peak particle velocity the displacements are showing sharp increase after 1.5m/s and recorded 89.6mm at 2.5m/s. This amount of displacements can be taken care of the dynamic rock supports such as cone bolt, which has yielding capacity of 200mm. However it is to be noted that the displacements during static condition due to mining activity, needs to be taken in to account and to be added to the displacements obtained from dynamic numerical modeling to select the displacement capacity of the dynamic support.

It is highly advantageous to have an appropriate instrumentation program to monitor the displacements and in situ loads on supports due to mining activity. This will help in deciding the remaining capacity of the support system both in terms of load and displacement and gives important information, whether the existing support can accommodate a severe rockburst if it happens in near future.

### 8.3 Suggestions for future research

This thesis presents the results of drift behavior under static and dynamic conditions through the 2Dimensional numerical modeling. Although the research in this work could be calibrated with the field in situ measurements and is able to demonstrate that the approach led to a proposed new methodology for dynamic rock supports design. However the following recommendations for future research are worth mentioning here.

- Study the support performance at intersections with respect to mining sequence using 3-dimensional modeling.
- Better define the shape and intensity of applied seismic wave by correlation with observed micro seismic activities at the mine, particularly major events causing rockbursts and fault slip bursts.
- Model the slip behavior of the MCB and other similar dynamic rock supports having slip mechanism.
- New generation of U-cells used to monitor the bolt in situ loads could be of immense help in further calibrating the dynamic model. It is recommended that the supports in rockburst prone areas may be monitored for their in situ loads and can be compared with the dynamic modeling results

## **8.4 Statement of Contribution**

This research has attempted for the first time to examine primary and secondary rock support performance in mine developments such as haulage drifts, with respect to the influences of lower-level and same-level mining activities. The study has integrated the use of numerical modelling tools and field instrumentation program to shed light on the rock support performance.

A new methodology for the selection of dynamic rock support pattern in burst-prone environment is devised. The methodology takes into account the energy, load and displacement capacities of the rock support as well as the applied kinetic energy due to seismic loading.

## 9 References

Abdellah.W (2012), Mine design lab, McGill University, Internal communication.

Barton, N.R., Lien, R and Lunde, J. (1974). Engineering classification of rock masses for the design of tunnel support. *Rock Mech.*, 6, 189-239.

Barton, N.(1988). Rock mass classification and tunnel reinforcement selection using the Q-system, In: *Rock Classification Systems for Engineering Purposes*, 59-88 (Louis Kirkaldie(ed)), ASTM STP 984, American Society for Testing and materials, Philadelphia.

Barton, N (2002). Some new Q-value correlations to assist in site characterization and tunnel design. *International Journal of Rock Mechanics and Mining Sciences*. 39, 185-216.

Beauchamp, L.A. (2006). *Ground support manual*. Mines and Aggregates Safety and Health Association (MASHA), North Bay ( Ontario): 285p

Biggs, (1964). *Introduction to structural dynamics*. New York: McGraw – Hill (1964).

Bieniawski, Z.T. (1989). *Engineering rock mass classifications*. New York: Wiley.

Bieniawski, Z.T. (1974). Geomechanics classification of rock masses and its application in tunneling. In: *Proceedings of the 3<sup>rd</sup> International Congress on Rock Mechanics*, Denver, 27-32.

Bjornfot, F. and Stephansson, O.(1984). Interaction of grouted rock bolts and hard rock masses at variable loading in a test drift of the Kiirunavaara Mine, Sweden. In:O.Stephansson, ed.Proceedings of the International Symposium on Rock Bolting. Rotterdam, The Netherlands: Balkema: pp. 377–395.

Blake and Hedley.(2003). Rockbursts: Case studies from North American Hard-rock Mines. Society for Mining, Metallurgy, and Exploration, Inc(SME), Littleton, Colorado, USA 80127, ISBN 0-87335-232-7.

Brady, B.H. and Brown, E.T. (1993) *Rock Mechanics For Underground Mining*. Chapman & Hall, 2nd edition.

CAMIRO (1996) Canadian rockburst research program 1990:1995— a comprehensive summary of five years of collaborative research on rock bursting in hard rock mines. CAMIRO Mining Division, Canada

CANMET, (2008). Design guidelines for the dynamic behavior of ground support tendons, Phase I: Technical information data sheets, by Denis labrie, Chantale Doucet and Michel Plouffe.

CANMET-MMSL.(2012). Technical information data sheets, version 2012-05-29, Natural resources, Canada

Charette F, Plouffe M (2007) Roofex—results of laboratory testing of a new concept of yieldable tendon. In: Potvin Y (ed) Deep mining 07. In: Proceedings of the 4th international seminar deep and high stress mining. Australian Centre for Geomechanics, Perth, pp 395–404

Clough, R. W. and J. Penzen (1975). Dynamics of Structures. United States of America, McGraw-Hill Book Company Inc.

Daehnke, A., Vanzyl, M & Roberts, M.K.C. (2001). Review and application of stope support design criteria. *Journal of the South African Institute of Mining and Metallurgy*, Vol. 101, No.3: 135-164.

Deb, D.and Das, C.D. (2010). Bolt-grout interactions in elasto-plastic rock mass using coupled FEM-FDM techniques. *Advances in Civil Engineering 2010*(Article ID 149810): 1–13.

Deere, D.U. (1968). Geological considerations. In: *Rock mechanics in engineering practice*, ( R.G.Stagg and D.C. Zienkiewicz.(Eds), division of Civil Engineering, School of Engineering, University of Wales, Swansea, John Wiley & Sons, New York, 1-20.

Deere,D.U. and Deere,D.W. (1988). The Rock Quality Designation(RQD) index in practice. In: *Rock Classification Systems for Engineering Purposes*, 91-101 (Louis Kirkaldie(ed)), ASTM STP 984, American Society for Testing and materials, Philadelphia

D.Jean Hutchinson and Mark.S. Diederichs, (1996). *Cablebolting in Underground Mines*, BITECH PUBLISHERS Ltd, Canada

Edelbro, C.(2003). *Rockmass strength – A Review*, Technical report, Department of Civil engineering, Lulia University of technology.

Farmer, I.W, and Shelton, P.D. (1980). Factors that affect underground rockbolt reinforcement systems. *Trans. Inst.min.Metall.*, 89, A68-A83.

Freeman, T.J. (1978). The behavior of fully grouted bolts in the Kielder experimental tunnel. *Tunnels and Tunnelling* 10: 37–40.

Gemant, A. and W. Jackson (1937). The Measurement of Internal Friction in Some Solid Dielectric Materials. The London, Edinburgh, and Dublin Philosophical Magazine & Journal of Science XXII: 960-983.

Genis, M., and Gercek, H., (2003), A numerical study of seismic damage to deep underground openings. In ISRM 2003- Technology roadmap for rock mechanics, South African Institute of Mining and Metallurgy.

Heal, D. (2007). Ground support for rockbursting conditions – theory and Practice, in Course Notes for Advanced ground support in underground mining (COR 0703), Perth, Australia, May, Australian Centre for Geomechanics, Section 5, 54.

Hadjigeorgiou, J & Charette, F. ( 2001). Rock bolting for underground excavations. Underground Mining Methods – Engineering fundamentals and international case studies, W.A. Hustruild and R.L. Bullock, Editors, Society for Mining, Metallurgy and exploration ( SME), Littleton ( Colorado), Chapter 63: 547-554.

Hedley, D.G.F. (1992), Rockburst Handbook for Ontario Hardrock mines. CANMET Special Publication SP92-1, Mining Research Laboratories, Energy, Mines and Resources Canada, Ottawa ( Ontario).

Hoek, E. and Brown, E.T. (1997). Practical estimates of rock mass strength. Int.J.Rock Mech.Min., 34(8), 1165-1186.

Hoek, E. (2000). *Practical rock engineering*. URL: <http://www.rockscience.com>

Hoek E. and Brown E.T. (1980). Underground Excavations in Rock, London: Institution of Mining. Metall

Hoek, E. (2007a). Practical Rock Engineering – Chapter 13: Design of large underground caverns. Lecture notes, Rockscience Inc., Toronto (Ontario): 29p.

Hoek, E., Kaiser, P.K & Bawden, W.F. (1995). Support of Underground Excavations in Hard Rock. A.A. Balkema Publishers, Rotterdam (Netherlands):215p

Hutchinson, J & Diederichs, M. (1995). Cablebolting in Underground Mines. Bitech Publishers, Richmond (British Columbia): 400p.

Hyett, A.J. and Mitri, H. (2012). Two new technologies for measuring the in situ performance of rock bolts. In: Abstract Volume of Proceedings of the Seventh International Symposium on Rockbolting and Rock Mechanics in Mining. Aachen, Germany: AIMS, abstract number -036.

Hyett, A.J., Moosavi, M., and Bawden, W.F. (1996). "Load distribution along fully grouted bolts, with emphasis on cable bolt reinforcement. International Journal for Numerical and Analytical Methods in Geomechanics 20(7): 517–544.

Hyett, A.J., Mitri, H., and Spearing, A.J.S. (2012) Validation of two new technologies for monitoring the in situ performance of rock bolts. In Proceedings of Aachen International Mining Symposia - 7th International Symposium, Rockbolting and Rock Mechanics in Mining, May 30-31, 2012, Aachen, Germany, pp. 177-190. Published by RWTH Aachen

ITASCA Consulting Group Inc. (2011). Dynamic Analysis, FLAC2D Fast Lagrangian Analysis of Continua. Minneapolis, Minnesota USA, Itasca Consulting Group.

ITASCA (2009) ,Itasca Consulting Canada. Geomechanics for Garson Deep FEL II study, February 2009

Jager AJ (1992) Two new support units for the control of rockburst damage. In: Kaiser PK, McCreath DR (eds) Proceedings of the international symposium rock support. Balkema, Rotterdam, pp621–631

Jager, A, Wojno, L.N and Henderson, N.B. (1990). New developments in the design and support of tunnels under high stress, Technical challenges in Deep-level Mining. SAIMM congress, Johannesburg.

Kaiser, P.K. (1993). Support of tunnels in burst-prone ground – Toward a rational design methodology: Proceedings of the 3<sup>rd</sup> International Symposium on Rockbursts and seismicity in Mines, 16-18 August, Kingston ( Canada), R.P. Young, Editor, A.A. Balkema Publishers, Rotterdam ( Netherlands): 13-27.

Kaiser, P.K., McCreath, D.R. and Tannant, D.D. (1997). Rockburst Support. In *Canadian Rockburst Research Program 1990-95*, Sudbury, ON: CAMIRO, Vol.2, 324 p.

Kirsten, H.A.D. (1993). Equivalence of mesh- and fiber-reinforced shotcrete at large deflections. *Can. Geotech. J.* 30, 418-440.

Kirsten, H.A.D. 1993. Equivalence of mesh- and fibre-reinforced shotcrete at large deflections. *Can. Geotech. J.* 30, 418-440.

Kunar, R. R., P. J. Beresford, et al. (1977). A Tested Soil-Structure Model for Surface Structures, in Proceedings of the Symposium on Soil-Structure Interaction Roorkee University, India, January, 1977 1: 137 – 144.

Lang, T. A. (1961 ). Theory and Practice of Rock Bolting, Trans. AIME, Trans. 220, 333-348

Li CC (2011a). Chapter 18. Rock support for underground excavations subjected to dynamic loads and failure. In: Zhou Y, Zhao J (eds) Advances in rock dynamics and applications. CRC Press, Taylor & Francis Group, Boca Rotan, pp 483–506

Li and Doucet.( 2012) Performance of D-Bolts Under Dynamic Loading in Rock Mech Rock Eng (2012) 45:193–204 DOI 10.1007/s00603-011-0202-1

Li CC (2010) A new energy-absorbing bolt for rock support in high stress rock masses. Int J Rock Mech Min Sci 47:396–404

Li CC (2011b) Performance of the D-bolt under static loading. Rock Mech Rock Eng. doi:10.1007/s00603-011-0198-6

Li, C.C (2010a). Field observations of rock bolts in high stress rock masses. Rock Mechanics and Rock Engineering 43(4): 491–496.

Li, T, Brown, E T, Coxon, J and Singh, U. (2004). Dynamic capable ground support development and application, in *Ground Support in Mining and Underground Construction* (eds: E Villaescusa and Y Potvin), pp 281-288 (Taylor and Francis Group: London)

Lindsay Moreau, V. (2012), Senior Ground Control Engineer, Garson Mine, Vale ltd, Sudbury, ON, Canada, .Personnel communication

Lysmer, J. and R. L. Kuhlemeyer (1973). Finite Dynamic Model for Infinite Media. *J. Eng. Mech* **95**(EM4): 859 - 877.

Martin, L. B., Tijani, M., and Hadj-Hassen, F. (2011). A new analytical solution to the mechanical behavior of fully grouted rock bolts subjected to pull-out tests. *Construction and Building Materials* **25**(2): 749–755.

McCreath CD, Kaiser PK (1992). Evaluation of current support practices in burst-prone ground and preliminary guidelines for Canadian hardrock mines. In: Kaiser PK, McCreath DR (eds) *Proceedings of the international symposium rock support*. Balkema, Rotterdam, pp 611–619

McGarr, A.(1997). A Mechanism for High Wall-rock Velocities in Rockbursts. *Pure and Applied Geophysics*, 150 (1997) 381–391, Birkhauser Verlag, Basel, 1997.

Mckenzie, R, ( 2002). Use of cone bolts in ground prone to rockburst, in Aziz, N(ed), *Coal 2002: Coal Operators conference*, University of Wollongong & the Australian Institute of Mining and Metallurgy, 169-175

Mehrotra, V. K. (1992). Estimation of Engineering Properties of Rock Mass. Ph. D. Thesis, University of Roorkee, Roorkee, India, p. 267.

Mercier-Langevin. F. (2010). Review of mining practices at depth at Agnico-Eagle's LaRonde mine. *CIM Journal*, Vol. 1, No. 3, pp.183-195

Metzger, D. R. (2003). Adaptive damping for dynamic relaxation problems with non-monotonic spectral response. *International Journal for Numerical Methods and Engineering* **56**: 57 – 80

Mikula(2012). Progress with empirical performance charting for confident Selection of ground support in seismic conditions, in a special issue on deep and high stress mining, Australian centre for Geomechanics, The University of Western Australia, 2012.

Mikula, P. A. and Lee, M. F. (2000). Bulk low grade mining at Mt Charlotte Mine, Proc. MassMin 2000 Conf., (ed. G. Chitombo), 623–635, Melbourne, Australasian Institute of Mining and Metallurgy.

Milev, A. M. and Spottiswood, S. M. (2005). Strong ground motion and site response in deep South African mines, J. S. Afr. Inst. Min. Metall., 105, (7), 515–524 and comment on that paper by Ortlepp, W. D. 2006. J. S. Afr. Inst. Min. Metall., 106, (7), 593–597, and reply to those comments by the original authors, J. S. Afr. Inst. Min. Metall., 106, (7), 598–599.

Mitri. H.S., (2000). Applied rock mechanics in underground mining- Focus on cable bolting technology, Short course, December 11-13, 2000, McGill University, Montreal.

Mitri, H.S. (2011). Evaluation of rock support performance through instrumentation and monitoring of bolt axial load. In Proceedings of Coal Operators' Conference, Wollongong, NSW, Australia, Feb 10-11, 2011, pp. 136-140. Published by the University of Wollongong

Mitri, H.S., Hyett, A. and Raju, D. (2012) New Monitoring Technologies for Measuring the in-situ Performance of Rock Bolts. In Proceedings of 31st International Conference on Ground Control in Mining, July 31-August 2, 2012, Morgantown, WV, Paper No. 34 (1-9). Published by Strata Products (USA) Inc.

Mitri, H.S. and Rajaie, H. (1991). Shear bond stresses along cable bolts: Proceedings of the 10th International Conference on Ground Control in Mining. Morgantown, WV: West Virginia University, 90–96.

Ortlepp. W.D., (1983). The Mechanism and Control of Rockbursts: Chapter 12: Rock Mechanics in Mining Practice, Budavari (ed.), S. Afr. Inst. Min. Met. series No. 5, pp. 257 - 282,

Ortlepp, W. D.(1993). *High ground displacement velocities associated with rockburst damage*. In *Rockbursts and Seismicity in Mines* (ed. Young, R. P.) (Balkema, Rotterdam 1993) pp. 101–106.

Ortlepp D (1992) Invited lecture: the design of support for the containment of rockburst damage in tunnels—an engineering approach. In: Kaiser PK, McCreath DR (eds) Proceedings of the international symposium on rock support, Sudbury, ON, Canada, Balkema, pp 593–609

Ortlepp D (1994) Grouted rock-studs as rockburst support: a simple design approach and an effective test procedure. J South Afr Inst Min, Metall, 94(2):4763

Ortlepp D, Stacey TR (1995) Technical note: safety and cost implications in the spacing of support. J South Afr Inst Min Metall, pp141–146

Palmstrom, A. (1995). Characterizing the Strength of Rock Masses for Use in Design of Underground Structures, Conf. Design and Construction of Underground Structures, New Delhi, pp. 43-52.

Pakalnis, V and D. Ames (1983). Load tests on mine screening. Underground support systems. Canadian Institute of Mining Metallurgy and Petroleum, Special Volume 35. Udd, J(ed) pp 79 – 83

Potvin et al. (2004), Surface support in Mining. Australian Centre for Geomechanics, 2004 - Technology & Engineering

Raju, D, Mitri, H.S, Denis Thibodeau and Lindsay Moreau, V.,(2012), Effect of Stope Sequencing on Support Performance of Haulage Drift, in 21<sup>st</sup> International conference on Mine Planning and Equipment Selection(MPES), November 28-30, 2012, New Delhi, India

Schach, R, Garshol, K & Heltzen, A.M. (1979). Rock Bolting: A practical Handbook, Pergamon Press, Oxford ( England): 84p

Seed, H. B. and I. Idriss (1969). "Influence of Soil Conditions on Ground Motion during Earthquakes." J. Soil Mech. Found., Div. ASCE, **95**: 99-137.

Shnorhokian S., Mitri H., Thibodeau D., and Moreau-Verlaan L. (2013). Optimizing stope sequence in a diminishing ore pillar: a case study. In *Proceedings of the 23<sup>rd</sup> World Mining Congress, 11 – 15 August, Montreal (Canada)*. Accepted.

Simser B (2001) Geotechnical review of the July 29, 2001. West ore zone mass blast and the performance of the Brunswick/NTC rockburst support system. Tech Rep

Simser, B.P (2007) The weakest link –ground support observations at some Canadian Shield hard rock mines, in Proceedings Fourth International Seminar on Deep and high stress mining( Deep Mining 07), Potvin(ed) 7-9 November 2007, Perth, Australia, Australian Centre for Geomechanics, Perth, PP, 335-348.

Simser et al.(2007). Field behavior and failure modes of modified cone bolts at the Craig, Laronde and Brunswick mines in Canada, In Challenges in Deep and High Stress Mining- Potvin, Hadjigeorgiou,

stacy(ed), Chapter 39, Australian Centre for Geomechanics, Perth, 2007, ISBN 978-0-9804185-1-4.

Singh, B and Goel, R.K. (1999). *Rock mass classification – A practical approach in civil engineering*, Elsevier, Netherlands.

Stacey, T.R., Ortlepp, W.D., and Kirsten H.AD., (1995), Energy-absorbing capacity of reinforced shotcrete, with reference to the containment of rockburst damage, S.Afr. inst. Min. Metall., V. 95, no. 3

Stillborg, B. (1994). Professional Users Handbook for Rock Bolting. Trans Tech Publications, 2nd Edition. Atlas Copco, Sweden.

Stille, H. (2001). Rock support in theory and practice. Underground Mining Methods – Engineering fundamentals and international case studies, W.A. Hustruild and R.L. Bullock, Editors, Society for Mining, Metallurgy and exploration (SME), Littleton (Colorado), Chapter 62: 535-546.

St-Pierre L, Hassani FP, Radziszewski PH, Ouellet J.(2009). Development of a dynamic model for a cone bolt. In: International Journal of Rock Mechanics & Mining Sciences 46 (2009) 107– 114.

Syed Ariff (2004). Studies on support design for Underground excavations, PhD thesis. Dept. Of Civil Engineering, Bangalore University, Bangalore, India

Saharan.M.R (2004). Dynamic modeling of rock fracturing by de stress blasting. PhD thesis, submitted to McGill University, 2004

Saharan. M.R., Mitri. H.S., and Jethwa. J.L, (2006). Rock fracturing by explosive energy: review of state-of-the-art. In Fragblast, Vol. 10, Nos. 1– 2, March–June 2006, 61 – 81

Shnorhokian S., Mitri H., Thibodeau D., and Moreau-Verlaan L. (2013). Optimizing stope sequence in a diminishing ore pillar: a case study. In Proceedings of the 23<sup>rd</sup> World Mining Congress, 11 – 15 August, Montreal (Canada). Accepted

Tang, B., Mitri, H.S., and Bouteldja, M. (2000). Finite element modeling of rock anchors. Proceedings of the ICE—Ground Improvement 4(2):65–71.

Tadolini, S. and Mitri, H.S. (2002). Field and numerical analysis of resin-grouted cable bolts used for coal mine longwall roof support. Hammah, Bawden, Curran and Telesnicki, eds. *Proceedings of the North American Rock Mechanics Symposium*. Toronto, ON, Canada: University of Toronto, pp. 713– 719.

Varden R, Lachenicht R, Player J, Thompson A, Villaescusa E (2008) Development and implementation of the Garford Dynamic Bolt at the Kanowna Belle Mine. In: 10th underground operators' conference, Launceston, Australia

Wagner, W.H ( 1984). Support requirements for rockburst conditions. Proceedings of the 1<sup>st</sup> International congress on Rockbursts and seismicity in Mines, September 1982, Johannesburg(South Africa), N.C.

Wei.W( 2010). Numerical modelling study of rock support system for deep mine haulage drift, Master's Thesis, submitted to McGill University, 2010.

Windsor, C.R. (2001). Cablebolting, Underground Mining methods – Engineering fundamentals and international case studies, W.A. Hustruidd and R.L. Bullock, Editors, Society for Mining, Metallurgy and exploration ( SME), Littleton ( Colorado), Chapter 64: 555-561.

Wojno and Kuijpers.(2001). Cone cable – New generation yieldable tendon for large deformations, in 4th International Symposium “Roofbolting in Mining” at the Aachen University of Technology on June 6 and 7, 2001.

Wu.R and Oldsen.J (2010). Development of a new yielding rock bolt—Yield-Lok bolt. In: The 44th US rock mechanics symposium, Salt Lake City, USA, ARMA, pp 10–197

[www.avengman.com](http://www.avengman.com)

[www.dsiunderground.com](http://www.dsiunderground.com)

[www.dynamicrocksupports.com](http://www.dynamicrocksupports.com)

[www.mansourmining.com](http://www.mansourmining.com)

Yao ,M, Chinnasane,D.R, Harding, D ( 2009), Mitigation plans for mining in highly burst-prone ground conditions at Vale Inco Copper cliff North mine: In Proceedings of the 3<sup>rd</sup> CANUS Rock Mechanics Symposium( ROCKENG09), Toronto, May 2009(ed:M.Diederichs and G. Graselli)

Yao, M., Chinnasane, R., and Harding, D., (2009). Mitigation Plans for Mining in Highly Burst-Prone Ground Conditions at Vale Inco Copper Cliff North Mine, ROCKENG09: Proceedings of the 3rd CANUS Rock Mechanics Symposium, Toronto, May 2009 (Ed: M.Diederichs and G. Grasselli), 2009.

Yi, X and Kaiser, P.K.(1993). Impact testing of rockbolt for design in rockburst conditions. In International Journal of Rock Mechanics and Mining Sciences & Geomechanical abstracts, 31(6):671-685.

Zhang, Y. and Mitri, H.S. (2006) A simple methodology for mine stope stability analysis. In the proceedings of Mine Planning & Equipment

Selection Symposium, Torino, Italy, September 20-22, Cardu, M., Ciccu,  
R., Lovera, E. and Michelotti, E. (eds), *Vol. 2, pp. 1465- 1470.*  
Published by FIORDO S.r.l. Galliate (NO) Italy.

## **10 Appendix**

## A-1 FLAC 2D Code for static analysis

Project: [Static-Prand Sec.prj] Static

Physical unit3: SI: meter-kilogram-second

Record Tree

:[new]

;Branch: branch A

:[NEWGRID.sav]

; Source: Simple grid

grid 268,120

gen 0.0,0.0 0.0,220.0 210.0,220.0 210.0,0.0 i=1,9 j=1,10

gen 210.0,0.0 210.0,220.0 220.0,220.0 220.0,0.0 i=9,12 j=1,10

gen 220.0,0.0 220.0,220.0 230.0,220.0 230.0,0.0 i=12,15 j=1,10

gen 230.0,0.0 230.0,220.0 240.0,220.0 240.0,0.0 i=15,18 j=1,10

gen 240.0,0.0 240.0,220.0 250.0,220.0 250.0,0.0 i=18,21 j=1,10

gen 250.0,0.0 250.0,220.0 255.0,220.0 255.0,0.0 i=21,24 j=1,10

gen 255.0,0.0 255.0,220.0 260.0,220.0 260.0,0.0 i=24,27 j=1,10

gen 260.0,0.0 260.0,220.0 265.0,220.0 265.0,0.0 i=27,30 j=1,10

gen 265.0,0.0 265.0,220.0 300.0,220.0 300.0,0.0 i=30,33 j=1,10

gen 300.0,0.0 300.0,220.0 365.0,220.0 365.0,0.0 i=33,36 j=1,10

gen 365.0,0.0 365.0,220.0 365.5,220.0 365.5,0.0 i=36,39 j=1,10

gen 365.5,0.0 365.5,220.0 365.75,220.00002 365.75,0.0 i=39,42 j=1,10

gen 365.75,0.0 365.75,220.00002 366.0,220.0 366.0,0.0 i=42,45 j=1,10

gen 366.0,0.0 366.0,220.0 400.0,220.0 400.0,0.0 i=45,48 j=1,10

gen 400.0,0.0 400.0,220.0 500.0,220.0 500.0,0.0 i=48,52 j=1,10

gen 0.0,220.0 0.0,245.0 210.0,245.0 210.0,220.0 i=1,9 j=10,13

gen 210.0,220.0 210.0,245.0 220.0,245.0 220.0,220.0 i=9,12 j=10,13

gen 220.0,220.0 220.0,245.0 230.0,245.0 230.0,220.0 i=12,15 j=10,13

gen 230.0,220.0 230.0,245.0 240.0,245.0 240.0,220.0 i=15,18 j=10,13

gen 240.0,220.0 240.0,245.0 250.0,245.0 250.0,220.0 i=18,21 j=10,13

gen 250.0,220.0 250.0,245.0 255.0,245.0 255.0,220.0 i=21,24 j=10,13

gen 255.0,220.0 255.0,245.0 260.0,245.0 260.0,220.0 i=24,27 j=10,13

gen 260.0,220.0 260.0,245.0 265.0,245.0 265.0,220.0 i=27,30 j=10,13  
gen 265.0,220.0 265.0,245.0 300.0,245.0 300.0,220.0 i=125,149 j=1,25  
gen 300.0,220.0 300.0,245.0 365.0,245.0 365.0,220.0 i=149,173 j=1,25  
gen 365.0,220.0 365.0,245.0 365.5,245.0 365.5,220.0 i=173,197 j=1,25  
gen 365.5,220.0 365.5,245.0 365.75,245.0 365.75,220.00002 i=197,221 j=1,25  
gen 365.75,220.00002 365.75,245.0 366.0,245.0 366.0,220.0 i=221,245 j=1,25  
gen 366.0,220.0 366.0,245.0 400.0,245.0 400.0,220.0 i=245,269 j=1,25  
gen 400.0,220.0 400.0,245.0 500.0,245.0 500.0,220.0 i=48,52 j=10,13  
gen 0.0,245.0 0.0,250.0 210.0,250.0 210.0,245.0 i=1,9 j=13,16  
gen 210.0,245.0 210.0,250.0 220.0,250.0 220.0,245.0 i=9,12 j=13,16  
gen 220.0,245.0 220.0,250.0 230.0,250.0 230.0,245.0 i=12,15 j=13,16  
gen 230.0,245.0 230.0,250.0 240.0,250.0 240.0,245.0 i=15,18 j=13,16  
gen 240.0,245.0 240.0,250.0 250.0,250.0 250.0,245.0 i=18,21 j=13,16  
gen 250.0,245.0 250.0,250.0 255.0,250.0 255.0,245.0 i=53,77 j=25,49  
gen 255.0,245.0 255.0,250.0 260.0,250.0 260.0,245.0 i=77,101 j=25,49  
gen 260.0,245.0 260.0,250.0 265.0,250.0 265.0,245.0 i=101,125 j=25,49  
gen 265.0,245.0 265.0,250.0 300.0,250.0 300.0,245.0 i=125,149 j=25,49  
gen 300.0,245.0 300.0,250.0 365.0,250.0 365.0,245.0 i=149,173 j=25,49  
gen 365.0,245.0 365.0,250.0 365.5,250.0 365.5,245.0 i=173,197 j=25,49  
gen 365.5,245.0 365.5,250.0 365.75,250.00002 365.75,245.0 i=197,221 j=25,49  
gen 365.75,245.0 365.75,250.00002 366.0,250.0 366.0,245.0 i=221,245 j=25,49  
gen 366.0,245.0 366.0,250.0 400.0,250.0 400.0,245.0 i=245,269 j=25,49  
gen 400.0,245.0 400.0,250.0 500.0,250.0 500.0,245.0 i=48,52 j=13,16  
gen 0.0,250.0 0.0,255.0 210.0,255.0 210.0,250.0 i=1,9 j=16,19  
gen 210.0,250.0 210.0,255.0 220.0,255.0 220.0,250.0 i=9,12 j=16,19  
gen 220.0,250.0 220.0,255.0 230.0,255.0 230.0,250.0 i=12,15 j=16,19  
gen 230.0,250.0 230.0,255.0 240.0,255.0 240.0,250.0 i=15,18 j=16,19  
gen 240.0,250.0 240.0,255.0 250.0,255.0 250.0,250.0 i=18,21 j=16,19  
gen 250.0,250.0 250.0,255.0 255.0,255.0 255.0,250.0 i=53,77 j=49,73  
gen 255.0,250.0 255.0,255.0 260.0,255.0 260.0,250.0 i=77,101 j=49,73  
gen 260.0,250.0 260.0,255.0 265.0,255.0 265.0,250.0 i=101,125 j=49,73  
gen 265.0,250.0 265.0,255.0 300.0,255.0 300.0,250.0 i=125,149 j=49,73  
gen 300.0,250.0 300.0,255.0 365.0,255.0 365.0,250.0 i=149,173 j=49,73  
gen 365.0,250.0 365.0,255.0 365.5,255.0 365.5,250.0 i=173,197 j=49,73  
gen 365.5,250.0 365.5,255.0 365.75,255.0 365.75,250.00002 i=197,221 j=49,73  
gen 365.75,250.00002 365.75,255.0 366.0,255.0 366.0,250.0 i=221,245 j=49,73  
gen 366.0,250.0 366.0,255.0 400.0,255.0 400.0,250.0 i=245,269 j=49,73

gen 400.0,250.0 400.0,255.0 500.0,255.0 500.0,250.0 i=48,52 j=16,19  
gen 0.0,255.0 0.0,260.0 210.0,260.0 210.0,255.0 i=1,9 j=19,22  
gen 210.0,255.0 210.0,260.0 220.0,260.0 220.0,255.0 i=9,12 j=19,22  
gen 220.0,255.0 220.0,260.0 230.0,260.0 230.0,255.0 i=12,15 j=19,22  
gen 230.0,255.0 230.0,260.0 240.0,260.0 240.0,255.0 i=15,18 j=19,22  
gen 240.0,255.0 240.0,260.0 250.0,260.0 250.0,255.0 i=18,21 j=19,22  
gen 250.0,255.0 250.0,260.0 255.0,260.0 255.0,255.0 i=53,77 j=73,97  
gen 255.0,255.0 255.0,260.0 260.0,260.0 260.0,255.0 i=77,101 j=73,97  
gen 260.0,255.0 260.0,260.0 265.0,260.0 265.0,255.0 i=101,125 j=73,97  
gen 265.0,255.0 265.0,260.0 300.0,260.0 300.0,255.0 i=125,149 j=73,97  
gen 300.0,255.0 300.0,260.0 365.0,260.0 365.0,255.0 i=149,173 j=73,97  
gen 365.0,255.0 365.0,260.0 365.5,260.0 365.5,255.0 i=173,197 j=73,97  
gen 365.5,255.0 365.5,260.0 365.75,260.0 365.75,255.0 i=197,221 j=73,97  
gen 365.75,255.0 365.75,260.0 366.0,260.0 366.0,255.0 i=221,245 j=73,97  
gen 366.0,255.0 366.0,260.0 400.0,260.0 400.0,255.0 i=245,269 j=73,97  
gen 400.0,255.0 400.0,260.0 500.0,260.0 500.0,255.0 i=48,52 j=19,22  
gen 0.0,260.0 0.0,280.0 210.0,280.0 210.0,260.0 i=1,9 j=22,25  
gen 210.0,260.0 210.0,280.0 220.0,280.0 220.0,260.0 i=9,12 j=22,25  
gen 220.0,260.0 220.0,280.0 230.0,280.0 230.0,260.0 i=12,15 j=22,25  
gen 230.0,260.0 230.0,280.0 240.0,280.0 240.0,260.0 i=15,18 j=22,25  
gen 240.0,260.0 240.0,280.0 250.0,280.0 250.0,260.0 i=18,21 j=22,25  
gen 250.0,260.0 250.0,280.0 255.0,280.0 255.0,260.0 i=21,24 j=22,25  
gen 255.0,260.0 255.0,280.0 260.0,280.0 260.0,260.0 i=24,27 j=22,25  
gen 260.0,260.0 260.0,280.0 265.0,280.0 265.0,260.0 i=27,30 j=22,25  
gen 265.0,260.0 265.0,280.0 300.0,280.0 300.0,260.0 i=125,149 j=97,121  
gen 300.0,260.0 300.0,280.0 365.0,280.0 365.0,260.0 i=149,173 j=97,121  
gen 365.0,260.0 365.0,280.0 365.5,280.0 365.5,260.0 i=173,197 j=97,121  
gen 365.75,260.0 365.75,280.0 366.0,280.0 366.0,260.0 i=221,245 j=97,121  
gen 366.0,260.0 366.0,280.0 400.0,280.0 400.0,260.0 i=245,269 j=97,121  
gen 365.5,260.0 365.5,280.0 365.75,280.0 365.75,260.0 i=197,221 j=97,121  
gen 400.0,260.0 400.0,280.0 500.0,280.0 500.0,260.0 i=48,52 j=22,25  
gen 0.0,280.0 0.0,500.0 210.0,500.0 210.0,280.0 i=1,9 j=25,34  
gen 210.0,280.0 210.0,500.0 220.0,500.0 220.0,280.0 i=9,12 j=25,34  
gen 220.0,280.0 220.0,500.0 230.0,500.0 230.0,280.0 i=12,15 j=25,34  
gen 230.0,280.0 230.0,500.0 240.0,500.0 240.0,280.0 i=15,18 j=25,34  
gen 240.0,280.0 240.0,500.0 250.0,500.0 250.0,280.0 i=18,21 j=25,34  
gen 250.0,280.0 250.0,500.0 255.0,500.0 255.0,280.0 i=21,24 j=25,34

gen 255.0,280.0 255.0,500.0 260.0,500.0 260.0,280.0 i=24,27 j=25,34  
gen 260.0,280.0 260.0,500.0 265.0,500.0 265.0,280.0 i=27,30 j=25,34  
gen 265.0,280.0 265.0,500.0 300.0,500.0 300.0,280.0 i=30,33 j=25,34  
gen 300.0,280.0 300.0,500.0 365.0,500.0 365.0,280.0 i=33,36 j=25,34  
gen 365.0,280.0 365.0,500.0 365.5,500.0 365.5,280.0 i=36,39 j=25,34  
gen 365.5,280.0 365.5,500.0 365.75,500.0 365.75,280.0 i=39,42 j=25,34  
gen 365.75,280.0 365.75,500.0 366.0,500.0 366.0,280.0 i=42,45 j=25,34  
gen 366.0,280.0 366.0,500.0 400.0,500.0 400.0,280.0 i=45,48 j=25,34  
gen 400.0,280.0 400.0,500.0 500.0,500.0 500.0,280.0 i=48,52 j=25,34  
model elastic i=1,8 j=1,9  
model elastic i=9,11 j=1,9  
model elastic i=12,14 j=1,9  
model elastic i=15,17 j=1,9  
model elastic i=18,20 j=1,9  
model elastic i=21,23 j=1,9  
model elastic i=24,26 j=1,9  
model elastic i=27,29 j=1,9  
model elastic i=30,32 j=1,9  
model elastic i=33,35 j=1,9  
model elastic i=36,38 j=1,9  
model elastic i=39,41 j=1,9  
model elastic i=42,44 j=1,9  
model elastic i=45,47 j=1,9  
model elastic i=48,51 j=1,9  
model elastic i=1,8 j=10,12  
model elastic i=9,11 j=10,12  
model elastic i=12,14 j=10,12  
model elastic i=15,17 j=10,12  
model elastic i=18,20 j=10,12  
model elastic i=21,23 j=10,12  
model elastic i=24,26 j=10,12  
model elastic i=27,29 j=10,12  
model elastic i=125,148 j=1,24  
model elastic i=149,172 j=1,24  
model elastic i=173,196 j=1,24  
model elastic i=197,220 j=1,24  
model elastic i=221,244 j=1,24

model elastic i=245,268 j=1,24  
model elastic i=48,51 j=10,12  
model elastic i=1,8 j=13,15  
model elastic i=9,11 j=13,15  
model elastic i=12,14 j=13,15  
model elastic i=15,17 j=13,15  
model elastic i=18,20 j=13,15  
model elastic i=53,76 j=25,48  
model elastic i=77,100 j=25,48  
model elastic i=101,124 j=25,48  
model elastic i=125,148 j=25,48  
model elastic i=149,172 j=25,48  
model elastic i=173,196 j=25,48  
model elastic i=197,220 j=25,48  
model elastic i=221,244 j=25,48  
model elastic i=245,268 j=25,48  
model elastic i=48,51 j=13,15  
model elastic i=1,8 j=16,18  
model elastic i=9,11 j=16,18  
model elastic i=12,14 j=16,18  
model elastic i=15,17 j=16,18  
model elastic i=18,20 j=16,18  
model elastic i=53,76 j=49,72  
model elastic i=77,100 j=49,72  
model elastic i=101,124 j=49,72  
model elastic i=125,148 j=49,72  
model elastic i=149,172 j=49,72  
model elastic i=173,196 j=49,72  
model elastic i=197,220 j=49,72  
model elastic i=221,244 j=49,72  
model elastic i=245,268 j=49,72  
model elastic i=48,51 j=16,18  
model elastic i=1,8 j=19,21  
model elastic i=9,11 j=19,21  
model elastic i=12,14 j=19,21  
model elastic i=15,17 j=19,21  
model elastic i=18,20 j=19,21

model elastic i=53,76 j=73,96  
model elastic i=77,100 j=73,96  
model elastic i=101,124 j=73,96  
model elastic i=125,148 j=73,96  
model elastic i=149,172 j=73,96  
model elastic i=173,196 j=73,96  
model elastic i=197,220 j=73,96  
model elastic i=221,244 j=73,96  
model elastic i=245,268 j=73,96  
model elastic i=48,51 j=19,21  
model elastic i=1,8 j=22,24  
model elastic i=9,11 j=22,24  
model elastic i=12,14 j=22,24  
model elastic i=15,17 j=22,24  
model elastic i=18,20 j=22,24  
model elastic i=21,23 j=22,24  
model elastic i=24,26 j=22,24  
model elastic i=27,29 j=22,24  
model elastic i=125,148 j=97,120  
model elastic i=149,172 j=97,120  
model elastic i=173,196 j=97,120  
model elastic i=221,244 j=97,120  
model elastic i=245,268 j=97,120  
model elastic i=197,220 j=97,120  
model elastic i=48,51 j=22,24  
model elastic i=1,8 j=25,33  
model elastic i=9,11 j=25,33  
model elastic i=12,14 j=25,33  
model elastic i=15,17 j=25,33  
model elastic i=18,20 j=25,33  
model elastic i=21,23 j=25,33  
model elastic i=24,26 j=25,33  
model elastic i=27,29 j=25,33  
model elastic i=30,32 j=25,33  
model elastic i=33,35 j=25,33  
model elastic i=36,38 j=25,33  
model elastic i=39,41 j=25,33

model elastic i=42,44 j=25,33  
model elastic i=45,47 j=25,33  
model elastic i=48,51 j=25,33  
; Attach grids  
attach aside from 125,1 to 149,1 bside from 30,10 to 33,10  
attach aside from 149,1 to 173,1 bside from 33,10 to 36,10  
attach aside from 173,1 to 197,1 bside from 36,10 to 39,10  
attach aside from 197,1 to 221,1 bside from 39,10 to 42,10  
attach aside from 221,1 to 245,1 bside from 42,10 to 45,10  
attach aside from 245,1 to 269,1 bside from 45,10 to 48,10  
attach aside from 53,25 to 77,25 bside from 21,13 to 24,13  
attach aside from 77,25 to 101,25 bside from 24,13 to 27,13  
attach aside from 101,25 to 125,25 bside from 27,13 to 30,13  
attach aside from 125,1 to 125,25 bside from 30,10 to 30,13  
attach aside from 48,10 to 48,13 bside from 269,1 to 269,25  
attach aside from 53,25 to 53,49 bside from 21,13 to 21,16  
attach aside from 48,13 to 48,16 bside from 269,25 to 269,49  
attach aside from 53,49 to 53,73 bside from 21,16 to 21,19  
attach aside from 48,16 to 48,19 bside from 269,49 to 269,73  
attach aside from 53,73 to 53,97 bside from 21,19 to 21,22  
attach aside from 21,22 to 24,22 bside from 53,97 to 77,97  
attach aside from 24,22 to 27,22 bside from 77,97 to 101,97  
attach aside from 27,22 to 30,22 bside from 101,97 to 125,97  
attach aside from 48,19 to 48,22 bside from 269,73 to 269,97  
attach aside from 125,97 to 125,121 bside from 30,22 to 30,25  
attach aside from 30,25 to 33,25 bside from 125,121 to 149,121  
attach aside from 33,25 to 36,25 bside from 149,121 to 173,121  
attach aside from 36,25 to 39,25 bside from 173,121 to 197,121  
attach aside from 42,25 to 45,25 bside from 221,121 to 245,121  
attach aside from 45,25 to 48,25 bside from 245,121 to 269,121  
attach aside from 48,22 to 48,25 bside from 269,97 to 269,121  
attach aside from 39,25 to 42,25 bside from 197,121 to 221,121  
mark i 77 101 j 49  
mark i 77 j 49 73  
mark i 101 j 49 73  
mark i 67 j 31  
unmark i 77 j 73

unmark i 101 j 73  
gen arc 257.5,246 260,254.8 33  
unmark i 67 j 31  
set dyn off  
;[stopes.sav]  
mark i 18 j 1 3  
mark i 9 j 1 3  
mark i 9 j 4  
mark i 18 j 4  
mark i 18 j 5  
mark i 9 j 5  
mark i 9 j 6  
mark i 18 j 6  
mark i 18 j 7  
mark i 9 j 7  
mark i 9 j 8  
mark i 18 j 8  
mark i 18 j 9  
mark i 9 j 9  
mark i 9 j 10  
mark i 18 j 10  
mark i 18 j 11  
mark i 18 j 12  
mark i 9 j 12  
mark i 9 j 11  
mark i 9 j 13 22  
mark i 18 j 13 22  
mark i 9 18 j 16  
mark i 10 18 j 10  
mark i 12 j 10 15  
mark i 15 j 10 15  
mark i 11 j 17 25  
mark i 9 j 22 25  
unmark i 11 j 17 25  
unmark i 12 j 17 25  
unmark i 15 j 17 25  
mark i 12 j 17 25

mark i 15 j 17 25  
mark i 18 j 23 25  
mark i 10 17 j 25  
mark i 9 j 26  
mark i 18 j 26  
mark i 17 j 27  
mark i 9 j 27  
mark i 9 j 28  
mark i 17 j 28  
mark i 17 j 29  
mark i 9 j 29  
mark i 9 j 30  
mark i 17 j 30  
mark i 9 j 31  
mark i 17 j 31  
mark i 17 j 32  
mark i 9 j 32  
mark i 9 j 33  
mark i 17 j 33  
mark i 9 j 34  
mark i 17 j 34  
mark i 10 17 j 1  
mark i 10 16 j 34  
mark i 18 j 27  
mark i 18 j 28  
mark i 18 j 29  
unmark i 17 j 29  
unmark i 17 j 28  
unmark i 17 j 27  
unmark i 17 j 30  
unmark i 17 j 31  
unmark i 17 j 32  
unmark i 17 j 33  
mark i 18 j 30  
mark i 18 j 31  
mark i 18 j 32  
mark i 18 j 33

mark i 18 j 34  
fix x i 1 j 1 34  
fix x i 39 j 1 34  
fix y i 1 39 j 34  
fix y i 1 39 j 1  
fix x i 2 39 j 1  
free x i 2 39 j 1  
fix x y i 39 j 1  
free x i 39 j 2 33  
free x y i 39 j 34  
free x y i 39 j 1  
fix x i 41 j 1 33  
fix x i 41 j 34  
fix y i 39 41 j 34  
fix y i 39 41 j 1  
free x i 41 j 1 33  
free y i 41 j 1  
free y i 41 j 2  
free y i 40 j 1  
free y i 40 j 34  
free y i 41 j 34  
free x i 41 j 34  
fix x i 39 j 1 34  
free x i 45 j 1 33  
free x i 45 j 33  
free x i 39 j 33  
free x i 45 j 32  
free x i 40 j 32  
free x i 39 j 32  
free x i 39 j 31  
free x i 40 j 30  
free x i 40 j 30  
free x i 39 j 30  
free x i 40 j 29  
free x i 40 j 29  
free x i 39 j 29  
free x i 39 j 28

```

free x i 39 j 27
free x i 39 j 26
free x i 39 j 25
free x i 39 j 10
free x i 39 j 9
free x i 39 j 8
free x i 39 j 7
free x i 39 j 6
free x i 39 j 5
free x i 39 j 4
free x i 39 j 3
free x i 38 44 j 2
free x i 39 j 1
free x i 39 j 34
fix x i 52 j 1 34
fix y i 46 52 j 1
fix y i 46 52 j 34
fix y i 40 45 j 34
fix y i 40 45 j 1
fix x i 1 52 j 1
; material
group 'Hanging wall:Left side' region 4 25
group 'Orebody:Middle' region 13 28
group 'Orebody:Middle' region 12 7
group 'Orebody:stope 1' region 10 11
group 'Orebody:stope 2' region 13 12
group 'Orebody:stope 3' region 16 11
group 'Orebody:stope 4' region 11 21
group 'Orebody:stope 5' region 14 21
group 'Orebody:stope 6' region 16 22
group 'Footwall:Right side' region 33 7
group 'Footwall:Haulage drift' region 78 34
group 'Footwall:Haulage drift' region 59 41
model mohr notnull group 'Hanging wall:Left side'
prop density=2782.0 bulk=1.66667E10 shear=1E10 cohesion=4800000.0
friction=38.0 dilation=9.0 tension=110000.0 notnull group 'Hanging wall:Left side'
model mohr notnull group 'Orebody:Middle'

```

prop density=4531.0 bulk=1.19E10 shear=8.2E9 cohesion=1.02E7 friction=43.0  
dilation=11.0 tension=310000.0 notnull group 'Orebody:Middle'  
model mohr notnull group 'Orebody:stope 1'  
prop density=4531.0 bulk=1.19E10 shear=8.2E9 cohesion=1.02E7 friction=43.0  
dilation=11.0 tension=310000.0 notnull group 'Orebody:stope 1'  
model mohr notnull group 'Orebody:stope 2'  
prop density=4531.0 bulk=1.19E10 shear=8.2E9 cohesion=1.02E7 friction=43.0  
dilation=11.0 tension=310000.0 notnull group 'Orebody:stope 2'  
model mohr notnull group 'Orebody:stope 3'  
prop density=4531.0 bulk=1.19E10 shear=8.2E9 cohesion=1.02E7 friction=43.0  
dilation=11.0 tension=310000.0 notnull group 'Orebody:stope 3'  
model mohr notnull group 'Orebody:stope 4'  
prop density=4531.0 bulk=1.19E10 shear=8.2E9 cohesion=1.02E7 friction=43.0  
dilation=11.0 tension=310000.0 notnull group 'Orebody:stope 4'  
model mohr notnull group 'Orebody:stope 5'  
prop density=4531.0 bulk=1.19E10 shear=8.2E9 cohesion=1.02E7 friction=43.0  
dilation=11.0 tension=310000.0 notnull group 'Orebody:stope 5'  
model mohr notnull group 'Orebody:stope 6'  
prop density=4531.0 bulk=1.19E10 shear=8.2E9 cohesion=1.02E7 friction=43.0  
dilation=11.0 tension=31000.0 notnull group 'Orebody:stope 6'  
model mohr notnull group 'Footwall:Right side'  
prop density=2916.0 bulk=4.1E10 shear=2.64E10 cohesion=5700000.0  
friction=54.9 dilation=10.0 tension=510000.0 notnull group 'Footwall:Right side'  
model mohr notnull group 'Footwall:Haulage drift'  
prop density=2916.0 bulk=4.01E10 shear=2.64E10 cohesion=5700000.0  
friction=54.9 dilation=10.0 tension=510000.0 notnull group 'Footwall:Haulage  
drift'  
group 'Footwall:Right side' region 57 60  
group 'Footwall:Right side' region 75 60  
model mohr notnull group 'Footwall:Right side'  
prop density=2916.0 bulk=4.1E10 shear=2.64E10 cohesion=5700000.0  
friction=54.9 dilation=10.0 tension=510000.0 notnull group 'Footwall:Right side'  
group 'Footwall:Haulage drift' region 85 60  
model mohr notnull group 'Footwall:Haulage drift'  
prop density=2916.0 bulk=4.01E10 shear=2.64E10 cohesion=5700000.0  
friction=54.9 dilation=10.0 tension=510000.0 notnull group 'Footwall:Haulage  
drift'  
; slot  
mark i 173 245 j 97  
mark i 173 245 j 25  
mark i 173 j 25 32

```
mark i 245 j 25 32
mark i 173 j 33 53
mark i 245 j 33 53
mark i 173 j 54 78
mark i 245 j 54 79
mark i 173 j 79 97
mark i 245 j 80 97
;insitu stress
initial sxx= -90.3e6 var 0, 22e6
initial syy=-50.2e6 var 0, 15e6
initial szz=-70.25e6 var 0, 14e6
history 4 xdisp i=101, j=61
history 5 xdisp i=101, j=61
history 6 xdisp i=77, j=62
history 7 ydisp i=89, j=74
history 8 xvel i=101, j=61
history 9 xvel i=77, j=61
set gravity=9.81
set =large
history 999 unbalanced
solve
solve
;[Drift.sav]
;Drift
model null region 87 61
group 'null' region 87 61
group delete 'null'
model null i 48 j 26
group 'null' i 48 j 26
group delete 'null'
solve
struct node 1 grid 79,73
struct node 2 254.21335,256.8728
struct node 3 grid 85,74
struct node 4 256.2974,257.21
struct node 5 grid 92,74
struct node 6 258.40164,257.23
```

```

struct node 7 grid 99,73
struct node 8 260.4691,256.95734
struct node 9 grid 77,72
struct node 10 252.6916,255.87042
struct node 11 grid 101,72
struct node 12 262.11148,255.82211
struct node 13 grid 77,70
struct node 14 253.20279,254.37643
struct node 15 grid 77,56
struct node 16 253.2,251.45874
struct node 17 grid 77,63
struct node 18 253.17831,252.91446
struct node 19 grid 101,70
struct node 20 261.78864,254.37488
struct node 21 grid 101,63
struct node 22 261.80136,252.9152
struct node 23 grid 101,56
struct node 24 261.8,251.47203
struct rockbolt begin node 1 end node 2 seg 10 prop 4001
struct rockbolt begin node 3 end node 4 seg 10 prop 4001
struct rockbolt begin node 5 end node 6 seg 10 prop 4001
struct rockbolt begin node 7 end node 8 seg 10 prop 4001
struct rockbolt begin node 9 end node 10 seg 10 prop 4001
struct rockbolt begin node 11 end node 12 seg 10 prop 4001
struct rockbolt begin node 13 end node 14 seg 10 prop 4001
struct rockbolt begin node 15 end node 16 seg 10 prop 4001
struct rockbolt begin node 17 end node 18 seg 10 prop 4001
struct rockbolt begin node 19 end node 20 seg 10 prop 4001
struct rockbolt begin node 21 end node 22 seg 10 prop 4001
struct rockbolt begin node 23 end node 24 seg 10 prop 4001
struct prop 4001
struct prop 4001 density 7800 spacing 1.2 e 2E11 radius 0.0090 cs_sstiff 4E7
cs_scoh 3644.0 yield 125000.0 pmom 457.266 cs_nstiff 1.3E11 cs_sfric 30.0
cs_ncoh 10000.0 perimeter 0.059 cs_nfric 30.0 tfstrain 0.09
solve
;MCB
struct node 133 grid 82,73
struct node 134 254.98952,257.35455

```

struct node 135 grid 89,74  
struct node 136 257.34036,257.5608  
struct node 137 grid 96,73  
struct node 138 259.85422,257.44  
struct node 139 grid 77,71  
struct node 140 252.6077,254.78146  
struct node 141 grid 77,67  
struct node 142 252.6,253.7456  
struct node 143 grid 77,59  
struct node 144 252.6,252.0879  
struct node 145 grid 101,71  
struct node 146 262.4,254.81296  
struct node 147 grid 101,67  
struct node 148 262.39957,253.75345  
struct node 149 grid 101,59  
struct node 150 262.39017,252.08646  
struct rockbolt begin node 133 end node 134 seg 10 prop 4001  
struct rockbolt begin node 135 end node 136 seg 10 prop 4001  
struct rockbolt begin node 137 end node 138 seg 10 prop 4001  
struct rockbolt begin node 139 end node 140 seg 10 prop 4001  
struct rockbolt begin node 141 end node 142 seg 10 prop 4001  
struct rockbolt begin node 143 end node 144 seg 10 prop 4001  
struct rockbolt begin node 145 end node 146 seg 10 prop 4001  
struct rockbolt begin node 147 end node 148 seg 10 prop 4001  
struct rockbolt begin node 149 end node 150 seg 10 prop 4001  
struct prop 4002 density 7800.0 spacing 1.2 e 2E11 radius 0.0090 cs\_sstiff 4E9  
cs\_scoh 3644.0 yield 150000.0 pmom 457.0 cs\_nstiff 1.3E11 cs\_sfrc 30.0  
cs\_ncoh 10000.0 perimeter 0.059 tfstrain 0.09  
struct prop 4003 density 7800.0 spacing 1.2 e 2E11 radius 0.0090 cs\_scoh  
3644.0 yield 150000.0 pmom 457.0 cs\_nstiff 1.3E11 cs\_sfrc 30.0 cs\_ncoh  
10000.0 perimeter 0.059 cs\_nfrc 30.0 tfstrain 0.09  
struct chprop 4002 range 210 210  
struct chprop 4002 range 209 209  
struct chprop 4002 range 208 208  
struct chprop 4003 range 207 207  
struct chprop 4003 range 206 206  
struct chprop 4003 range 205 205  
struct chprop 4003 range 204 204

struct chprop 4003 range 203 203  
struct chprop 4003 range 202 202  
struct chprop 4003 range 201 201  
struct chprop 4002 range 200 200  
struct chprop 4002 range 199 199  
struct chprop 4002 range 198 198  
struct chprop 4003 range 197 197  
struct chprop 4003 range 196 196  
struct chprop 4003 range 195 195  
struct chprop 4003 range 194 194  
struct chprop 4003 range 193 193  
struct chprop 4003 range 192 192  
struct chprop 4003 range 191 191  
struct chprop 4002 range 190 190  
struct chprop 4002 range 189 189  
struct chprop 4002 range 188 188  
struct chprop 4003 range 187 187  
struct chprop 4003 range 186 186  
struct chprop 4003 range 185 185  
struct chprop 4003 range 184 184  
struct chprop 4003 range 183 183  
struct chprop 4003 range 182 182  
struct chprop 4003 range 181 181  
struct chprop 4002 range 180 180  
struct chprop 4002 range 179 179  
struct chprop 4002 range 178 178  
struct chprop 4003 range 177 177  
struct chprop 4003 range 176 176  
struct chprop 4003 range 175 175  
struct chprop 4003 range 174 174  
struct chprop 4003 range 173 173  
struct chprop 4003 range 172 172  
struct chprop 4003 range 171 171  
struct chprop 4002 range 170 170  
struct chprop 4002 range 169 169  
struct chprop 4002 range 168 168  
struct chprop 4003 range 167 167

struct chprop 4003 range 166 166  
struct chprop 4003 range 165 165  
struct chprop 4003 range 164 164  
struct chprop 4003 range 163 163  
struct chprop 4003 range 162 162  
struct chprop 4003 range 161 161  
struct chprop 4002 range 160 160  
struct chprop 4002 range 159 159  
struct chprop 4002 range 158 158  
struct chprop 4003 range 157 157  
struct chprop 4003 range 156 156  
struct chprop 4003 range 155 155  
struct chprop 4003 range 154 154  
struct chprop 4003 range 153 153  
struct chprop 4003 range 152 152  
struct chprop 4003 range 151 151  
struct chprop 4002 range 150 150  
struct chprop 4002 range 149 149  
struct chprop 4002 range 148 148  
struct chprop 4003 range 147 147  
struct chprop 4003 range 146 146  
struct chprop 4003 range 145 145  
struct chprop 4003 range 144 144  
struct chprop 4003 range 143 143  
struct chprop 4003 range 142 142  
struct chprop 4003 range 141 141  
struct chprop 4002 range 140 140  
struct chprop 4002 range 139 139  
struct chprop 4002 range 138 138  
struct chprop 4003 range 137 137  
struct chprop 4003 range 136 136  
struct chprop 4003 range 135 135  
struct chprop 4003 range 134 134  
struct chprop 4003 range 133 133  
struct chprop 4003 range 132 132  
struct chprop 4003 range 131 131  
struct chprop 4002 range 130 130

```
struct chprop 4002 range 129 129
struct chprop 4002 range 128 128
struct chprop 4003 range 127 127
struct chprop 4003 range 126 126
struct chprop 4003 range 125 125
struct chprop 4003 range 124 124
struct chprop 4003 range 123 123
struct chprop 4003 range 122 122
struct chprop 4003 range 121 121
```

```
:[Stope-1.sav]
```

```
:[Stope-2.sav]
```

```
group 'Orebody:stope 1' region 10 11
model mohr group 'Orebody:stope 1'
prop density=4531.0 bulk=1.19000003E10 shear=8.2E9 cohesion=1.02E7
friction=43.0 dilation=11.0 tension=310000.0 group 'Orebody:stope 1'
group 'Backfill:Stope1' region 10 11
group 'Backfill:Stope1' region 9 11
model mohr notnull group 'Backfill:Stope1'
prop density=2000.0 bulk=8.33334E7 shear=3.84615E7 cohesion=1000000.0
friction=30.0 dilation=0.0 tension=10000.0 notnull group 'Backfill:Stope1'
model null group 'Orebody:stope 2'
solve
```

```
:[stope-3.sav]
```

```
model mohr group 'Orebody:stope 2'
prop density=4531.0 bulk=1.19000003E10 shear=8.2E9 cohesion=1.02E7
friction=43.0 dilation=11.0 tension=310000.0 group 'Orebody:stope 2'
group 'Backfill:CRF' region 13 11
model mohr notnull group 'Backfill:CRF'
prop density=2000.0 bulk=8.33333E7 shear=3.84615E7 cohesion=1000000.0
friction=30.0 dilation=0.0 tension=10000.0 notnull group 'Backfill:CRF'
model null group 'Orebody:stope 3'
solve
```

```
:[Stope-4.sav]
```

```
model mohr group 'Orebody:stope 3'
prop density=4531.0 bulk=1.19000003E10 shear=8.2E9 cohesion=1.02E7
friction=43.0 dilation=11.0 tension=310000.0 group 'Orebody:stope 3'
group 'Backfill:CRF' region 16 11
model mohr notnull group 'Backfill:CRF'
```

```

prop density=2000.0 bulk=8.33333E7 shear=3.84615E7 cohesion=1000000.0
friction=30.0 dilation=0.0 tension=10000.0 notnull group 'Backfill:CRF'

model null group 'Orebody:stope 4'

solve

;[Stope-5.sav]

model mohr group 'Orebody:stope 4'

prop density=4531.0 bulk=1.19000003E10 shear=8.2E9 cohesion=1.02E7
friction=43.0 dilation=11.0 tension=310000.0 group 'Orebody:stope 4'

group 'Backfill:CRF' region 13 23

model mohr notnull group 'Backfill:CRF'

prop density=2000.0 bulk=8.33333E7 shear=3.84615E7 cohesion=1000000.0
friction=30.0 dilation=0.0 tension=10000.0 notnull group 'Backfill:CRF'

group 'Backfill:CRF' region 10 22

group 'Orebody:stope 5' region 13 22

model mohr notnull group 'Orebody:stope 5'

prop density=4531.0 bulk=1.19E10 shear=8.2E9 cohesion=1.02E7 friction=43.0
dilation=11.0 tension=310000.0 notnull group 'Orebody:stope 5'

model mohr notnull group 'Backfill:CRF'

prop density=2000.0 bulk=8.33333E7 shear=3.84615E7 cohesion=1000000.0
friction=30.0 dilation=0.0 tension=10000.0 notnull group 'Backfill:CRF'

model null group 'Orebody:stope 5'

solve

;[Stope-6.sav]

model mohr group 'Orebody:stope 5'

prop density=4531.0 bulk=1.19000003E10 shear=8.2E9 cohesion=1.02E7
friction=43.0 dilation=11.0 tension=310000.0 group 'Orebody:stope 5'

group 'Backfill:CRF' region 13 22

model mohr notnull group 'Backfill:CRF'

prop density=2000.0 bulk=8.33333E7 shear=3.84615E7 cohesion=1000000.0
friction=30.0 dilation=0.0 tension=10000.0 notnull group 'Backfill:CRF'

model null group 'Orebody:stope 6'

solve

```

**A2 - Pictures of field instrumentation and others during this study**



Figure A2-1 Cone bolt failing under shear force

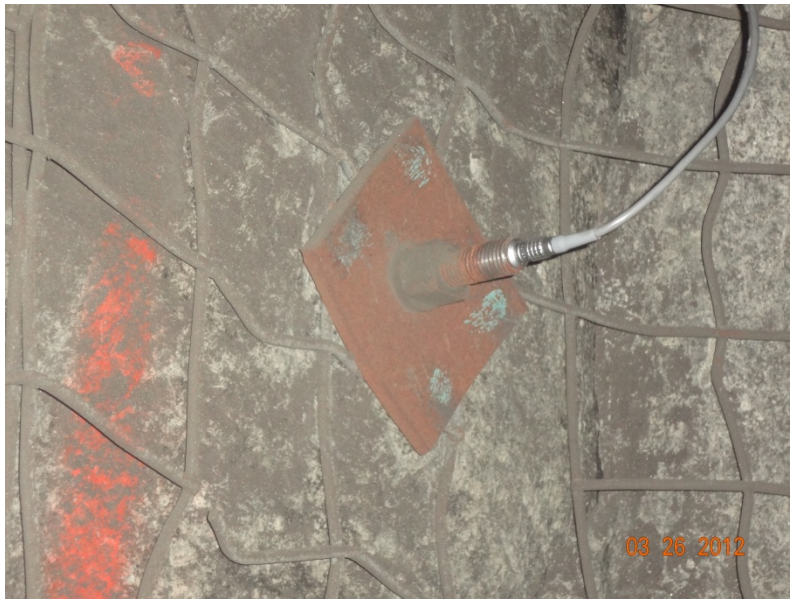


Figure A2-2 U-Cells in the drift wall and roof taking load



Figure A2-3 Drift wall condition before and after miner rockburst



Figure A2-4 Installation of MPBX in drift wall



Figure A2-5 Installation of U-Cell in drift wall